

**Palladium-Catalysed Enantioselective  
Hydrogenation of *N*-acetyl  
dehydrophenylalanine methyl ester**

Thesis submitted in accordance with the requirement of Cardiff University  
for the degree of Doctor of Philosophy

by

Nicola Jane Colston B.Sc.

UMI Number: U202157

All rights reserved

INFORMATION TO ALL USERS

The quality of this reproduction is dependent upon the quality of the copy submitted.

In the unlikely event that the author did not send a complete manuscript and there are missing pages, these will be noted. Also, if material had to be removed, a note will indicate the deletion.



UMI U202157

Published by ProQuest LLC 2013. Copyright in the Dissertation held by the Author.  
Microform Edition © ProQuest LLC.

All rights reserved. This work is protected against  
unauthorized copying under Title 17, United States Code.



ProQuest LLC  
789 East Eisenhower Parkway  
P.O. Box 1346  
Ann Arbor, MI 48106-1346

## Acknowledgements

I would like to thank my supervisors, Prof. Graham J. Hutchings, Prof. Peter B. Wells, Dr. Paul McMorn, for their help and support throughout this project. This project was financed in part by Robinson Brothers, thank you.

There are many other people who have helped me throughout my work. Dr. Mike Coogan, for his help and guidance during organic syntheses, Rob Jenkins for his constant help with many NMR spectra, Dr. Dave Willock and Ed Jefferey for computer modelling. All the technical staff, Ricki, Robin, Rob (again) and Alun. Gaz and Steve in the stores for being 'open all hours'. Also, thanks to Pat, for the little chats and bars of chocolates.

Special thanks to all the people in the lab, Becky, Nick, Darragh (Des), Owain, John, Lee and anyone else that I've forgotten. Thanks for being such excellent company (joke Des!). An extra special thanks to Dr. Philip Landon for putting up with me throughout this long four years.

Finally, I'd like to thank all my family and friends for their constant encouragement, love and support. Thanks all.

<b><i>Chapter 1</i></b>	page
<b>1.1 Catalysis</b>	1
<b>1.2 Definitions and Terms</b>	2
<b>1.3 Kinetics of Catalysed Reactions</b>	3
<b>1.4 Hydrogenation of the Carbon-Carbon Double Bond</b>	6
<b>1.5 Enantioselective Synthesis</b>	9
<b>1.6 Homogeneous Catalysis</b>	10
1.6.1 Homogeneous Catalysis for Enantioselective Carbon-Carbon Double Bond Hydrogenation	11
1.6.2 Homogeneous Catalysis for Enantioselective Carbon-Oxygen Double Bond Hydrogenation	13
<b>1.7 Heterogeneous Catalysis</b>	14
<b>1.8 Enantioselective Hydrogenation Using Modified Metal Catalysts</b>	15
1.8.1 Platinum Catalysed Reactions	17
1.8.1.1 Variation of modifier structure	19
1.8.1.2 The adsorption model	21
1.8.1.2A Conformations of cinchona alkaloids	22
1.8.1.2B Adsorption mode of ethyl pyruvate	25
1.8.1.2C Mechanism	25
1.8.1.3 The chemical shielding model	28
1.8.2 Palladium Catalysed Reactions	29
1.8.2.1 Hydrogenation of carbon-oxygen double bonds	29



1.8.2.1A	Mechanism	29
1.8.2.2	Hydrogenation of carbon-carbon double bonds	32
1.8.2.2A	Mechanism	34
1.8.2.3	Hydrogenation of carbon-nitrogen double bonds	36
1.8.2.3A	Mechanism	37
<b>1.9</b>	<b>The Target Reaction</b>	<b>39</b>
1.9.1	Homogeneous Catalysis of NADPME	39
1.9.1.1	Mechanism	41
1.9.2	Heterogeneous Catalysis of NADPME	43
1.9.3	Objectives	43
<b>1.10</b>	<b>References</b>	<b>44</b>

## *Chapter 2*

<b>2.1</b>	<b>Materials</b>	<b>52</b>
2.1.1	Reactants	52
2.1.1.1	Preparation of dehydrophenylalanine azlactone	52
2.1.1.2	Preparation of ( <i>E</i> )- <i>N</i> -acetyl dehydrophenylalanine methyl ester	52
2.1.1.3	Preparation of ( <i>E</i> )- <i>N</i> -acetyl dehydrophenylalanine ethyl ester	53
2.1.1.4	Preparation of ( <i>E</i> )- <i>N</i> -acetyl dehydrophenylalanine butyl ester	53
2.1.1.5	Preparation of ( <i>E</i> )- <i>N</i> -acetyl dehydrophenylalanine $\pm$ 2-butyl ester	53
2.1.1.6	Preparation of ( <i>E</i> )- <i>N</i> -acetyl dehydrophenylalanine + ( <i>R</i> )-2-butyl ester	54
2.1.1.7	Preparation of ( <i>E</i> )- <i>N</i> -acetyl dehydrophenylalanine	54
2.1.1.8	Preparation of the hydrochloride salt of dehydrophenylalanine methyl ester	55
2.1.1.9	Preparation of ( <i>E</i> )-dehydrophenylalanine methyl ester	55
2.1.1.10	Preparation of ( <i>E</i> )-phenyl cinnamic acid methyl ester	56

2.1.1.11 Preparation of diazomethane	56
2.1.2 Catalysts	58
2.1.2.1 Deposition-reduction method of catalyst preparation	58
2.1.2.2 Wet impregnation method of catalyst preparation	59
2.1.2.3 Re-reduction of catalyst samples	59
2.1.2.4 Premodification of catalyst with cinchona alkaloid	59
2.1.3 Cinchona Alkaloid Modifiers	60
2.1.3.1 Preparation of 10,11-dihydroderivatives	61
2.1.3.2 Preparation of quaternised cinchonine using methyl iodide	61
2.1.4 Other Modifiers	61
2.1.4.1 Preparation of (2S, 1'S)-N-[2'-naphthyl) ethyl]-2-amino propionic acid	62
2.1.5 Other Materials	63
<b>2.2 Apparatus</b>	
2.2.1 Parr Autoclave and Buchi Pressflow Controller	64
2.2.2 Chiral Gas Chromatography	65
2.2.3 Mass Spectrometry	66
2.2.4 Polarimetry	66
2.2.5 Fourier Transform Infra-Red (FT-IR)	66
2.2.6 Nuclear Magnetic Resonance Spectroscopy (NMR)	66
2.2.7 Electron Microscopy	67
2.2.8 Atomic Absorption Measurements (AA)	67
2.2.9 X-Ray Diffraction (XRD)	67
2.2.10 Measurements of Surface Area and Metal Dispersion	67
<b>2.3 Procedures</b>	67
2.3.1 Hydrogenations	67
2.3.2 Hydrogenations: Kinetics	68

---

2.3.3	Hydrogenations: Deuterium Tracer Studies	68
2.3.4	Product Recovery and Analysis	69
2.3.4.1	Derivatisation by diazomethane	69
2.3.5	Accuracy and Reproducibility of GC Analysis	70
2.3.6	NMR for Characterisation of Reactants	71
2.3.7	NMR for the Study of Modifier: Reactant Interaction	71
2.3.8	Atomic Absorption Measurements	72
2.3.9	X-Ray Diffraction Measurements	73
2.3.10	Chemisorption Measurements	73
<b>2.4</b>	<b>References</b>	<b>73</b>
 <b><i>Chapter 3</i></b>		
<b>3.1</b>	<b>The Standard Reaction</b>	<b>75</b>
3.1.1	Choice of Catalyst	75
3.1.2	Choice of Alkaloid Modifier	77
3.1.2.1	Effect of modifier on reaction rate	78
3.1.3	Reaction Conditions	79
3.1.3.1	Conditions for kinetic measurements	79
3.1.3.2	Conditions for standard (micro-scale) reactions	80
3.1.4	Characterisation of the Standard Reaction	80
3.1.4.1	Effect of stirring speed on rate of reaction	80
3.1.4.2	Variation of enantiomeric excess with hydrogen pressure	81
3.1.4.3	Dependence of enantiomeric excess on conversion	82
3.1.4.4	Variation of enantiomeric excess with temperature	83
3.1.4.5	Variation of enantiomeric excess with mass of modifier	84
3.1.4.6	Definition of standard conditions	86
<b>3.2</b>	<b>Kinetics of NADPME Hydrogenation</b>	<b>87</b>
3.2.1	Kinetics of the Unmodified Reaction	88

---

3.2.1.1 Effect of mass of catalyst	88
3.2.1.2 Effect of hydrogen pressure	90
3.2.1.3 Effect of mass of reactant	91
<b>3.2.2 Kinetics of the Cinchonine Modified Reaction</b>	<b>92</b>
3.2.2.1 Effect of mass of catalyst	92
3.2.2.2 Effect of hydrogen pressure	94
3.2.2.3 Effect of mass of reactant	96
3.2.2.4 Effect of temperature	96
<b>3.3 Solvent Effects</b>	<b>98</b>
3.3.1 Reactions in Various Solvents	98
3.3.2 Reactions in Mixed Solvents	101
3.3.2.1 Methanol/water mixtures	101
3.3.2.2 <i>N,N</i> -dimethylformamide/water mixtures	103
<b>3.3 Deuterium Tracer Studies</b>	<b>104</b>
<b>3.5 Investigation of the Reactant Modifier Interaction</b>	<b>106</b>
3.5.1 Alteration of the Ester Function of NADPME	106
3.5.2 Alteration of the <i>N</i> -Acetyl Function of NADPME	109
3.5.3 Alteration of the Phenyl Group of NADPME	110
3.5.4 Variation of Modifier	110
<b>3.6 Effect of pH on the Standard Reaction</b>	<b>112</b>
3.6.1 Effect of Acid	112
3.6.2 Effect of Base	114
<b>3.7 Hydrogenation of NADPME Catalysed by Pd/titania</b>	<b>118</b>
3.7.1 Catalyst Preparation	118
3.7.2 Effect of Palladium Loading	119

---

3.7.3 Reactions in Various Solvents	124
3.7.4 Conclusion	125
<b>3.8 Cinchonidine Modified Hydrogenations</b>	125
3.8.1 Effect of Cinchonidine Concentration on Enantiomeric Excess	125
3.8.2 Effect of Modifier on Rate	127
3.8.3 Reactions in Various Solvents	131
3.8.4 Reactions in Mixed Solvents	134
3.8.5 Variations on the Standard Reaction	135
3.8.5.1 Quaternised cinchonidine	135
3.8.5.2 Pre-modified catalyst	136
3.8.6 Spectroscopic Investigations	137
<b>3.9 Reactions Involving Other Cinchona Alkaloids</b>	142
<b>3.10 References</b>	144

## *Chapter 4*

<b>4.1 Preliminary Considerations</b>	145
4.1.1 A Comparison of Catalysts (1) and (2)	145
4.1.2 Deuterium Tracer Work	145
4.1.3 Comments on the Standard Reaction	146
<b>4.2 Kinetics of Racemic and Enantioselective NADPME Hydrogenation</b>	148
4.2.1 Competitive and Non-competitive Adsorption Under	148

---

Reaction Conditions.	
4.2.2 Order in NADPME	149
4.2.3 Order in Hydrogen	150
4.2.4 Activation Energy	151
4.2.5 Dependence of Rate on Catalyst Mass	151
4.2.6 Conclusion	152
4.2.7 Variation of Enantiomeric Excess with Hydrogen Pressure and Catalyst Mass	152
<b>4.3 A Model for Cinchonine-Modified Hydrogenation of NADPME.</b>	<b>153</b>
4.3.1 Pathways to Products	153
4.3.2 Adsorption and Reaction of NADPME at Alkaloid-Modified Sites	154
4.3.2.1 Origin of the reactant-modifier interaction	154
4.3.2.2 Reactant conformations	156
DPME	
NADPME	157
4.3.2.3 Reactant:modifier interaction at the enantioselective site	158
4.3.2.4 Enantioselective hydrogenation	161
DPME	161
NADPME	162
4.3.2.5 Modification by protonated cinchonine	163
4.3.3 Adsorption and Reaction of NADPME at Unmodified Sites	164
4.3.4 Adsorption and Reaction of Adducts at Surface Sites	165
4.3.5 Conclusions	167

---

<b>4.4</b>	<b>Effects of Solvent</b>	168
4.4.1	The Effect of Conformational Behaviour of Cinchona Alkaloids in NADPME Hydrogenation	168
4.4.2	The Effect of Solvent on the Nature of the Modifier-Reactant Interaction	168
4.4.3	Conclusions	171
<b>4.5</b>	<b>The Effect of pH on the Standard Reaction</b>	172
4.5.1	The Reactant-Modifier Interaction	172
4.5.2	The Effect of Additives	
4.5.2.1	Solutions containing acetic acid	173
4.5.2.2	Solutions containing potassium hydroxide	175
4.5.2.3	Solutions containing trifluoroacetic acid	176
4.5.3	The Effect of pH on the Optimum Modifier:Reactant Ratio	177
4.5.4	Conclusion	177
<b>4.6</b>	<b>Effects of Other Experimental Variables</b>	178
4.6.1	Variation in Reactant Structure	178
4.6.2	Variation in Modifier Structure	180
4.6.3	Conclusions	181
<b>4.7</b>	<b>Effects of Changing Catalyst Support</b>	182
4.7.1	Method of Preparation of Pd/titania	182
4.7.2	Comparison of Pd/titania with Pd/alumina	182
4.7.3	Effect of Palladium Loading	183
4.7.4	Conclusions	185
<b>4.8</b>	<b>Cinchonidine-Modified Hydrogenation of NADPME</b>	186

---

<b>4.8.1</b>	<b>Variation of Enantiomeric Excess with Modifier:Reactant Ratio</b>	<b>187</b>
4.8.1.1	Reactions Involving low modifier:reactant ratios	187
	<i>Cinchonine and cinchonidine</i>	187
	<i>Quinine and quinidine</i>	188
4.8.1.2	Reactions at high modifier:reactant molar ratio	189
	<i>Quinine and quinidine</i>	189
	<i>Cinchonine and cinchonidine</i>	189
<b>4.8.2</b>	<b>Variation of Experimental Conditions for Cinchonidine-Modified Reactions</b>	<b>192</b>
4.8.2.1	Effect of modifier on rate	192
4.8.2.2	Solvent effects	193
4.8.2.3	Reactions in acetic acid mixtures	194
	<i>Reactions in methanol/acetic acid and in ethanol/acetic acid</i>	194
	<i>Reactions in DCM/acetic acid</i>	195
4.8.2.4	Effect of varying standard conditions	195
	<i>Quaternised cinchonidine</i>	195
<b>4.8.3</b>	<b>Conclusions</b>	<b>196</b>
<b>4.9</b>	<b>References</b>	<b>196</b>



## Abstract

The enantioselective hydrogenation of *N*-acetyl dehydrophenylalanine methyl ester (NADPME) in solution over cinchona-modified Pd/alumina at 293 K and 10 bar hydrogen pressure. Experimental variables that influenced enantiomeric excess included the dielectric constant and pH of the reaction medium, the reactant:modifier molar ratio, and hydrogen pressure. The highest value achieved for the enantiomeric excess was 32%(*S*).

A deuterium tracer study confirmed that the reaction was one of carbon-carbon double bond saturation. Improvement of enantiomeric excess by addition of small amounts of water to high dielectric constant solvents (e.g. *N,N*-dimethylformamide) suggested that NADPME dimerised in solution but that the monomeric form participated in enantioselective reaction. Kinetic studies showed that both reactant and modifier were strongly adsorbed at the catalyst surface and that hydrogen was relatively weakly adsorbed. Comparison of results over Pd/alumina and Pd/titania indicated no direct support effect but suggested a dependence of enantiomeric excess on Pd particle size.

The interaction between NADPME and cinchonine was investigated by systematic variation of the structures of both reactant and modifier, and by the use of NMR spectroscopy and molecular modelling. Replacement of the -NHAc group in NADPME or quaternisation of the quinuclidine-N in cinchonine each caused complete loss of enantioselectivity, indicating that H-bonding between these two functions was an essential precursor to selective enantioface adsorption and preferential enantiomer formation in the product. Values of the enantiomeric excess provided by cinchonidine, quinine and quinidine revealed that the behaviour of cinchonine, which included inversion of the sense of enantioselectivity with increasing concentration, was atypically complex due in part to its low solubility.

The results have been interpreted in terms of the adsorption model. The relatively low values of enantiomeric excess achieved indicate that the two relevant conformational states of adsorbed-NADPME are not greatly differentiated with respect to their energies of adsorption.

# Chapter 1

## 1.1 Catalysis

Catalysis is at the heart of the modern chemicals industry [1]. The major high volume chemicals, e.g. sulphuric acid, nitric acid, ammonia, methanol, ethene are all formed in catalytic processes, as are the hydrocarbon fuels for petrol, diesel, and aeroengines. Polymers and plastics are formed in catalysed reactions, and many processes in the fine chemicals industry that were formerly operated as stoichiometric processes are now being replaced by more environmentally-friendly catalytic processes. Catalytic processes remove sulphur, nitrogen and heavy metals to very low levels before oil is processed in fuel production and auto-exhaust catalysts reduce the concentrations of unburnt fuel, carbon monoxide and nitrogen oxides in vehicle emissions. The pharmaceutical and agrochemical industries together with other smaller scale manufacturers use catalytic processes for simple molecular transformations such as hydrogenation [2, 3] and carbonylation.

Where the addition of a catalyst increases the number of phases present in a system we speak of *heterogenous catalysis* [4a]. In the majority of the processes mentioned above the catalyst is a solid and the reactants are in a fluid phase, so these are heterogeneously catalysed reactions. However, a number of important processes such as alkene polymerisations proceed with the catalyst in the same phase as one or more of the reactants, in which case the process is one of *homogeneous catalysis*.

The special area of concern for this investigation is enantioselective hydrogenation, and with regards to this, homogeneous catalysts have proved highly effective and selective, though expensive to prepare and difficult to separate from the product. Heterogeneous catalysts have proved less selective – except in certain cases – but are less expensive to make and are more convenient in use.

Any general definition of ‘catalysis’ and ‘catalyst’ applies equally to heterogeneous and homogeneous catalysts and to the processes in which they participate.

## 1.2 Definitions and Terms

Chemical reactions are characterised by changes in the arrangement and bonding of atoms in molecules. These changes are accompanied by a change in free energy – usually a diminution – by the absorption or evolution of heat, and by changes in the ordering of the system. The rates at which such processes occur are determined by the frequency of collision between reactant molecules and by the energy pathway for the conversion of reactants to products. The Arrhenius equation,  $k = Ae^{-E/RT}$ , (where  $k$  is the rate coefficient,  $A$  is a constant which includes the collision frequency,  $E$  is the activation energy, and  $T$  the temperature) describes both catalysed and uncatalysed reactions.

A catalyst is defined as a substance that increases the rate at which a chemical reaction approaches equilibrium without itself being consumed in the process [4b]. There are three important aspects to this definition [4c]. First, catalysts could, in principle, increase rate either by providing for an increase in the collision frequency or by reducing the activation energy barrier between reactants and products. Because the collision frequency of molecules from a fluid phase with a two-dimensional surface is much lower than their collision frequency in the three-dimensional fluid phase, heterogeneous catalysts operate at an inherent disadvantage. Their efficacy relies on their being able to provide a lower energy pathway for conversion of reactants to products; part of that saving in activation energy compensates for the reduced collision frequency, and the remainder contributes to the observed increase in rate. Second, catalysts do not feature in expressions for the equilibrium constant and hence they do not influence positions of equilibrium. Catalysts accelerate the forward and backward reactions to an equal degree, and they cannot be used as magical devices to circumvent thermodynamic constraints. Third, the catalyst surface should be regenerated after each reaction turnover, giving materials with an infinite lifetime. In practice, the rigorous conditions at a catalyst surface may lead to irreversible changes of morphology (e.g. crystal planes exposed) or of composition (e.g. formation of carbides) or undesirable side-reactions may lead to the deposition of poisons; hence catalytic activity tends to fall with time. In some instances, the processes leading to catalyst deactivation can be reversed and the catalyst regenerated, in others deactivation is irreversible [5, 6].

Reactant molecules approaching a solid surface are first subject to weak van der Waals interactions and, on closer approach may enter into chemical combination with the surface [4d]. The overall process is termed *adsorption*. The van der Waals interaction defines the *physically adsorbed* or *physisorbed* state, whereas the chemical interaction defines the *chemically adsorbed* or *chemisorbed* state. Progress from the physisorbed state to the chemisorbed state may or may not be an activated process. Where chemisorption is accompanied by dissociation it is termed *dissociative chemisorption*. Molecules adsorbed at surfaces are termed *adsorbates* and the surface itself is the *adsorbent*. The locations at which adsorbates are chemisorbed are termed *active sites* and adsorbents that catalyse reaction are called *active phases*. The process whereby adsorbates leave the surface is termed *desorption*. [Nomenclature in Heterogeneous Catalysis was defined by IUPAC in 1977 [7]].

### 1.3 Kinetics of Catalysed Reactions

In order to write a rate equation for a surface-catalysed reaction it is necessary to know, the relationship between the surface coverage and the concentration (or pressure) of each species involved in the rate determining step (or the species from which it was derived) in the fluid phase [8]. In general, if a reactant A, exerting a pressure  $P_A$  in the gas phase (or a concentration  $[A]$  in the solution phase), adsorbs without dissociation and is in equilibrium with adsorbed-A at a surface, then its surface coverage,  $\theta_A$ , is given by the Langmuir equation:

$$\theta_A = b_A P_A / (1 + b_A P_A). \quad (1)$$

Derivation of this equation involves the assumption that all adsorption sites at the surface are of equal energy, i.e. the heat of adsorption,  $-\Delta H_{ads}$ , is independent of  $\theta$ . Other adsorption equations are available based on assumptions that  $-\Delta H_{ads}$  decreases linearly or exponentially with coverage. Langmuir equations are most commonly used in practice in interpretations of the kinetics of catalysed reactions.

If reactant A dissociates into  $n$  species on adsorption, the above equation becomes:

$$\theta_A = b_A^{1/n} P_A^{1/n} / (1 + b_A^{1/n} P_A^{1/n}) \quad (2)$$

and so, for example, for hydrogen:

$$\theta_H = b_{H_2}^{1/2} P_{H_2}^{1/2} / (1 + b_{H_2}^{1/2} P_{H_2}^{1/2}). \quad (3)$$

Where A is very strongly adsorbed (i.e.  $b_A$  is very large) or its pressure or concentration is very high, so that  $b_A P_A \gg 1$ , equation (1) reduces to:

$$\theta_A \rightarrow 1 \quad (\text{i.e. full surface coverage}). \quad (4)$$

This means that  $\theta_A$  is independent of  $P_A$ .

Alternatively, where A is so weakly adsorbed that  $b_A P_A \ll 1$ , equation (1) reduces to:

$$\theta_A = b_A P_A \quad (5)$$

(i.e. the surface coverage of A increases in direct proportion to the pressure of A). By the same token, for weak dissociative hydrogen adsorption:

$$\theta_A = b_{H_2}^{1/2} P_{H_2}^{1/2}. \quad (6)$$

Where A and B adsorb at a surface in competition:

$$\theta_A = b_A P_A / (1 + b_A P_A + b_B P_B) \quad (7)$$

$$\text{and } \theta_B = b_B P_B / (1 + b_A P_A + b_B P_B). \quad (8)$$

Where A is more strongly adsorbed than B,  $\theta_A$  again approaches unity.

As an example, consider the hydrogenation of ethene over Pd at room temperature, which is zero or negative order in ethene and first order in hydrogen [9]. Reaction of ethene with deuterium produces all possible deuteriated ethenes and ethanes from which it is concluded that adsorbed- $C_2X_4$  and adsorbed-X are in kinetically fast equilibrium with adsorbed- $C_2X_5$  [X = H or D]. The rate determining step is proposed to be the removal of adsorbed-ethyl from the surface as ethane by reaction with adsorbed-H, thus:



$$\text{Therefore: } \text{rate} = k \theta_{C_2H_5} \theta_H. \quad (7)$$

Now  $\theta_{C_2H_5} = K \theta_{C_2H_4} \theta_H$ , where K is the equilibrium constant, so:

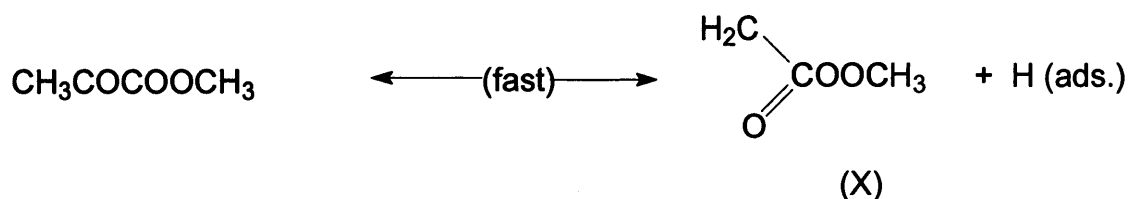
$$\text{rate} = k.K \theta_{C_2H_4} \theta_H \theta_H = k' \theta_{C_2H_4} \theta_H^2. \quad (8)$$

Supposing that ethene is very strongly adsorbed by comparison with hydrogen, then  $\theta_{C_2H_4} = b_{C_2H_4} P_{C_2H_4} / (1 + b_{C_2H_4} P_{C_2H_4} + b_{H_2}^{1/2} P_{H_2}^{1/2}) \Rightarrow 1$  by application of equations (3) and (7), and  $\theta_H = b_{H_2}^{1/2} P_{H_2}^{1/2} / (1 + b_{C_2H_4} P_{C_2H_4} + b_{H_2}^{1/2} P_{H_2}^{1/2}) \Rightarrow b_{H_2}^{1/2} P_{H_2}^{1/2} / b_{C_2H_4} P_{C_2H_4}$ . Substituting these values into equation (8) gives:

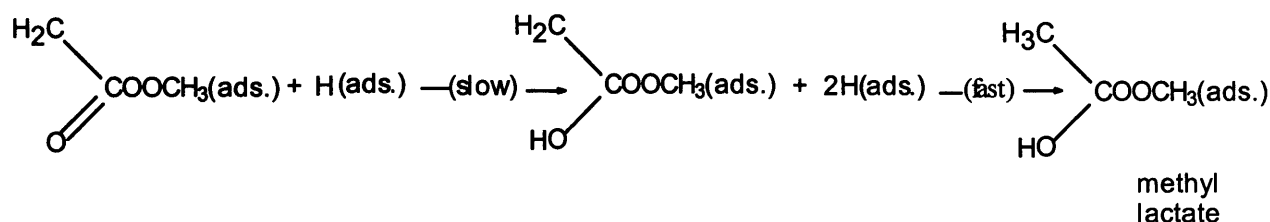
$$\text{rate} = k'.1. [b_{H_2}^{1/2} P_{H_2}^{1/2} / b_{C_2H_4} P_{C_2H_4}]^2 = k'' P_{H_2}^1 P_{C_2H_4}^{-2}$$

This treatment interprets the first order in hydrogen; orders in ethene are usually zero or negative, but not as negative as  $-2$ , which may reflect a failure of the system to comply with the assumptions of an energetically uniform surface made in deriving the Langmuir equations.

Another example worth consideration is the enantioselective hydrogenation of methyl pyruvate over cinchonidine-modified Pd [10]. Here the ester undergoes fast dissociative adsorption and reformation:



and the rate determining step is considered to be the slow addition of hydrogen to give the enol which then, being an alkene, undergoes kinetically fast hydrogenation over Pd to methyl lactate:



Given that the ester is strongly adsorbed ( $\theta_X \rightarrow 1$ ) and the hydrogen is weakly adsorbed ( $\theta_H \propto P_{\text{H}_2}^{1/2}$ ) then:

$$\text{rate} = k\theta_X\theta_H = [\text{methyl pyruvate}]^0 \cdot P_{\text{H}_2}^{1/2}$$

which interprets the observed zero and half orders in organic reactant and hydrogen respectively.

Catalysed reactions show rates that vary with temperature and it is common practice for investigators to report activation energies. The Arrhenius equation (above) describes the variation of the rate coefficient,  $k$ , with temperature. If the temperature range is such that the surface coverages of the reacting species (in the rate-determining step) do not vary with temperature, then the variation of  $k$  with temperature is followed by that of the reaction rate. So a plot of  $\ln(\text{reaction rate})$  against  $1/T(\text{K})$  should be linear with a gradient equal to  $-E_{\text{act}}/R$ . Where the above coverage condition is obeyed the activation energy so obtained is a *true*

*activation energy*. However, virtually all chemisorptions are exothermic and so, by Le Chatelier's Principle, surface coverage will have a tendency to decrease as temperature is raised. Thus, on raising temperature, the rate should increase because the rate coefficient increases, but it should fall if the surface coverage of a crucial intermediate falls. There may therefore be two effects working in opposition. Supposing that the crucial intermediate referred to is in an adsorption equilibrium then, according to the van't Hoff isochore equation, the variation of its coverage with temperature will be governed by its heat of adsorption, so that the measured activation energy will be equal to the true activation (measured in  $\text{kJ mol}^{-1}$ ) minus the heat of adsorption (also measured in  $\text{kJ mol}^{-1}$ ). The activation energy derived under these conditions is called an *apparent activation energy*. There is a tendency to treat high activation energies (say  $40 \text{ kJ mol}^{-1}$  or more) as true values and to suspect that low values (say  $10 \text{ kJ mol}^{-1}$ ) are apparent activation energies. Care must be exercised, however, because other conditions such as diffusion limitation can cause values of activation energy to be low [11]. However, where low values are recorded, and diffusion or other artefacts can be shown to be absent, then it is likely that the temperature dependence of the rate is governed both by kinetic and coverage effects.

If the coverage effect is zero, then the measured orders of reaction should be the same at all temperatures used to determine the activation energy. However, the number of investigations where the orders have been measured at each temperature are diminishingly small.

Some workers report all their values as apparent activation energies on the basis that the coverage effect must be operative in principle and that they do not have the detailed information required to establish that their values are true activation energies. The value of the activation energy, if high, is useful as contributory evidence that the reaction is not diffusion controlled.

## 1.4 Hydrogenation of the Carbon-Carbon Double Bond

The hydrogenation of organic compounds over finely divided metals was actively researched in the last quarter of the nineteenth century, culminating in the award of the



Nobel Prize to Sabatier in 1912. Here we shall restrict attention to the saturation of the carbon-carbon double bond, but removal of carbon-nitrogen and carbon-oxygen unsaturation by addition of hydrogen can also be achieved by use of metal catalysts.

The metals of Groups 8, 9, and 10, i.e. Fe, Ru, Os, Co, Rh, Ir, Ni, Pd, and Pt, are all catalytically active for hydrogenation when used as supported metals [12]. Early work with metal films and silica-supported metals identified Rh as the most active metal, closely followed by Ru and Pd in that order [13]. Thus the second transition series metals in these groups are the most active. Of these, palladium holds pride of place for organic chemists, probably because Pd/charcoal is active without any pretreatment.

The simplest hydrogenation is the conversion of ethene to ethane. Generally, over all metals of Groups 8, 9, and 10, this reaction is of zero or slightly negative order in ethene and of positive order in hydrogen [12]. The activation energy is usually close to  $35 \text{ kJ mol}^{-1}$ . This indicates that ethene is the more strongly adsorbed reactant and achieves high surface coverage whereas hydrogen is relatively weakly adsorbed and achieves low surface coverage. The situation over Pd is more complex because, at ambient and modest temperatures, Pd is in the H-rich phase and so, in principle, adsorbed-H can be established at the surface not only by dissociative adsorption of gaseous  $\text{H}_2$  but also by emergence of dissolved-H atoms from the bulk at the surface [14].

Alkene hydrogenations are generally considered to be structure insensitive, i.e. the activity and kinetics are independent of the structure (particle size, shape) of the active phase. However, when an active metal such as Pd is supported on a reducible oxide such as titania, and is reduced at a high temperature (say, 773 K), the so-called Strong Metal Support Interaction (SMSI) is induced [15] and activity is reduced.

As indicated above, the reaction of  $\text{C}_2\text{H}_4$  with  $\text{D}_2$  over any metal does not give  $\text{C}_2\text{H}_4\text{D}_2$  as the sole product; indeed, all possible deuterated ethanes being formed together with deuterium-containing ethenes [9]. This leads to a most important conclusion: namely, that saturation occurs by the consecutive addition of two H- or D-atoms and that ethene is first converted to a *half-hydrogenated state*, adsorbed- $\text{C}_2\text{X}_5$  (where  $\text{X} = \text{H}$  or  $\text{D}$ ). Kemball examined this reaction over many metal films and developed a mathematical approach which permitted the calculation of the D-distribution in the product [16, 17].

He assumed that adsorbed-ethene and adsorbed-ethyl were the only two hydrocarbon species involved in reaction (ethane, being saturated, is not adsorbed as such). Next, it was proposed (i) that the chance of adsorbed-ethene reacting with adsorbed-H and being converted to adsorbed-ethyl relative to its chance of undergoing desorption was  $p:1$ , (ii) that the chance of adsorbed-ethyl decomposing to adsorbed-ethene and adsorbed-H relative to its chance of reacting with adsorbed-H and forming gaseous ethane was  $r:1$ , and (iii) that the relative chances of adsorbed-ethene acquiring adsorbed-D rather than adsorbed-H was  $q:1$  and of adsorbed-ethyl so doing was  $s:1$ . There are 6 isotopically distinguishable adsorbed-ethenes and 12 isotopically distinguishable adsorbed-ethyls. Hence, 18 simultaneous steady state equations can be written which involve the 18 surface coverages and the four disposable parameters just defined. By supplying values for  $p$ ,  $q$ ,  $r$ , and  $s$ , and solving the equations, a calculated product composition can be obtained compared with the experimental; the two are then brought into agreement by iteration. Bond and co-workers showed that the product compositions from ethene-deuterium reactions over alumina-supported Ru, Rh, Pd, Re, Os, Ir and Pt could all be so interpreted [9, 18 – 20], and it was thereby firmly established that ethene is hydrogenated to ethane via a half-hydrogenated state.

Butene exists as the positional and geometric isomers but-1-ene, cis-but-2-ene, and trans-but-2-ene, and these alkenes are all hydrogenated to butane over these transition metals. Hydrogenation is accompanied by isomerisation, i.e. by both double bond migration and by cis/trans interconversion [9]. Generally, isomerisation is faster over Ru, Rh, and Pd than over Os, Ir, Pt. Over Pd the butene fraction often achieves its thermodynamic equilibrium composition ( $\text{trans-b-2} > \text{cis-b-2} > \text{b-1}$ ) before complete conversion to butane. These processes of double bond migration and cis/trans isomerisation are a direct result of the formation of the adsorbed-2-butyl half hydrogenated state. This chemistry has found important application in the process of fat hardening in which triglycerides containing multiply unsaturated  $C_{18}$ -ester side chains are selectively hydrogenated over Ni/silica to less unsaturated products [21].

Probably all metal-catalysed reactions which involve carbon-carbon double bond saturation by hydrogen involve the formation of an intermediate half-hydrogenated state, and this will be assumed in the interpretation of the results of the reaction under investigation.

When  $^{14}\text{C}$ -labelled ethene was adsorbed onto supported Ni, Pd, and Pt it was found that a proportion could be hydrogenated off as labelled-ethane or displaced by unlabelled ethene, but that a substantial proportion was irreversibly adsorbed as a dehydrogenated residue – the so-called hydrocarbonaceous species [22]. This result was later corroborated by surface science studies [23]. Remarkably, however, there is evidence that these hydrocarbonaceous species are not simple poisons, but may indeed be an important constituent of a healthy catalyst, contributing to H-atom transfer from the metallic surface to other adsorbed species [14]. Thus, it is not the case that alkene hydrogenations occur at otherwise clean metal surfaces; rather, there is a complex residue of permanently-retained hydrocarbonaceous matter at the metallic surface which is a constituent of the active surface. This will also be the case in the hydrogenation of complex molecules, such as those that undergo enantioselective hydrogenation, but no account has been taken so far of any analogous permanently adsorbed residues in such reactions.

## 1.5 Enantioselective Synthesis

The synthesis of optically pure compounds is of great importance, especially in the pharmaceutical and agrochemical industries. Research in this field is growing rapidly with the major aim of developing selective and highly active heterogeneous catalysts for asymmetric synthesis. This review concentrates on the synthesis of chiral compounds from prochiral reactants.

A molecule is prochiral when addition to a double bond or replacement of two equivalent groups at a particular atom leads to the creation of a new stereogenic centre in the molecule [24].

Transformation of these prochiral compounds via hydrogenation (Figure 1.5.1) can result in the preferential formation of one of the enantiomers; i.e. one of the configurations, *R* or *S*, prevails at the new stereogenic centre. This is known as enantioselective synthesis.

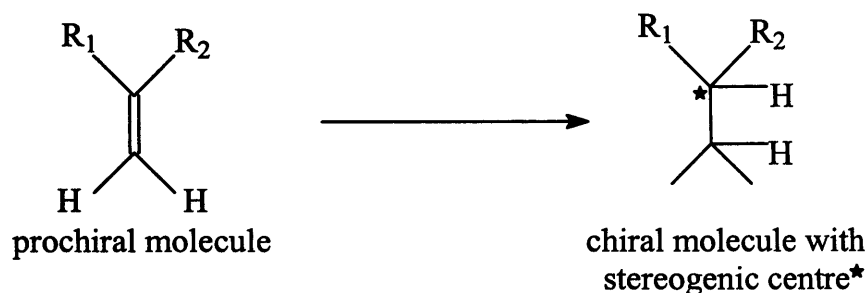


Figure 1.5.1 Hydrogenation of a prochiral compound to produce a chiral product.

The degree of enantioselectivity is quantified in terms of the enantiomeric excess (e.e.) which is defined as [25]:

$$\text{Enantiomeric excess (e.e.)\% (R)} = 100(R - S) / (R + S)$$

The achievement of enantioselection requires that a chiral entity is present in the reaction whether the reaction is catalysed homogeneously, where no phase boundaries exist between catalyst and reactant, or heterogeneously, where the catalyst and reactant are separated by a phase boundary. The way in which the chiral entity is incorporated into the reaction system can vary depending on the type of catalysis used.

## 1.6 Homogeneous Catalysis

In homogeneous catalysis the incorporation of a chiral entity is most simply achieved by use of a chiral ligand as a constituent of the catalytically active complex. There are many literature reviews on enantioselective hydrogenation involving homogeneous catalysts and the description below is representative of a very wide subject which is beyond the scope of this Chapter.

### 1.6.1 Homogeneous Catalysis for Enantioselective Carbon-Carbon Double Bond Hydrogenation

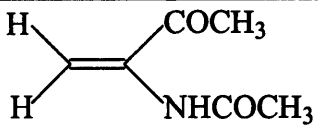
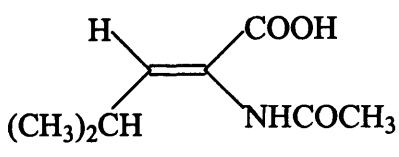
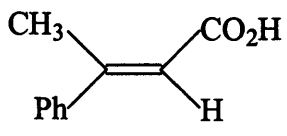
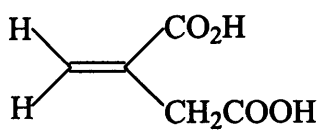
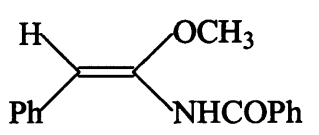
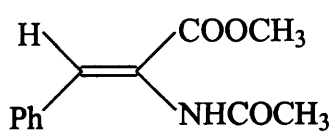
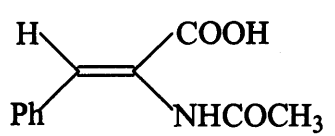
Knowles and Sabacky [26] provided some of the first examples of the enantioselective hydrogenation of carbon-carbon double bonds using complexes of Rh(I) with chiral phosphine ligands. Initially low values of enantiomeric excess were achieved, less than 10%, for a variety of reactants. It was soon realised that higher enantioselectivities could be achieved when the olefin met certain requirements. These were:

- (i) a carbonyl group or equivalent should be located  $\beta$  to the olefinic function.
- (ii) the group cis to the  $\beta$  group should be electron withdrawing.
- (iii) a hydrogen atom should occupy one of the remaining positions around the carbon-carbon double bond.

The knowledge of the importance of reactant structure coupled with the development of a wide range of bidentate chiral ligands led rapidly to an improvement in the values of enantiomeric excess achieved for these systems [27]. Some of the best applications listed in Table 1.6.1, use rhodium as the metal centre. There are reports in the literature of hydrogenations of similar reactants using ruthenium as the metal centre, but the enantioselectivities are generally lower.

Entry 6 in Table 1.6.1 is *N*-acetyl dehydrophenylalanine methyl ester (NADPME), which is the target reactant in the present investigation. Therefore a more detailed account of the homogeneously catalysed hydrogenation of this reactant, as is in Section 1.8.2.

Table 1.6.1 Values of enantiomeric excess reported for the homogeneously catalysed hydrogenation of various reactants using chiral rhodium complexes.

Reactant	<sup>a</sup> Chiral ligand	e.e./%	Ref.
	( <i>R, R</i> )-DIPAMP	92 ( <i>S</i> )	28
	( <i>S, S</i> )-CHIRAPHOS	100 ( <i>R</i> )	29
	MMPP	71 ( <i>S</i> )	30
	<i>R</i> -CAPP	95 ( <i>R</i> )	30
	<i>R</i> -BINAP	97 ( <i>R</i> )	28
	( <i>R, R</i> )-DIPAMP	90 ( <i>R</i> )	31
	( <i>R, R</i> )-DIPAMP	96 ( <i>R</i> )	32

<sup>a</sup> all chiral ligands were complexed with rhodium; their structures are shown in Figure 1.6.1.

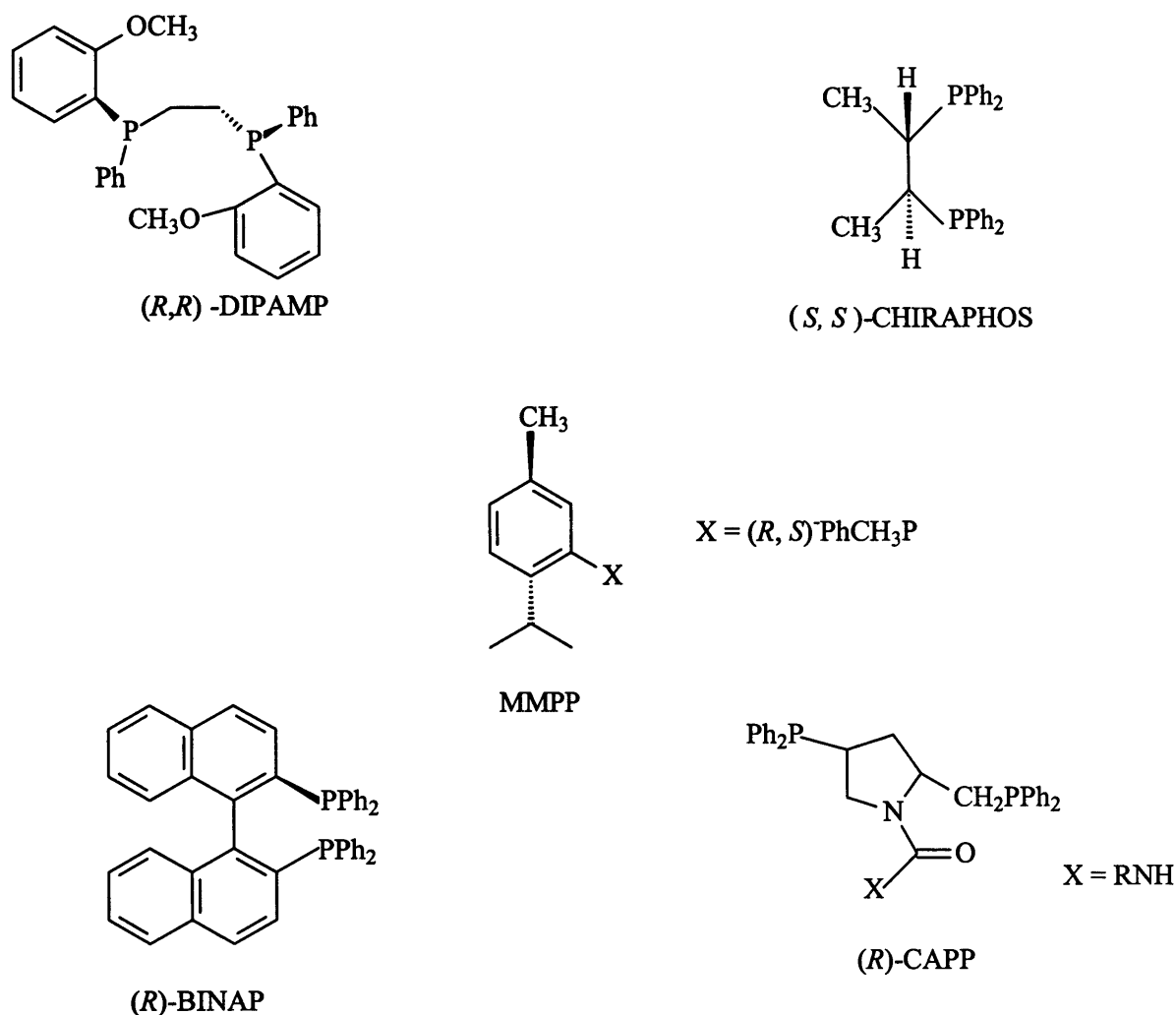
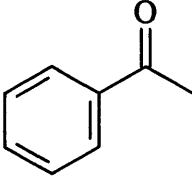
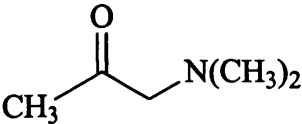
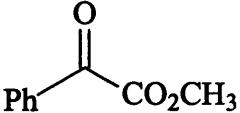
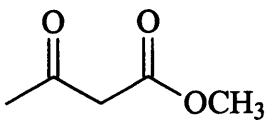


Figure 1.6.1 The structures of the chiral ligands used in the homogeneous catalysis of the reactants shown in Table 1.6.1.

## 1.6.2 Homogeneous Catalysts for Enantioselective Hydrogenation of Carbon-Oxygen Double Bonds

In contrast to  $>\text{C}=\text{C}<$  hydrogenations, rhodium catalysts are less selective and active than ruthenium catalysts towards  $>\text{C}=\text{O}$  reductions. However, it is still necessary for the reactant to possess some functionality  $\alpha$  or  $\beta$  to the carbonyl group for high values of enantiomeric excess to be achieved. Table 1.6.2 illustrates some of the best examples.

Table 1.6.2 Values of enantiomeric excess reported in the enantioselective hydrogenation of various ketonic reactants

Reactant	Catalyst	e.e./%	Ref
	rhodium	80	30
	ruthenium	96	30
	ruthenium	86	31
	ruthenium	99	30

Thus, homogeneous catalysis offers high selectivity for a variety of reactants but the disadvantages associated with this type of catalysis, such as, separation and recycling of the catalyst, is still a problem. As a result there are increasing demands placed on the chemist to develop highly efficient heterogeneous catalysts for these types of reactions.

## 1.7 Heterogeneous Catalysis

Heterogeneous catalysis takes place at a phase boundary when the catalyst and reactant are in different phases. Thus, various routes can be used to achieve enantioselectivity, each incorporating a chiral entity in the reaction system. These are: (i) the catalyst surface may be inherently chiral [33], (ii) the active phase may be supported on a chiral support [34, 35], (iii) a chiral compound (a modifier) may be adsorbed onto an achiral active phase in such a way as to create a local chiral environment at the surface. The most promising strategy from a synthetic point of view, is (iii), the use of metal catalyst



in the presence of a chiral modifier, and this method is discussed in the following sections.

## 1.8 Enantioselective Hydrogenations Catalysed by Alkaloid-Modified Metal Catalysts

For these systems the choice of both modifier and catalyst are important factors in providing the desired hydrogenation product with high enantiomeric excess.

Table 1.8.1 Values of enantiomeric excess achieved for various modifiers in the platinum-catalysed hydrogenation of ethyl pyruvate (EtPy) and methyl pyruvate (MePy).

Modifier	Reactant	e.e./%	Ref
Cinchonidine <sup>a</sup>	EtPy	77 ( <i>R</i> )	37
Cinchonine <sup>a</sup>	EtPy	56 ( <i>S</i> )	37
Dihydrocinchonidine <sup>a</sup>	MePy	82 ( <i>R</i> )	38
Quinine <sup>a</sup>	MePy	61( <i>R</i> )	39
Quinidine <sup>a</sup>	MePy	55( <i>S</i> )	38
Brucine	MePy	20( <i>S</i> )	39, 40
Codeine	MePy	5( <i>S</i> )	41
Oxycodone	MePy	15 ( <i>R</i> )	40

<sup>a</sup> For the structures of the various cinchona alkaloids refer to Section 2.1.3, Figure 2.1.7.

Table 1.8.1 shows a comparison of values of enantiomeric excess achieved with various chiral alkaloid-modifiers in the hydrogenation of pyruvate esters over platinum with Figure 1.8.1 illustrates the differences in the (racemic) hydrogenation of hydroxymethylpyrone using nickel, palladium and platinum in the absence of modifier.

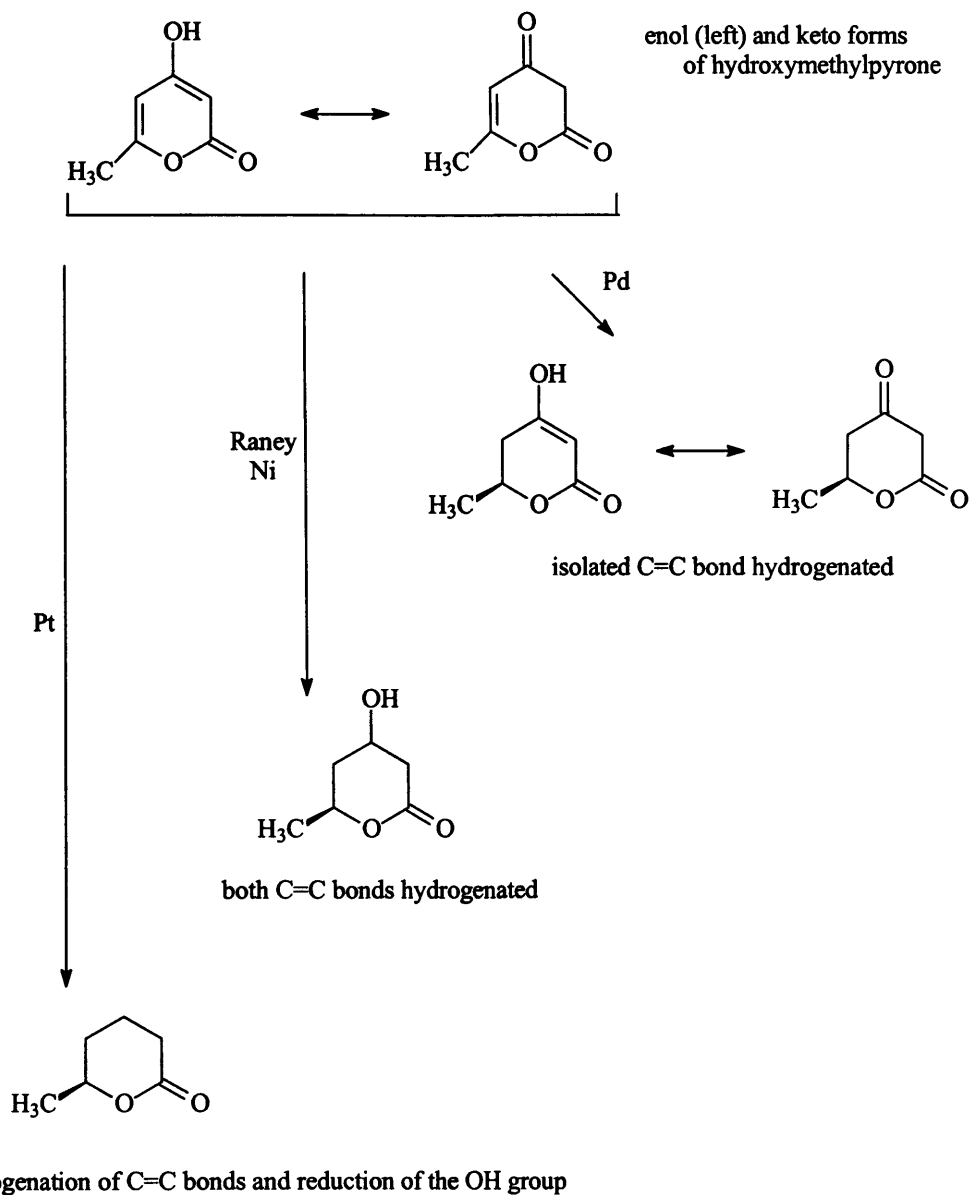


Figure 1.8.1 Differences in catalytic selectivity of nickel, palladium and platinum illustrated by reference to the hydrogenation of hydroxymethylpyrone [39].

As shown in Table 1.8.1, superior values of enantiomeric excess are achieved for reactions using the cinchona alkaloids as opposed to those of the strychnos and morphine alkaloid families [38]. Also, of the cinchona alkaloids, cinchonidine and cinchonine give the best performances, a scenario echoed throughout the literature. As a result the use of cinchonine and more predominantly cinchonidine as chiral modifier for enantioselective reactions is very common. The choice of metal catalyst used in conjunction with these

modifiers is often dependent on the desired hydrogenation product, as highlighted in Figure 1.8.1.

Nickel, palladium and platinum, despite their nominally similar electronic configurations, show several significant differences in their chemistry. It appears that palladium is a more selective hydrogenation catalyst for the reduction of  $>C=C<$  bonds in those olefins which possess more than one reducible functional group and the ease of hydrogenation often decreases in the order  $Pd > Rh > Pt > Ni \gg Ru$  [40]. The differences in activity have been related to fundamental differences in the interaction of hydrogen on these surfaces [41]. Typically, over cinchona-modified platinum systems, a first order dependence of rate on hydrogen pressure is observed whereas, over cinchona-modified palladium systems a half order dependence is observed.

Another difference is the isomerisation activity associated with each metal. Palladium and nickel often promote double bond migration in olefins, a situation not observed over platinum [42]. This can ultimately effect the type of hydrogenation taking place and more importantly the stereochemical outcome of the reaction, this is exemplified in the hydrogenation of ethyl pyruvate over platinum and palladium [43].

The most extensively studied enantioselective metal catalysts are Raney nickel modified by tartaric acid [44], and platinum or palladium modified by cinchona alkaloids. The next sections describe the latter.

### 1.8.1 Platinum Catalysed Enantioselective Hydrogenation

In 1979, Orito *et al.* [45] reported the use of cinchona-modified platinum for the enantioselective hydrogenation of  $\alpha$ -keto esters, especially methyl pyruvate. This system has now been extended to include a broad range of  $\alpha$ -functionalised ketones; some of the most successful applications are presented in Table 1.8.2.

There are several characteristic features of Pt-catalysed enantioselective hydrogenations. The first is that selectivity increases with increasing modifier concentration to a maximum [46, 47] and that this optimum is reached at low concentrations of alkaloid, i.e. at high reactant:modifier molar ratios. This is exemplified in the hydrogenation of ketopantolactone where the highest enantiomeric excess was achieved using a

reactant:modifier molar ratio of 237 000:1 [48]. Another important feature is that the modified reaction is accompanied by a significant increase in rate compared to that of the unmodified reaction.

Table 1.8.2 Examples of high values of enantiomeric excess achieved for the hydrogenation of various reactants over cinchona-modified platinum.

Reactant type	Reactant	Modifier	e.e./%( <i>R</i> )	Reference
$\alpha$ -keto esters	ethyl pyruvate	cinchonidine	97.5	49,50
$\alpha$ -keto acids	4-phenyl-2-oxybutyric acid	O-methyl-cinchonidine	85.0	51
$\alpha$ -diketones	butan-2,3-dione	cinchonidine	90.0	52, 53
$\alpha$ -ketolactones	ketopantolactone	cinchonidine	91.5	48
<sup>a</sup> $\alpha$ -ketoamides	N-2,2,2-trifluoroethylpyruvamide	cinchonidine	60.0	54
$\alpha,\alpha,\alpha$ -trifluoroketones	trifluoroacetophenone	cinchonidine	61.0	55, 56
$\alpha$ -ketoacetals	pyruvaldehyde dimethyl acetal	cinchonidine	96.5	57, 58

<sup>a</sup> both linear and cyclic structures.

In an attempt to understand and hence improve these systems extensive studies have been made regarding the modifier structure and the nature of the reactant-modifier interaction. The model system is the hydrogenation of ethyl pyruvate to the corresponding *R* and *S* lactates over cinchonidine-modified platinum, Figure 1.8.2.

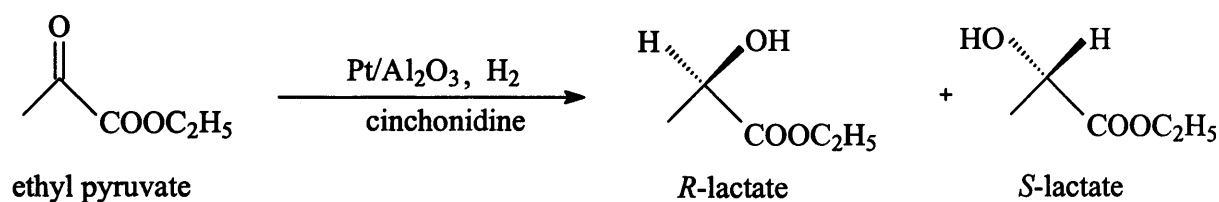


Figure 1.8.2 Ethyl pyruvate hydrogenation over cinchonidine-modified platinum.

## 1.8.1.1 Variation of the modifier structure

Systematic variation of the modifier structure has illuminated the reaction mechanism and has enabled crucial parts of the modifier to be identified. The structure of cinchonidine is shown in Figure 1.8.3, for the general structures of the cinchona alkaloids see Section 2.1.3, Figure 2.1.7.

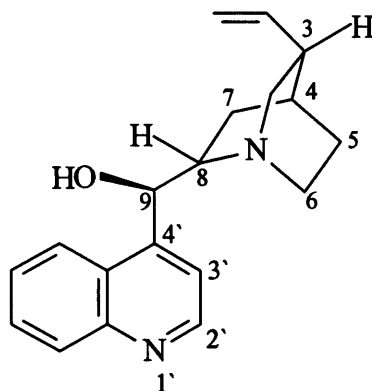


Figure 1.8.3 Structure of cinchonidine

- (i) The absolute configuration at C<sub>8</sub> determines the direction of chiral induction. This is exemplified by the reverse enantiodirecting properties of the cinchona alkaloids which have the reverse configurations at this carbon. In the hydrogenation of ethyl pyruvate over Pt, cinchonidine produces *R*-lactate as the major isomer and cinchonine the *S*-lactate.
- (ii) The basic N-atom of the quinuclidine ring system is required for interaction of the carbonyl O-atom of ethyl pyruvate, (“the docking moiety”). Enantioselectivity is lost when these alkaloids are quaternised at the quinuclidine-N atom [43, 53, 59].
- (iii) The extended aromatic ring system (“the anchoring moiety”) is necessary for the adsorption onto the metal surface. Essentially the anchoring moiety must adsorb onto the Pt surface at two or more adsorption sites. This is the case for both the anthracene, naphthalene and quinoline ring systems and modifiers containing these rings can produce moderate to high enantioselectivities (examples (1), (2) and (3), Figure 1.4.4). However, when the anchoring moiety is reduced to just one aromatic ring system, such as, benzene or pyridine the values of enantiomeric excess drop to zero under otherwise identical conditions, (examples (4) and (5), Figure 1.8.4), [60].

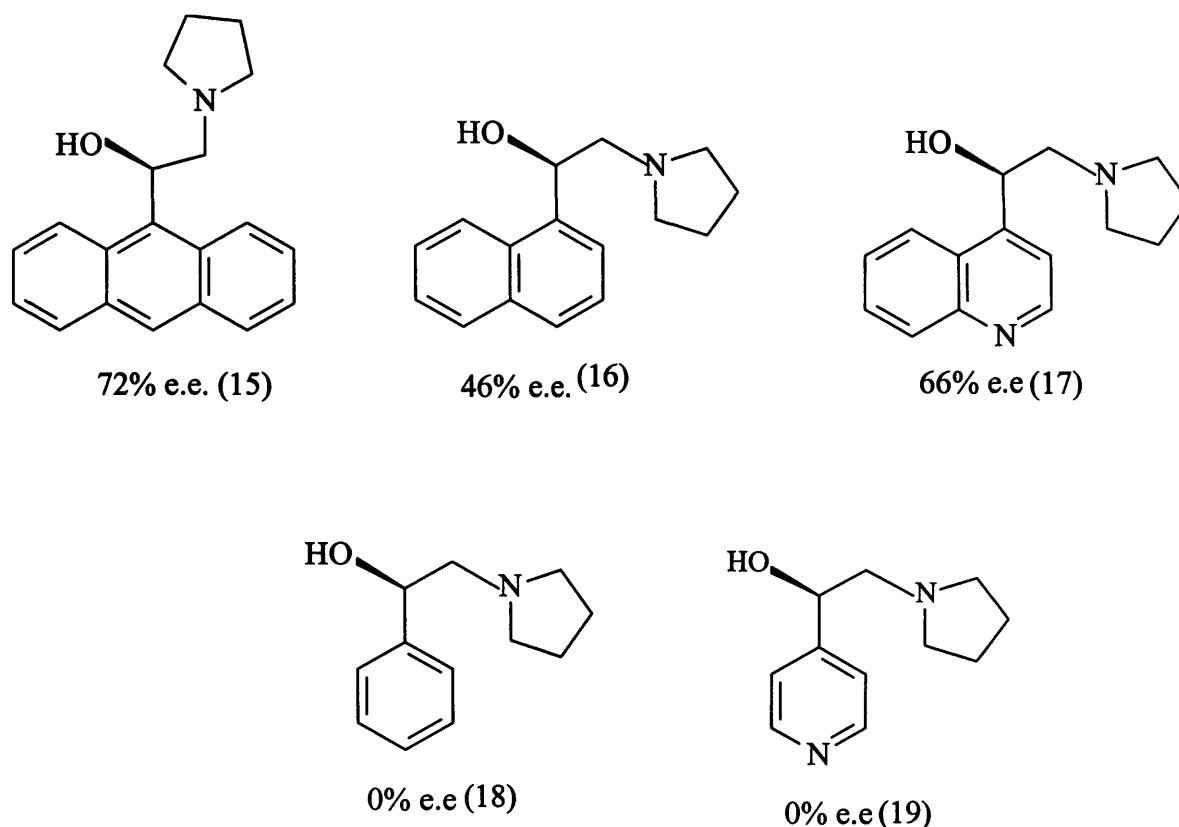


Figure 1.8.4 Values of enantiomeric excess achieved for the hydrogenation of ethyl pyruvate over cinchonidine-modified platinum at 75 bar hydrogen pressure [60, 61].

The exact adsorption mode of these modifiers onto a platinum and palladium surface is still the subject of investigation, although it is generally accepted from spectroscopic investigations that flat parallel  $\pi$ -adsorption through the aromatic ring moiety onto the surface occurs. Other experimental evidence obtained by completing hydrogenations over a range of temperature indicates that the parallel adsorption of the modifier becomes tilted at temperatures above 328 K and that partial hydrogenation of the quinoline moiety also occurs. U.V. analysis determined that thermal desorption of the modifier then takes place [63], producing e.e.s inferior to those at lower temperatures for the same reaction system.

For modifiers which contain a N-heteroatom in the aromatic ring moiety, other adsorption modes may be possible. Baiker *et al.* observed three species interacting

with the metal surface for cinchonidine on platinum and two adsorption modes on palladium. With regards to the palladium surface, the first adsorption mode was the flat parallel  $\pi$ -adsorption and the other involved  $\sigma$ -bonding between the surface and the lone pair of electrons on the quinoline -N atom. They also documented that adsorption of the cinchona alkaloids is weaker on palladium than on platinum and that the relative stability of the species are also different for both metals. The contrasting behaviour for adsorption over palladium and platinum is thought to be due to the different d-orbital diffuseness [62].

- (iv) The substituent groups at C<sub>9</sub> influence the selectivity. O-methylation (OCH<sub>3</sub>) of the OH group has a marginal but positive effect on enantiomeric excess [64], whereas substitution of OH by H (thereby rendering C<sub>9</sub> achiral) reduces but does not eliminate enantioselectivity.

For reactions over cinchona-modified platinum the enantioselection is accompanied by a significant rate enhancement for formation of *both* enantiomers. Wells and Webb quote values of initial rate of about 1290 mmol h<sup>-1</sup> g<sup>-1</sup> for modified (enantioselective) reactions and just 50 mmol h<sup>-1</sup> g<sup>-1</sup> for the unmodified (racemic) reaction [65]. Several mechanistic models have been proposed to account for the rate enhancement and the enantioselective behaviour induced by reaction modifiers. The model most widely accepted is the adsorption model outlined below, although an alternative model, which conceives of the crucial modifier-reactant interaction as occurring in solution, has also been described.

#### 1.8.1.2 The Adsorption Model

In the adsorption model it is proposed that molecules of alkaloid adsorb onto the metal catalyst surface, thereby creating a chiral environment at certain adjacent unoccupied sites. This model is consistent with adsorption isotherms, which indicate that the alkaloid adsorbs on both the Pt active phase and on a silica support [66].

Other evidence obtained from H/D-exchange experiments [67], NEXAFS studies [68] and molecular modelling and various other experiments, such as, ultra high [68] suggests that the alkaloid adsorbs with its aromatic ring system parallel onto the Pt surface. Proposals have been made for an alternative mode of adsorption of the modifier onto the Pt surface via the nitrogen atom of the quinoline moiety [62], but this has to be

confirmed. So far, spectroscopic methods such as NEXAFS indicate adsorption via the aromatic  $\pi$ -electron system as the only important adsorption process.

Originally Wells and co-workers proposed that the adsorption of the alkaloid onto the Pt surface occurred in an ordered non-close-packed arrangement [66]. The shaped ensembles so formed were proposed to be enantiodiscriminant with respect to the adsorption of methyl pyruvate molecules and hence were able to facilitate an enantioselective outcome (The Template Model). However, Wells and Roberts' XPS and LEED studies later showed that high surface coverage of the modifier is achieved but that the adsorption is not ordered.

Modelling of the adsorption of 10,11-dihydrocinchonidine on the (111)-face of a Pt single crystal has been investigated extensively and measurement of the relative conformations in solution has led to an understanding of the various modes the adsorbed cinchona alkaloids can adopt [69].

#### 1.8.1.2A Conformations of Cinchona Alkaloids

Cinchona alkaloid molecules are composed of two relatively rigid moieties, an aliphatic quinuclidine ring and an aromatic quinoline ring, connected via carbon atom numbered 9 (Figure 1.8.3). There is free rotation around the single bonds C<sub>4</sub> and C<sub>9</sub>, C<sub>8</sub> and C<sub>9</sub>, C<sub>3</sub> and C<sub>10</sub> and between C<sub>9</sub> and O. Rotations around these bonds lead to major and minor changes in the conformations of the cinchona alkaloids. Molecular mechanics indicate that there are four states of minimum energy for cinchonine, cinchonidine, quinine and quinidine. Those for cinchonidine are depicted in Figure 1.8.5.

Several NMR techniques [COSY (Correlation Spectroscopy), NOESY (Nuclear Overhauser Enhancement Spectroscopy), NOE-difference and vicinal couplings] are used to assign conformations and to determine the relative occupations of the lowest energy states of the modifier in solution [70]. This is achieved mainly from the NOE's between protons of the quinoline and quinuclidine rings and between the proton pairs of the lowest energy states shown in Figure 1.8.5.

The closed 1 and 2 states are defined as those in which the lone pair on the quinuclidine-N points towards the quinoline ring, whereas the open 3 and 4 states are those which the lone pair points away from the quinoline ring.



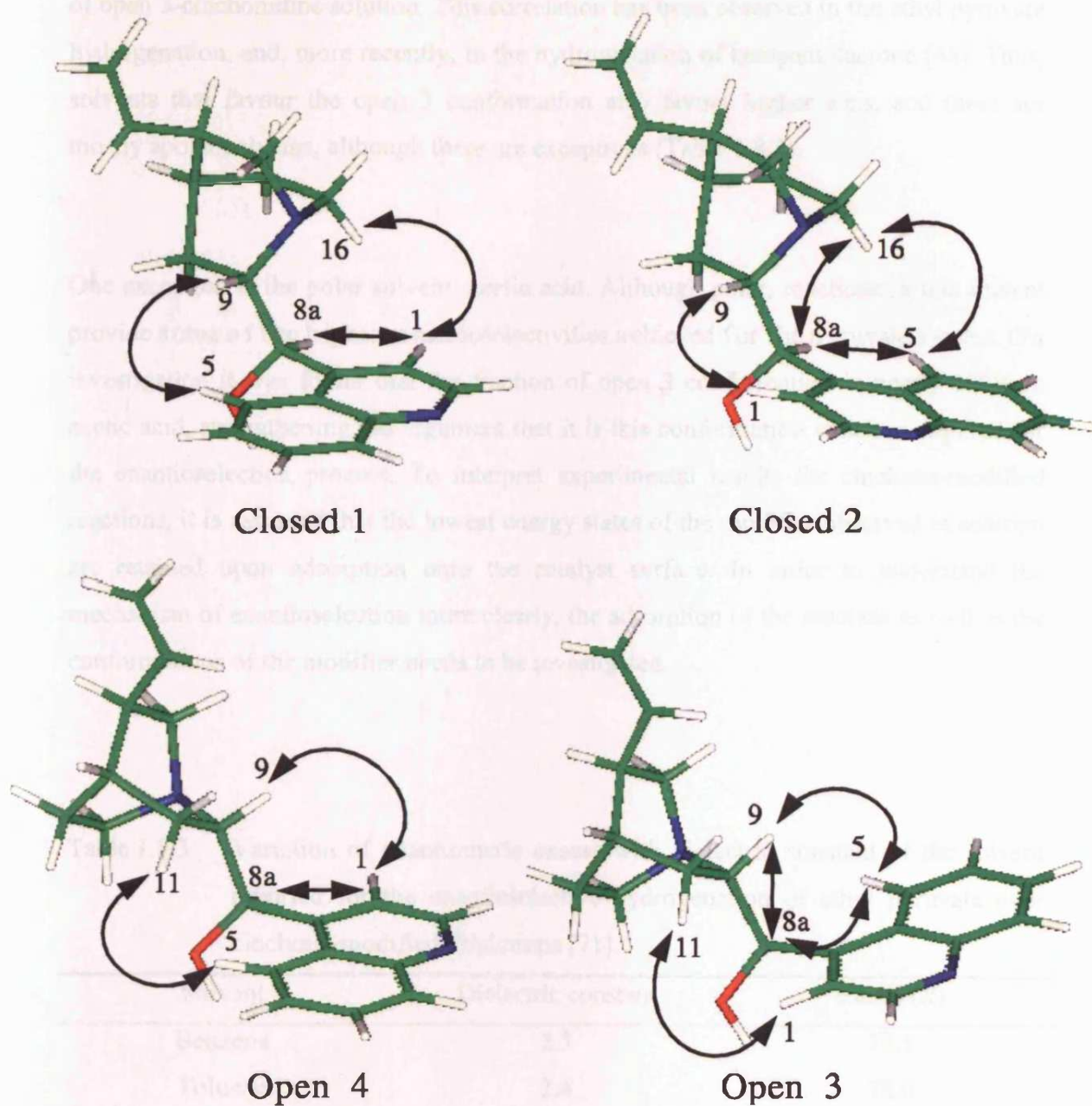


Figure 1.8.5 The four lowest energy conformations of cinchonidine. The pairs of numbered H-atoms are those which are identified, by their interactions, in H NMR spectra.

These techniques show that, for cinchonidine, the open 3 conformer is the most stable in apolar solvents but that, as solvent polarity is increased, the closed 1 and 2 states are stabilised relative to open 3. Ultimately, open 3 becomes the minor conformer.

There is a positive correlation between favourable enantiomeric excess and the fraction of open 3-cinchonidine solution. This correlation has been observed in the ethyl pyruvate hydrogenation, and, more recently, in the hydrogenation of ketopantolactone [48]. Thus, solvents that favour the open 3 conformation also favour higher e.e.s, and these are mostly apolar solvents, although there are exceptions (Table 1.8.3).

One exception is the polar solvent, acetic acid. Although polar, reactions in this solvent provide some of the highest enantioselectivities achieved for the pyruvate system. On investigation it was found that the fraction of open 3 conformation is nearly 100% in acetic acid, strengthening the argument that it is this conformation which is required for the enantioselection process. To interpret experimental results for cinchona-modified reactions, it is assumed that the lowest energy states of the modifier observed in solution are retained upon adsorption onto the catalyst surface. In order to understand the mechanism of enantioselection more clearly, the adsorption of the reactant as well as the conformations of the modifier needs to be investigated.

Table 1.8.3 Variation of enantiomeric excess with dielectric constant of the solvent reported for the enantioselective hydrogenation of ethyl pyruvate over cinchona-modified Pt/alumina [71].

Solvent	Dielectric constant	e.e./% ( <i>R</i> )
Benzene	2.3	78.5
Toluene	2.4	78.0
Acetic acid	6.2	86.5
DCM	8.9	71.5
Butan-2-one	13.4	69.0
Butan-1-ol	17.3	67.5
Acetone	21.0	65.0
Ethanol	25.3	52.5

### 1.8.1.2B Adsorption Mode of Ethyl Pyruvate

Recently, Burgi, Schogl and Baiker [72] reported their findings of an *in situ* XANES study of the adsorption mode of ethyl pyruvate on the surface of Pt (111). These studies demonstrated that the adsorption mode of ethyl pyruvate is influenced by coadsorbed hydrogen on the platinum surface, highlighting the need for more *in situ* spectroscopic methods to be used to investigate all the interactions occurring during the enantioselective process. There was evidence for the co-existence of ethyl pyruvate species in two adsorption modes, one orientated parallel (flat  $\pi$ -bonded) and one perpendicular (lone pair bonded) to the Pt surface, the former being stabilised with respect to the latter. Earlier proposals suggest that it is the flat  $\pi$ -bonded ethyl pyruvate which is relevant in the enantio-differentiating transition state (see below). Despite the parallel and perpendicular forms of pyruvate ester co-existing, the idea that the parallel mode is the most important for the enantioselection, is still feasible. This is because the hydrogen bonding between the quinuclidine nitrogen atom of the modifier and the oxygen atom of the  $\alpha$ -carbonyl of ethyl pyruvate in the enantio-differentiating transition state favours the  $\pi$ -bonded species. Burgi and Baiker suggest that the lone pair bonded species could be a precursor state of the final  $\pi$ -bonded species.

### 1.8.1.2C Mechanism

The conformation of the alkaloid and the adsorption mode of ethyl pyruvate both play a role in determining the enantioselectivity of the reaction, but they are not the only factors which need to be considered.

Kinetic and thermodynamic properties also play a role. When pyruvate adsorbs onto the platinum surface it does so via enantioface pre-*R* or enantioface pre-*S*. Hydrogenation of pre-*R* leads to the formation of *R*-lactate and hydrogenation of pre-*S* leads to *S*-lactate (Figure 1.8.6). If the rate constant for formation of *S*-lactate from pre-*S* ( $k_2$ ) equals the rate constant for formation of *R*-lactate from pre-*R* ( $k_1$ ) then the enantioselection is due only to selective enantioface adsorption and no kinetic influences are operative. If, however, the rate constants for the formation of the two isomers are not equal then the enantioselection is due to both kinetic and thermodynamic properties.

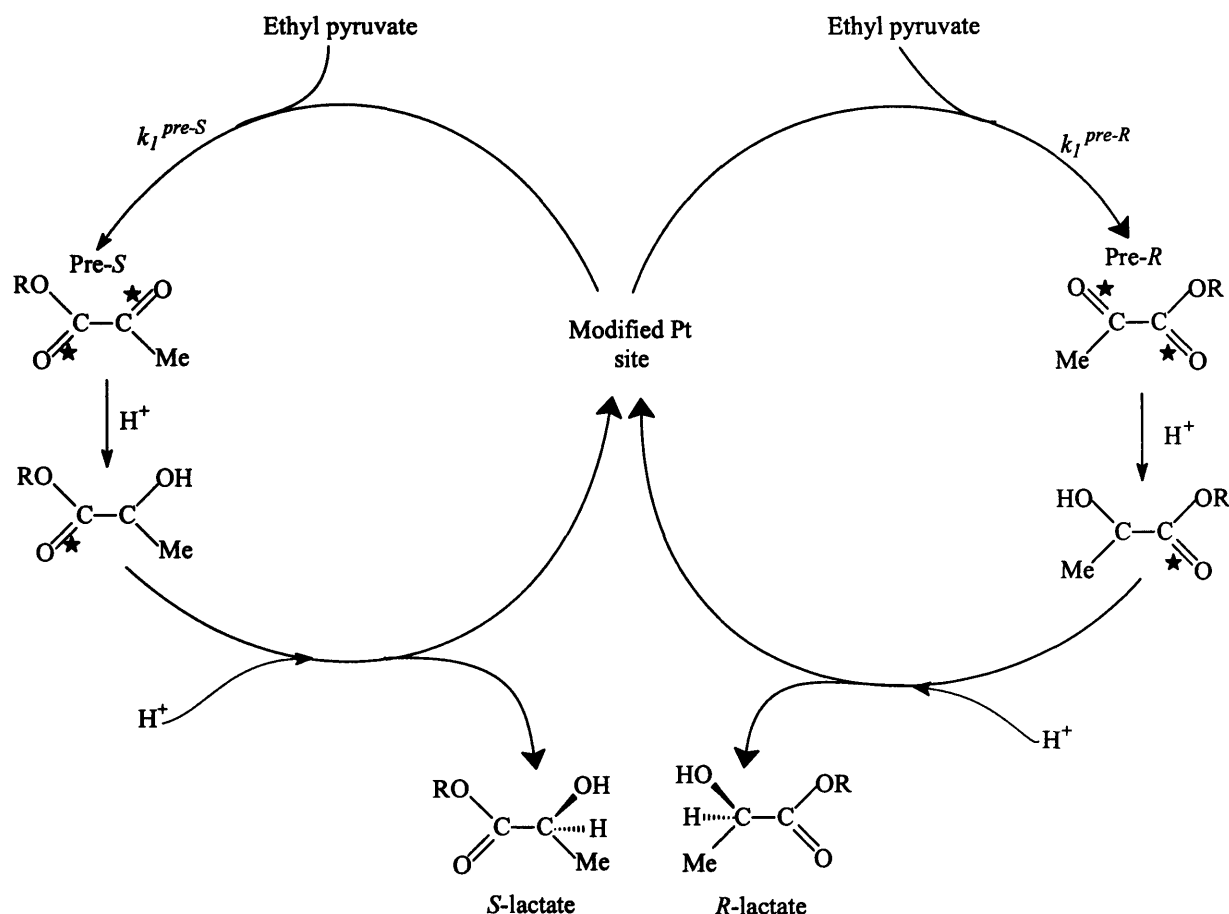
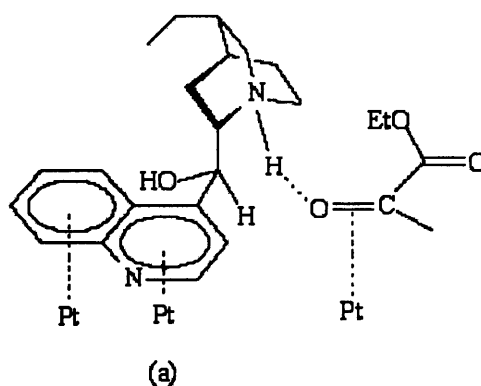


Figure 1.8.6 Schematic representation of ethyl pyruvate hydrogenation

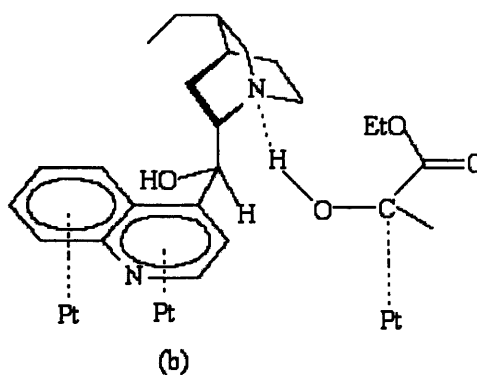
Semi quantitative modelling can provide an estimate of the relative surface coverage of both enantiofacial forms in the adsorbed state and, if no kinetic influences are operating, predict the enantioselectivity of the reaction. Interaction energies have been calculated for reactant-modifier interactions assuming that the aromatic rings of the modifier and the carbonyl groups of the pyruvate are in the same plane [73, 74]. Unfortunately, the metal-reactant interaction energies cannot at present be calculated. From these calculations the cinchonidine:pyruvate ester interactions are less restrictive for enantioface *pre-R* than for *pre-S* resulting in the preferential enantioselective synthesis of *R*-lactate. Similar calculations for cinchonine:pyruvate ester demonstrate that the reverse is true, i.e. the interactions are less restrictive for *pre-S* than *pre-R*, leading to the enantioselection in favour of *S*-lactate.

For the cinchona-modified pyruvate system the enantioselectivity is accompanied by a significant rate enhancement for formation of both enantiomers. Most workers propose that there is a 1:1 interaction between modifier and substrate with the suggestion that the adsorbed modifier stabilises intermediates of the pyruvate ester via the quinuclidine nitrogen. The lifetime of the stabilised intermediate is then increased, and hence its concentration, thereby leading to the observed rate enhancement.

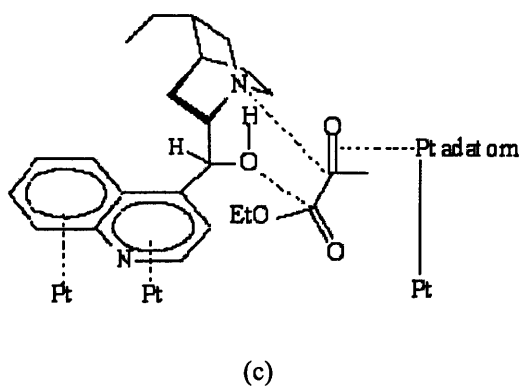
Baiker *et al.* and Schwalm *et al.* [75] proposed that it is the protonated cinchona modifier that interacts with the oxygen of the carbonyl group in ethyl pyruvate, thereby activating ethyl pyruvate for hydrogenation and dictating the enantioface adsorption and hence enantioselectivity. (scheme a).



Wells and co-workers offer a similar interpretation whereby the addition of the first hydrogen to the oxygen of the carbonyl group (the half-hydrogenated state) is stabilised by a hydrogen bond interaction with the nitrogen atom of the quinuclidine system (scheme b) [74].



In contrast, Augustine *et al.* [76] postulated that the cinchona molecule is adsorbed via the  $\pi$ -system of the quinoline close to a platinum ad-atom on which both hydrogen atoms and ethyl pyruvate are adsorbed (scheme c). In this proposal, the quinuclidine-N atom interacts with the keto group, whereas the ester carbonyl of ethyl pyruvate interacts with the lone pair



of the hydroxy group, giving a pseudo-six membered ring conformation. This pseudo-six membered ring was proposed to be relatively stable and dictates the stereochemical outcome of the reaction. These proposals are not unlike and all agree on the basic concepts of the adsorption model, even if the structures of the intermediates are still a matter of dispute.

### 1.8.1.3 The chemical shielding model

A quite different model has been suggested by Margitfalvi and co-workers [77, 78], who have proposed that the modifier in the closed-1 conformation provides an umbrella concave with respect to the reactant so that, as the resulting shielded complex approaches the surface, only one enantioface of the molecule is exposed for adsorption (Figure 1.8.7). Enantioselectivity is then determined by the modifier in solution, and the only function of the catalyst is to act as a source of adsorbed-H.

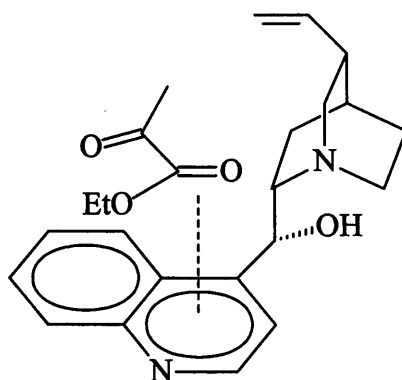


Figure 1.8.7 The adduct between cinchonidine and ethyl pyruvate proposed in the chemical shielding model [78].

The adsorption model and the chemical shielding model may not be mutually exclusive, but may represent two processes that occur to greater or lesser extents during the enantioselective hydrogenation.

## 1.8.2 Palladium Catalysed Reactions

The most frequently studied cinchona-alkaloid modified palladium hydrogenations are those of pyruvate esters and of  $\alpha,\beta$ -unsaturated acids. Oxime hydrogenation has been studied to a much lesser extent.

### 1.8.2.1 Hydrogenation of carbon-oxygen double bonds

Cinchonidine-modified palladium has modest activity towards pyruvate ester hydrogenation and provides enantioselectivity in the opposite sense to that observed for the same reaction over cinchonidine-modified platinum. Evidence from D-tracer studies [79] suggests that this observation is a result of the reactant being hydrogenated in its enol form over palladium as opposed to its keto form over platinum (Figure 1.8.7). In the reaction of methyl pyruvate with  $D_2$ , the methyl group adjacent to the  $\alpha$ -keto group underwent exchange so that the product was  $CX_3CX(OX)COOCH_3$ , where X = H or D. This indicated dissociative adsorption of the H atom from the methyl group followed by rehydrogenation to give the enol. The hydrogenation was then that of a carbon-carbon double bond rather than of a keto group.

#### 1.8.2.1A Mechanism

Hydrogenation of intermediate B (Figure 1.8.8) was proposed to be the rate-determining step in this mechanism. Furthermore, different solvents affect the formation of the enol, and hence the observed e.e is also affected.

Figure 1.8.8 shows the formation of the enol as intermediate C and its conversion in a kinetically fast process to *R*-lactate. The experimentally observed preferential formation of *S*-lactate was interpreted as follows.

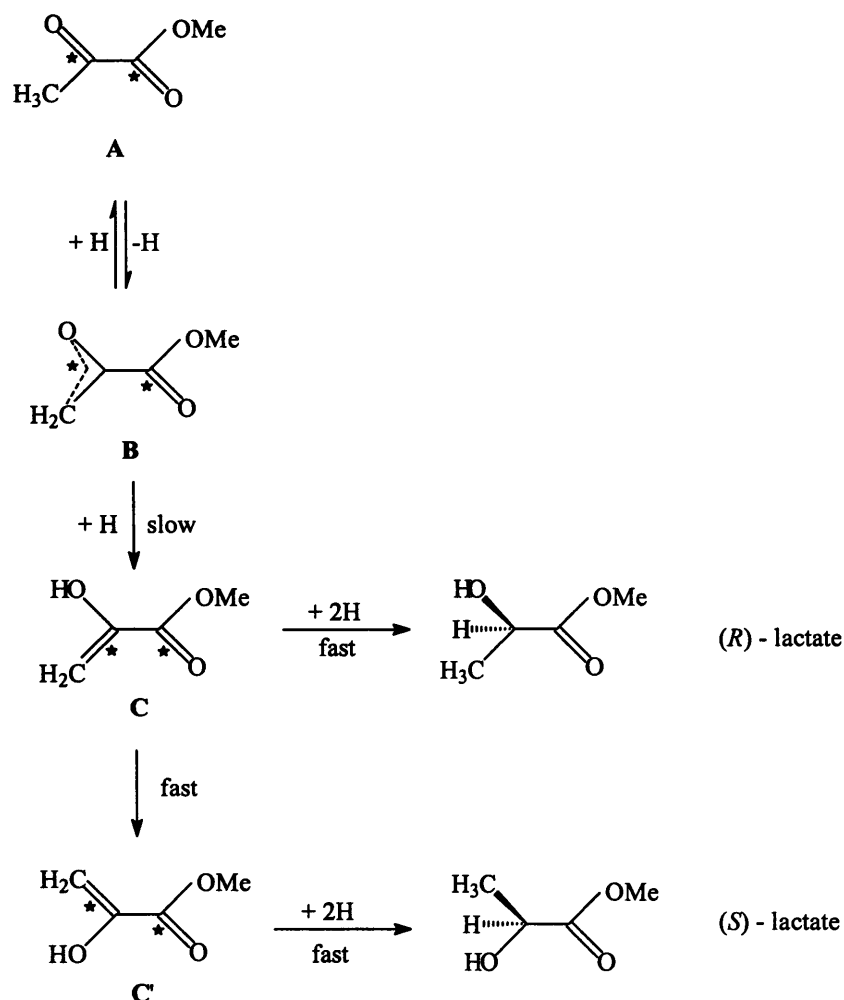


Figure 1.8.8 Mechanism for the enantioselective hydrogenation of pyruvate ester over cinchonidine-modified palladium, (adapted from Wells and co-workers. [79]).

Intermediate **C** experiences considerable intramolecular repulsion due to the syn-configuration of the adsorbed  $>\text{C}=\text{C}<$  and  $>\text{C}=\text{O}$  groups. This repulsion is relieved by conversion of **C** to **C'**, and subsequent hydrogenation of **C'** yields *S*-lactate as product. Thus, the observed preference for *S*-product was interpreted provided the conversion of **C** to **C'** is somewhat faster than conversion of **C** to *R*-lactate. The enantiomeric excess achieved in this reaction was normally low, typically 20%, and showed poor reproducibility, which was not inconsistent with a mechanism involving competition between kinetically fast processes.



The opposite enantiodirecting effect observed for pyruvate ester hydrogenation over cinchonidine-modified palladium is not the only difference between the two metals. Table 1.8.4 highlights some of the main general differences for enantioselective hydrogenations conducted over cinchona-modified palladium and platinum.

Table 1.8.4 Differences between enantioselective hydrogenations conducted over cinchona-modified palladium and platinum

Platinum catalysed enantioselective hydrogenations	Palladium catalysed enantioselective hydrogenations
1. Optimum enantioselectivity achieved with small additions of modifier.	1. Optimum enantioselectivity achieved using larger quantities of modifier.
2. Substantial rate enhancement for modified reactions.	2. No rate enhancement for modified reactions, the fastest rates are observed for racemic hydrogenation.
3. Higher values of enantiomeric excess are observed for reactions conducted in solvents having lower dielectric constants.	3. Higher values of enantiomeric excess are observed for reactions conducted in solvents having higher dielectric constants.
4. In general: cinchonidine-modified hydrogenations provide an excess of the <i>R</i> -enantiomer and cinchonine-modified hydrogenations an excess of the <i>S</i> -enantiomer.	4. In general: cinchonidine-modified hydrogenations provide an excess of the <i>S</i> -enantiomer and cinchonine-modified hydrogenations an excess of the <i>R</i> -enantiomer.
5. Good performance in the enantioselective reduction of $>C=O$ functions.	5. Good performance in the enantioselective reduction of $>C=C<$ function

The most striking difference between the enantioselective hydrogenations over palladium by comparison with those over platinum is the lack of any rate enhancement. For these systems the rate decreases with increasing amounts of modifier, such that the racemic reaction occurring at the unmodified catalyst surface remains a significant reaction. This may be the reason why enantioselective hydrogenations over palladium require much larger amounts of modifier to obtain the highest enantioselectivity. Perhaps the modifier

acts as a catalyst poison, reducing the number of unmodified sites available for racemic reaction.

### 1.8.2.2 Hydrogenations of carbon-carbon double bonds

Cinchona-modified palladium is typically used for the enantioselective hydrogenation of carbon-carbon double bonds and this is well documented in the literature. Figure 1.8.9 illustrates some of the highest enantioselectivities achieved in  $>C=C<$  hydrogenations catalysed by modified-Pd.

The enantioselective hydrogenation of 4-hydroxy-6-methyl-2-pyrone (Figure 1.8.9, **(V)**) over cinchona-modified Pd/alumina provides one of the highest enantioselectivities achieved to date for such systems. Initially, lower values of enantiomeric excess were achieved for this reaction due to the slow rate and the limited stability of the reaction modifier under the experimental conditions. This is partly due to the fact that palladium is more active for the partial hydrogenation of the aromatic ring system of the cinchona alkaloids than the other Pt group metals [86]. This ultimately affects the adsorption of the cinchona alkaloid and its effectiveness in achieving enantioselection. Baiker resolved this problem by starting the reaction with small amounts of modifier (between 2.5 and 10 mg) and subsequently dosing minute quantities of modifier ( $0.25 - 1.0 \text{ mg h}^{-1}$ ) to the system as the reaction proceeded. This had the effect of optimising the concentration of modifier on the Pd surface and maintained higher values of enantiomeric excess.

With regards to  $\alpha,\beta$ -unsaturated acids the highest enantioselectivity was reported by Nitta and Kobiro in the hydrogenation of (E)- $\alpha$ -phenylcinnamic acid over cinchonidine-modified Pd (Figure 1.8.9, **(I)**). Performance for this reaction was effected by the polarity of the solvent, catalyst dispersion and mass of modifier, such that enantioselectivity increased with increasing dielectric constant of the solvent in the order: DMF > MeOH > EtOH > PrOH > BuOH > THF > ethyl acetate. Optimum Pd dispersion was 61% ( $\sim 2.7 \text{ nm}$  Pd particle size) achieved using 5% Pd/TiO<sub>2</sub>. The optimum modifier concentration was  $6.0 \text{ mmol dm}^{-3}$  [80 -82, 87].

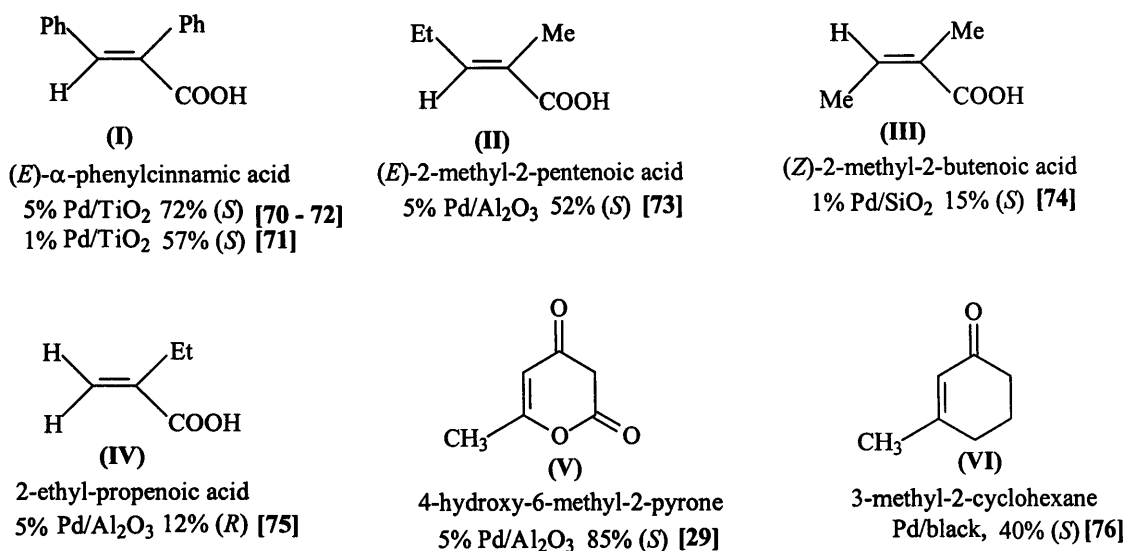


Figure 1.8.9 Structures of some unsaturated compounds with values of enantiomeric excess achieved when hydrogenated over alkaloid-modified palladium. [For (I) – (V) alkaloid = cinchonidine, for (VI) alkaloid = dihydrovinpocetine (a vinca alkaloid).

Hydrogenation of  $\alpha,\beta$ -unsaturated acids that contain no aromaticity afford inferior values of enantiomeric excess although in most instances the sense of the enantioselectivity observed is the same, i.e., cinchonidine provides an excess of the *S*-enantiomer and cinchonine provides an excess of the *R*-enantiomer. However, one exception where the opposite sense in enantioselectivity has been observed is the hydrogenation of (*E*)-2-ethyl-2-propenoic acid in which the carbon-carbon double bond is terminal (Figure 1.8.9 (IV)). Under the experimental conditions used double bond migration occurred to form tiglic acid ((*E*)-2-methyl-2-butenoic acid). This hydrogenated preferentially in favour of the *R*-enantiomer. The low enantioselectivity (12% (*R*)) observed for this system and for those of other alkenoic acids may be a result of competing hydrogenations of reactant isomers occurring under the experimental conditions.

Enantioselective hydrogenation of the esters of unsaturated acids results in racemic products, as does the hydrogenation of unsaturated acids over Pd modified with N-

methyl quaternised cinchonine or cinchonidine. This experimental evidence suggests that the fundamental interaction between reactant and modifier required for enantioselection, occurs via the OH group of the reactant and the quinuclidine-N of the modifier. Two models proposed for this interaction are outlined below.

It is important to note that misleading results can be observed when N-allyl and N-benzyl quaternised forms of cinchonidine or cinchonine are used to demonstrate the importance of the quinuclidine-N in enantioselective processes over Pd. One such result was reported for the hydrogenation of (E)- $\alpha$ -phenylcinnamic acid over Pd/TiO<sub>2</sub> modified with N-benzyl cinchonidinium chloride [87]. The authors reported an enantiomeric excess of 57%(S) for reactions using this modifier as compared to 61%(S) achieved with cinchonidine, under otherwise identical conditions. This suggested that the quinuclidine-N was not involved in the interaction between reactant and modifier. On the contrary, when N-methyl quaternised cinchonidine was used a complete loss of enantioselectivity was observed. It was later proposed that under experimental conditions debenylation of N-benzyl cinchonidine was occurring resulting in the formation of cinchonidine hydrochloride which is a known active modifier.

#### 1.8.2.2A Mechanism

##### *The monomer-modifier interaction model*

This model suggests that there is a 1:1 H-bonding interaction between the OH of the acid and the quinuclidine-N of the adsorbed modifier (assumed to be in the open 3 conformation, see Figure 1.8.5). Simple energy profiles of this interaction show that for cinchonidine and reactant a lower energy state is observed for the precursor which would give the *S*-product on hydrogenation, compared to that which would give the *R*-product. Likewise, for cinchonine as modifier, the lowest energy state is observed for the precursor

which yields the *R*-product on hydrogenation. This interprets the sense of enantioselectivities observed for reactions over cinchonidine-modified and cinchonine-modified Pd.

*The dimer-modifier interaction model*

The monomer-modifier interaction model is simple but fails to take into account the possible interaction of the modifier with dimers of these acids, which exist in equilibrium with the monomers. The extent of dimerisation is solvent dependant and is greater in apolar media. Evidence accumulated by Baiker in respect of the hydrogenation of (Z)-2-methyl-2-butenoic acid (tiglic acid) suggest that the dimer-modifier interaction is not just with the quinuclidine-N of the modifier but also with the OH group at C<sub>9</sub> [88]. This proposal was tested by conducting hydrogenations in toluene over dihydrocinchonidine-modified Pd/alumina in the presence of the strong bulky base DBU (1, 8-diazabicyclo[5.4.0]undec-7-ene). DBU is able to complex with the dimer to form DBU(acid)<sub>2</sub>. It was noted that enantioselectivity was unaffected when the concentration of DBU was such that some free acid dimers were still available in solution, but when sufficient base was added so that this was not the case then the enantioselectivity dropped to zero. Furthermore, conversion of the C<sub>9</sub>OH group in cinchonidine to C<sub>9</sub>-OR (where R = methyl, allyl or benzyl) also destroyed the enantioselectivity. These observations together with other theoretical calculations indicate that there are three important hydrogen bond interactions necessary to provide enantioselectivity for tiglic acid hydrogenation over cinchona-modified Pd. These are between: (i) acid monomers to form dimers, (ii) the carboxyl-H of an acid molecule and the quinuclidine-N and (iii) the C<sub>9</sub>-OH and the carbonyl-O of the other acid molecule in the dimer (Figure 1.8.10). Enantioselective hydrogenation of the >C=C< double bond of the acid molecule which interacts with the quinuclidine-N then occurs.

The interactions shown in the model below (Figure 1.8.10) may be favourable for the smaller alkenoic acids but not as favourable for bulkier reactants, such as (E)- $\alpha$ -phenylcinnamic acid and 4-hydroxy-6-methyl-2-pyrone, where the interactions are subject to a greater degree of steric hindrance. For these reactants the monomer-modifier interaction may be more applicable, a factor which is exemplified by higher enantioselectivities being observed for reactions conducted in more polar solvents, where the monomer dominates over the dimer.

For enantioselective reactions over cinchona-modified palladium no acceleration in reaction rate is observed. This may be a result of the bond undergoing not being directly

involved in the interaction with the quinuclidine-N, and so no stabilisation of intermediates occurs during the hydrogenation process.

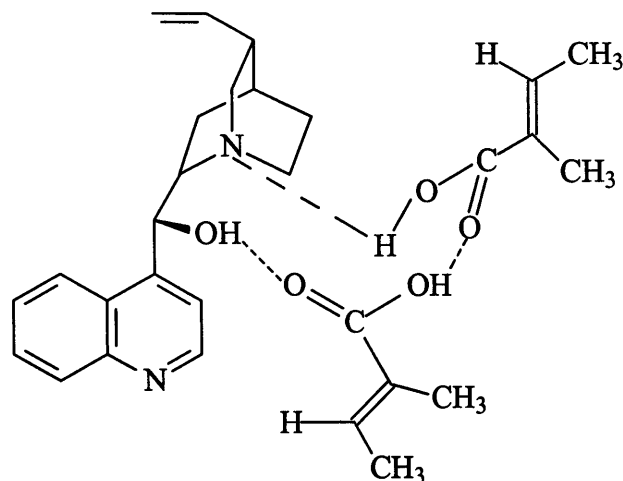


Figure 1.8.10 Representation of the tiglic acid dimer bonded to the C<sub>9</sub>-OH and the protonated quinuclidine-N of cinchonidine.

### 1.8.2.3 Hydrogenations of carbon-nitrogen double bonds

Enantioselective hydrogenation of carbon-nitrogen double bonds over cinchona-modified metals has received little attention compared to the other reactions described above. Baiker *et al.* recently reported their findings for the combined hydrogenation-hydrogenolysis of pyruvic acid oxime over Pd/alumina (Figure 1.8.11) [89]. Values of the enantiomeric excess achieved were small and particularly susceptible to changes in both modifier concentration and solvent.

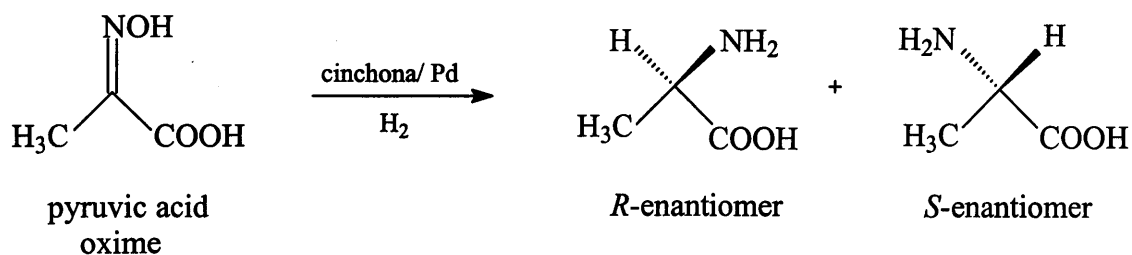


Figure 1.8.11 Enantioselective hydrogenation of pyruvic acid oxime

The authors reported the sense in enantioselectivity changing from 4.2(*R*) to 1.7(*S*) for cinchonidine-modified hydrogenations conducted in ethanol and acetic acid respectively. Likewise, another inversion in enantioselectivity was observed with modifier concentration such that, at low concentrations (modifier:oxime molar ratio =  $10^{-4}$  -  $10^{-2}$ ) an excess of the *S*-enantiomer was observed (e.e.=1 – 5% ) whereas at higher concentrations (molar ratio =  $10^{-1}$  –  $10^0$ ) an excess of the *R*-enantiomer, (e.e. = 2 – 14 % respectively). Another important feature of this system was that, under a modifier:oxime molar ratio of 1:1 both cinchonine and cinchonidine afforded an excess of the same enantiomer.

Under the same experimental conditions ephedrine was used as modifier and afforded the highest enantioselectivity reported to date of 26%(*S*).

#### 1.8.2.3A Mechanism

Crystal structures have been obtained for 1:1 cinchonidine:oxime adducts and these provide models for the interactions occurring between reactant and modifier in the adsorbed state. It was found that the interaction was complex and involved CD-oxime chains in an extensive hydrogen bond network. First, oxime molecules are connected to each other by H-bonds between the hydroxyl and carboxyl functional groups. Second, the carboxyl OH group is connected to the hydroxyl group of cinchonidine and the basic nitrogen of the next cinchonidine molecule in the chain (Figure 1.8.12). An analogous crystal structure was observed for the ephedrine:oxime adduct.

It is clear from the representation below that both the OH group at C<sub>9</sub> and the quinuclidine-N of the modifier are involved in the interaction with pyruvic acid oxime. However, it is unclear whether both are actually required for enantioselection to take place whereas, in the hydrogenation of tiglic acid, substitution of the OH group at C<sub>9</sub> completely destroyed the enantioselectivity as did quaternisation of the quinuclidine-N.

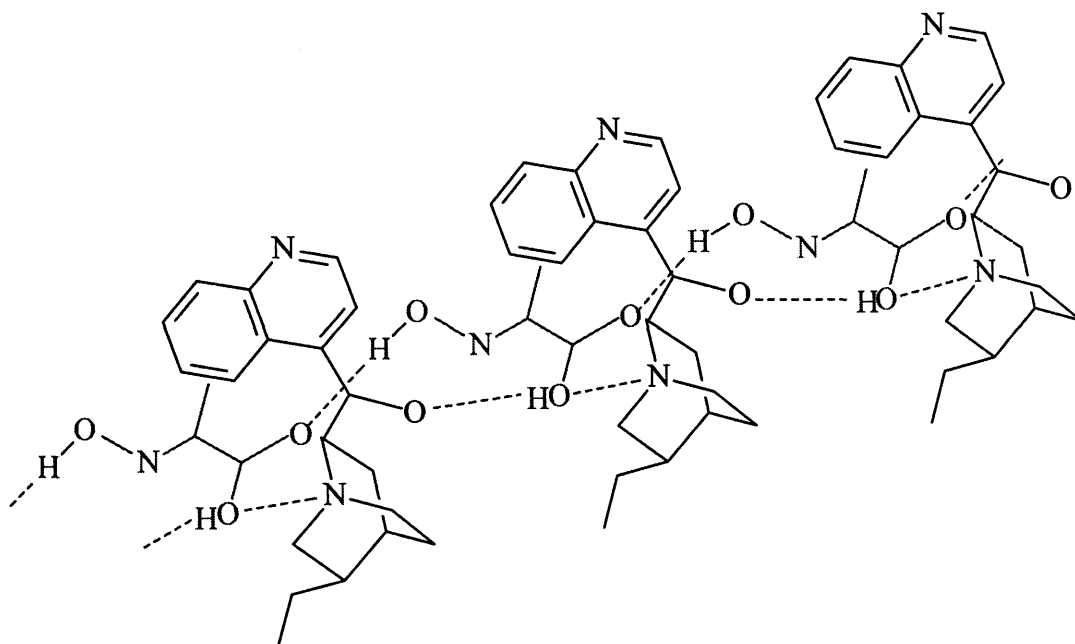


Figure 1.8.12 Part of the chain in the cinchonidine-oxime structure. Adapted from Baiker *et al.* [89].

In contrast to these proposals Bartok *et al.* recently reported that for the hydrogenation of the  $>C=N<$  bond in methyl 1-pyrroline-2-carboxylate the important interaction required for enantioselection was that between the reactant molecule and the OH group at C<sub>9</sub> of cinchonidine [90]. Reactions completed with various quaternised cinchonidinium salts, including the methyl cinchonidinium salt, showed no loss in enantioselectivity, whereas, reactions where the OH group at C<sub>9</sub> was replaced with OMe showed no enantioselectivity.

Enantioselective hydrogenation of pyruvic acid oxime over cinchona-modified Pd is one way to produce the desired chiral amino acid, although the values of enantiomeric excess achieved are very low. These enantioselectivities can be dramatically improved when a diastereoselective route is used. These hydrogenations take place in three parts, first the  $\alpha$ -keto acid is caused to undergo reductive amination with an optically active amine, and the product is then hydrogenated over Pd/C before undergoing hydrogenolysis to release the amino acid (Figure 1.8.13). Values of enantiomeric excess between 12 – 81% have been reported in the final product.



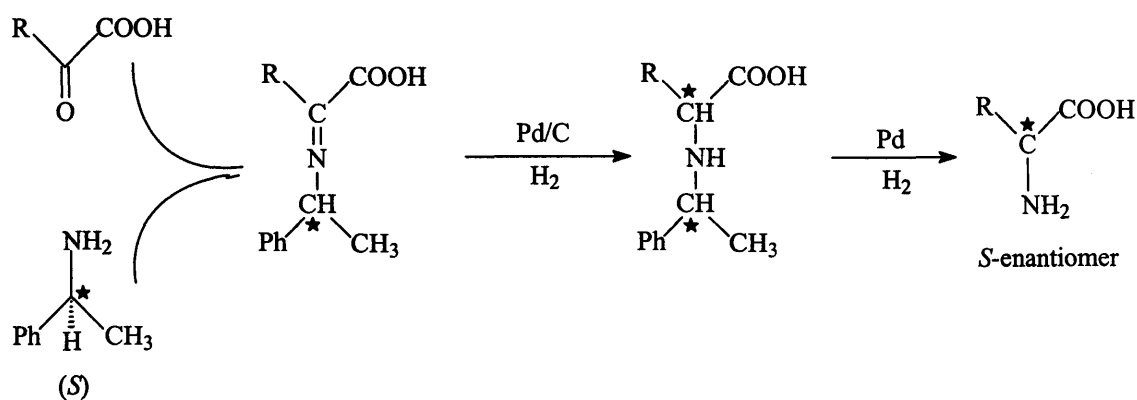


Figure 1.8.13 Diastereoselective route for achieving chiral amino acids from  $\alpha$ -keto acids

Diastereoselective hydrogenation is beyond the scope of this review and will not be discussed further.

## 1.9 The Target Reaction

The target reaction for this investigation, is the enantioselective hydrogenation of *N*-acetyl dehydrophenylalanine (NADPME) to the corresponding *R*- and *S*-enantiomers of *N*-acetyl phenylalanine methyl ester (Figure 1.8.1).

Many pharmaceutically active substances, such as L-DOPA, are amino acids. Synthesising natural and non-natural amino acids in high enantiomeric purity is a challenging problem for modern chemistry. The enantioselective hydrogenation of enamides, such as, NADPME is often the crucial step in amino acid synthesis. To date there are several homogeneous hydrogenation catalysts that can catalyse this reaction efficiently and these are outlined in Section 1.8.1. However, increasing demands are placed on the chemist to develop highly efficient heterogeneous catalysts for these reactions, so that the advantages this offers can be exploited

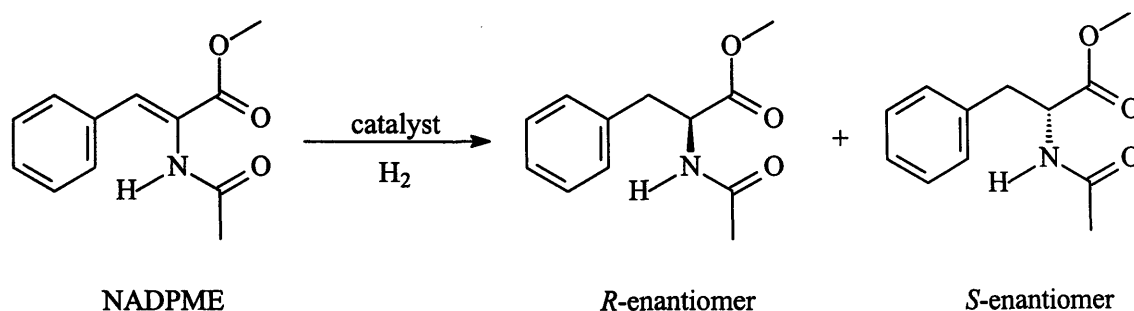


Figure 1.9.1 The hydrogenation of *N*-acetyl dehydrophenylalanine methyl ester (NADPME) to the corresponding *R*- and *S*-enantiomers of *N*-acetyl phenylalanine methyl ester.

### 1.9.1 Homogeneous Catalysis of NADPME

There are many homogeneous catalysts which are able to hydrogenate NADPME and related derivatives with high enantiomeric excess. Table 1.9.1 shows some of the best applications of homogeneous catalysts for the hydrogenation of NADPME and the free acid, *N*-acetyl dehydrophenylalanine (NADP).

Table 1.9.1 Values of enantiomeric excess achieved for NADP and NADPME hydrogenation using various chiral ligands

Chiral ligand	Reactant	e.e./%	Reference
CHIRAPHOS	NADP	97	64
BINAP	NADPME	92	65, 66
DIPAMP	NADPME	90	93
DIPAMP	NADP	96	92 – 96
DuPHOS	NADP	99	93, 95
DuPHOS	NADPME	99	93, 94
PYRPHOS	NADPME	99	97

The chiral ligands in Table 1.9.1 can either complexed with rhodium or ruthenium with very few references in the literature of the use of other transition metals. For the selective hydrogenation of dehydroamino acids rhodium is the preferred choice giving slightly better performances [66, 92].

With the exception of reactions using DuPHOS as the chiral ligand, hydrogenation of the E and Z isomers of the reactants shown in Table 1.9.1 are done so at different rates, with the Z-isomer being hydrogenated more selectively [94,95].

### 1.9.1.1 Mechanism

The mechanism shown in Figure 1.9.2 is for the hydrogenation of NADPME catalysed by Rh-DIPAMP or Rh-CHIRAPHOS complexes. Halpern and Landis described the coordination of NADPME to the activated complex and its further reaction in two different cycles: the 'Minor Manifold' and the 'Major Manifold' [93].

Catalytic hydrogenations are undertaken either using a catalyst precursor or with an in situ prepared catalyst. Common catalyst precursors are cyclooctadiene (COD) or norbornadiene (NBD) complexes of Rh. This complex also contains the chelating chiral ligand and a non-co-ordinating anion, such as,  $\text{BF}_4^-$  or  $\text{SF}_6^-$ . First the diene precursor is hydrogenated forming molecules which have a lower affinity to Rh than the educts and can be replaced by two co-ordinating solvent molecules. This bis-solvent complex is the catalytically active species shown as **(I)** in Figure 1.4.2. NADPME then displaces the solvent molecules and chelates with Rh side on with its double bond and with one electron pair of the O of its amido group (complex **(II)** and **(II')**, Figure 1.5.2). Two complexes are formed which upon hydrogenation will result in the preferential formation of *R*- or *S*-products. Of these two complexes Pre-*R* is more stable and this exists predominantly (complex **(II)** in the Major Manifold). Reaction steps thus far are reversible and it is the oxidative addition of  $\text{H}_2$  which is the first irreversible step in the cycle and therefore dictates the enantioselection. The major reactant complex **(III)** reacts far more slowly with  $\text{H}_2$  than the minor reactant complex **(III')** and for this reason the major reactant complex forms the minor product. The final step in the cycle is reaction of

the dihydro complex (III) and (IV) with the hydrido alkyl complex which eliminates the product and rebuilds the bis-solvent complex (I), and so the whole cycle can start again.

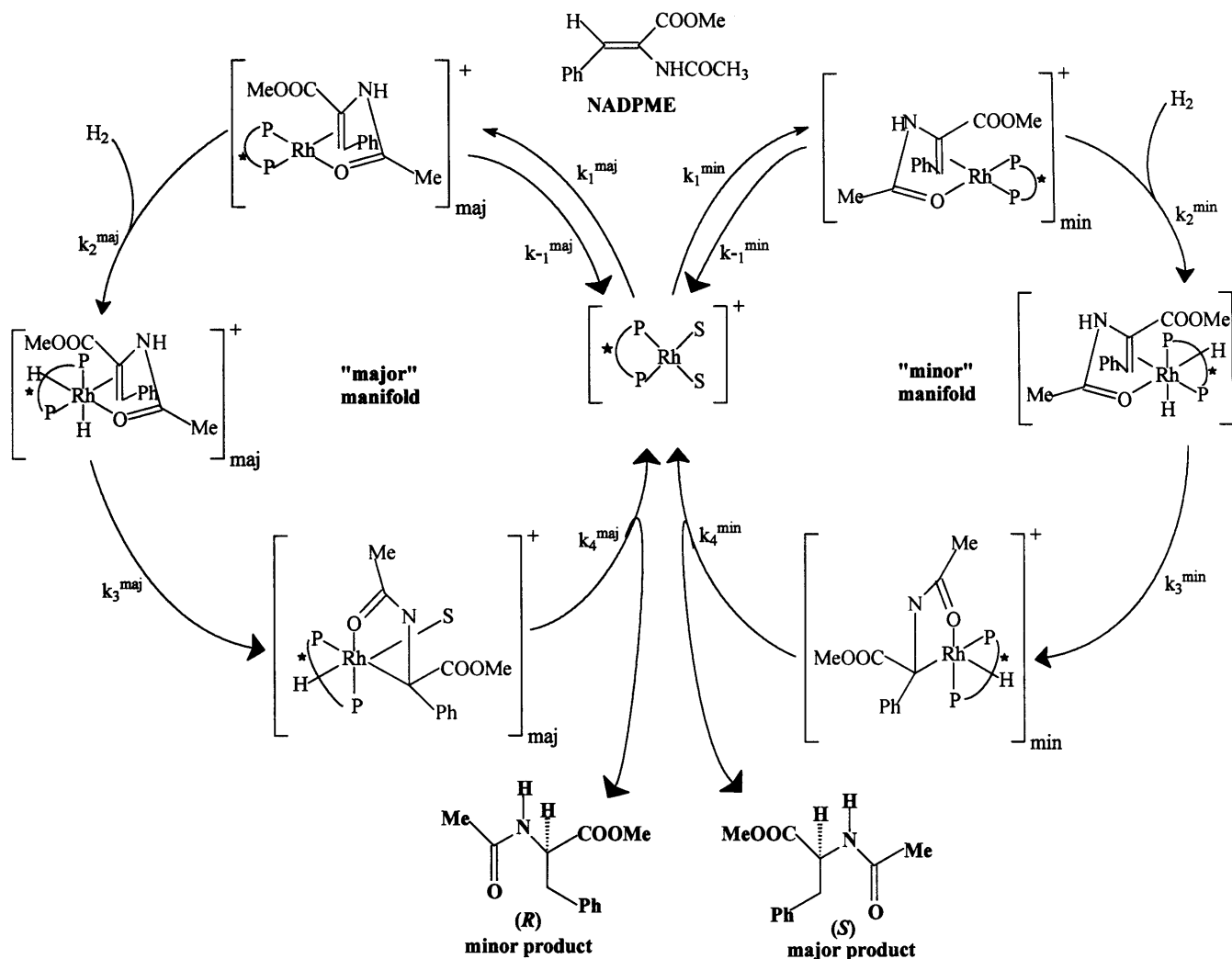


Figure 1.9.2 Schematic representation of the homogeneously catalysed enantioselective hydrogenation of NADPME

In conclusion the target reaction can be successfully hydrogenated using various homogeneous catalysts giving extremely high values of enantiomeric excess. However due to the advantages that heterogeneous catalysts offers an alternative route for producing these amino acids precursors is of considerable importance

## 1.9.2 Heterogeneous Catalysis of NADPME

Heterogeneous catalysis, although used predominantly in processes involved in industrial chemistry, is still in the early stages of progress in the fine chemical industry. Competing with the performance of homogeneous catalysts has been difficult but not unachievable. There are now several heterogeneous catalysts in use, and in the process of being developed for use in producing optically active compounds. One of the most promising strategies in this area is the use of modified-metal catalysts, such as platinum or palladium, modified with cinchona alkaloids or nickel modified with tartaric acid. Although these applications have been quite substrate specific, there is in recent years a broadening of reactants, which can be produced this way. The most notorious are the  $\alpha$ - and  $\beta$ -keto esters and to a lesser extent,  $\alpha,\beta$ -unsaturated acids. Such reactants can be enantioselectively hydrogenated, with values of enantiomeric excess greater than 85%. However,  $\alpha,\beta$ -unsaturated esters, to date, show no enantioselectivity via this route. Fundamentally, NADPME is an  $\alpha,\beta$ -unsaturated ester which has been re-functionalised with a *N*-acetyl group. The objectives of the present investigation are outlined below in Section 1.9.3.

## 1.9.3 Objectives of the Present Investigation

The objectives of this investigation were:

- (1) To devise a heterogeneous catalytic system for the enantioselective hydrogenation of NADPME.
- (2) To investigate the mechanism of this enantioselective reaction.
- (3) To explore the role of the modifier in determining the sense of the enantioselectivity.
- (4) To investigate the hydrogenation of related compounds so as to understand NADPME hydrogenation in context.
- (5) To identify the factors that limit enantioselectivity and reaction rate.

## 1.9 References

1. Handbook of Heterogeneous Catalysis, (Eds. G. Ertl, H. Knozinger, J. Weitkamp), VCH, Weinheim (2003), Volume 4 and 5, pp1559 – 2122 and 2123 – 2447.
2. P. Kukula, R. Prins, *Topics in Catal.*, **25** (2003) 29.
3. M. Besson, C. Pinel, *Topics in Catal.*, **25** (2003) 43.
4. G. C. Bond in 'Heterogeneous Catalysis: Principles and Applications', Oxford, 1974, (a) p.12, (b) p.6, (c) p.9, (d) p.20.
5. R. Hughes, 'Deactivation of Catalysts', Academic Press, London, 1984.
6. L. L. Hegedus, R. W. McCabe, 'Catalyst Poisoning' Chemical Industries Monograph 17, Marcel Dekker, New York, 1984.
7. R. L. Burwell Jr., *Advan. Catal.*, **26** (1977) 351.
8. K. J. Laidler, 'Chemical Kinetics' McGraw Hill, New York, (1950), pp256-320.
9. G. C. Bond, J. J. Phillipson, P. B. Wells, J. M. Winterbottom, *Trans. Faraday Soc.*, **62** (1966) 433.
10. P. B. Wells, A. G. Wilkinson, *Topics in Catal.*, **5** (1998) 39.
11. G. Emig, R. Ditmeyer in 'Handbook of Heterogeneous Catalysis', (Eds. G. Ertl, H. Knozinger, J. Weitkamp), Volume 3, pp 1209 – 1212.
12. V. Ponec, G. C. Bond, 'Catalysis by Metals and Alloys', *Stud. Surf. Sci. Catal.*, Elsevier, Amsterdam, **95** (1995).

- 13 O. Beeck, *Discuss. Faraday Soc.*, **8** (1950) 118.
- 14 W. Palczewska in 'Hydrogen Effects in Catalysis', (Eds. Z. Paal, P. C. Menson), Dekker, New York and Basal, (1988) p. 373.
- 15 'Strong Metal Support Interactions', ACS Symposium Series 298, (Eds. R. T. K. Baker, S. J. Touster, J. A. Dunesic), ACS, Washington DC, 1986.
- 16 C. Kemball, *J. Chem. Soc.*, (1956) p. 735.
- 17 C. Kemball, P. B. Wells, *J. Chem. Soc. (A)*, (1968) 444.
- 18 G. C. Bond, G. Webb, P. B. Wells, *Trans. Faraday Soc.*, **61** (1965) 999.
- 19 G. C. Bond, J. J. Phillipson, P. B. Wells, J. M. Winterbottom, *Trans. Faraday Soc.*, **62** (1966) 433.
- 20 J. Grant, R. B. Moyes, P. B. Wells, *J. Chem. Soc. Faraday Trans. I*, **69** (1973) 1779.
- 21 J. W. Veldsink, M. J. Bouma, N-H. Shoon, A. A. C. M. Beenackers, *Cat. Rev. Sci Ergg.*, **39** (1997) 253.
- 22 K. Campbell, S. J. Thomson, *Prog. Surf. Membrane Sci.*, **9** (1975) 163.
- 23a G. A. Somorjai in 'Introduction to Surface Catalysis, Wiley, New York, 1994, p.507.
- 23b 'Handbook of Heterogeneous Catalysis', (Eds. G. Ertl, H. Knozinger, J. Weitkamp), VCH, Weinheim (2003), Volume 1, pp 151 – 153.
- 24 R.A. Sheldon, *Chirotechnology, Industrial Synthesis of Optically Active Compounds*, Marcel Dekker, New York 1993 pp82 – 84.
- 25 G.V. Smith, F. Notheisz, *Heterogeneous Catalysis in Organic Chemistry*,

- Academic Press, 1999, pp97 –115.
- 26 W.S. Knowles, M.J. Sabacky, *J. Chem. Soc. Chem. Comm.*, (1968) 1443.
- 27 H.B. Kagan in 11, 1.
- 28 U. Nagel, J. Albrecht, *Top. Catal.*, **5** (1998) 3.
- 29 B. R. James, A. Pacheco, S.J. Rettig, I.S. Thorburn, R.J. Ball, J.A. Ibers, *J. Mol. Catal.*, **41** (1987) 147.
- 30 T.J. Hall, PhD thesis, University of Hull, 1997.
- 31 W.S. Knowles, M.J. Sabacky, B.D. Vineyard, D.J. Weinkauff, *J. Am. Chem. Soc.*, **97** (1995) 2567.
- 32 W.S Knowles, M.J. Sabacky, B.D. Vineyard, *J. Chem. Soc. Chem. Commun.*, (1972) 10.
- 33 A. Ahmadi, G. Attard, J. Fehiu, A. Rodes, *Langmuir*, **7** (1999) 2420.
- 34 G.M. Schwab, L. Rudolph, *Naturwiss*, **20** (1932) 362.
- 35 S. Akabori, S. Sakurai, Y. Izumi, Y. Fujii, *Nature*, **178** (1956) 323.
- 36 P.A. Meheux, A. Ibbotson, P.B. Wells, *J. Catal.*, **125** (1991) 387
- 37 S. P. Griffiths, PhD thesis, University of Hull, 1997.
- 38 P.B. Wells, K.E. Simons, J.A. Slipszenko, S. P. Griffiths, D.F. Ewing, *J. Mol. Catal. A:Chem.*, **146** (1999) 159.
- 39 W.R. Huck, T. Burgi, T. Mallat, A. Baiker, *J. Catal.*, **200** (2001) 171.



- 40 H.U. Blaser, H.P. Jalett, D.M. Monti, J.T. Wehrli, A. Baiker, *Stud. Surf. Sci. Catal.*, **67** (1991) 147.
- 41 G.W. Watson, R.P.K. Wells, D.J. Willock, G.J. Hutchings, *J. Chem. Soc. Chem. Commun.*, (2000) 705.
- 42 K. Borszeczy, T. Mallat, A. Baiker, *Catal. Lett.*, **59** (1999) 95.
- 43 G. Webb, P.B. Wells, *Catal. Today*, **12** (1992) 319.
- 44 T. Osawa, T. Harada, A. Tai, *Catal. Today*, **37** (1997) 465.
- 45 Y. Orito, S. Imai, S. Niwa, *J. Chem. Soc. Japan*, (1979) 118.
- 46 A. Baiker, *J. Mol. Catal. A: Chem.*, **115** (1997) 473.
- 47 P.B. Wells, K.E. Simons, J.A. Slipszenko, S.P. Griffiths, D.F. Ewing, *J. Mol. Catal. A: Chem.*, **112** (1996) 93.
- 48 M. Schurch, O. Schwalm, T. Mallat, J. Weber, A. Baiker, *J. Catal.*, **169** (1997) 275.
- 49 B. Torok, K. Felfoldi, G. Szakonyi, K. Balazsik, M. Bartok, *Catal. Lett.*, **52** (1998) 81.
- 50 X. Zuo, H. Liu, M. Liu, *Tetrahedron Lett.*, **39** (1998) 1941.
- 51 H.U. Blaser, H.P. Jalett, *Stud. Surf. Sci. Catal.*, **78** (1993) 139.
- 52 M. Studer, V. Okafor, H.U. Blaser, *J. Chem. Soc. Chem. Commun.*, (1998) 1053.
- 53 J.A. Slipszenko, S. P. Griffiths, K.E. Simons, W.A.H. Vermeer, P.B. Wells, *J. Catal.*, **179** (1998) 267.
- 54 N. Kunzle, A. Szabo, M. Schurch, G. Wang, T. Mallat, A. Baiker, *J. Chem. Soc. Chem. Comm.*, (1998) 1377.

- 55 T. Mallat, M. Bodmer, A. Baiker, *Catal. Lett.*, **44** (1997) 95.
- 56 T. Mallat, M. Bodmer, A. Baiker, in F.E.Herkes (Ed.), *Catalysis of Organic Reactions*, Marcel Dekker, New York, 1998, p.75.
- 57 B. Torok, K. Felfoldi, K. Basazsik, M. Bartok, *J. Chem. Soc. Chem. Commun.*, (1999) 1725.
- 58 M. Studer, S. Burkhardt, H.U. Blaser, *J. Chem. Soc. Chem. Commun.* (1999) 1727.
- 59 T. Mallat, A. Baiker, *App. Catal. A:Gen.*, **200** (2000) 3.
- 60 M. Schurch, T. Heinz, R. Aeischmann, T. Mallat, A. Baiker, *J. Catal.*, **173** (1998) 187.
- 61 A. Pfaltz, T. Heinz, *Topics in Catal.*, **4** (1997) 229.
- 62 D. Ferri, T. Burgi, A. Baiker, *J. Catal.*, **210** (2002)160.
- 63 R.L.Augustine, S.K. Tanielyan, *J. Mol. Catal. A:Chem.*, **112** (1996) 93.
- 64 K. Borszegy, T. Burgi, Z. Zhaohui, T. Mallat, A. Baiker, *J. Catal.*, **187** (1999) 160.
- 65 G. Webb, P.B. Wells, *Catal. Today*, **12** (1992) 319.
- 66 I. M. Sutherland, A. Ibbotson, P.B. Wells, *J. Catal.*, **125** (1990) 77.
- 67 G. Bond, P.B. Wells, *J. Catal.*, **150** (1994) 329.
- 68 T.J. Hall, P. Johnston, W.A.H. Vermeer, S.R. Watson, P.B. Wells, *Stud. Surf. Sci. Catal.*, **101** (1996) 221.
- 69 P.B.Wells, R.P.K. Wells, Chapter 6 in: *Chiral Catalysts Immobilisation and*

- Recycling, (eds. De Vos et al.), Wiley-VCH, Weinheim, 2000, p123.
- 70 T. Burgi, A. Baiker, *J. Am. Chem. Soc.*, **120** (1998) 12920.
- 71 X. Li, PhD Thesis, Cardiff of University, 2001.
- 72 T. Burgi, F. Atamny, A. Knop-Gericke, M. Havecker, T. Schedel-Niedrig, R. Schlogl, A. Baiker, *Catal. Lett.*, **66** (2000) 109.
- 73 K. E. Simons, PhD Thesis, University of Hull, 1994.
- 74 K.E. Simons, P.A. Meheux, S.P. Griffiths, I.M. Sutherland, P. Johnston, P.B. Wells, A.F. Carley, M.K. Rajumon, M.W. Roberts, A. Ibbotson, *Recl. Trav. Chim. Pays-Bas* **113** (1994) 465.
- 75 A. Baiker, T. Mallat, B. Minder, O. Schwalm, K.E. Simons, J. Weber, in "Chiral Reactions in Heterogeneous Catalysis" (G. Jannes, V. Dubois, Eds.), Plenum Press, New York, 1995 p95.
- 76 R.L. Augustine, S.K. Tanielyan, *J. Mol. Catal. A: Chem.*, **112** (1996) 93.
- 77 J.L. Margitfalvi, E. Tfirst, *J. Mol. Catal. A: Chem.*, **134** (1999) 81.
- 78 J.L. Margitfalvi, E. Talas, E. Tfirst, C. Kumar, A. Gergely, *App. Catal. A: Gen.*, **191** (2000) 177.
- 79 T. J. Hall, P. Johnston, W. A. H. Vermeer, S. R. Watson, P. B. Wells, *Stud. Surf. Sci. Catal.*, **101** (1996) 221.
- 80 Y. Nitta, Y. Ueda, T. Imanaka, *Chem. Lett.*, (1994) 1095.

- 81 Y. Nitta, T. Kubota, Y. Okamoto, *Chem. Soc. Japan*, **74** (2001) 2161
- 82 Y. Nitta, K. Kobiro, Y. Okamoto, *Chem. Lett.*, (1996) 897.
- 83 I. Kun, B. Torok, K. Felfoldi, M. Bartok, *App. Catal. A: Gen.*, **203** (2000) 71.
- 84 Y. Nitta, K. Kobiro, Y. Okamoto, *Proc. 70<sup>th</sup> Ann. Mtg. Chem. Soc. Japan*, **1** (1996) 573.
- 85 K. Borszeky, T. Mallat, A. Baiker, *Catal. Lett.*, **59** (1999) 95.
- 86 W.R. Huck, T. Mallat, A. Baiker, *J. Catal.*, **193** (2000) 1.
- 87 Y. Nitta, K. Kobiro, *Chem. Lett.*, (1995) 165.
- 88 K. Borszeky, T. Burgi, Z. Zhaohui, T. Mallat, A. Baiker, *J. Catal.*, **187** (1999) 160.
- 89 K. Borszeky, T. Mallat, R. Aeschiman, W.B. Schweizer, A. Baiker, *J. Catal.*, **161** (1996) 451.
- 90 G. Szollosi, I. Kun, M. Bartok, *Chirality*, **13** (2001) 619.
- 91 W.D Lubell, M. Kitamura, R. Noyori, *Tet :Asymm.*, **2** (1991) 543.
- 92 H. Kawano, T. Ikariya, Y. Ishii, M. Saburi, S. Yoshikawa, Y. Uchida, H. Kumobayashi, *J. Chem. Soc. Perkin Trans. 1* (1989) 1571.
- 93 W.S. Knowles, M.J. Sabacky, B.D. Vineyard, G. L. Bachman, D.J. Weinkauff *J. Am. Chem. Soc.*, **99** (1997) 5946.
- 94 W.S. Knowles, *Acc. Chem. Res.*, **16** (1983) 106.
- 95 M.J. Burk, J.E. Feaster, R.L. Harlow, *Tet.: Asymm.*, **2** (1991) 569.

- 96 M.J. Burk, *J. Am. Chem. Soc.*, **113** (1991) 8518.
- 97 M.J. Burk, J.E. Feaster, R.L. Harlow, *Organometallics*, **9** (1990) 2653.
- 98 M.J. Burk, J.E. Feaster, W.A. Nugent, R.L. Harlow, *J. Am. Chem. Soc.*, **115** (1993) 10125.
- 99 U. Nagel, E. Kinzel, J.G. Andrade, G. Prescher, *Chem. Ber.*, **119** (1986) 3326.

# *Chapter 2*

## 2.1 Materials

### 2.1.1 Reactants

All procedures follow exactly those practised by Robinson Brothers.

#### 2.1.1.1 Preparation of dehydrophenylalanine azlactone

Benzaldehyde (55 g), *N*-acetylglycine (61 g) and sodium acetate (43 g) were suspended in ethyl acetate (125 ml) in a 1 L glass container. Acetic anhydride was added (36 g) and the mixture stirred and heated to 85 – 90°C and maintained at this temperature for 20 h. The resultant solution was cooled to 50°C and de-ionised water (382 ml) added to precipitate the product. The mobile slurry was stirred at 30 – 35°C for 30 min, then cooled to 0 – 5°C. After 1 h at this temperature the slurry was filtered under vacuum using a buchner funnel and washed with de-ionised water. The product was characterised using IR, NMR and mass spectrometry.

$^1\text{H}$  NMR ( $d_4$ -  $\text{CD}_3\text{OD}$ , 400 MHz),  $\delta$ : 2.2, (singlet, 3H), 6.9 (singlet, 1H), 7.3 (multiplet, 3H), 7.9 (multiplet, 2H).

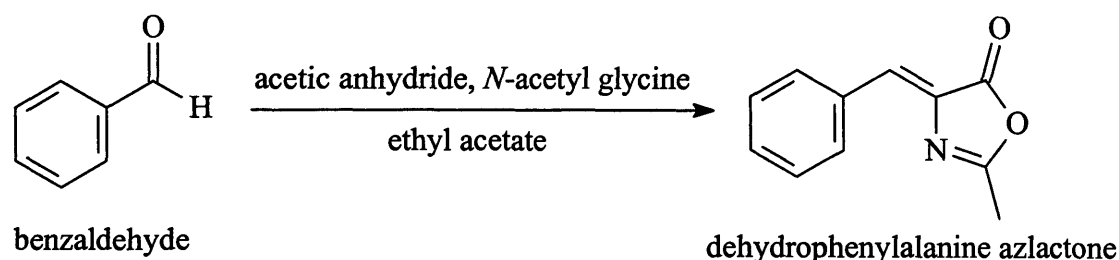


Figure 2.1.1 Preparation of dehydrophenylalanine azlactone

#### 2.1.1.2 Preparation of (E)- *N*-acetyl dehydrophenylalanine methyl ester (NADPME)

Dehydrophenylalanine azlactone (15 g) was slurried in methanol (50 ml) and stirred at room temperature for 1 h. To this suspension a 25% solution of sodium methoxide in methanol was added drop-wise, ensuring no increase in temperature. Addition was complete when a brown solution formed. After stirring for 1 h, the solution was cooled in an ice bath until crystallisation occurred. The mixture was filtered under vacuum using a

buchner funnel and dried overnight at 50°C. The product was characterised by IR, NMR and mass spectrometry.

$^1\text{H}$  NMR ( $d_4$ -  $\text{CD}_3\text{OD}$ , 400 MHz),  $\delta$ : 2.2 (singlet, 3H), 3.9 (singlet, 3H), 7.0 (singlet, 1H), 7.5 (multiplet, 6H).

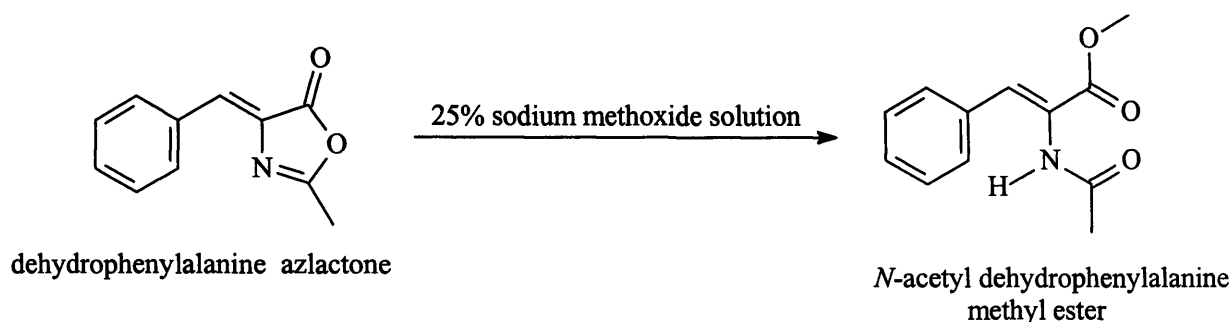


Figure 2.1.2 Preparation of *N*-acetyl dehydrophenylalanine methyl ester

#### 2.1.1.3 Preparation of *N*-acetyl dehydrophenylalanine ethyl ester

This preparation followed that described in Section 2.1.1.2, with the 25% sodium methoxide being replaced by a 25% solution of sodium ethoxide in ethanol.

$^1\text{H}$  NMR ( $d_4$ -  $\text{CD}_3\text{OD}$ , 400 MHz),  $\delta$ : 1.0 (multiplet, 2H), 1.2 (multiplet, 3H), 2.0 (singlet, 3H), 7.0 (multiplet, 6H).

#### 2.1.1.4 Preparation of *N*-acetyl dehydrophenylalanine butyl ester

This preparation followed that described in Section 2.1.1.2, with the 25% sodium methoxide being replaced by a 25% solution of potassium butoxide in butan-1-ol.

$^1\text{H}$  NMR ( $d_4$ -  $\text{CD}_3\text{OD}$ , 400 MHz),  $\delta$ : 1.0, (multiplet, 2H), 1.1 (multiplet, 2H), 1.4 (multiplet, 3H), 2.0 (singlet, 3H), 2.2 (singlet, 3H), 3.2 (multiplet, 2H), 6.0 (singlet, 1H), 7.2 (multiplet, 6H).

#### 2.1.1.5 Preparation of *N*-acetyl dehydrophenylalanine $\pm$ 2 butyl ester

Dehydrophenylalanine azlactone (5 g) was dissolved in toluene (30 ml) and  $\pm$  butan-2-ol (5 ml) and equivalent moles of t-potassium butoxide added. The mixture was stirred for 12 h, and the solvent removed by rotary evaporation. The product was dissolved in dichloromethane (20 ml) and washed with acidified water. The resulting DCM layer was



removed by rotary evaporation and the product characterised by NMR.

$^1\text{H}$  NMR ( $d_4$ -  $\text{CD}_3\text{OD}$ , 400 MHz),  $\delta$ : 1.2, (multiplet, 3H), 1.5 (multiplet, 2H), 2.0, (multiplet, 3H), 2.2, (singlet, 3H), 4.1, (multiplet, 1H), 7.2, (multiplet, 7H).

#### 2.1.1.6 Preparation of *N*-acetyl dehydrophenylalanine (+)-*R*-2-butyl ester

This preparation followed that described in Section 2.1.1.5, with  $\pm$  butan-2-ol being replaced by (+)-*R*-butan-2-ol.

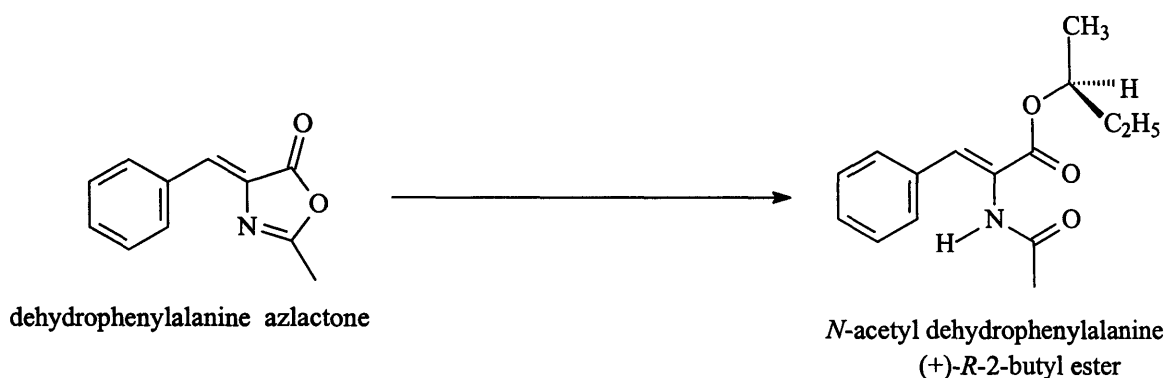
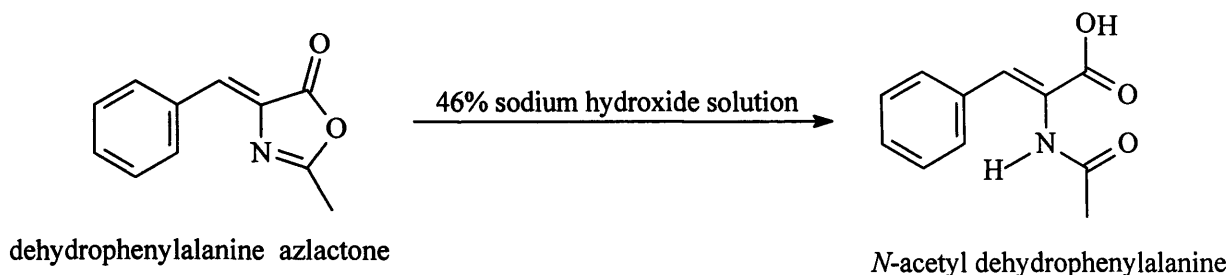


Figure 2.1.3 Preparation of *N*-acetyl dehydrophenylalanine (+)-*R*-2-butyl ester

#### 2.1.1.7 Preparation of *N*-acetyl dehydrophenylalanine (NADP)

Dehydrophenylalanine azlactone (10 g) was added to de-ionised water (30 ml) in a glass beaker (50 ml) at room temperature. To this suspension a 46% sodium hydroxide solution (10 ml) was added drop-wise so as to maintain the pH between 12.5 - 13.0 and to limit the temperature rise to 40°C. The reaction mixture was stirred overnight. The pH of the mixture was then adjusted to about 1 using concentrated hydrochloric acid. The slurry was cooled to 0 – 5°C and stirred for a further hour. The product was filtered under vacuum using a buchner funnel and washed with de-ionised water. The wet solid was then dried overnight in an oven at 40°C. The product was characterised using IR, NMR and mass spectrometry.

$^1\text{H}$  NMR ( $d_4$ -  $\text{CD}_3\text{OD}$ , 400 MHz),  $\delta$ : 2.2 (singlet, 3H), 6.9 (singlet, 1H), 7.5 (multiplet, 6H), 12.4 (singlet, 1H).

Figure 2.1.4 Preparation of *N*-acetyl dehydrophenylalanine

## 2.1.1.8 Preparation of dehydrophenylalanine methyl ester hydrochloride salt

NADPME (5 g) was dissolved in a 0.5 M HCl/toluene solution and placed in a round-bottomed flask (100 ml). A Dean-Stark reflux apparatus was then attached to this flask and the solution refluxed overnight at 85°C. The solution was cooled to room temperature and the solvent removed by rotary evaporation to yield the salt [1].

$^1\text{H}$  NMR ( $d_4$ -  $\text{CD}_3\text{OD}$ , 400 MHz),  $\delta$ : 2.1 (singlet, 3H), 2.2 (multiplet, 3H), 4.9 (singlet, 1H), 6.0 (multiplet, 5H).

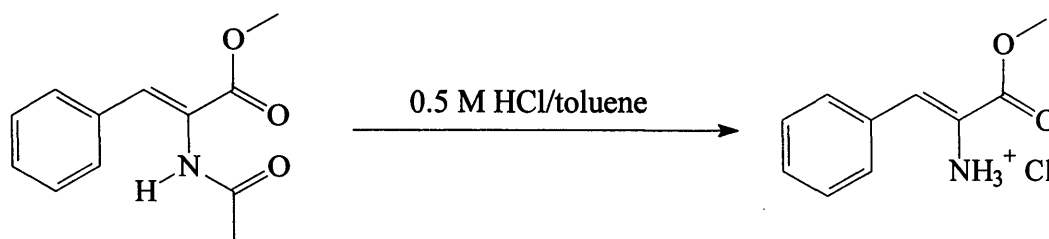


Figure 2.1.5 Preparation of the hydrochloride salt of dehydrophenylalanine methyl ester

## 2.1.1.9 Preparation of dehydrophenylalanine methyl ester

The hydrochloride salt of dehydrophenylalanine methyl ester was dissolved in dichloromethane (DCM, 20 ml) and subsequently washed twice with a saturated brine medium (2 x 10 ml). The DCM layer was isolated and the solvent removed by rotary evaporation to yield the product. The product was characterised by NMR and consumed within two days of synthesis.

### 2.1.1.10 Preparation of *E*-methyl cinnamic acid methyl ester

Phenyl cinnamic acid (Fluka, 5 g) was dissolved in a mixture of methanol (50 ml) and concentrated hydrochloric acid (2 ml) in a round-bottomed flask (100 ml). The mixture was refluxed for 5 h, cooled and solvent removed by rotary evaporation. Conversion of the acid to the ester was confirmed with NMR.

$^1\text{H}$  NMR ( $\text{d}_4\text{-CD}_3\text{OD}$ , 400 MHz),  $\delta$ : 2.1 (singlet, 3H), 3.9 (singlet, 3H), 7.3 (multiplet, 5H), 7.6 (singlet, 1H).

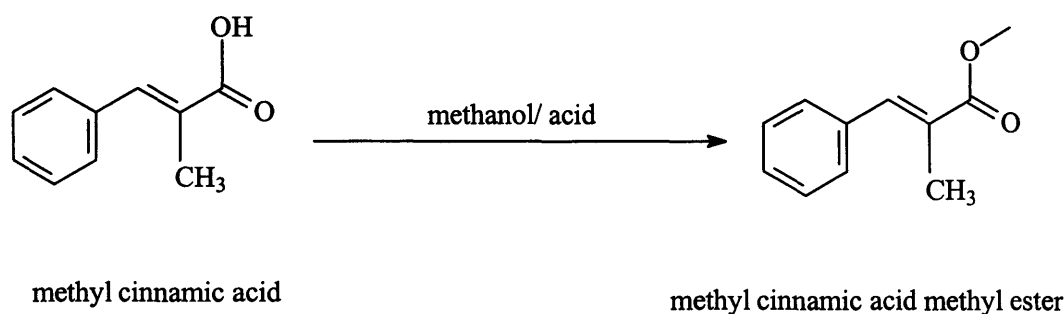


Figure 2.1.6 Preparation of methyl cinnamic acid methyl ester

### 2.1.1.11 Preparation of diazomethane

Diazomethane was prepared using specialised glassware (Figure 2.1.7) purchased from Aldrich. The procedure was as follows. The distillation flask (125 ml), fitted with a long-stem dropping funnel, was connected to a condenser. The condenser was then connected by means of an adapter to an Erlenmeyer flask (250 ml). An outlet tube ran from this Erlenmeyer flask, through a hole in the stopper to a second Erlenmeyer flask. The outlet tube was fed nearly to the bottom of the second Erlenmeyer flask, which was not stoppered. Both receivers were cooled in a salt-ice mixture to approximately  $0^\circ\text{C}$ . Ether was placed in both receivers, 10 ml in the first and 35 ml in the second (ensuring that the outlet tube in the second flask lay below the surface of the ether).

Potassium hydroxide (6 g) was dissolved in water (10 ml), Carbitol (diethylene glycol momoethyl ether, ethoxy diglycol) (35 ml) and ether (10 ml) in the distilling flask (125

ml). The dropping funnel was adjusted so that the stem was just above the surface of the solution. A solution of p-tolylsulfonyl methyl nitrosamide (21.5 g) in ether was placed in the dropping funnel. The distillation flask was then heated to 70 – 75°C using a water bath and magnetic stirring commenced. All the p-tolylsulfonyl methyl nitrosamide solution was then added at a regular rate over a twenty minute period. When this was complete additional ether (~50 – 100 ml) was placed in the dropping funnel and added at the same rate until the distillate was colourless.

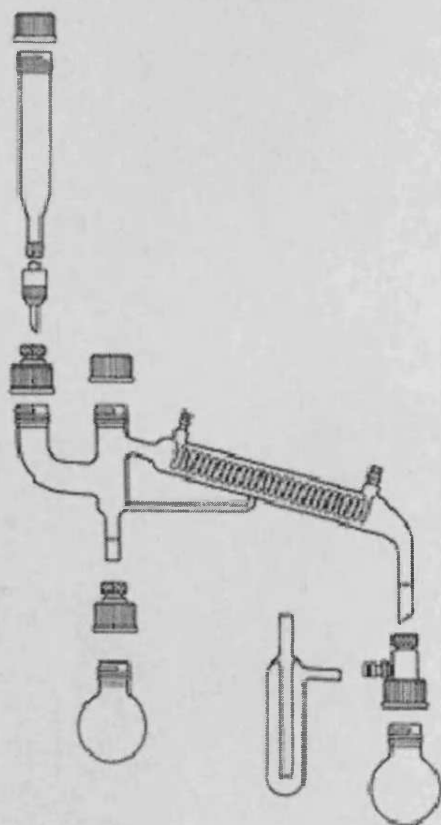


Figure 2.1.7 Glassware for preparation of diazomethane

Diazomethane was collected as a solution in ether and stored in a refrigerator [2].

## 2.1.2 Catalysts

Two 5% Pd/alumina catalysts (Johnson Matthey, batch numbers 99300, 99306) were used throughout this project. Information supplied stated that both catalysts have palladium particle size distributions extending from 2 - 20 nm. The metal assay was 4.97 - 5.03% Pd.

Palladium catalysts prepared in the laboratory by deposition-reduction method (A) and by wet impregnation method (B) are listed in Table 2.1.1.

Table 2.1.1 Catalysts prepared in the laboratory

Catalyst precursor	Support	Preparation method <sup>a</sup>	Finished catalyst	Quantity prepared / g
K <sub>2</sub> PdCl <sub>4</sub>	anatase	A	1% Pd/TiO <sub>2</sub>	2
K <sub>2</sub> PdCl <sub>4</sub>	anatase	A	2% Pd/TiO <sub>2</sub>	2
K <sub>2</sub> PdCl <sub>4</sub>	anatase	A	5% Pd/TiO <sub>2</sub>	2
K <sub>2</sub> PdCl <sub>4</sub>	anatase	A	10% Pd/TiO <sub>2</sub>	2
K <sub>2</sub> PdCl <sub>4</sub>	anatase	A	20% Pd/TiO <sub>2</sub>	2
K <sub>2</sub> PdCl <sub>4</sub>	anatase	A	5% Pd/TiO <sub>2</sub>	7
K <sub>2</sub> PdCl <sub>4</sub>	Anatase	A	10% Pd/TiO <sub>2</sub>	7
K <sub>2</sub> PdCl <sub>4</sub>	Anatase	A	20% Pd/TiO <sub>2</sub>	7
Pd(NO <sub>3</sub> ) <sub>2</sub>	Anatase	B	2% Pd/TiO <sub>2</sub>	2
Pd(NO <sub>3</sub> ) <sub>2</sub>	γ- alumina	B	5% Pd/Al <sub>2</sub> O <sub>3</sub>	2

<sup>a</sup>For method A see Section 2.1.2.1.; for method B see Section 2.1.2.2.

### 2.1.2.1 Deposition-reduction method of catalyst preparation

Titanium dioxide (2 g anatase) was added to distilled water (30 ml) in a round-bottomed flask (100 ml). An appropriate amount of potassium tetrachloropalladite (K<sub>2</sub>PdCl<sub>4</sub>) was added to this suspension and pH ~ 11 achieved by addition of powdered potassium hydroxide. The suspension was then boiled under reflux for 1 h. To this mixture an excess of sodium borohydride was added (approximately three times the stoichiometric amount) and after 30 min the suspension was cooled. The catalyst was filtered under

vacuum using a buchner funnel, washed with de-ionised water, and left in the funnel to dry overnight [3].

#### 2.1.2.2 Wet impregnation method of catalyst preparation

Titanium dioxide (2 g anatase) and sodium hydroxide (0.14 M, 4 ml) was added to distilled water (30 ml) in a conical flask (100 ml). The mixture was stirred for 10 min at room temperature. A solution of palladium nitrate (0.028 M, 10 ml) was added drop-wise to the mixture, ensuring no change in temperature, and the mixture stirred for a further 30 min. The supported salt was then filtered, washed with de-ionised water and dried in an oven overnight at 110°C. Reduction of the supported salt was achieved using a tube furnace at 250°C with a continuous flow of 5% H<sub>2</sub>/He for 10 h. The catalyst was then cooled under the same flow to room temperature before exposure to air [4].

#### 2.1.2.3 Re-reduction of catalyst samples

Re-reductions of the JM catalysts (batches 99300 and 99306) were made occasionally using a tube-furnace. Various reduction temperatures were employed but the same procedure was followed. The catalyst sample (3.0 g) was placed in a ceramic boat and placed inside a Pyrex tube furnace. A continuous flow of 5% H<sub>2</sub>/He was passed over the catalyst sample to ensure the removal of air from inside the tube. The temperature was then raised to that appropriate for reduction (see Chapter 3) and maintained at this value for 2 h. The sample was then cooled to room temperature under the same gas flow, after which it was stored in a glass vial and used within 48 h.

#### 2.1.2.4 Pre-modification of catalyst with cinchona alkaloid

Pre-modification of catalyst samples with cinchonidine were made using various alkaloid concentrations. The procedure was as follows: Pd/alumina (2) (50 mg) was added to methanol (10 ml) and subsequently placed inside the autoclave. Stirring was commenced at 1 bar hydrogen pressure and 298 K for 30 minutes. The autoclave was then opened and the appropriate amount of cinchonidine added to the catalyst mixture. Stirring was then

commenced for a further 30 minutes in the absence of hydrogen. Once this was complete the reactant was added and hydrogenation under standard conditions started.

### 2.1.3 Cinchona Alkaloids

Cinchona alkaloids and simple derivatives have been used as catalyst modifiers. Most experiments have involved use of cinchonine or cinchonidine; these compounds are 'near enantiomers' their structures differing only in the configurations at the chiral carbon atoms C<sub>8</sub> and C<sub>9</sub> (Figure 2.1.8).

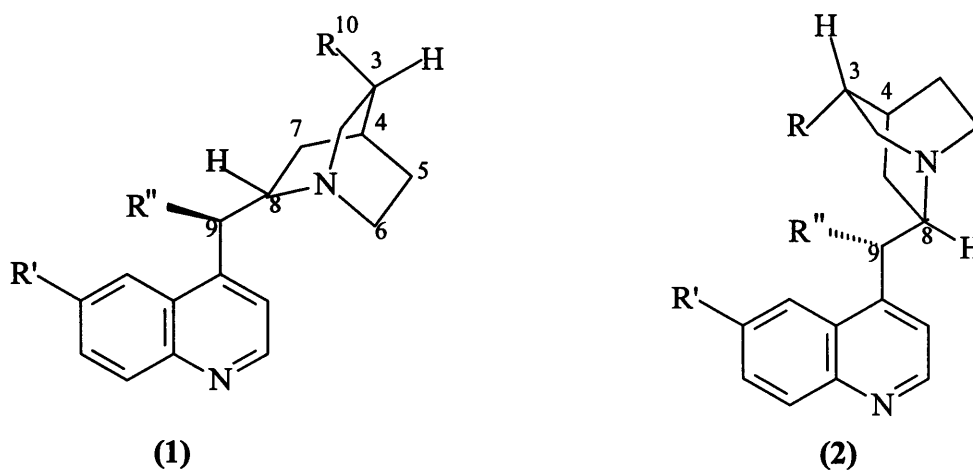


Figure 2.1.8 Structures and configurations of the cinchona alkaloids

	(1)	(2)	Substituents
	Cinchonidine (CD)	Cinchonine (CN)	R = C <sub>2</sub> H <sub>5</sub> , R' = H, R'' = OH
	Quinine (QN)	Quinidine (QD)	R = C <sub>2</sub> H <sub>5</sub> , R' = OMe, R'' = OH
	Dihydro-derivatives		R = C <sub>2</sub> H <sub>5</sub>
	Dihydroquinine chlorobenzoate	Dihydroquininidine chlorobenzoate	R = C <sub>2</sub> H <sub>5</sub> , R' = OMe, R'' = C <sub>6</sub> H <sub>5</sub> COO
Atom	C <sub>8</sub> C <sub>9</sub>	C <sub>8</sub> C <sub>9</sub>	
Configuration	S R	R S	

The natural cinchona alkaloids supplied by Fluka and were used as received. Their stated purities were quoted as: cinchonidine ~ 99%, cinchonine ~ 98.7% quinine ~ 99%, quinidine ~ 99% dihydroquinidine chlorobenzoate ~ 99% and dihydroquinidine chlorobenzoate ~ 99%.

#### 2.1.3.1 Preparation of 10,11-dihydro-derivatives

The appropriate alkaloid (5 g) was dissolved in 0.5M sulphuric acid (30 ml) and added to 5% Pd/C (0.1 g). The mixture was placed in a stainless steel autoclave and hydrogenated at 1 bar hydrogen pressure at 298 K for 3 h. The resulting solution was filtered to remove the catalyst and neutralised with 0.5M sodium hydroxide solution whereupon the dihydro-derivative precipitated. The product was separated, washed, dried at 353 K, and re-crystallised from an ethanol/water mixture. Hydrogenation of the vinyl group was confirmed using NMR [5].

#### 2.1.3.2 Preparation of quaternised cinchonine using methyl iodide

Cinchonine (1 g) was placed in a conical flask (100 ml) with methanol (20 ml). One equivalent of methyl iodide (0.21 ml) was added to the reaction mixture and the mixture stirred at 298 K for 24 h. The solvent was removed by rotary evaporation and the product identified by NMR [6].

#### 2.1.4 Other Modifiers

Modifiers from the strychnos and morphine alkaloid families were investigated; their structures are shown in Figure 2.1.9. Both were used as received.



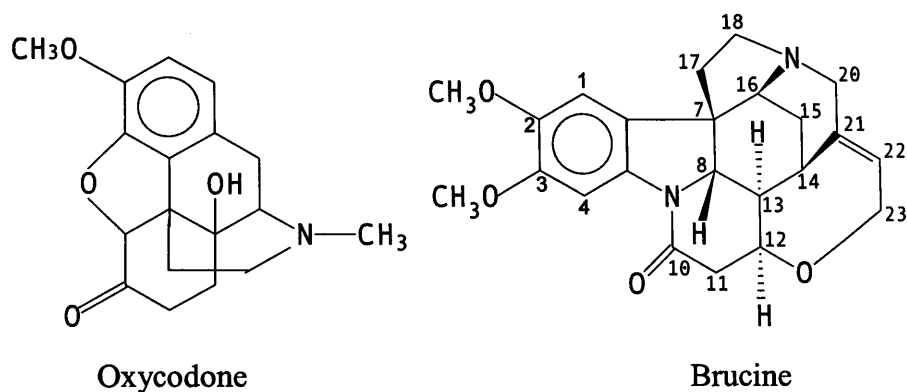


Figure 2.1.9 Structures of oxycodone and brucine

#### 2.1.4.1 Preparation of (2*S*, 1'*S*)-*N*-[1'-(1-naphthyl)ethyl]-2-amino propionic acid ethyl ester

(*S*)-1-(1-naphthyl)ethylamine (5.8 mg) and ethyl pyruvate (1.2 g) were mixed in acetic acid (2 ml) and added to 5% Pt/alumina catalyst (50 mg). The mixture was transferred to an autoclave and stirred at 25 bar H<sub>2</sub> pressure for 1 h. After filtration of the catalyst the solvent was removed by distillation under vacuum (100°C). The residue was dissolved in ether and an excess of potassium carbonate was added. The mixture was stirred for 1 h at room temperature. Filtration and removal of the solvent in vacuo yielded an oily product. Flash chromatography with hexane/ethyl acetate (5:1) afforded (2*S*, 1'*S*)-*N*-[1'-(1-naphthyl)ethyl]-2-amino propionic acid ethyl ester (Figure 2.1.10.). Yield ca. 20% [7].

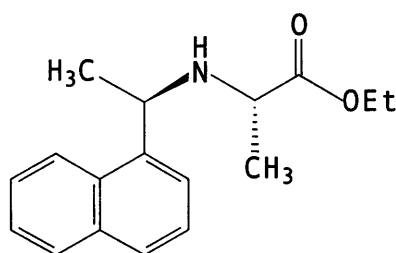


Figure 2.1.10 The structure of (2*S*, 1'*S*)-*N*-[1'-(1-naphthyl)ethyl]-2-amino propionic acid ethyl ester

## 2.1.5 Other Materials

Table 2.1.2 lists all other chemicals used; they were used as received unless otherwise stated.

Table 2.1.2 Other materials used in the investigation

Material	Supplier	Purity
Methanol	Fisher Chemicals	99
Dichloromethane	Fisher Chemicals	99
Acetic acid	Fisher Chemicals	99.5
Trifluoroacetic acid	Fluka	99
Ethanol	Fisher Chemicals	99
Tetrahydrofuran	Fisher Chemicals	99
N,N-dimethyl formamide	Aldrich	98
Dimethyl sulfoxide	Aldrich	97
Formamide	Fluka	99
Toluene	Fisher Chemicals	99
L-proline	Aldrich	99+
Sodium methoxide (solution)	Aldrich	98
Sodium ethoxide (solution)	Aldrich	96
Ethyl acetate	Aldrich	99
Acetic anhydride	Aldrich	99
Benzaldehyde	Aldrich	99.5
Sodium borohydride	Aldrich	99
Acetylglycine	Aldrich	99
methylcinnamic acid	Aldrich	99
Butanol	Fisher	99
Butan-2-ol	Fluka	≥ 99.5
R-butan-2-ol	Fluka	≥ 98
S-butan-2-ol	Fluka	≥ 99
N-acetyl phenylalanine	Aldrich	99
Titanium dioxide (anatase)	Degussa	50 m <sup>2</sup> g <sup>-1</sup>
Aluminium oxide	Condea	148 m <sup>2</sup> g <sup>-1</sup>

Table 2.1.2 continued

Material	Supplier	Purity
Potassium chloropalladite	Johnson Matthey	Batch 13
Potassium (II) nitrate	Strem	(99.9) % Pd – 42.0
Hydrogen gas	BOC	99.995
Air	BOC	-
Helium gas	BOC	99.5
Deuterium gas		2.8 Grade
Deuterated water (D <sub>2</sub> O)	Aldrich	99.96 - D
Deuterated methanol (CD <sub>3</sub> OD)	Euriso-top	99.8 - D
Deuterated dichloromethane (CD <sub>2</sub> Cl <sub>2</sub> )	Aldrich	99.5 - D

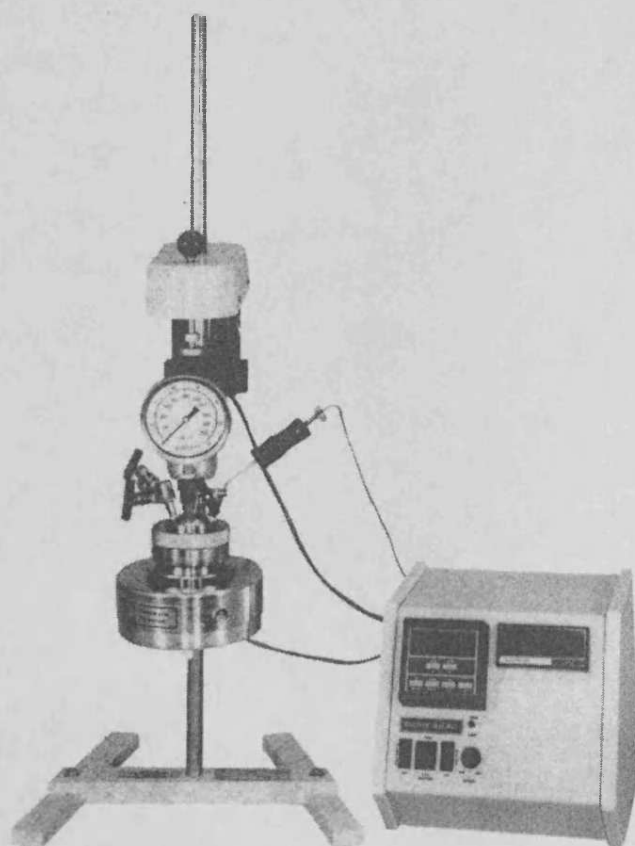
## 2.2 Apparatus

### 2.2.1 Parr Autoclave and Buchi Pressflow Controller

Hydrogenations were performed in a 50 ml stainless steel reactor, Figure 2.2.1. The reactor consisted of four parts: a cylinder, a head, two metal half-jackets and an outer metal-jacket. It was assembled by placing the head in the groove gasket of the cylinder via a Teflon O-ring. The two metal half-jackets were then secured around this join and the outer metal jacket was secured around the two half-jackets. All ensured the pressure integrity of the reactor. The reactor was equipped with a 1/12 hp variable speed motor and a temperature sleeve which fitted around the cylinder when required. Temperature and motor speed were achieved using a series 4840 controller. The reactor and controller can be seen in Figure 2.2.1. The working upper limits for reactor pressure, temperature and motor speed were, 80 bar, 220°C and 1000 revolutions per minute (rpm) respectively.

Hydrogen and helium (purge gases) were dosed into the system using a Buchi Pressflow gas control unit. The required pressure was set at the control unit. As hydrogen was consumed during reaction the Buchi unit detected the pressure decrease and admitted further hydrogen in order to maintain the set pressure. It recorded the amount of

hydrogen consumed and relayed this information via a serial cable to a RM computer, where it was displayed as a function of time. This data could then be saved as a Microsoft Excel spreadsheet for analysis.



4591 Micro Reactor with 4841 Controller

Figure 2.2.1 Picture of 50 ml Parr Autoclave with series 4841 temperature controller

### 2.2.2 Chiral Gas Chromatography

Separation and analysis of enantiomers was achieved using a Varian CP-3800 gas chromatograph equipped with a 25 m Chirasil-L-Val capillary column and a FID detector. The results were displayed on a RM computer and processed using Varian Star software.

### 2.2.3 Mass Spectrometry

Mass spectrometry was used for the characterisation of organic reactants prepared and the products formed after hydrogenation. The mass spectrometer used was a VG Visions Platform 2. All samples (~0.001 g) were dissolved in acetone and was analysed by a trained technician.

### 2.2.4 Polarimetry

The AA 1000 Optical Activity polarimeter was used to determine the nature of the hydrogenation products of reactions completed using unmodified catalysts.

### 2.2.5 Fourier Transform Infra-Red (FTIR)

Infra-red spectra were obtained using a Perkin-Elmer 2000 FTIR spectrometer at a resolution of  $4.0\text{ cm}^{-1}$  (higher resolution spectra revealed no additional information in the spectra) and the co-addition of 200 scans. The spectra were displayed and analysed using PE spectrum 200 software. For information regarding modifier-reactant interactions, spectra were obtained using a solution cell of 1 mm path length (calcium fluoride windows) and a cinchonidine concentration of 0.01M.

Spectra obtained for characterisation purposes were achieved using nujol mulls with sodium chloride plates.

### 2.2.6 Nuclear Magnetic Resonance Spectroscopy (NMR)

$^1\text{H}$  and  $^{13}\text{C}$  NMR spectra were recorded using a Bruker 400 MHz NMR spectrometer at room temperature. An internal standard (e.g. TMS) was not necessary as the spectrometer was configured to lock automatically on the deuterium signal of the chosen solvent.

### 2.2.7 Electron Microscopy

Scanning electron microscopy (SEM) and transmission electron microscopy (TEM) were used to obtain information on the morphology of the catalysts used. SEM was carried out in the Earth Sciences Department of Cardiff University and TEM at the Biology Department, Hull University. Both instruments were operated by trained technical staff.

### 2.2.8 Atomic Absorption Measurements.

Atomic absorption measurements were used to obtain percentage metal content of the catalysts prepared in the laboratory. The measurements were recorded on a varian 2000 AA.

### 2.2.9 X-ray Diffraction Measurements (XRD)

X-ray diffraction patterns were produced using a Siemens D5000 diffractometer using Cu K $\alpha$  radiation ( $\lambda = 1.54 \text{ \AA}$ ). This was a self-service machine.

### 2.2.10 Measurements of Surface Area and Metal Dispersion

Surface area measurements were performed using a Micromeritics ASAP 2000 and chemisorption measurements using the Micromeritics Auto Chem 2910.

## 2.3 Procedures

### 2.3.1 Hydrogenations

The standard procedure for a typical hydrogenation of *N*-acetyl dehydrophenylalanine methyl ester (NADPME) was as follows. NADPME (100 mg, 0.46 mmol) and cinchonine (15 mg, 0.05 mmol) were dissolved in methanol (10 ml). The catalyst (100

mg) was placed either directly inside the steel reactor, or inside a glass liner and the liner placed in the reactor. The solution of reactant and modifier was then added to the catalyst and the reactor closed. The reactor was purged twice with helium and twice with hydrogen at a pressure of 3 bar to remove air. The reactor was then pressurised with hydrogen to 10 bar at ambient temperature (293 – 295 K) and stirring commenced (1000 rpm). Reaction time was normally 3 h, within which time 100% conversion was normally achieved.

### 2.3.2 Hydrogenations: Kinetics

In order to obtain kinetic information for the modified and unmodified hydrogenation of *N*-acetyl dehydrophenylalanine methyl ester the reactant amount, pressure, temperature and catalyst amount were each varied individually. Hydrogenations were carried out as described in Section 2.3.1 above, but the amount of reactant was increased to at least 1.5 g (6.8 mmol) so that reliable uptake time curves could be recorded. Rate curves were obtained for reactions in which the variables were: NADPME, 1.5 g to 4.5 g (6.8 mmol – 20.5 mmol); hydrogen pressure, 1 to 70 bar; catalyst mass, 200 mg to 1.2 g; temperature 280 to 309 K. When each individual parameter was being held constant the standard amounts were: NADPME mass – 3.0 g (13.7 mmol); hydrogen pressure – 10 bar; catalyst mass – 200 mg; cinchonine mass – 120 mg (0.4 mmol); temperature – 295 K.

### 2.3.3 Hydrogenations: Deuterium Tracer Studies

Deuterium tracer studies were undertaken to investigate the possibility of tautomers of NADPME being present under certain hydrogenation conditions [8]. The reactor was purged with a slow flow of deuterium for 30 min prior to a reaction being carried out, to ensure the removal of hydrogen from inside the reactor. ‘Hydrogenations’ then followed the procedure described in Section 2.3.1.

### 2.3.4 Product Recovery and Analysis

Products were analysed using chiral gas chromatography. Before analysis was undertaken the catalyst was filtered from the reaction mixture and the resulting solution diluted. Correct dilution of the products was crucial for their separation, and for accurate and reproducible analysis of the enantiomers. Product concentrations less than  $0.4 \text{ g l}^{-1}$  and greater than  $0.8 \text{ g l}^{-1}$  could not be analysed accurately. Reactions were normally allowed to run to completion. The product concentration was then known and the required dilution could be made. For a standard hydrogenation, 1 ml of reaction solution was diluted in 10 ml of the same solvent and  $0.1 \mu\text{l}$  of this solution was injected onto to the column. The enantiomeric excess (e.e.), obtained from integration of the peak areas for the *R* and *S* products, is defined as:

$$\text{enantiomeric excess/\%} = \frac{(R - S)}{(R + S)} \times 100$$

where  $R$  = peak area of *R*-enantiomer  
 $S$  = peak area of *S*-enantiomer

The GC operating conditions were as follows: injector temperature, 603 K; column temperature, 428 K; detector temperature, 613 K; hold time at 428 K, 30 min; split flow ratio, 50:1; column flow rate,  $1 \text{ ml min}^{-1}$  He.

#### 2.3.4.1 Derivatisation by diazomethane

*N*-acetyl phenylalanine required esterification with diazomethane prior to GC analysis. To the reaction solution containing NADP, aliquots of diazomethane solution were added, whereupon effervescence of the solution occurred. Esterification of NADP was complete when further addition of diazomethane solution produced no further effervescence. The product solution was then analysed as described in Section 2.3.4.



### 2.3.5 Accuracy and Reproducibility of GC Analysis

Calibration of the GC was required to ensure the accurate and reproducible analysis of enantiomers. The *R* and *S* enantiomers of *N*-acetyl phenylalanine methyl ester (NAPME) could not be purchased. As a result they were prepared from the hydrogenation of *N*-acetyl dehydrophenylalanine methyl ester (NADPME). A series of standard solutions for GC calibration were made using various combinations of two solutions.

*Solution 1* was the result of the hydrogenation of NADPME over Pt/alumina under standard conditions. The solution was first analysed using a polarimeter and then by chiral GC. Both methods indicated that *solution 1* contained equal amounts of the *R* and *S* enantiomers of NAPME and the product was thus racemic.

*Solution 2* was the result of the homogeneous hydrogenation of NADPME using (*R,R*)-dipamp as catalyst. The value of the enantiomeric excess determined by GC analysis was 89%(*R*).

The values of e.e. expected from the prepared standards varied in the range of 8 – 80%(*R*). A second series of standards was prepared in a similar manner using (*S,S*)-dipamp as the homogeneous catalyst. This allowed values of e.e. in favour of the *S*-enantiomer to be incorporated in the calibration. The results are shown in Figure 2.3.1. Each experimental value plotted is an average of three results for a given sample; in every case the three results concurred to within  $\pm 0.7$ .

The standard deviations for the results shown in Figure 2.3.1 were small. This indicated that the experimental and the expected e.e. values were in good agreement, and that the GC was accurately analysing the products. GC calibration was repeated periodically, to ensure that no deterioration in performance had occurred.

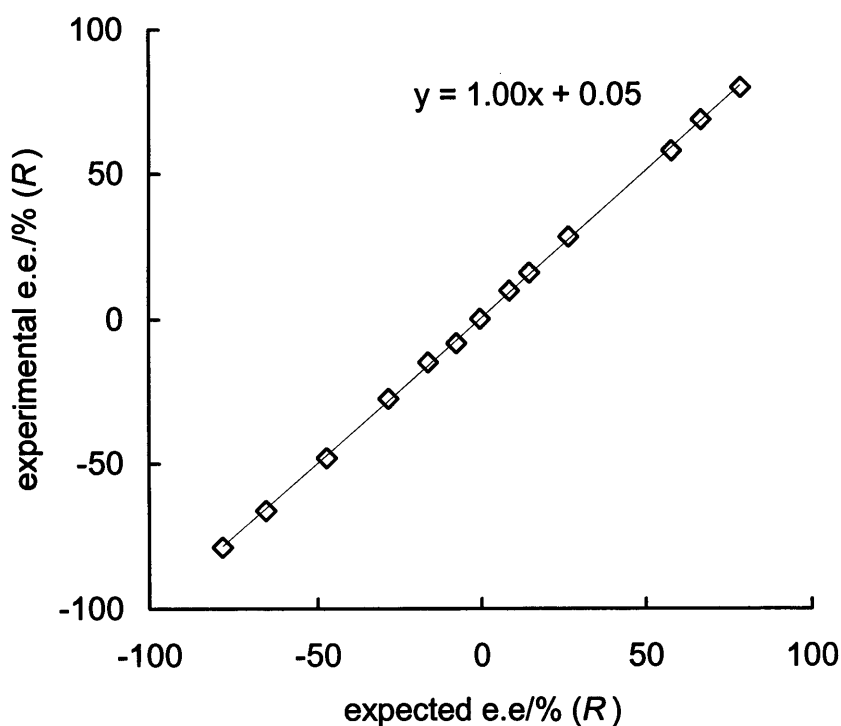


Figure 2.3.1 GC calibration plot: correlation between experimentally determined e.e. and the known values for prepared standards

### 2.3.6 NMR for the Characterisation of Reactants

The organic reactants prepared were characterised using  $^1\text{H}$  and  $^{13}\text{C}$  NMR techniques. For the initial characterisation of reactants COSEY spectra were also obtained. Solutions were prepared by dissolving small amount of reactant in 1 ml of deuterated solvent ( $\text{CDCl}_3$  or  $\text{CD}_3\text{OD}$ ).

### 2.3.7 NMR for the Study of Modifier : Reactant Interactions

NMR studies of cinchonidine conformations and of cinchonidine:reactant interactions were achieved by recording  $^1\text{H}$  NMR spectra, followed by NOESY spectra, for the samples involved. Two deuterated solvents were used,  $\text{CD}_2\text{Cl}_2$  and  $\text{CD}_3\text{OD}$  (0.5 ml). A constant amount of NADPME was used (5 mg) with various amounts of cinchonidine (0.5 mg, 2.5 mg, and 7.5 mg).

### 2.3.8 Atomic Absorption Measurements

Atomic absorption measurements were performed using the apparatus described in 2.2.8. A range of standard solutions were made from a stock solution of palladium of 1 000 ppm. The concentrations of the standards were between 10 – 100 ppm. The results are presented in Table 2.3.1. The calibration graph shown in Figure 2.3.2 was used to determine the concentration of palladium in catalyst samples.

Table 2.3.1 Atomic absorption measurements of the prepared standards of palladium

Standard concentration /ppm	Absorbance	Absorbance after subtraction of absorbance attributed to water
10	0.1693	0.1575
20	0.2726	0.2608
40	0.4808	0.4690
60	0.7352	0.7234
80	0.8001	0.7883
100	0.9061	0.8943

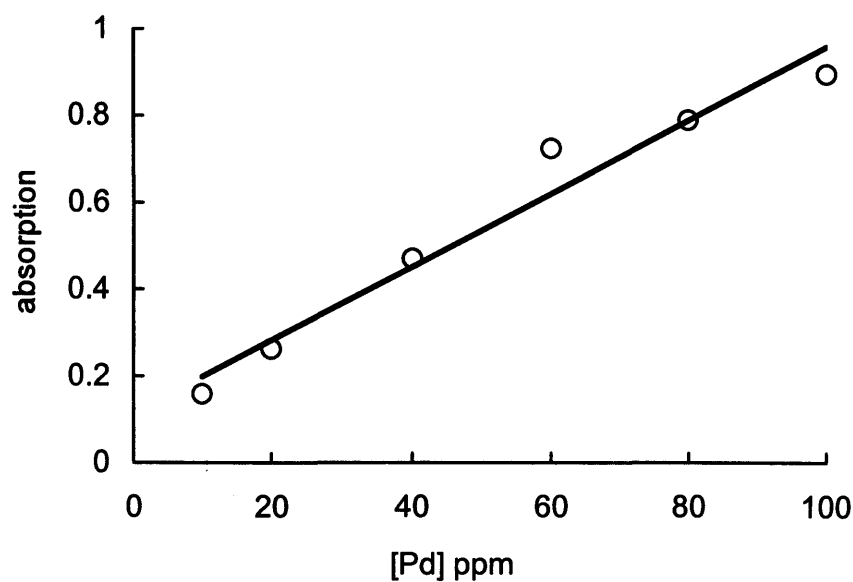


Figure 2.3.2 Variation of absorption with Pd concentration for six standard solutions

### 2.3.9 X-ray Diffraction Measurements

XRD measurements were performed using the apparatus described in 2.2.9. The catalyst sample was evenly dispersed on an aluminium holder and the holder placed in the machine. Scans were recorded for values of  $2\theta$  between  $10^\circ$  and  $100^\circ$  over a period of 10 min.

### 2.3.10 Chemisorption Measurements

Chemisorption measurements were made to ascertain the metal dispersion in catalyst samples. The apparatus used was described in Section 2.2.10. A small amount of glass wool was inserted firmly into the bottom of the U-tube followed by 0.3 g of catalyst. This ensured that catalyst sample could not be blown round the U-bend by flowing gases. The U-tube was then secured to the apparatus and the program started. The program was divided into two parts. First, a temperature programmed reduction (TPR) was implemented to clean and reduce the catalyst surface. This was achieved by passing  $H_2/He$  (flow rate  $0.5 \text{ ml min}^{-1}$ ) over the catalyst surface at  $150^\circ\text{C}$  for 1 h. The sample was then cooled to a baseline temperature before the second stage of the program (chemisorption of CO onto the Pd) was initiated. An initial pulse of CO in a known loop volume (1.02 ml) was made (bypassing the catalyst) so that a reading was displayed on the monitor that corresponded to the loop volume (i.e. no chemisorption of CO onto catalyst surface). Repeated pulses of CO were then passed over the catalyst sample until the output displayed a constant value corresponding to the initial injection volume. From this, a calibration factor  $k = (\text{loop volume}/\text{final constant reading})$ , was determined. The total volume of CO chemisorbed (ml) was then determined using the equation below.

$$\text{Total volume chemisorbed (ml)} = \sum (\text{loop volume} - (k \times \text{display reading after each CO pulse}))$$

This value was then converted to the total volume chemisorbed at STP,  $V_{\text{chem, STP}}$ , in the usual way

$$\text{Volume chemisorbed} = \frac{\text{total volume chemisorbed}}{(\text{ml STP})} \times \frac{273}{\text{room temp}} \times \frac{\text{atm P}}{760}$$

The percentage metal dispersion, D, was calculated on the assumption that CO chemisorbs in a bridging mode on palladium [9]. This introduces a stoichiometric factor of 2 into the equation below. Dispersion is defined as the fraction of metal atoms situated at the available metal surface. So for a catalyst sample of mass m, and metal loading L, and for Pd (RMM = 105.42):

$$D = (2V_{\text{chem, STP}} \times 105.42 \times 100) / 22414Lm$$

## 2.4 References

- 1 C. Black, *Org. Syn. Coll.*, **1**(1992) 34.
- 2 F. Arndt, *Org. Syn. Coll.*, **2** (1999) 165.
- 3 A. Tungler, *J. Mol. Catal. A:Chem.*, **179** (2002) 107.
- 4 R.L. Augustine et al., *J. Mol. Catal. A:Chem.*, **95** (1995) 277.
- 5 W.R. Huck, T. Burgi, T. Mallat, A. Baiker, *J. Catal.*, **200** (2001) 171.
- 6 A. Baiker et al., *Catal. Lett.*, **80** (2002) 3.
- 7 S.P. Griffiths, PhD thesis, University of Hull, 1997.
- 8 K. Borszky, T. Burgi, Z. Zhaouhui, T. Mallat, A. Baiker, *J. Catal.*, **187** (1999) 160.
- 9 A. Baiker, A. Pfaltz, M. Schurch, T. Mallat, T. Heinz, B. Minder *J. Catal.*, **160** (1996) 261.
- 10 G.A. Somarjai, *Introduction to Surface Chemistry and Catalysis*, Wiley, New York, 1994, p90.

# *Chapter 3*

### 3.1 The Standard Reaction

The target reaction in this work has been the enantioselective hydrogenation of *N*-acetyl dehydrophenylalanine methyl ester (NADPME) to *N*-acetyl phenylalanine methyl ester using alkaloid modified metal catalysts (Figure 3.1.1).

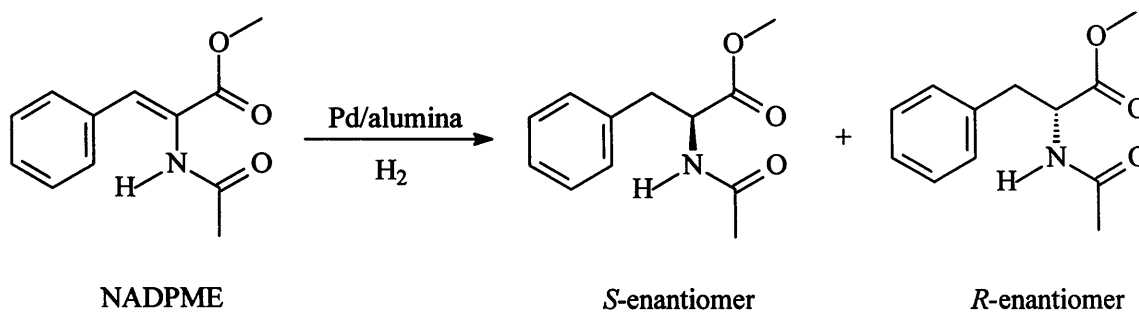


Figure 3.1.1 The hydrogenation of *N*-acetyl dehydrophenylalanine methyl ester (NADPME) to the corresponding *R*- and *S*- enantiomers of *N*-acetyl phenylalanine methyl ester

Various catalysts and modifiers were screened to establish their effectiveness for the enantioselective hydrogenation of NADPME.

#### 3.1.1 Choice of Catalyst

Rhodium, platinum and palladium on various supports were used to determine the most suitable catalyst for the hydrogenation (Table 3.1.1). The conditions reported by Nitta for the enantioselective hydrogenation for  $\alpha,\beta$ -unsaturated acids were taken as a guide [1]. The cinchona alkaloid cinchonine was chosen as modifier for this catalyst screening exercise. Palladium was the only effective catalyst for the enantioselective hydrogenation of the carbon – carbon double bond in NADPME. Rhodium catalysed the hydrogenation to give racemic product both in the absence and presence of cinchonine. Platinum also catalysed the required hydrogenation, but NMR spectra of the products showed that significant hydrogenation of the amide carbonyl group and of the aromatic ring had also occurred. Reducing the temperature of the Pt-catalysed reaction from 298 K to 263 K did not favour the desired reaction.

A brief study was made of cinchonine adsorption on these catalysts by UV spectroscopy. Fast adsorption on Pd/alumina and Pt/alumina was observed, but no adsorption occurred on Rh/alumina over a 2 h period. The reason for the different behaviour of Rh/alumina is unclear, but it should be noted that cinchona-modified Rh is not an effective catalyst for enantioselective pyruvate ester hydrogenation.

Table 3.1.1 Performance of various catalysts in the cinchonine modified hydrogenation of NADPME

Entry	Supplier	Batch number	Catalyst <sup>a</sup>	e.e. /%
1	Johnson Matthey	99300	5% Pd/alumina	10.0 ( <i>S</i> )
2	Johnson Matthey	99306	5% Pd/alumina	8.0 ( <i>S</i> )
3	Engelhard		5% Pd/carbon	5.0 ( <i>S</i> )
4	Engelhard		10% Pd/carbon	4.5 ( <i>S</i> )
5	Engelhard		5% Pd/silica	4.0 ( <i>S</i> )
6	Engelhard		5% Pd/calcium carbonate <sup>b</sup>	0
7	Engelhard		5% Pd/strontium carbonate <sup>b</sup>	0
8	Johnson Matthey		5% Rh/alumina	0
9	Johnson Matthey		5%Pt/alumina	Many unidentified products

<sup>a</sup>All catalysts used as received. <sup>b</sup>low activity, conversion <100%.

[Conditions: 20 ml methanol, 500 mg NADPME, 0.1 g catalyst, 5 mg cinchonine, 10 bar hydrogen pressure, T = 298 K, 1000 rpm, reaction time = 6 h, 100% conversion].

Pd/alumina was the most effective of the catalysts tested and was adopted as the standard catalyst for this investigation. It had been reduced by the manufacturer, and required no re-reduction before use. Table 3.1.2 compares the values of the enantiomeric excess achieved for catalyst used as received and catalyst re-reduced in 1 bar flowing hydrogen



at various temperatures. Performance was not improved by re-reduction, and hence normal procedure was to use catalyst as received. The footnotes to the Tables which follow, indicate the use of catalyst (1) or catalyst (2); catalyst (1) was that shown in Entry 1 in Table 3.1.1, and catalyst (2) was that shown in Entry 2 in Table 3.1.1.

Table 3.1.2 Values of enantiomeric excess for as-received and re-reduced catalysts

Reduction temperature /K	e.e. /% ( <i>S</i> )
Used as received	9.0
423	7.5
473	10.0
573	7.0
673	9.0

[Conditions: 20 ml methanol, 500 mg NADPME, 0.1 g catalyst (1), 5 mg cinchonine, 10 bar hydrogen pressure, T = 298 K, 1000 rpm, reaction time = 6 h, 100% conversion].

### 3.1.2 Choice of Alkaloid Modifier

The effectiveness of representative members of the cinchona, morphine and strychnos families of alkaloids as modifiers for NADPME hydrogenation over Pd/alumina was evaluated (Table 3.1.3). These alkaloids all induce enantioselectivity in  $\alpha$ -ketoester hydrogenation [2, 3], although the performances of the strychnos and morphine alkaloids are usually inferior to that of the cinchona alkaloids [4, 5]. A similar pattern of behaviour was observed for NADPME hydrogenation.

The highest enantioselectivities were achieved with cinchonine and 10,11-dihydrocinchonine, which favoured formation of the *S*-enantiomer. Cinchonidine and 10,11-dihydrocinchonidine afforded an excess of the *R*-enantiomer but both were less effective than cinchonine and dihydrocinchonine under the conditions used. This contrasts with most reports in the literature in which cinchonidine is usually superior to cinchonine as modifier [6]. Moreover, in the hydrogenation of  $\alpha,\beta$ -unsaturated acids, cinchonine normally favours the *R*-product and cinchonidine the *S*-product. Therefore,

the sense of the enantioselectivities recorded in Table 3.1.3 was unexpected. Saturation of the vinyl group in cinchonine and cinchonidine had no effect on the sense or magnitude of the enantiomeric excess. It is probable that, under the chosen conditions, saturation of the vinyl group occurred rapidly before significant hydrogenation of NADPME had taken place.

Table 3.1.3 Values of enantiomeric excess provided by various modifiers tested in the hydrogenation of NADPME over Pd/alumina.

Alkaloid type	Modifier	e.e./%
Cinchona	Cinchonine	9.0 ( <i>S</i> )
Cinchona	10,11-Dihydrocinchonine	9.5 ( <i>S</i> )
Cinchona	Cinchonidine	3.5 ( <i>R</i> )
Cinchona	10,11-Dihydrocinchonidine	4.0 ( <i>R</i> )
Cinchona	Quinine	0
Cinchona	Quinidine	1.0 ( <i>R</i> )
Morphine	Oxycodone	3.5 ( <i>S</i> )
Morphine	Codeine	1.5 ( <i>R</i> )
Strychnos	Brucine	0.5 ( <i>S</i> )
-	3-(1-Naphthyl)-L-alanine	1.0 ( <i>S</i> )

[Conditions: 20 ml methanol, 500 mg NADPME, 0.1 g catalyst (1), 5 mg modifier, 10 bar hydrogen pressure, T = 298 K, 1000 rpm, reaction time = 6 h, 100% conversion].

The more sterically hindered cinchona alkaloids quinine and quinidine gave racemic product. The morphine and strychnos alkaloids were ineffective and were not studied further.

### 3.1.2.1 Effect of modifier on reaction rate

Figure 3.1.2 shows the hydrogen uptake curves obtained during NADPME hydrogenation in the presence and in the absence of cinchonine. A fast initial uptake of hydrogen was observed in both reactions, which was attributed to the equilibration of hydrogen between the gas phase and the solution phase and, for the enantioselective

hydrogenation only, the saturation of the vinyl group in cinchonine. NADPME hydrogenation, which followed these initial fast processes, occurred at initial rates measured as described in Section 3.2. These initial rates were  $48 \text{ mmol h}^{-1} \text{ g}^{-1}$  for the racemic reaction and  $10 \text{ mmol h}^{-1} \text{ g}^{-1}$  for the enantioselective reaction. Thus, the effect of the presence of the modifier was to reduce reaction rate. Further reduced rates were observed with increasing mass of cinchonine. This is typical for enantioselective reductions of carbon – carbon double bonds over cinchona modified Pd [6 - 9].

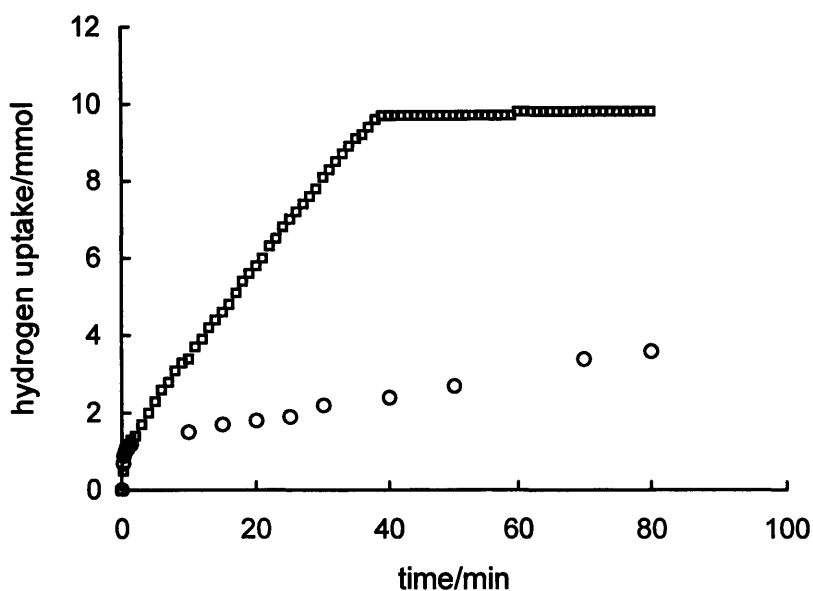


Figure 3.1.2 Typical hydrogen uptake curves recorded for (□) unmodified and (○) cinchonine modified hydrogenation of NADPME.

[Conditions for racemic reaction: 20 ml methanol, 2.0 g NADPME, 0.2 g catalyst (1), 10 bar hydrogen pressure,  $T = 298 \text{ K}$ , 1000 rpm. Conditions for enantioselective reaction were as for racemic reaction with the addition of 60 mg cinchonine].

### 3.1.3 Reaction Conditions

#### 3.1.3.1 Conditions for kinetic measurements

To obtain kinetic information for the modified hydrogenation of NADPME, the mass of reactant was increased to at least 1.0 g (4.5 mmol), so that reliable uptake time curves could be recorded. The mass of cinchonine and catalyst were increased proportionally so

as to maintain the same molar ratios as those for standard conditions. The amount of solvent used was 30 ml. Hydrogenations were then carried out under the same experimental conditions as for those of the standard reaction. The footnotes to the Tables and Figures which follow, state the amount of reactant, modifier and catalyst used in obtaining all kinetic measurements.

### 3.1.3.2 Conditions for standard (micro-scale) experiments

Micro-scale (standard) reactions were carried out on a small quantitative scale. These were: 10 ml solvent, 100 – 500 mg reactant, 50 mg – 250 mg catalyst and cinchonine between 10 – 50 mg. Footnotes to the Tables and Figures which follow state the exact amounts used.

### 3.1.4 Characteristics of the Standard Reaction

The initial investigation determined the most suitable catalyst to be Pd/alumina (1) and the most effective modifier to be cinchonine. Optimisation of the experimental conditions for NADPME hydrogenation over cinchonine-modified palladium was then carried out to obtain a set of standard conditions for future experiments. To determine these standard conditions the effects on enantiomeric excess of varying stirring speed, hydrogen pressure, temperature, and modifier concentration were studied, as was the effect of conversion. Methanol was used as solvent; it is shown later to be one of the most effective for the reaction.

#### 3.1.4.1 Effect of stirring speed on rate of reaction

Over the range studied the rate of stirring had very little effect on the rate of hydrogenation (Figure 3.1.3). This demonstrated that the rate was not limited by the mass transport of hydrogen from the gas phase through the liquid phase to the catalyst surface. For the purpose of defining conditions for the standard reaction, a stirring speed of 1000 rpm was adopted.

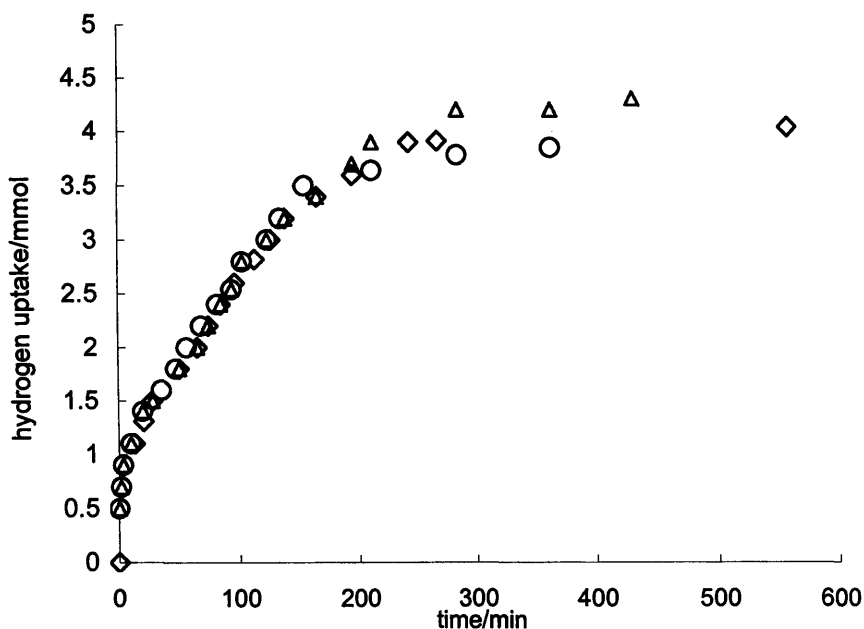


Figure 3.1.3 Dependence of rate of reaction on stirring rate. Rate of stirring/rpm: ◇, 600; ○, 800; △, 1000.

[Conditions: 30 ml methanol, 1.0 g NADPME, 0.2 g catalyst (1), 40 mg cinchonine, CN:NADPME molar ratio = 0.03, 10 bar hydrogen pressure,  $T = 298$  K, 1000 rpm, reaction time = 24 h].

#### 3.1.4.2 Variation of enantiomeric excess with hydrogen pressure

Figure 3.1.4 illustrates the dependence of enantiomeric excess on hydrogen pressure. An increase was observed over the range 1 to 10 bar, after which there was a sharp decrease. This behaviour contrasts with many enantioselective hydrogenations using cinchona modified Pd and Pt, where enantiomeric excess increases or remains constant as hydrogen pressure is increased [9, 10]. 10 bar hydrogen pressure was adopted as the standard pressure in subsequent reactions.

Conditions for the reactions were: 20 ml methanol, 500 mg NADPME, 0.1 g catalyst (1), 5 mg cinchonine,  $T = 298$  K, 1000 rpm, reaction time = 6 h, 100% conversion.

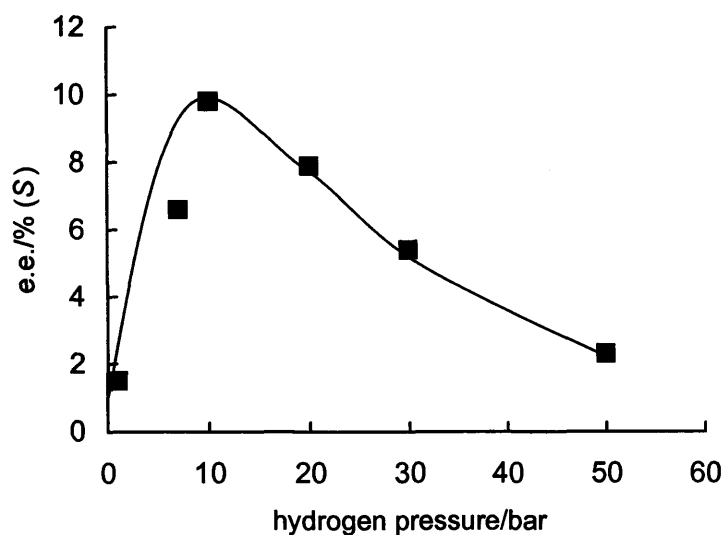


Figure 3.1.4 Variation of enantiomeric excess with hydrogen pressure for the cinchonine modified hydrogenation of NADPME. For conditions, see text.

#### 3.1.4.3 Dependence of enantiomeric excess on conversion

Enantiomeric excess was independent of conversion as shown in Table 3.1.4 and Figure 3.1.5. A similar conversion independence has been reported for the enantioselective hydrogenation of methoxypyrene over cinchona modified Pd [11].

Table 3.1.4 Dependence of enantiomeric excess on conversion

Time /min	Conversion /%	e.e. /% (S)
0	0	0
5	5	8.0
10	7	9.0
20	15	8.5
30	28	9.0
60	56	9.0
120	89	9.0
180	100	9.5

[Conditions: 10 ml methanol, 100 mg NADPME, 0.05 g catalyst (2), 10 mg cinchonine, 10 bar hydrogen pressure, T = 298 K, 1000 rpm].

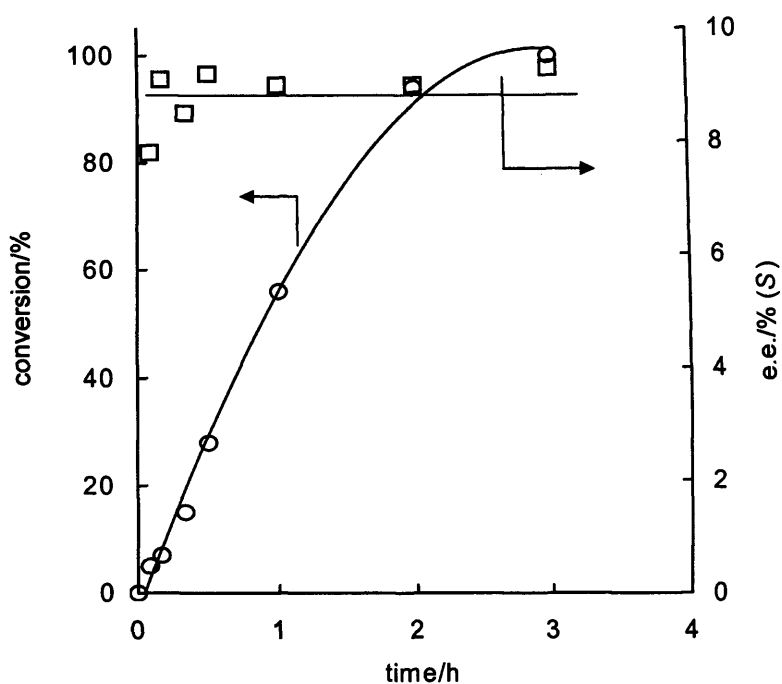


Figure 3.1.5 Dependence of enantiomeric excess on conversion.

Reaction was complete after three hours, and this was therefore adopted as the standard reaction time.

#### 3.1.4.4 Variation of enantiomeric excess with temperature

The dependence of enantiomeric excess on temperature for two cinchonine concentrations is shown in Table 3.1.5 and Figure 3.1.6.

Table 3.1.5 Variation of enantiomeric excess with temperature  
at two cinchonine concentrations

T/K	e.e./% ( <i>S</i> ) [CN:NADPME molar ratio = 0.01] <sup>a</sup>	e.e./% ( <i>S</i> ) [CN:NADPME molar ratio = 0.02] <sup>b</sup>
268	8.0	10.0
283	8.0	9.0
298	7.5	10.0
303	7.0	8.0
313	7.0	8.0

<sup>a</sup> 7 mg cinchonine. <sup>b</sup> 15 mg cinchonine. For conditions see Figure 3.1.6.

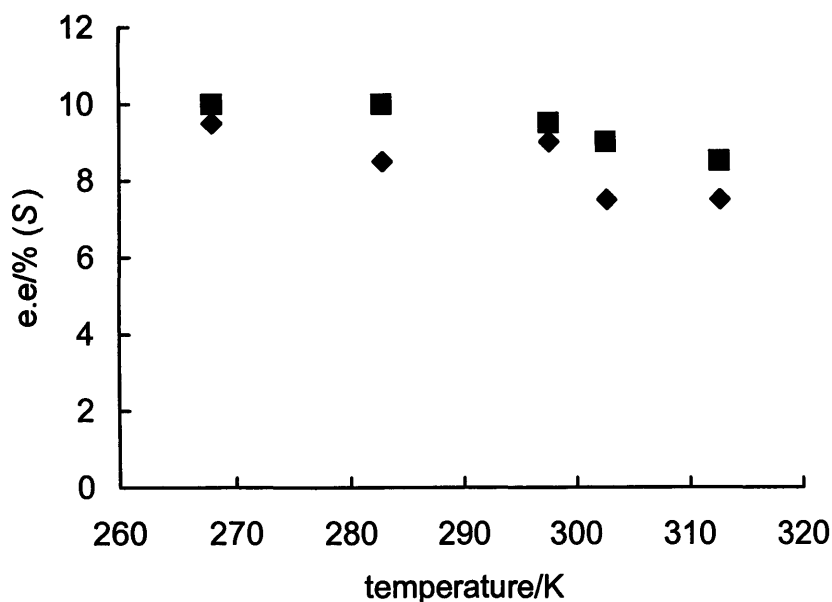


Figure 3.1.6 Variation of e.e. with temperature at two cinchonine concentrations:◆, 7 mg cinchonine;■, 15 mg cinchonine.

[Conditions: 20 ml methanol, 500 mg NADPME, 0.1 g catalyst (1), 10 bar hydrogen pressure, 1000 rpm, reaction time = 6 h, 100% conversion,].

The reproducibility of GC analysis for measuring enantioselectivity for a given sample is higher ( $\pm 0.7\%$ ) than the reproducibility of measurements of enantioselectivity between duplicate experiments ( $\pm 1.5\%$ ). Thus, the differences in enantiomeric excess recorded for 7 mg cinchonine and 15 mg cinchonine (Figure 3.1.6) are within the range of the experimental error. Thus, variation of reaction temperature had no substantial effect on enantiomeric excess.

#### 3.1.4.5 Variation of enantiomeric excess with mass of modifier

The amount of cinchonine used as modifier influenced enantiomeric excess (Table 3.1.6 and Figure 3.1.7).

With concentration of NADPME kept constant the enantiomeric excess showed maximum values for CN:NADPME molar ratios in the range 0.006 – 0.03. Variation of the ratio outside of this range resulted in lower values of the enantiomeric excess. When



Table 3.1.6 Variation of enantiomeric excess with mass of cinchonine.

Mass of CN /mg	CN:NADPME molar ratio	e.e. /% ( <i>S</i> )
0.5	0.004	7.0
1	0.006	10.0
2	0.01	9.5
3	0.02	9.0
4	0.03	9.5
10	0.07	7.5
20	0.14	6.0
40	0.20	5.5
<sup>a</sup> 50	0.42	4.0
<sup>a</sup> 80	0.60	3.0
100	0.72	2.0
<sup>a</sup> 150	1.0	2.0
<sup>a</sup> 200	2.0	0
<sup>a</sup> 300	2.7	0

<sup>a</sup> solutions saturated with cinchonine. For CN = 200 and 300 mg conversion = zero [Conditions: 10 ml methanol, 100 mg NADPME, 0.05 g catalyst (2), 10 bar hydrogen pressure, T = 298 K, 1000 rpm, reaction time = 3h, 100% conversion except in saturated solutions].

the amounts of cinchonine used exceeded 50 mg the solutions were saturated in alkaloid and were of equal cinchonine concentration. However the enantiomeric excess did not plateau but continued to decrease steadily (unfilled points, Figure 3.1.7). When 200 and 300 mg cinchonine was used no reaction occurred; under these conditions the alkaloid may have crystallised out over the palladium surface thus rendering it inactive.

As the concentration of cinchonine increased, so the pH of the reaction medium increased. It will be shown later (Section 3.6) that such an increase in pH has an unfavourable effect on enantiomeric excess.

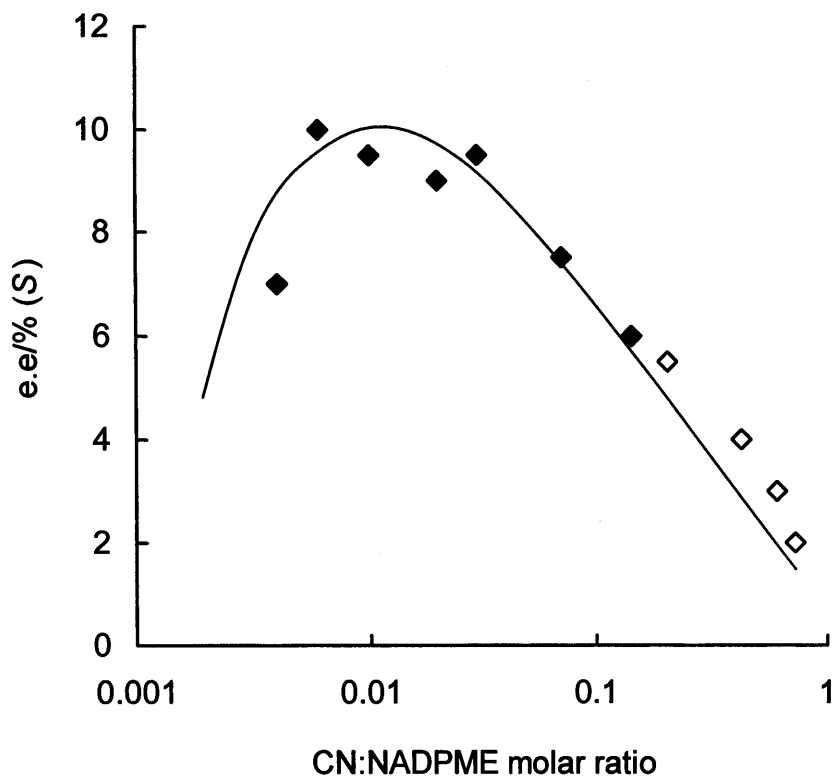


Figure 3.1.7 Semi logarithmic presentation of the variation of enantiomeric excess with cinchonine:NADPME molar ratio under standard conditions. [NADPME] = constant throughout. Unfilled points indicate solutions saturated with cinchonine. For conditions see Table 3.1.6.

It was concluded that optimum performance was obtained in this reaction by use of CN:NADPME molar ratios in the range 0.007 to 0.03, and values at the upper end of this range were normally adopted.

#### 3.1.4.6 Definition of standard conditions

The standard reaction conditions as described in this section are: 100 mg (0.46 mmol) NADPME, cinchonine as modifier with CN:NADPME molar ratios between 0.006 – 0.03, catalyst (1) and catalyst (2), 10 bar hydrogen pressure,  $T = 298$  K, 1000 rpm, reaction time 3 h and 100 % conversion.

## 3.2 Kinetics of NADPME hydrogenation

The effects on initial rate of varying mass of catalyst, hydrogen pressure and mass of reactant have been investigated as has the effect of temperature. To obtain reliable hydrogen uptake curves the mass of NADPME was increased from 100 mg (as used under the standard conditions) to 3.0 g for all kinetic measurements (with the exception of variation of mass of NADPME, for conditions see Chapter 2, Section 2.3.2).

Hydrogen uptake curves obtained for such hydrogenations show a fast consumption of hydrogen in the initial few minutes of reaction (Section 3.1, Figure 3.1.2). This is attributed to equilibration of hydrogen between the gas phase and solution phase. To determine the initial rate of reaction the apparent consumption of hydrogen due to dissolution in the solvent had to be distinguished from the real consumption due to NADPME hydrogenation. This was achieved by (i) fitting a polynomial curve to the data points, (ii) differentiating this curve to obtain an equation for its gradient at any point, and (iii) determining the gradient at zero time, which represented the initial rate. An example serves to demonstrate the method.

*An example of determination of initial rate:* Figure 3.2.1 shows results obtained from the hydrogenation of NADPME over cinchonine modified Pd. Conditions were: 20 ml methanol, 3.0 g NADPME, 60 mg cinchonine, 0.2 g Pd/alumina (2), 10 bar hydrogen pressure,  $T = 298 \text{ K}$ , and 1000 rpm.

Equation (1) describes the curve shown in black in Figure 3.2.1. Differentiation gives equation (2), which represents the gradient of the curve at any point.

$$y = -7.1 \times 10^{-5} x^2 + 6.3 \times 10^{-2} x + 0.70 \quad \leftarrow(1)$$

$$\text{rate} = dy / dx = -0.000142 x + 0.063 \quad \leftarrow(2)$$

Thus, the tangent to the curve at time zero (i.e.  $x = 0$ ) is  $0.063 \text{ mmol min}^{-1}$  which represents the initial rate of this reaction. The tangent is shown in blue in Figure 3.2.1.

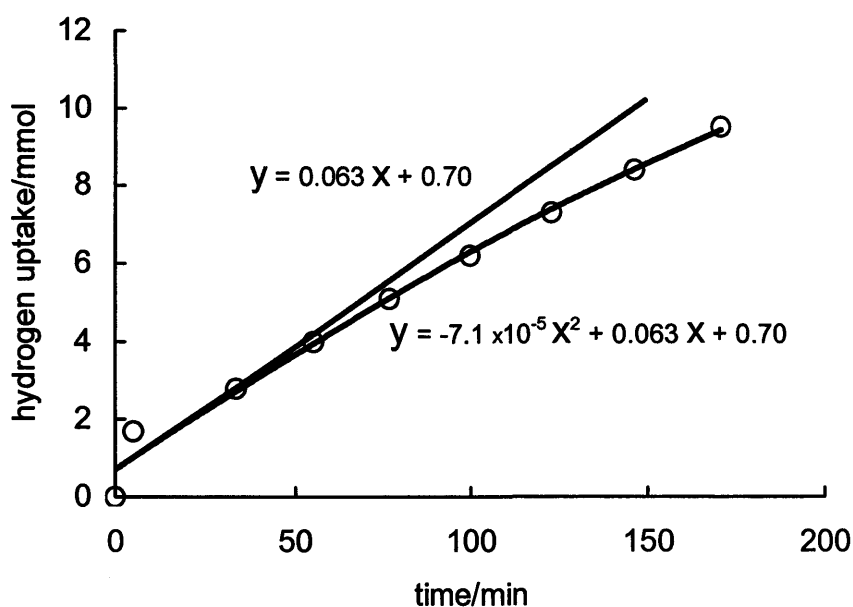


Figure 3.2.1 Typical variation of hydrogen uptake with time for NADPME hydrogenation. Conditions in text. The graph shows the experimental points, the polynomial curve fitted to the points, and the gradient at zero time which represents the initial rate.

### 3.2.1 Kinetics of the Unmodified Reaction

#### 3.2.1.1 Effect of mass of catalyst

Figure 3.2.2 shows the variation of hydrogen uptake with mass of catalyst for NADPME hydrogenation over unmodified Pd. The initial rates are presented in Table 3.2.1.

Table 3.2.1 Dependence of initial rate on mass of catalyst

Mass of catalyst /g	Initial rate /mmol min <sup>-1</sup>
0.2	0.050
0.4	0.119
0.6	0.247
1.2	0.727

[Conditions: 20 ml methanol, 3.0 g NADPME, catalyst (2), 10 bar hydrogen pressure, T= 298 K, 1000 rpm, reaction time 24 h].

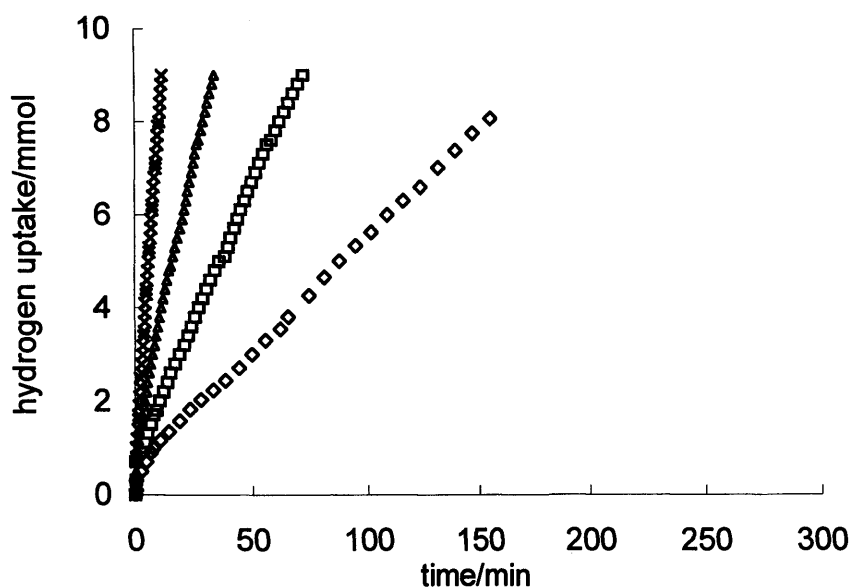


Figure 3.2.2 Dependence of hydrogen uptake on mass of catalyst. Mass of catalyst: ◇, 0.2 g; □, 0.4 g; △, 0.6 g; ×, 1.2 g. For conditions see Table 3.2.1

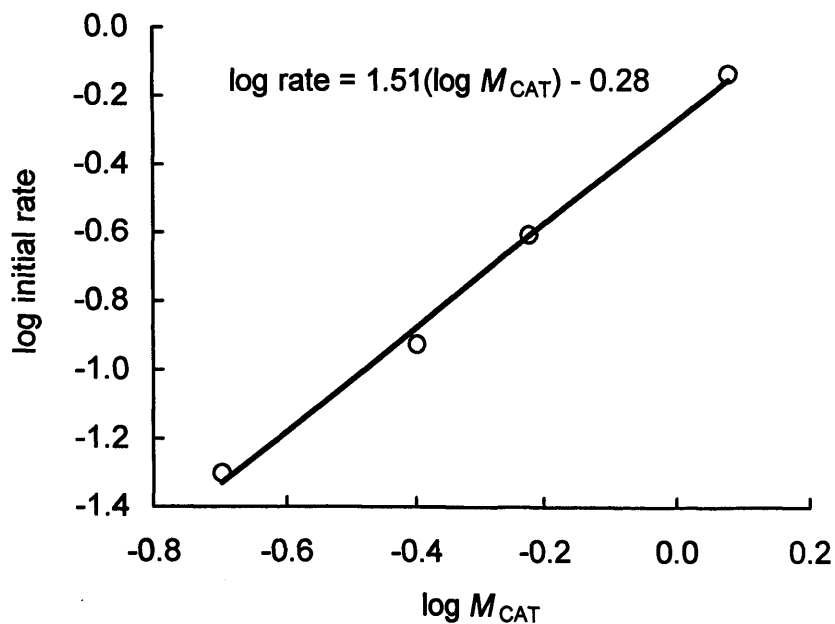


Figure 3.2.3 Logarithmic presentation of initial rate dependence on mass of catalyst. For conditions and original data see Table 3.2.1.

Initial rate increased with increasing mass of catalyst (Table 3.2.1). The order of reaction with respect to catalyst mass was determined from a logarithmic presentation of initial

rate against catalyst mass as 1.5, (Figure 3.2.3). This suggests no mass transport limitation.

### 3.2.1.2 Effect of hydrogen pressure

The dependence of hydrogen uptake on hydrogen pressure over the range 7 – 30 bar is shown in Figure 3.2.4 and in Table 3.2.2.

Table 3.2.2 Dependence of initial rate on hydrogen pressure

Hydrogen pressure /bar	Initial rate /mmol min <sup>-1</sup>
7	0.046
10	0.062
20	0.087
30	0.118

[Conditions: 20 ml methanol, 3.0 g NADPME, 200 mg catalyst (2), T = 298 K, 1000 rpm, reaction time 24 h].

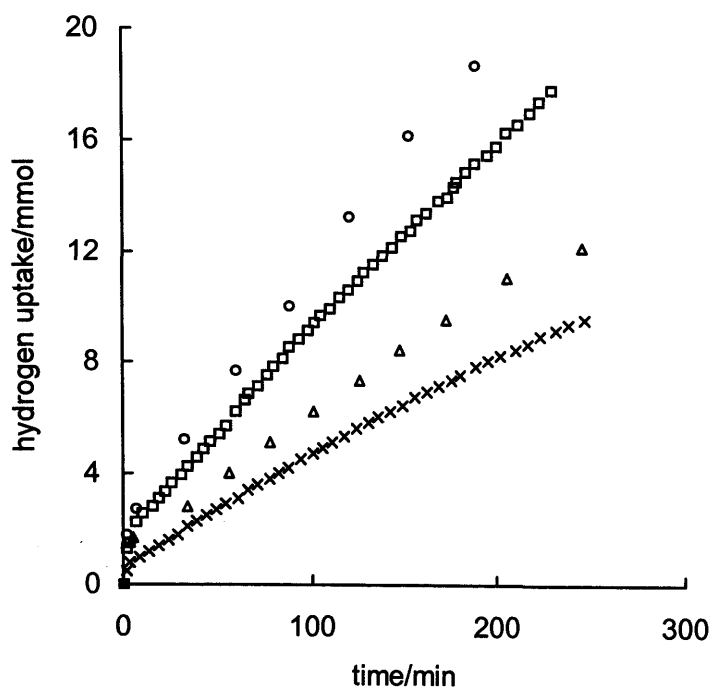


Figure 3.2.4 Dependence of rate of hydrogen uptake on hydrogen pressure. Hydrogen pressure: x, 7 bar; Δ, 10 bar; □, 20 bar; ○, 30 bar. For conditions see Table 3.2.2

The initial rate increased as a function of hydrogen pressure and the logarithmic presentation of these results in Figure 3.2.5 shows the order in hydrogen to be 0.6. Comparable half order dependencies in hydrogen pressure are reported in the literature for enantioselective hydrogenations over palladium [13].

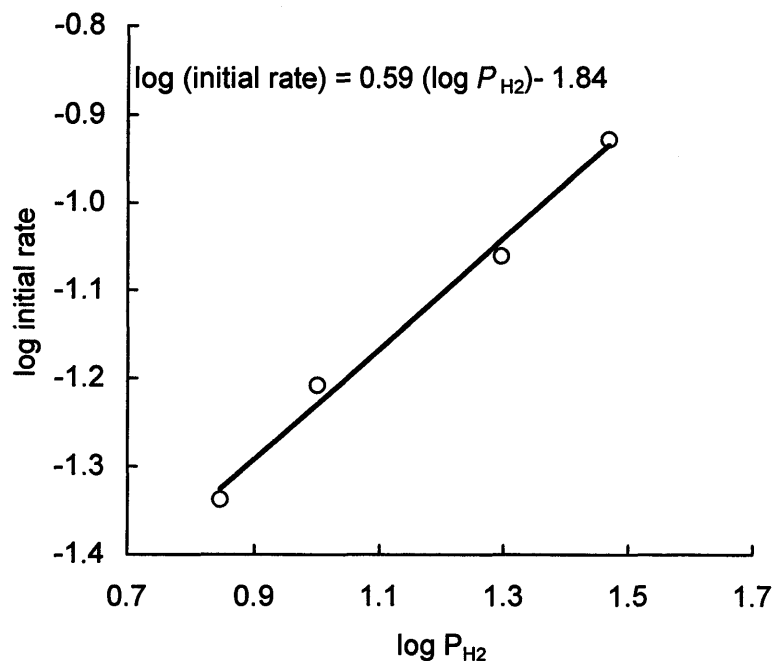


Figure 3.2.5 Logarithmic presentation of initial rate dependence on hydrogen pressure. For conditions see Table 3.2.2.

### 3.2.1.3 Effect of mass of reactant

Figure 3.2.6 shows hydrogen uptake curves obtained using various concentrations of NADPME.

Reactions were carried out over 0.2 g Pd/alumina (2) at 10 bar hydrogen pressure and room temperature at a stirring speed of 1000 rpm for 24 h. The rate of NADPME hydrogenation was independent of mass of NADPME, thus the reaction is of zero order with respect to [NADPME].

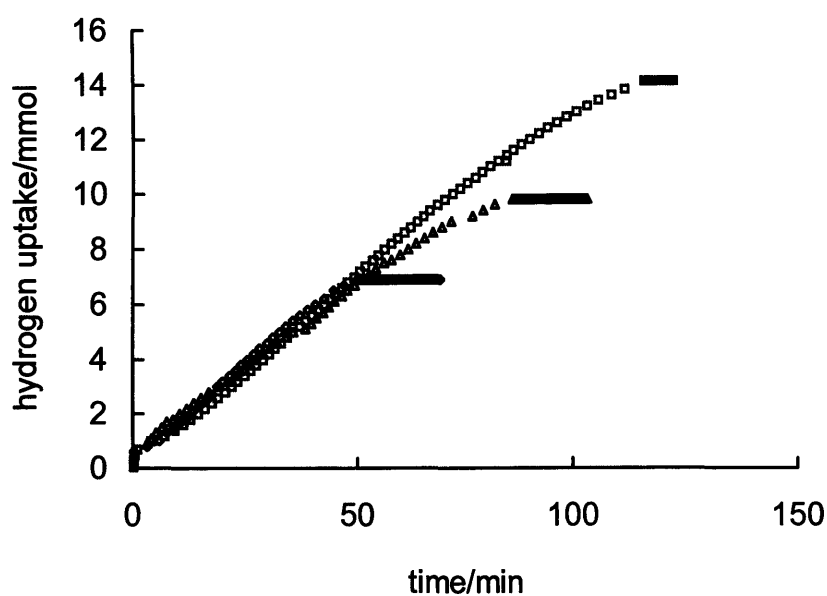


Figure 3.2.6 Dependence of hydrogen uptake on mass of NADPME. Mass of NADPME:  $\diamond$ , 1.5 g;  $\Delta$ , 3.0 g;  $\square$ , 4.5 g.

Thus, the overall rate equation for NADPME hydrogenation over unmodified Pd/alumina is given by:

$$\text{Rate} = k [M_{\text{CAT}}]^{1.5} [\text{NADPME}]^0 [P_{\text{H}_2}]^{0.6}$$

### 3.2.2 Kinetics of the Cinchonine-Modified Hydrogenation

For reactions involving 3.0 g (13.8 mmol) NADPME, 60 mg (0.2 mmol) of cinchonine was used. This provided a CN:NADPME molar ratio of 0.015 a value within the optimum conditions determined in Section 3.1.4.5.

#### 3.2.2.1 Effect of mass of catalyst

Figure 3.2.7 shows the dependence of hydrogen uptake on mass of catalyst. The initial rates and values of the enantiomeric excess are given in Table 3.2.3, and the logarithmic plot for the determination of the order in catalyst mass is shown in Figure 3.2.8.



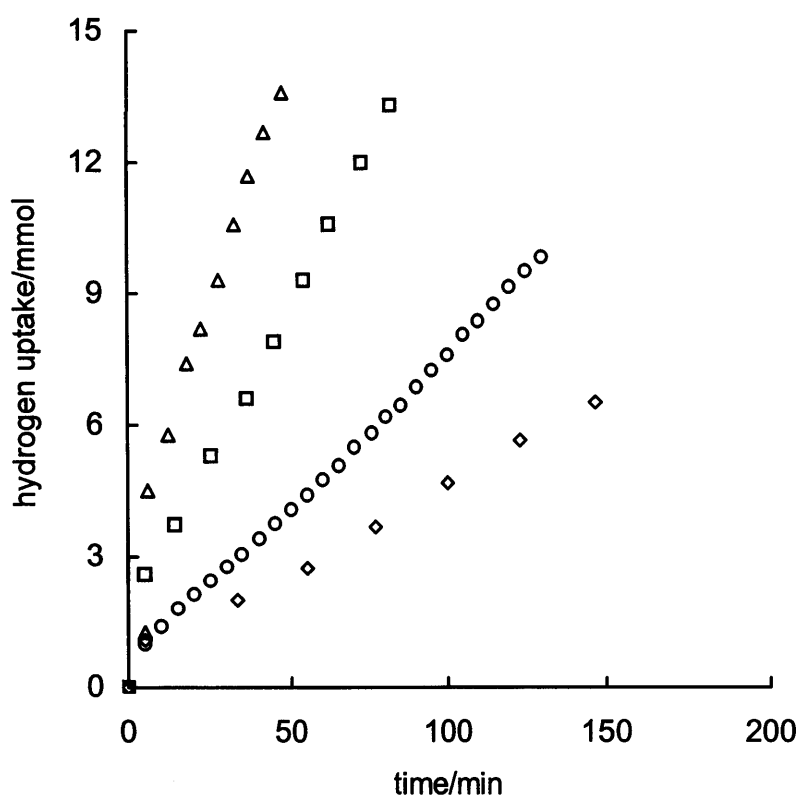


Figure 3.2.7 Dependence of hydrogen uptake on mass of catalyst. Mass of catalyst:  $\diamond$ , 0.2 g;  $\circ$ , 0.4 g;  $\square$ , 0.6 g;  $\Delta$ , 1.2 g. For conditions see Table 3.2.3.

Table 3.2.3 Dependence of initial rate and enantiomeric excess on mass of catalyst

Mass of catalyst /g	Initial rate /mmol min <sup>-1</sup>	e.e. /%(S)
0.2	0.046	7.0
0.4	0.070	8.0
0.6	0.173	7.0
1.2	0.366	6.5

[Conditions: 20 ml methanol, 3.0 g NADPME, catalyst (1), 60 mg cinchonine, 10 bar hydrogen pressure, T = 298 K, 1000 rpm, reaction time = 24 h, 100% conversion].

The values of enantiomeric excess in Table 3.2.3 are in agreement with those obtained under standard conditions and are similar in magnitude over the range of catalyst mass. The initial rate increases with mass of catalyst, the order in catalyst mass being 1.2 (Figure 3.2.8).

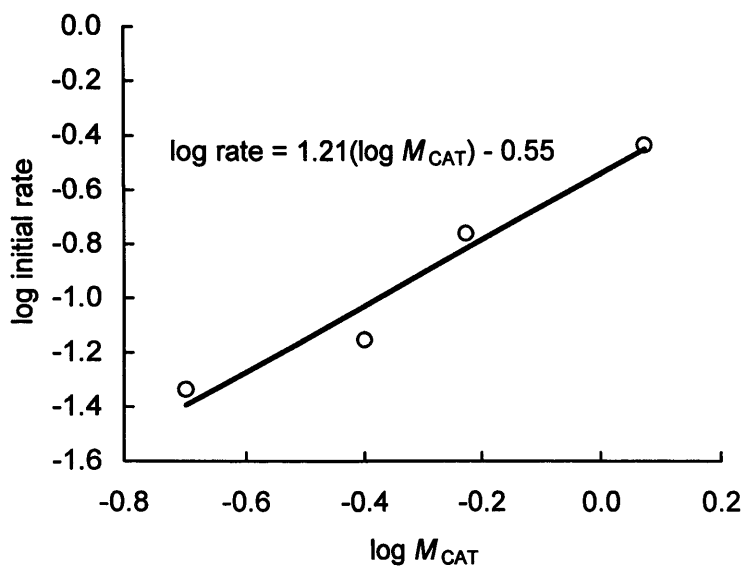


Figure 3.2.8 Logarithmic presentation of initial rate dependence on mass of catalyst. For conditions see Table 3.2.3.

### 3.2.2.2 Effect of hydrogen pressure

Figure 3.2.9 shows the hydrogen uptake curves observed with variation of hydrogen pressure over the range 7 – 50 bar.

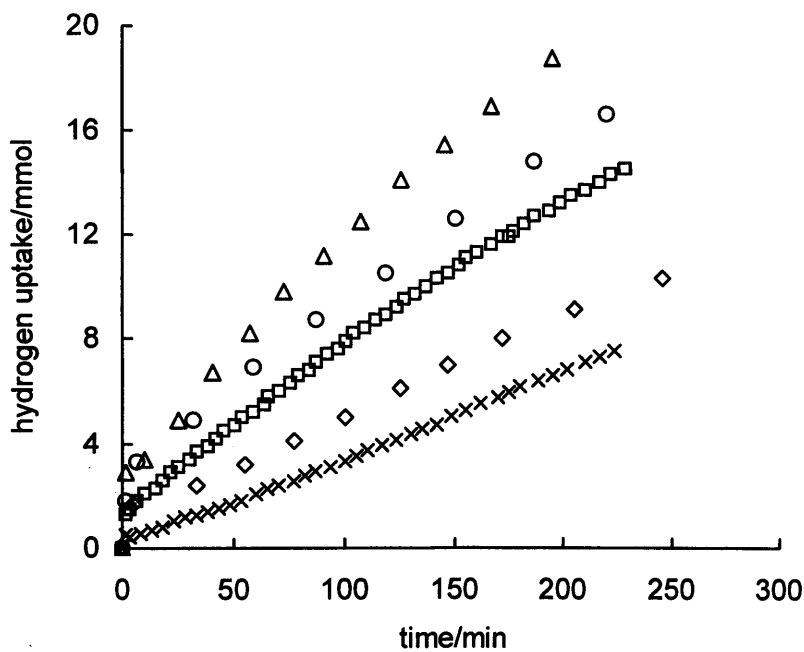


Figure 3.2.9 Dependence of hydrogen uptake on hydrogen pressure. Hydrogen pressure: x, 7 bar; ◇, 10 bar; □, 20 bar; ○, 30 bar; △, 50 bar. For conditions see Table 3.2.4.

The initial rates and enantioselectivities are presented in Table 3.2.4. The logarithmic plot (Figure 3.2.10) indicates an order in hydrogen pressure of 0.6. The values of enantiomeric excess over the same range show a similar pattern to that observed under standard reaction conditions. Curiously, for reaction conducted at 1 bar the hydrogen uptake curve was the same as that observed at 7 bar, but the value of enantiomeric excess was low (Table 3.2.4). This may be indicative of a different hydrogenation regime operating at ambient pressure.

Table 3.2.4 Dependence of initial rate and values of enantiomeric excess on hydrogen pressure

Hydrogen pressure /bar	Initial rate /mmol min <sup>-1</sup>	e.e. /%(S)
1	0.040	1.5
7	0.040	6.5
10	0.047	7.5
20	0.075	6.0
30	0.092	4.5
50	0.124	2.0

[Conditions: 20 ml methanol, 3.0 g NADPME, 0.2 g catalyst (1), 60 mg cinchonine, T = 298 K, 1000 rpm, reaction time = 24 h, 100% conversion].

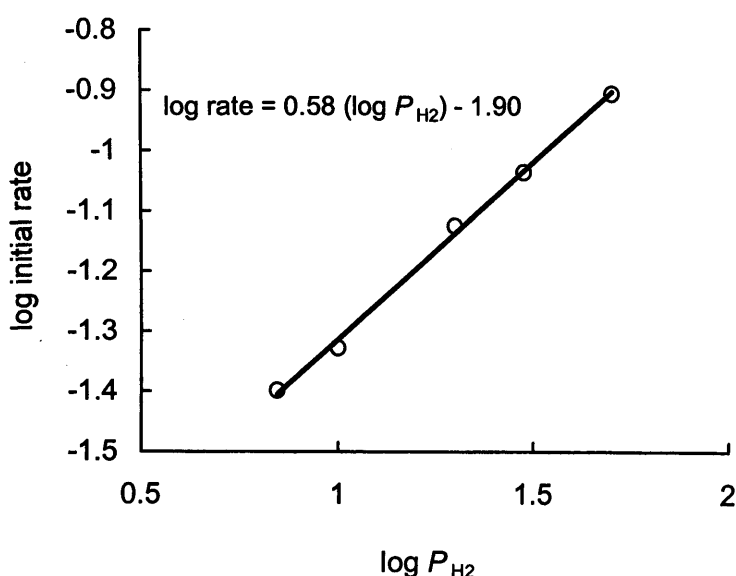


Figure 3.2.10 Logarithmic presentation of initial rate dependence on hydrogen pressure. For conditions see Table 3.2.4.



### 3.2.2.3 Effect of mass of reactant

Figure 3.2.11 shows the hydrogen uptake curves obtained using various NADPME concentrations. Initial rate was independent of mass of NADPME and the reaction is thus of zero order.

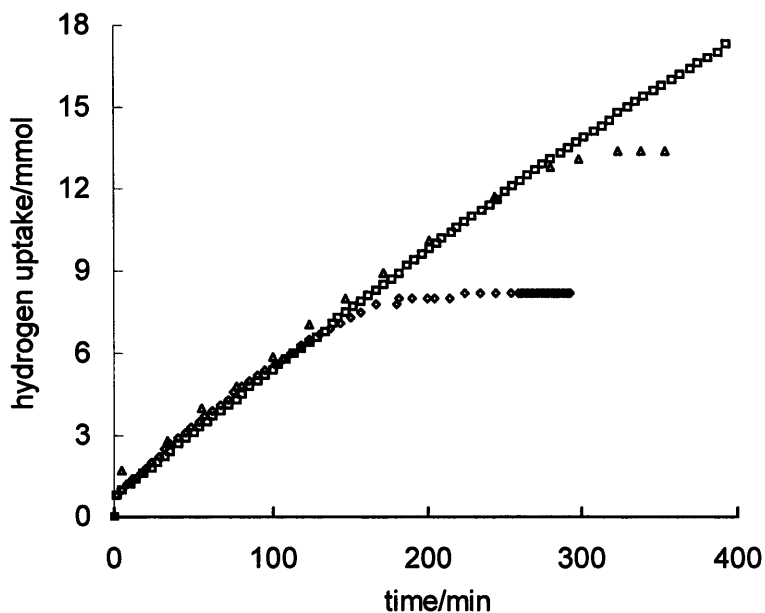


Figure 3.2.11 Dependence of hydrogen uptake on mass of NADPME. Mass of NADPME: ◇, 1.5 g; △, 3.0 g; □, 4.5 g.

[Conditions: 20 ml methanol, 0.2 g catalyst (1), 60 mg cinchonine, 10 bar hydrogen pressure,  $T = 298$  K, 1000 rpm, reaction time = 24 h, 100% conversion].

Thus, the overall rate equation for the hydrogenation of NADPME over cinchonine modified Pd is given by:

$$\text{Rate} = k [M_{\text{CAT}}]^{1.2} [\text{NADPME}]^0 [P_{\text{H}_2}]^{0.6}$$

Similar rate equations apply to the unmodified and the cinchonine-modified hydrogenations.

### 3.2.2.4 Effect of temperature

The effect of temperature on initial rate was measured over the range 280 – 309 K (Table 3.2.5)

Table 3.2.5 Influence of temperature on initial rate for the cinchonine-modified hydrogenation of NADPME

Temperature/ K	Initial rate/mmol min <sup>-1</sup>
280	0.011
289	0.031
299	0.055
309	0.090

[Conditions: 20 ml methanol, 3.0 g NADPME, 0.2 g catalyst (2), 60 mg cinchonine, 10 bar hydrogen pressure, 1000 rpm, reaction time = 24 h].

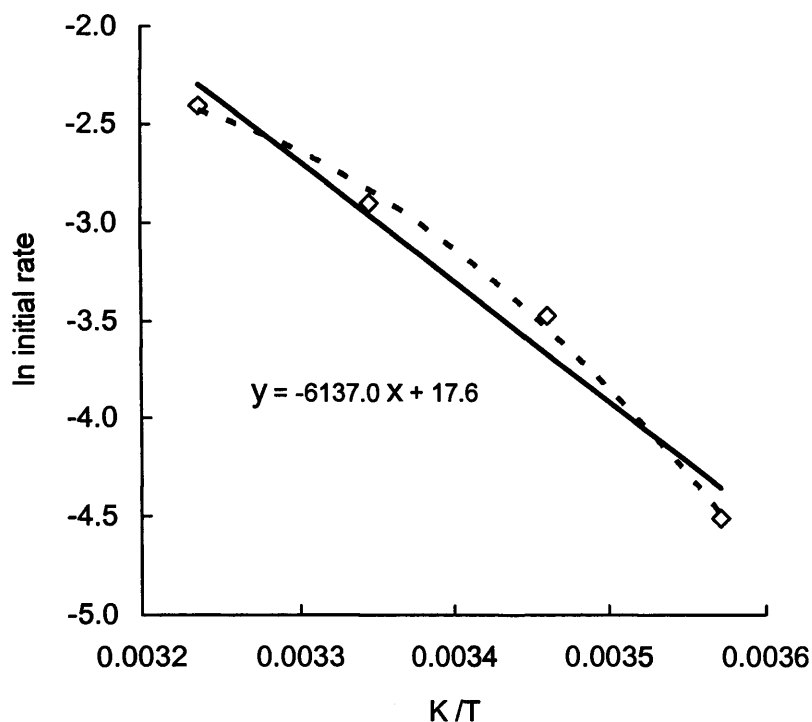


Figure 3.2.12 Arrhenius plot for determination of activation energy

The points in Figure 3.2.12 lie on a shallow curve (dotted blue curve) indicating mass transfer limitation at higher temperatures. The Arrhenius line (black line) is an approximation; the activation energy determined from this line was 51 kJ mol<sup>-1</sup>.

### 3.3 Solvent Effects

#### 3.3.1 Reactions in Various Solvents.

The variation of enantiomeric excess with mass of cinchonine for reactions conducted under standard conditions in various solvents is shown in Table 3.3.1 and Figure 3.3.1.

Table 3.3.1 Variation of enantiomeric excess with cinchonine concentration for reactions in various solvents

CN:NADPME molar ratio	e.e./% ( <i>S</i> )			
	Methanol	Ethanol	<sup>a</sup> DCM	<sup>b</sup> DMF
0.006	7.0	4.0	0	7.0
0.02	9.0	5.0	2.5	13.0
0.07	8.0	6.0	3.0	18.0
0.2	5.0	4.0	<sup>c</sup> 2.0	<sup>c</sup> -
0.4	<sup>c</sup> 4.0	<sup>c</sup> 3.5	<sup>c</sup> 1.0	<sup>c</sup> -
1.0	<sup>c</sup> 2.0	<sup>c</sup> 2.0	<sup>c</sup> 0	<sup>c</sup> -

<sup>a</sup> Dichloromethane. <sup>b</sup> *N,N*-Dimethyl formamide. <sup>c</sup> Cinchonine-saturated reaction medium, conversion too low to measure e.e. accurately.

[Conditions: 10 ml solvent, 100 mg NADPME, 0.05 g catalyst (2), 10 bar hydrogen pressure, T = 298 K, 1000 rpm, reaction time = 3 h].

Similar trends were observed with each solvent, enantiomeric excess first increasing and later decreasing as the mass of cinchonine was increased.

Maximum values of enantiomeric excess were observed for CN:NADPME molar ratios in the range 0.02 to 0.07. Solvents giving the highest enantioselectivities were *N,N*-dimethylformamide and methanol. Cinchonine showed limited solubility in all solvents which, when exceeded, caused a decrease in rate and enantioselectivity.

The overall effect of solvent on enantiomeric excess was DMF > MeOH > EtOH > DCM suggesting a correlation between dielectric constant of solvent and enantioselectivity. This was probed further by use of a wider range of solvents (Table 3.3.2). Reactions were conducted in ten solvents and one mixed solvent, the dielectric constant of the solvents ranging from 2.3 to 111.0. Values of enantiomeric excess were recorded for reactions conducted under standard conditions, the molar ratio of CN:NADPME being 0.07 in all reactions (Table 3.3.2, Figures 3.3.2 and 3.3.3).

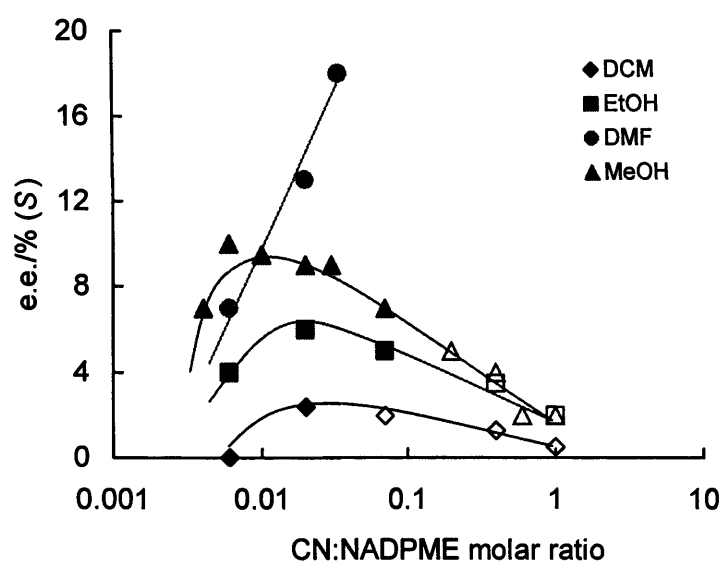


Figure 3.3.1 Semi logarithmic presentation of the variation of enantiomeric excess with cinchonine concentration for reactions in various solvents. [NADPME] = constant throughout. For conditions see Table 3.3.1. Unfilled points indicate reaction mediums saturated with cinchonine.

Table 3.3.2 Effect of dielectric constant of the solvent on enantiomeric excess and initial rate for cinchonine modified hydrogenation of NADPME

Solvent	Dielectric constant	<sup>a</sup> e.e. /%	Initial Rate /mmol min <sup>-1</sup>
Toluene	2.3	2.0 (S)	0.013
Acetic acid	6.1	2.0 (R)	- <sup>b</sup>
Tetrahydrofuran	7.6	3.0 (S)	0.025
Dichloromethane	8.9	4.0 (S)	0.023
DCM/acetic acid		2.0 (R)	- <sup>b</sup>
Ethanol	24.5	5.0 (S)	0.038
Methanol	32.7	9.0 (S)	0.063
<i>N,N</i> -Dimethylformamide	36.7	18.0 (S)	0.050
Dimethylsulfoxide	46.5	0	0
Water	78.3	20.0 (S)	0.069
Formamide	111.0	1.0 (S)	0.009

<sup>a</sup>[Conditions: 10 ml solvent, 100 mg NADPME, 0.05 g catalyst (2), 10 mg cinchonine, T = 298 K, 10 bar hydrogen pressure, 1000 rpm, reaction time = 3 h. <sup>b</sup> not measured

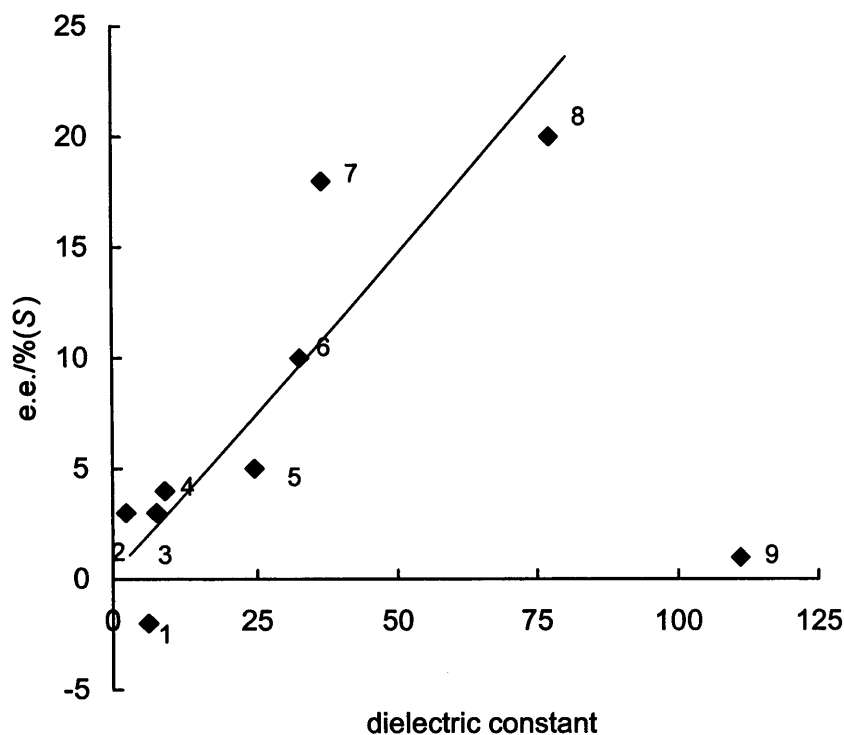


Figure 3.3.2 Variation of enantiomeric excess with dielectric constant of solvent. Key: 1 acetic acid, 2 toluene, 3 tetrahydrofuran, 4 dichloromethane, 5 ethanol, 6 methanol, 7 *N,N*-dimethylformamide, 8 water, 9 formamide. For conditions see Table 3.3.2.

For seven of the ten solvents enantiomeric excess increased with increasing dielectric constant of the solvent, in the order: DMF > methanol > ethanol > dichloromethane > tetrahydrofuran > toluene (Figure 3.3.2). The exceptional solvents were dimethylsulfoxide, formamide, acetic acid and DCM/acetic acid. The first two of these solvents appeared to poison the reaction, whereas normal reaction was observed for reactions in acetic acid and DCM/acetic acid but a reversal of the sense of enantioselectivity was recorded.

The solvents that promoted the highest enantioselectivities were those in which the reaction proceeded most rapidly (Figure 3.3.3).



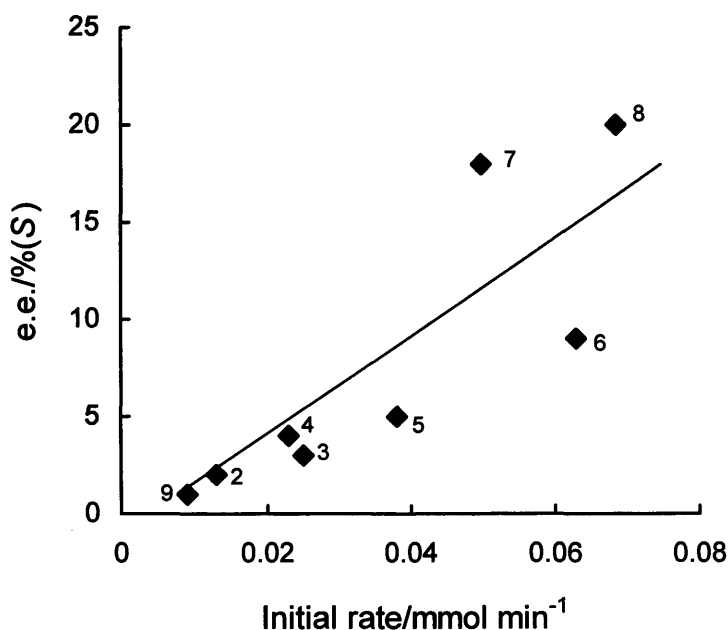


Figure 3.3.3 Correlation between enantiomeric excess and the initial rate. Key: 2 toluene, 3 tetrahydrofuran, 4 dichloromethane, 5 ethanol, 6 methanol, 7 *N,N*-dimethylformamide, 8 water, 9 formamide

### 3.3.2 Reactions in Mixed Solvents

The highest enantioselectivity was achieved using water as solvent. However, both reactant and modifier showed poor solubility in this solvent which resulted in low reproducibility. Consequently the effect of water was studied by use of various water/methanol and water/DMF mixtures as solvent. Reactions were conducted in triplicate to assure reproducible results.

#### 3.3.2.1 Methanol/water mixtures

Reactions in methanol conducted using the optimum mass of cinchonine (10 mg) showed higher enantioselectivities when small amounts of water were added to the reaction (Table 3.3.3 and Figure 3.3.4). The maximum increase in enantiomeric excess occurred approximately at 3% by volume of water added, after which further addition of water resulted in a decrease in enantioselectivity to a value similar to that observed in the absence of water.

Table 3.3.3 Values of enantiomeric excess for triplicated reactions conducted in various water/methanol mixtures.

Water added /% by volume	e.e. /% (S)	e.e. /% (S)	e.e. /% (S)
0	7.0	7.0	7.5
1	7.0	9.0	8.0
2	8.0	13.0	11.0
3	12.0	12.0	13.0
4	11.0	9.5	10.0
5	10.0	9.0	9.0
7	6.0	8.0	7.0
10	7.0	8.0	7.0
15	5.0	6.0	6.0

[Conditions: 10 ml solvent, 100 mg NADPME, 0.05 g catalyst (2), 10 mg cinchonine, 10 bar hydrogen pressure, T = 298 K, 1000 rpm, reaction time = 3 h].

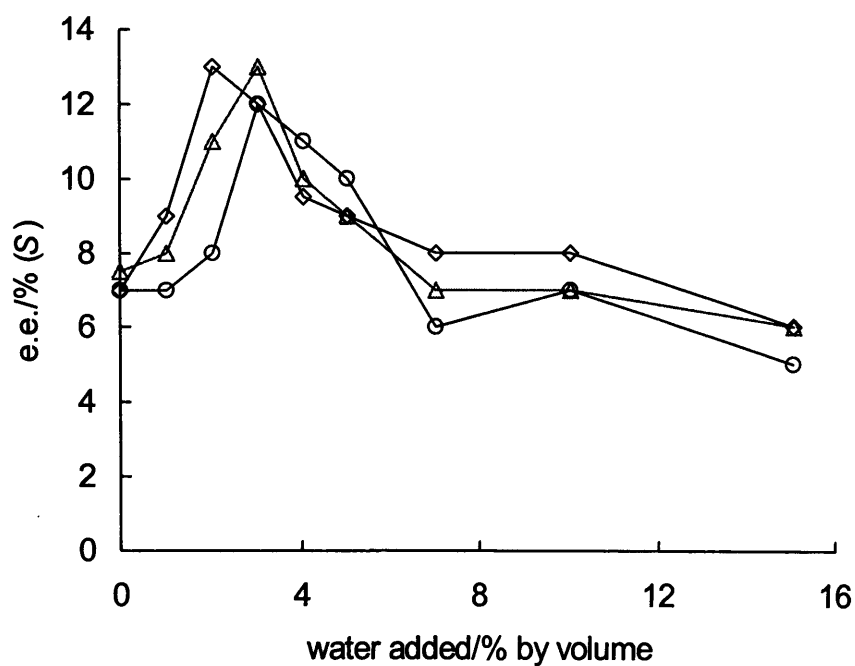


Figure 3.3.4 Variation of enantiomeric excess with water content for triplicated reactions in methanol/water mixtures. For conditions see Table 3.3.3.

3.3.2.2 *N,N*-Dimethylformamide/water mixtures

A similar pattern of behaviour was observed when water was added to dimethylformamide as solvent (Table 3.3.4 and Figure 3.3.5). In this system, the enantiomeric excess increased from 19% to 33%, and high enantioselectivity was maintained over a substantial range of solvent composition.

Table 3.3.4 Values of enantiomeric excess for duplicated reactions in various *N,N* Dimethylformamide/water mixtures.

Water added /% volume	e.e. /% ( <i>S</i> )	e.e. /% ( <i>S</i> )
0	18.0	19.0
3	29.0	31.0
5	28.0	29.0
10	31.0	33.0
12	32.0	30.0
15	24.0	27.0
20	24.0	27.0

[Conditions: 10 ml solvent, 100 mg NADPME, 0.05 g catalyst (2), 10 mg cinchonine, 10 bar hydrogen pressure,  $T = 298\text{ K}$ , 1000 rpm, reaction time = 3 h].

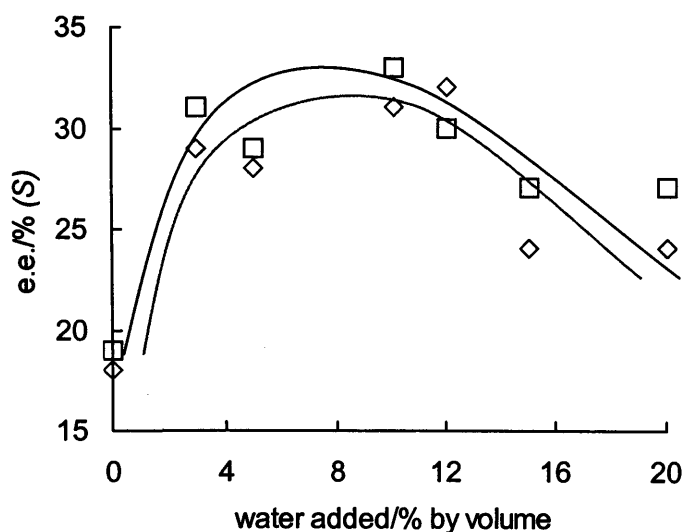


Figure 3.3.5 Variation of enantiomeric excess with water content for duplicated reactions in *N,N*-dimethylformamide/water mixtures. For conditions see Table 3.3.4.

### 3.4 Deuterium Tracer Studies

NADPME has the potential to exist in a tautomeric form, (Figure 3.4.1). It was necessary to examine whether this tautomer contributed to product formation under the experimental conditions used.

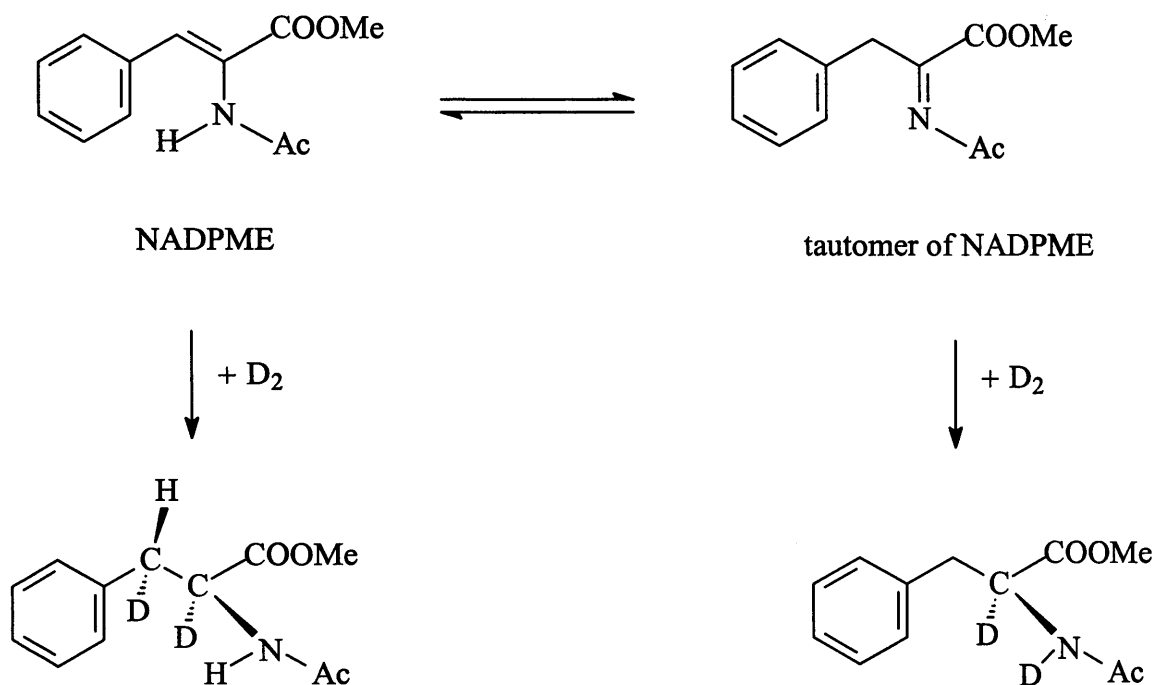


Figure 3.4.1 Structure of NADPME and the tautomeric form

Reactions were conducted under standard conditions and in various solvents using 10 bar deuterium pressure. HNMR data for the hydrogenation product for reaction using methanol as solvent are presented in Table 3.4.1. The spectra are shown in Figure 3.4.2.

For reactions in methanol the integrals attributed to  $CH$  and  $CH_2$  groups in the product diminished due to the presence of deuterium at these locations. The integral attributed to the proton of the  $NH$  group is of the size that would be expected, indicating no exchange of hydrogen for deuterium. Thus, deuterium addition only occurred across the carbon-carbon double bond and reaction via the tautomeric form was negligible.

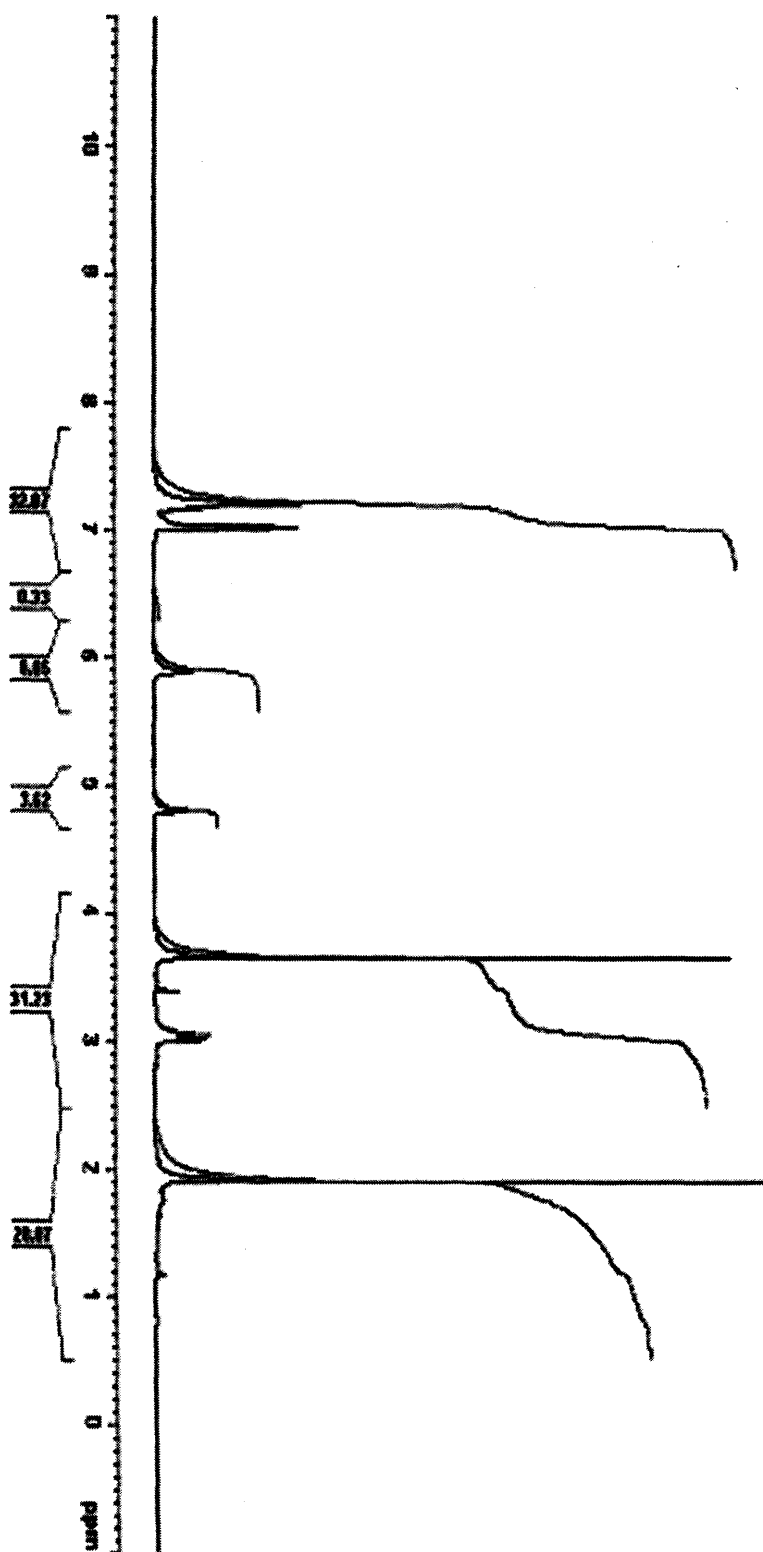


Figure 3.4.2  $^1\text{H}$ NMR for the product spectra of NADPME hydrogenation in deuterium

Table 3.4.1 Measured integrals from <sup>1</sup>HNMR spectra for the product of NADPME hydrogenation in hydrogen and in deuterium.

Functional group of assigned protons	Chemical shift (ppm)	Product integrals			
		Reaction in hydrogen		Reaction in deuterium	
		cms	<sup>a</sup> normalised	cms	<sup>a</sup> normalised
N-COCH <sub>3</sub>	3.8	9.3	3.2	9.2	3.1
COOCH <sub>3</sub>	1.9	8.7	3.0	8.9	3.0
CH	4.8	2.9	1.0	1.6	0.5
CH <sub>2</sub>	3.0	6.2	2.1	4.3	1.5
NH	5.9	2.7	0.9	2.9	1.0
Aromatic ring	7.0	14.7	5.1	14.7	5.0

<sup>a</sup> Integrals were normalised with respect to the integral for the protons on the COOCH<sub>3</sub> functional group.

Reactions in *N,N*-dimethylformamide, *N,N*-dimethylformamide/10%water, and methanol/3% water were also examined. Unfortunately, the <sup>1</sup>HNMR of the reaction product from each of these reactions was inconclusive.

### 3.5 Investigation of the Reactant Modifier Interaction

Systematic variations of reactant structure were made to assess the influence of the particular functional groups of NADPME on its enantioselective hydrogenation. Three functionalities were altered: the ester group, the *N*-acetyl group and the phenyl ring.

Reactions were conducted under the standard conditions and with the optimum mass of cinchonine known to be optimal for NADPME, since there was not the opportunity to optimise the system for each component. The masses of reactant (100 mg) and of catalyst (50 mg) were maintained constant throughout.

## 3.5.1 Alteration of the ester function of NADPME

The structures of NADPME and five related compounds are shown in Figure 3.5.1.

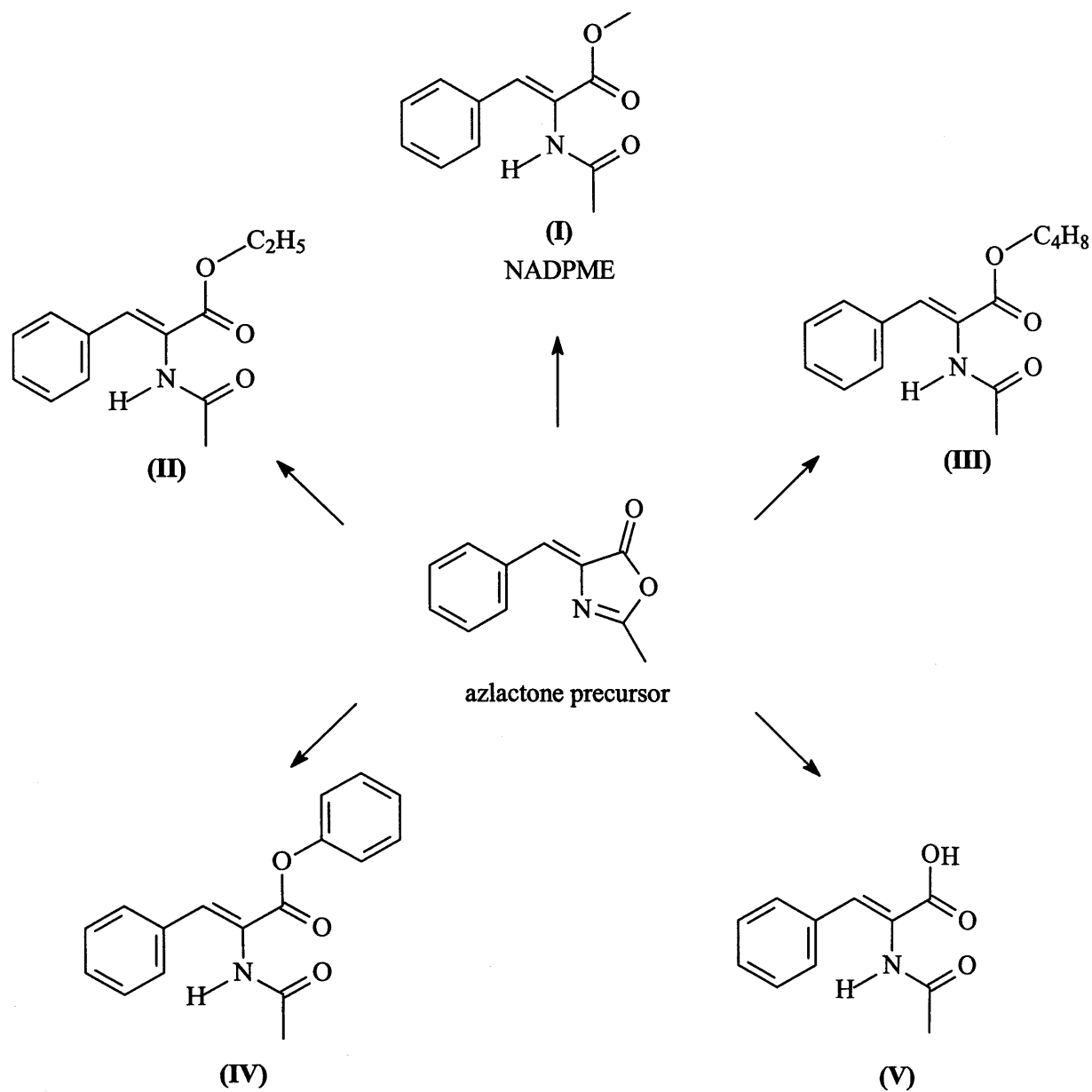


Figure 3.5.1 Structures of the azlactone precursor, NADPME and four derivatives.

Table 3.5.1 Values of enantiomeric excess observed in the products of hydrogenation of NADPME and in five related compounds

	Reactant	e.e./ % ( <i>S</i> )
(I)	<sup>a</sup> <i>N</i> -acetyl dehydrophenylalanine methyl ester	10.0
(II)	<sup>a</sup> <i>N</i> -acetyl dehydrophenylalanine ethyl ester	4.0
(III)	<sup>b</sup> <i>N</i> -acetyl dehydrophenylalanine butyl ester	3.0
(IV)	<sup>b</sup> <i>N</i> -acetyl dehydrophenylalanine benzyl ester	2.0
(V)	<sup>a</sup> <i>N</i> -acetyl dehydrophenylalanine	5.0
Azlactone precursor	<sup>a</sup> <i>N</i> -acetyl dehydrophenyl azlactone	8.0

<sup>a</sup> hydrogenated over catalyst (1), <sup>b</sup> hydrogenated over catalyst (2). [Conditions: 10 ml methanol, 100 mg reactant, 0.05 g catalyst, mass of cinchonine such that CN : reactant molar ratio = 0.07, 10 bar hydrogen pressure, T = 298 K, 1000 rpm, reaction time = 3 h].

Enantioselectivity decreased with increasing size of the alkyl group in the ester function in the order: methyl (I) > ethyl (II) > butyl (III) > benzyl (IV) (Table 3.5.1).

Direct hydrogenation of the azlactone precursor had the potential to create two chiral centres: one by hydrogenation of the >C=C< function and the other from the hydrogenation of >C=N-. However, under experimental conditions the azlactone ring opened forming the methyl ester, NADPME; this was confirmed by GC and NMR spectroscopy. Therefore, the similarity in e.e. observed for NADPME and the azlactone precursor was to be expected.

Hydrogenation of *N*-acetyl dehydrophenylalanine (V) resulted in a lower enantioselectivity compared to NADPME. This result was perhaps unexpected as  $\alpha,\beta$ -unsaturated acids are usually hydrogenated over cinchona modified Pd with enantioselectivities ranging from 20 to 72 % [14 - 16]. This result is discussed later.



### 3.5.2 Alteration of the *N*-acetyl function of NADPME

Replacing the *N*-acetyl group of NADPME with a methyl group to form (VI) resulted in a complete loss of enantioselectivity (Table 3.5.2). This is consistent with reports in the literature that  $\alpha,\beta$ -unsaturated esters are not enantioselectively reduced over cinchona-modified Pd [2]. Hydrogenations of dehydrophenylalanine (VII) and of its hydrochloride salt (VIII) resulted in values of the enantioselectivity similar to those observed for NADPME (Table 3.5.2).

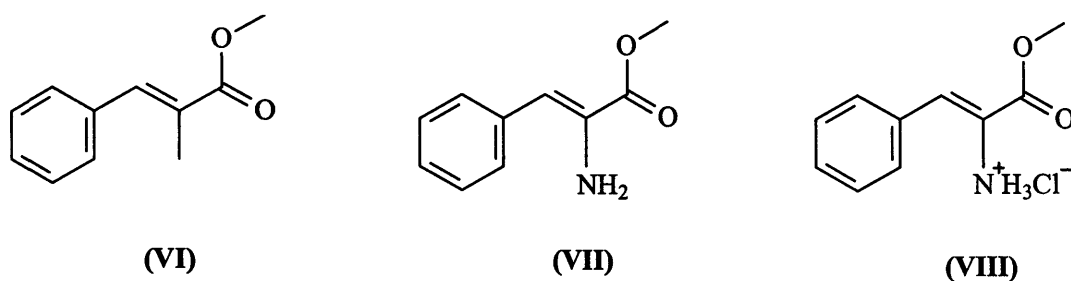


Figure 3.5.2 Structures of the methyl ester of methyl cinnamic acid (VI), dehydrophenylalanine (VII), and the hydrochloride salt of dehydrophenylalanine (VIII).

Table 3.5.2 Values of enantiomeric excess observed in the products of hydrogenation of three compounds related to NADPME

Reactant	e.e./% ( <i>S</i> )
(VI)	0
(VII)	11.0
(VIII)	14.0

[Conditions: 10 ml methanol, 100 mg reactant, 0.05 g catalyst (1), CN:reactant molar ratio = 0.07, 10 bar hydrogen pressure, T = 298 K, 1000 rpm, reaction time = 3 h].

The marginal improvement in e.e. observed for the hydrochloride salt (VIII) was probably due to a pH effect (see Section 3.6).

### 3.5.3 Alteration of the phenyl group of NADPME

Alterations made to the phenyl moiety of NADPME had no obvious effect on the values of enantiomeric excess achieved (Table 3.5.3).

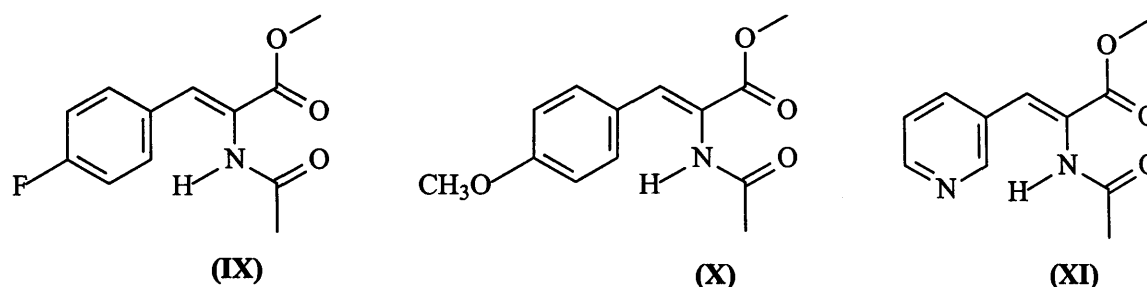


Figure 3.5.3 Structures of *N*-acetyl dehydro-4-fluorophenylalanine methyl ester (IX), *N*-acetyl dehydro-4-methoxyphenylalanine methyl ester (X) and *N*-acetyl dehydro-3-pyridylalanine methyl ester (XI).

Table 3.5.3 Values of enantiomeric excess observed in the products of hydrogenation of phenyl derivatives of NADPME

Reactant	e.e./% ( <i>S</i> )
(IX)	7.0
(X)	9.0
(XI)	9.0

[Conditions: 10 ml methanol, 100 mg reactant, 0.05 g catalyst (2), CN:reactant molar ratio = 0.07, 10 bar hydrogen pressure, T = 298 K, 1000 rpm, reaction time = 3 h].

### 3.5.4 Variation of Modifier

Five derivatives of cinchonine were studied to gain information regarding interactions between NADPME and the modifier. Reactions were conducted under the standard conditions already described for cinchonine modified hydrogenations. Table 3.5.4 shows the values of enantiomeric excess achieved and the extent of conversion over a 24 h

period.

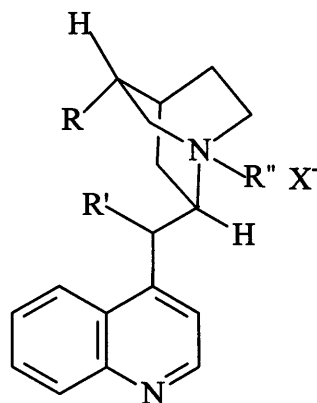


Figure 3.5.4 General structure of cinchonine derivatives

Table 3.5.4 Conversions and values of enantiomeric excess observed in NADPME hydrogenation over Pd/alumina modified by various derivatives of cinchonine. R, R', R'' and X<sup>-</sup> defined in Figure 3.5.4.

	R	R'	R''	X <sup>-</sup>	e.e. /% (S)	Conversion /%
Cinchonine	C <sub>2</sub> H <sub>3</sub>	OH	-	-	9.0	100
Dihydrocinchonine	C <sub>2</sub> H <sub>5</sub>	OH	-	-	9.5	100
Cinchonine mono- hydrochloride	C <sub>2</sub> H <sub>3</sub>	OH	H	Cl	14.0	42
Quaternised cinchonine	C <sub>2</sub> H <sub>3</sub>	OH	CH <sub>3</sub>	I	0	26
Quaternised cinchonine	C <sub>2</sub> H <sub>3</sub>	OH	CH <sub>3</sub>	Cl	0	40
4-chlorobenzoate quinidine	C <sub>2</sub> H <sub>5</sub>	COphCl	-	-	9.5	100

[Conditions: 10 ml methanol, 100 mg NADPME, 0.05 g catalyst (1), mass of modifier varied so that modifier:NADPME molar ratio = 0.07, 10 bar hydrogen pressure, T = 298 K, 1000 rpm, reaction time = 24 h].

As previously reported, no difference in modifier performance was observed between cinchonine and dihydrocinchonine with e.e. ~ 9% and full conversion reached after 3 h.

For cinchonine modified hydrogenations the actual effective modifier is dihydrocinchonine, as rapid reduction of the vinyl group occurred under the experimental conditions used.

Lower conversions in 24 h were observed for reactions carried out in the presence of the halide salts of cinchonine. This might be explained by supposing that the anions adsorbed on the surface and effectively poisoned the catalyst. The lowest conversion was recorded for reactions carried out in the presence of iodide anions; this is consistent with reports that the strengths of adsorption of the halide anions decrease in the order:  $I^- > Br^- > Cl^- > F^-$  [17]. Clearly, the lowest conversion was observed for the most strongly adsorbed anion.

Racemic product was formed with the N-methyl halide salts (entries 4 and 5), whereas, e.e. = 14% was observed with the hydrochloride salt. An interpretation of these observations relies on models to be advanced in Chapter 4 as does the result recorded as entry 6 in Table 3.5.4, where the enantioselectivity was unaffected.

## 3.6 Effect of Additives on the Standard Reaction

### 3.6.1 Effect of Acid

The effect of an acid additive on enantioselectivity for NADPME hydrogenation was studied using two acids, acetic acid and trifluoroacetic acid.

Reactions in methanol conducted using the optimum mass of cinchonine (10 mg) showed higher enantioselectivities when small amounts of acetic acid were added to the reaction (Table 3.6.1 and Figure 3.6.1). The maximum increase in enantiomeric excess occurred between 0.008 – 0.016 by volume of acetic acid added, after which further addition of acetic acid resulted in a decrease in enantioselectivity. The highest enantioselectivities were recorded for hydrogenations over catalyst (1), although catalyst (1) and (2) showed similar patterns of behaviour over the range studied.

Table 3.6.1 Values of the enantiomeric excess observed for NADPME hydrogenation for various methanol/acetic acid mixtures

Volume of acetic acid added (ml)	pH of reaction medium	e.e./%(S)	
		Catalyst (1)	Catalyst (2)
0	8.4	9.5	9.0
0.005	8.0	10.0	9.0
0.008	7.0	13.0	9.5
0.011	6.5	16.0	12.0
0.016	5.5	14.5	11.5
0.019	4.5	8.5	10.0
0.024	4.0	8.0	5.5
0.031	2.0	6.0	5.0

[Conditions: 10 ml methanol, 100 mg NADPME, 0.05 g catalyst, 10 mg cinchonine, 10 bar hydrogen pressure, T = 298 K, 1000rpm, reaction time = 3h].

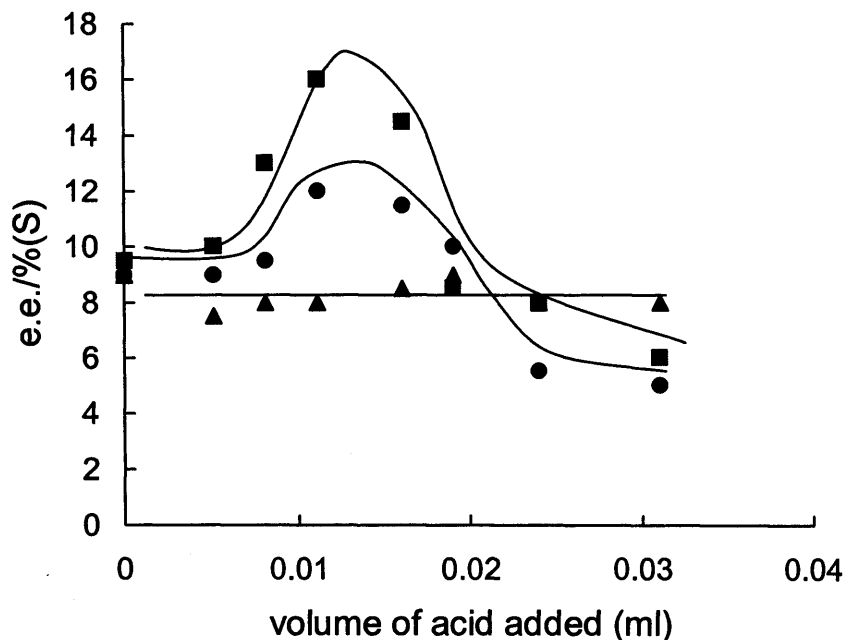


Figure 3.6.1 Values of enantiomeric excess achieved in the hydrogenation of NADPME over catalysts (1,  $\square$ ) and (2,  $\bullet$ ) for various volumes of acetic acid and for hydrogenation of NADPME over catalyst (2,  $\blacktriangle$ ) for various volumes of trifluoroacetic acid. For conditions see Table 3.6.1.

When trifluoroacetic acid was used in place of acetic acid a different effect of acid on enantioselectivity was observed (Figure 3.6.1). The value of enantiomeric excess varied only slightly over the range studied. This may indicate that weak and strong acids interact differently with the modifier, reactant or both, and thus, have a different effect on enantioselectivity. This result is discussed later.

### 3.6.2 Effect of Base

Various quantities of powdered potassium hydroxide were added to the reaction media and the results are presented in Table 3.6.2 and Figure 3.6.2.

Table 3.6.2 Values of the enantiomeric excess observed for NADPME hydrogenation for various methanol/potassium hydroxide mixtures

Mass of potassium hydroxide added (mg)	pH of the reaction medium	e.e./%( <i>S</i> )	
		Catalyst (1)	Catalyst (2)
0	8.4	9.5	9.0
10	9.5	7.0	6.0
50	10.5	4.0	4.0
130	11.0	0	0

[Conditions: 10 ml methanol, 100 mg NADPME, 0.05 g catalyst, 10 mg cinchonine, 10 bar hydrogen pressure, T = 298 K, 1000rpm, reaction time = 3h].

The value of enantiomeric excess decreased with the addition of powdered potassium hydroxide to the reaction media, such that for masses greater than 130mg, zero enantioselectivity was observed.

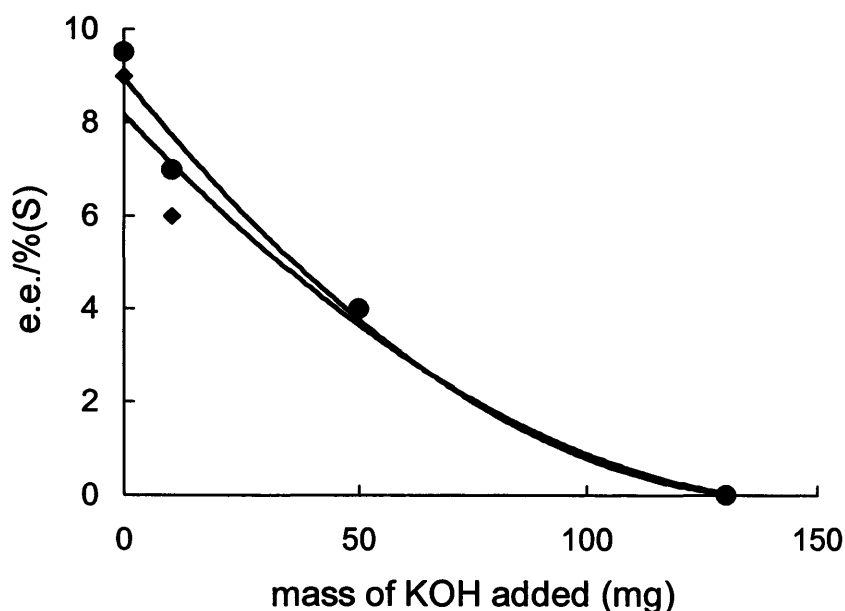


Figure 3.6.2 Values of enantiomeric excess achieved for the hydrogenation of NADPME over catalyst (1, ♦) and catalyst (2, ●) for various masses of potassium hydroxide added to the reaction media. For conditions see Table 3.6.2.

This detrimental effect on enantioselectivity for reactions conducted in basic media had implications for the definition of the standard conditions (see Section 3.1.4.6). The optimum mass of cinchonine of 1 – 10 mg gave reaction media having pH values between 8.0 and 8.4. Further addition of cinchonine raised the pH of the reaction medium and decreased enantioselectivity. In light of the results in Table 3.6.1 the optimum mass of cinchonine was re-assessed using reaction media buffered at pH = 6 using acetic acid (equivalent to the addition of 0.011 ml acetic acid under standard reaction conditions). The results are recorded in Table 3.6.3 and Figure 3.6.3.

Higher enantioselectivities were observed for hydrogenations conducted in buffered reaction media, with maximum values of enantiomeric excess recorded over a wider range of CN:NADPME molar ratios. A small decrease in the enantiomeric excess was observed when the CN:NADPME molar ratio exceeded 0.42, but the value remained

constant at 7% (*S*) thereafter. This contrasts with the results obtained for hydrogenations carried out under standard unbuffered conditions where, at CN:NADPME molar ratio exceeding 0.42 reaction solutions became saturated with cinchonine and the enantiomeric excess decreased to zero.

Table 3.6.3 NADPME hydrogenation over catalyst (2). Variation of enantiomeric excess with mass of cinchonine under (a) unbuffered conditions, (b) buffered condition pH = 6.

Mass of cinchonine /mg	CN:NADPME molar ratio	e.e./% ( <i>S</i> )	
		<sup>a</sup> Unbuffered conditions	<sup>b</sup> Buffered solutions at pH = 6
0.5	0.004	7.0	6.0
1	0.007	10.0	7.0
2	0.01	9.5	9.0
3	0.02	9.0	11.0
4	0.03	9.5	13.0
10	0.07	7.5	11.0
20	0.14	6.0	11.0
40	0.20	5.5	11.5
50	0.42	<sup>c</sup> 4.0	10.5
80	0.60	<sup>c</sup> 3.0	7.5
100	0.72	<sup>c</sup> 2.0	7.0
150	1.0	<sup>c</sup> 2.0	7.0
200	2.0	<sup>d</sup> 0	7.0
300	2.7	<sup>d</sup> 0	7.0

<sup>c</sup> solutions saturated with cinchonine. <sup>d</sup> solutions saturated with cinchonine; no reaction observed.

[Conditions: 10 ml methanol, 100 mg NADPME, 0.05 g catalyst (2), 10 bar hydrogen pressure, T = 298 K, 1000 rpm, reaction time = 3 h].



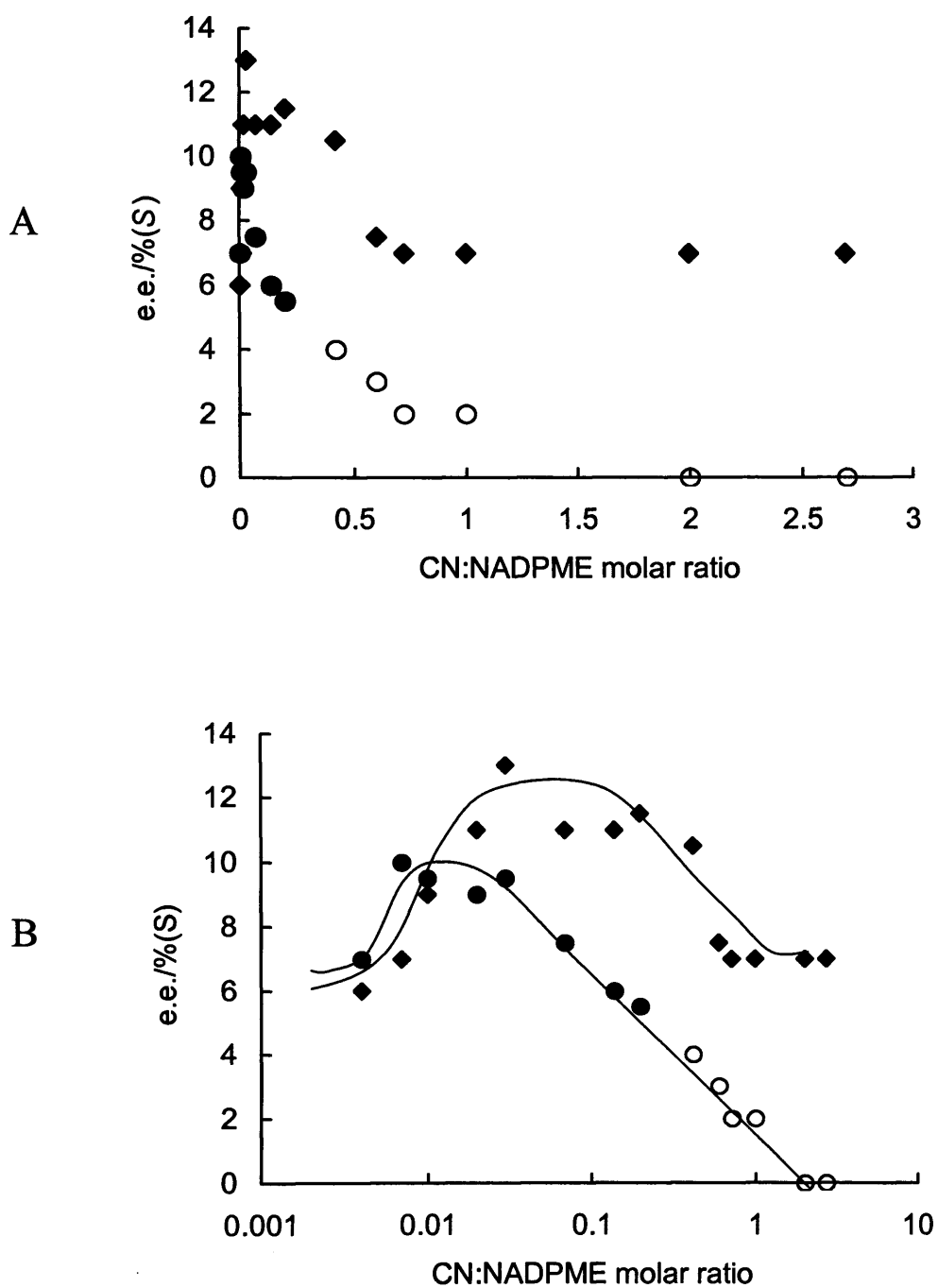


Figure 3.6.3 **A** - Variation of enantiomeric excess with CN:NADPME molar ratio. Mass of NADPME was constant throughout (100 mg, 0.46 mmol). (●), not buffered; (◆), buffered pH 6.. **B** - semi logarithmic presentation of **A**. Unfilled points indicate solutions saturated with cinchonine. For conditions see Table 3.6.3.

### 3.7 Hydrogenation of NADPME Catalysed by Pd/titania

According to literature reports, Pd/titania is the most effective catalyst for the hydrogenation of  $\alpha,\beta$ -unsaturated acids [14]; a range of such catalysts was prepared to investigate their effectiveness in NADPME hydrogenation.

#### 3.7.1 Catalyst Preparation

Palladium/titania catalysts were prepared as described in Sections 2.1.2.1 and 2.1.2.2 by (i) deposition-reduction, method (A) and (ii) wet impregnation, method (B). Table 3.7.1 compares their performance with that of the two Johnson Matthey 5% Pd/alumina catalysts used in the main body of this investigation and 5% Pd/alumina(A), a catalyst prepared in the laboratory by deposition-reduction.

Table 3.7.1 Variation of enantiomeric excess with CN:NADPME molar ratio for NADPME hydrogenations over various Pd/titania Pd/alumina catalysts

Entry	Catalyst	e.e./%(S)					
		CN:NADPME molar ratio					
		0.006	0.01	0.02	0.04	0.07	0.1
1	<sup>b</sup> 5% Pd/titania (A)	8.0	8.5	12.0	16.5	17.0	13.0
2	<sup>b</sup> 5% Pd/titania (B)	9.0	13.0	16.0	17.0	17.0	14.0
3	<sup>a</sup> 5% Pd/alumina (1)	10.0	9.0	9.5	10.0	7.0	8.0
4	<sup>a</sup> 5% Pd/alumina (2)	8.0	9.5	9.0	9.5	7.5	7.0
5	<sup>b</sup> 5% Pd/alumina (A)	9.0	13.0	14.5	14.0	14.0	13.5
6	<sup>c</sup> 5% Pd/titania (A)	7.5	8.0	8.5	8.0	7.5	7.0

<sup>a</sup> Supplied by Johnson Matthey. <sup>b</sup> Prepared in the laboratory, scale of preparation = 2 g.

<sup>c</sup> Prepared in the laboratory, scale of preparation = 7 g.

[Conditions: 10 ml methanol, 0.1 g NADPME, 0.05 g catalyst, cinchonine as modifier, 10 bar hydrogen pressure, T = 298 K, 1000 rpm, reaction time = 3 h].

The method of preparation made but little difference to the performance of these Pd/titania catalysts (Entries 1 and 2). These Pd/titania catalysts were superior to the Johnson Matthey Pd/aluminas at most CN:NADPME ratios (compare Entries 1 and 2 with 3 and 4). The Pd/alumina prepared by deposition-reduction (Entry 5) gave higher values of the enantiomeric excess than the Johnson Matthey Pd/alumina but was not as effective as the Pd/titania samples. It was clear, therefore, that titania was satisfactory as a support.

The Pd/titania samples reported in Entries 1 and 2 were taken from batches that had been prepared on a 2 g scale. A second preparation was undertaken on a 7 g scale, using the deposition-reduction method, and the performance of a sample from this batch is recorded in Entry 6. Unfortunately, 5% Pd/titania prepared on this scale gave a performance which showed no benefit over that of the Johnson Matthey Pd/aluminas. The reason for the failure of this scale-up is unknown.

### 3.7.2 Effect of palladium loading

The influence of metal loading on performance was investigated by preparing 1%, 2%, 5%, 10%, and 20% Pd/titania catalysts on a 2 g scale using the deposition-reduction method. As indicated in Section 2, their Pd contents by atomic adsorption analysis were 0.94, 1.81, 4.63, 9.71 and 19.89% respectively, and the dispersions of the Pd active phase, determined by CO chemisorption, were 58, 46, 31, 20, and 12.5% respectively. The performance of these catalysts under standard conditions is shown in Table 3.7.2 and in Figure 3.7.1.

The region of best performance for each catalyst is shown in red in Table 3.7.2. It is immediately evident, both from this Table and from Figure 3.7.1, that the optimum loading for Pd on titania was 2%. The performance of 2% Pd/titania was best or equalled the best at every value of the CN:NADPME ratio, although this catalyst was unique in providing its best performance at values of the ratio of 0.14 and 0.16.

Table 3.7.2 NADPME hydrogenation over Pd/titania. Influence of Pd loading on enantiomeric excess for reactions involving various modifier:reactant ratios

<sup>a</sup> Pd loading	e.e./%(S)								
	CN:NADPME molar ratio								
	0.01	0.02	0.04	0.08	0.10	0.14	0.16	0.40 <sup>b</sup>	0.6 <sup>b</sup>
1%	13.0	16.0	17.0	16.5	14.5	13.0	12.5	7.0	5.0
2%	13.0	16.0	18.5	19.0	19.0	20.5	22.0	10.0	5.0
5%	8.5	12.0	16.5	16.0	13.0	-	10.0	5.0	2.0
10%	7.0	10.0	14.0	14.5	12.5	11.5	12.0	5.0	3.0
20%	7.5	8.0	12.0	12.5	10.0	10.0	9.0	3.0	2.0

<sup>a</sup> All catalysts prepared in the laboratory, preparation scale = 2 g. <sup>b</sup> Reactions carried out at molar ratios  $\geq 0.4$  were saturated with cinchonine. For conditions see Table 3.7.1.

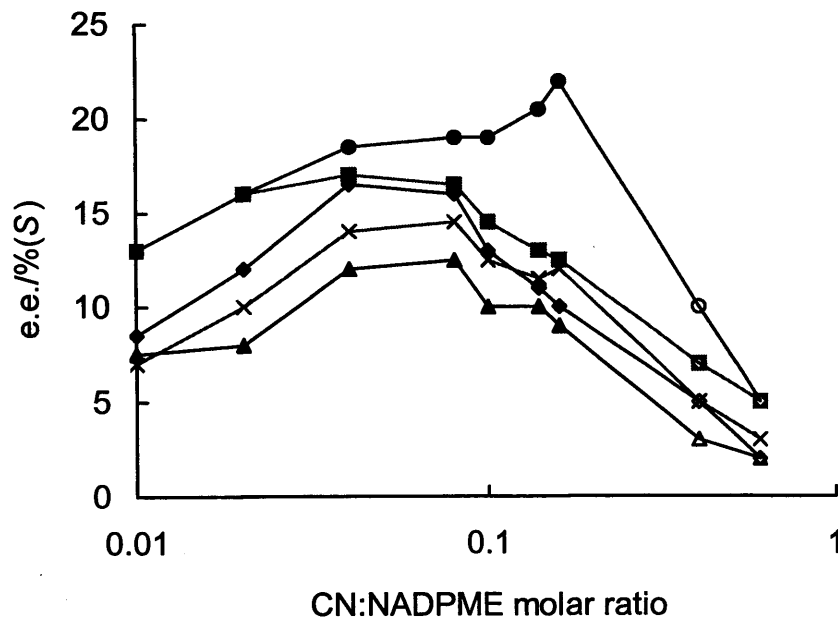


Figure 3.7.1 Semi-logarithmic presentation of variation of enantiomeric excess with CN:NADPME molar ratio for hydrogenations over Pd/titania catalysts of various % metal loading. Unfilled points indicate reaction media saturated with cinchonine. For conditions see Table 3.7.2.

The relative performances of the catalysts over the range of conditions were: 2% Pd/titania > 1% Pd/titania > 5% Pd/titania > 10% Pd/titania > 20% Pd/titania. Figure 3.7.2 shows the variation of enantiomeric excess, measured under conditions optimum for each catalyst (see Table 3.7.2), with Pd dispersion. The highest enantioselectivity was achieved with a dispersion of 46%, i.e. the optimum Pd particle size (on the cubic particle model) was about 2.7 nm.

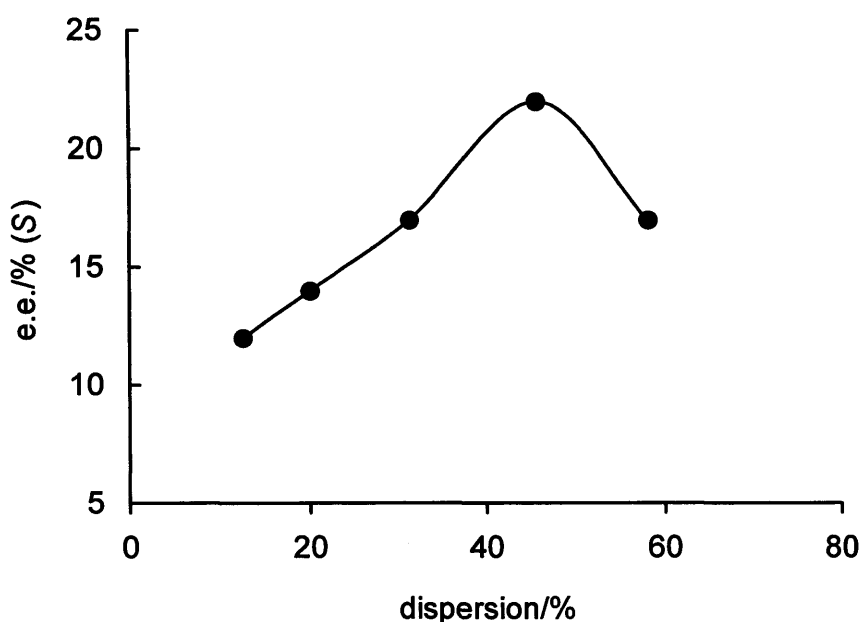


Figure 3.7.2 Dependence of enantiomeric excess on % dispersion of Pd on titania for the cinchonine-modified hydrogenation of NADPME

There would appear to be a case for further investigations of the effects of catalyst preparation on the performance of Pd/titania, as the dispersion of the active phase has a marked effect on enantioselectivity.

The morphology of representative catalysts used in this study was examined by scanning electron microscopy (SEM) and by high resolution transmission electron microscopy (HRTEM). Micrographs for 5% Pd/alumina (2) and for 5% Pd/titania are shown in Figures 3.7.3 – 6. 5% Pd/alumina contained alumina grains of fairly uniform size and shape (SEM), visible Pd particles (HRTEM) being about 7.3 nm in diameter. 5% Pd/titania, on the other hand, contained grains of irregular size and shape and the relatively few visible Pd particles were about 4.2 nm in size.

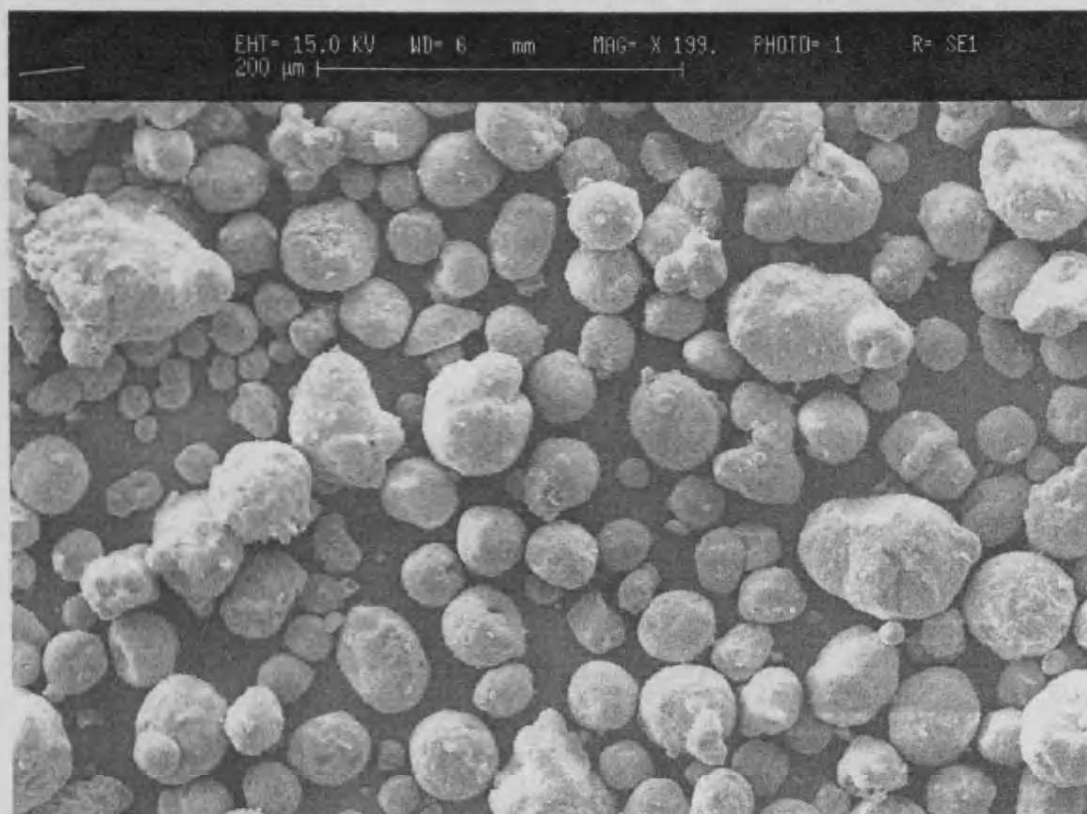


Figure 3.7.3 SEM of 5% Pd/alumina (2)

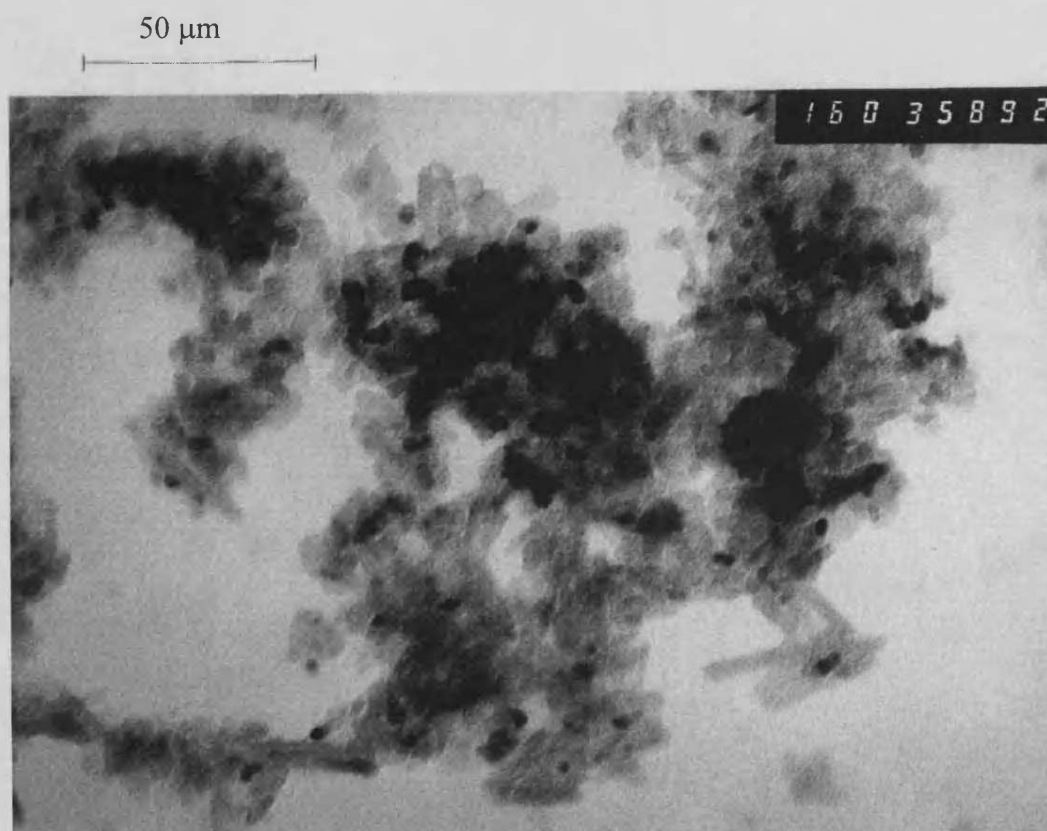


Figure 3.7.4 TEM of 5% Pd/alumina (x 480 magnification)

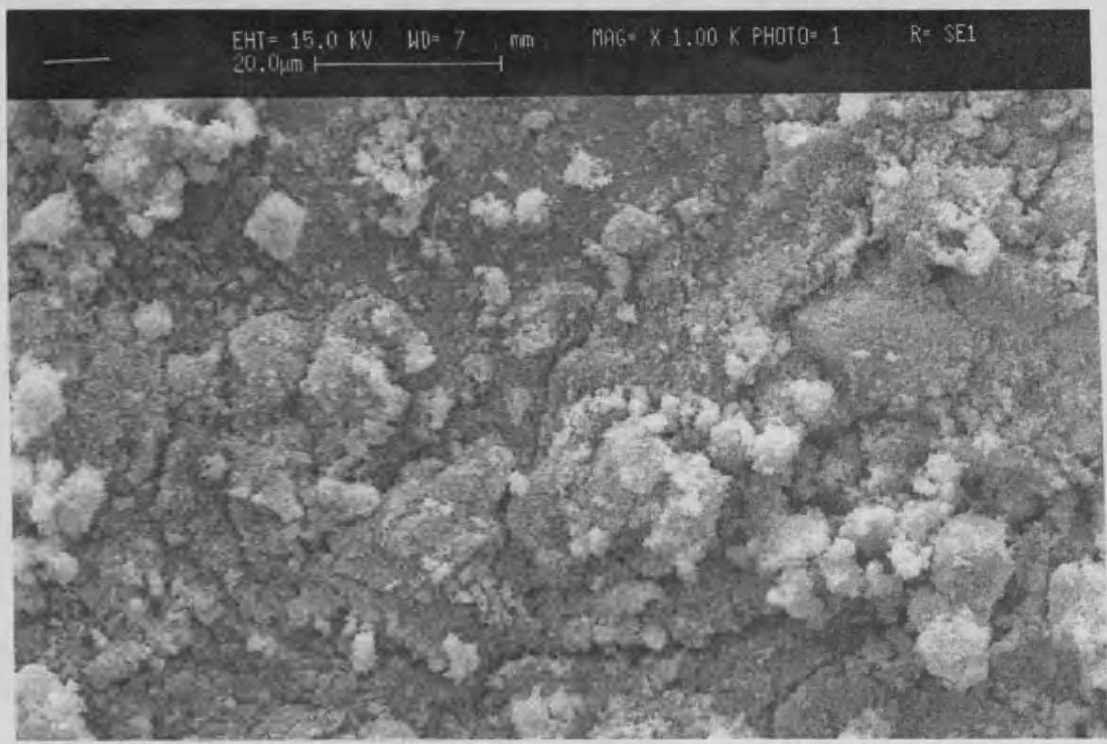


Figure 3.7.5 SEM of 5% Pd/titania

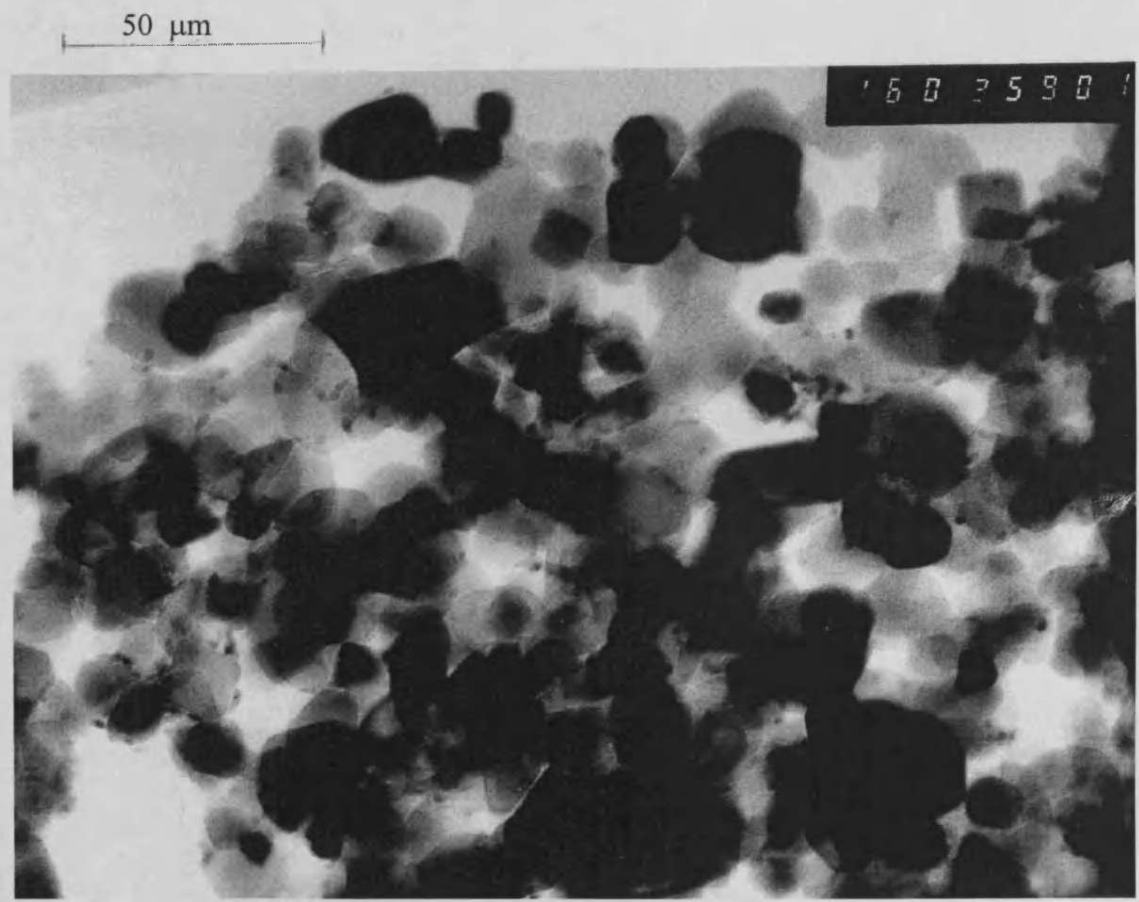


Figure 3.7.6 TEM of 5% Pd/titania (x 480 magnification).

### 3.7.3 Reactions in various solvents

The highest enantioselectivities over cinchonine-modified Pd/alumina are reported in Section 3.3 for reactions conducted in methanol, in dimethylformamide, and in mixtures of these solvents with water. Accordingly, the performance of 2% and 5% Pd/titania was determined under these conditions and compared with that of the Johnson Matthey 5% Pd/alumina (2) catalysts and 5% Pd/alumina(A). The performances of these catalysts are compared in Table 3.7.3.

Table 3.7.3 Values of enantiomeric excess achieved for NADPME hydrogenation over cinchonine-modified Pd catalysts in various solvents

Solvent	e.e./%( <i>S</i> ) Catalyst			
	2% Pd/titania (A)	5% Pd/titania (A)	5% Pd/alumina (2)	5% Pd/alumina (A)
Methanol	22.0	17.0	10.0	15.0
Methanol/3% by volume of water	18.0	16.0	13.0	18.5
DMF	27.0	25.5	18.0	20.0
DMF/10% by volume of water	24.0	24.5	32.0	27.0

[Conditions: 10 ml solvent, 0.1 g NADPME, 0.05 g catalyst, mass of cinchonine used was the optimum determined for each catalyst, (see Table 3.7.3), 10 bar hydrogen pressure, T = 298 K, 1000 rpm, reaction time = 1 h]

For each catalyst, reactions in DMF afforded higher enantioselectivities than reactions in methanol, and the value of 27% provided by 2% Pd/titania was the highest recorded over this catalyst. The presence of water, though beneficial in reactions over Pd/alumina, was deleterious in reactions over Pd/titania. This may be related to cinchonine solubility. As noted above, reactions over Pd/titania required higher concentrations of cinchonine to achieve optimum performance. Over 2% Pd/titania optimum enantioselectivity in methanol occurred at or near the point of saturation (Figure 3.7.1) and hence the addition of water to methanol may have caused the solubility of cinchonine to be exceeded.



### 3.7.4 Conclusions

Although the high performance of Pd/titania for  $\alpha,\beta$ -unsaturated acids recorded by Nitta et al. [14] (e.e.  $\sim 72\%$ ) has not been replicated here, the best performance provided by 2% Pd/titania was comparable to the best performance provided by 5% Pd/alumina, and under several sets of comparable conditions Pd/titania was more enantioselective than Pd/alumina.

## 3.8 Cinchonidine-Modified Hydrogenations

The effectiveness of various chiral modifiers for NADPME hydrogenation were recorded in Section 3.1, Table 3.1.3. These results were obtained using the optimum modifier: NADPME molar ratio as determined for cinchonine. Under those conditions cinchonidine-modified hydrogenations favoured a low value of enantiomeric excess in favour of the *R*-enantiomer (3.4 %(*R*)). As cinchonidine is substantially more soluble than cinchonine, it cannot be assumed that reaction conditions used were the optimum in respect of cinchonidine concentration.

### 3.8.1 Effect of Cinchonidine Concentration on Enantiomeric Excess

The variation of the sense and magnitude of the enantiomeric excess with cinchonidine concentration is presented in Table 3.8.1 and Figure 3.8.1. The experimental conditions determined for cinchonine modified hydrogenations were employed as standard for these hydrogenations.

At CD:NADPME molar ratios between 0.006:1 to 0.02:1 cinchonidine favoured the formation of *R*-product. This reversal of enantioselectivity by comparison to that provided by cinchonine was as expected [16]. However, as the cinchonidine concentration was increased there was an unexpected inversion in the sense of the enantioselectivity, an enantiomeric excess of 21.5%(*S*) being achieved at a CD:NADPME molar ratio of 1:1. Constant values at  $\sim 18\%$ (*S*) were observed after this optimum.

Table 3.8.1 Variation of enantiomeric excess with mass of cinchonidine (CD)

Mass of cinchonidine /mg	CD:NADPME molar ratio	e.e. /%
1	0.006	3.4 ( <i>R</i> )
2	0.01	3.0 ( <i>R</i> )
3	0.02	3.0 ( <i>R</i> )
4	0.03	0
10	0.07	1.0 ( <i>S</i> )
20	0.14	2.0 ( <i>S</i> )
40	0.20	2.5 ( <i>S</i> )
50	0.40	8.0( <i>S</i> )
80	0.60	16.5( <i>S</i> )
150	1.00	21.5 ( <i>S</i> )
300	2.00	18.0 ( <i>S</i> )
400	2.70	18.0 ( <i>S</i> )

[Conditions: 10 ml methanol, 0.1 g NADPME, 0.05 g Pd/alumina (2), 10 bar hydrogen pressure, T = 298 K, reaction time = 3 h].

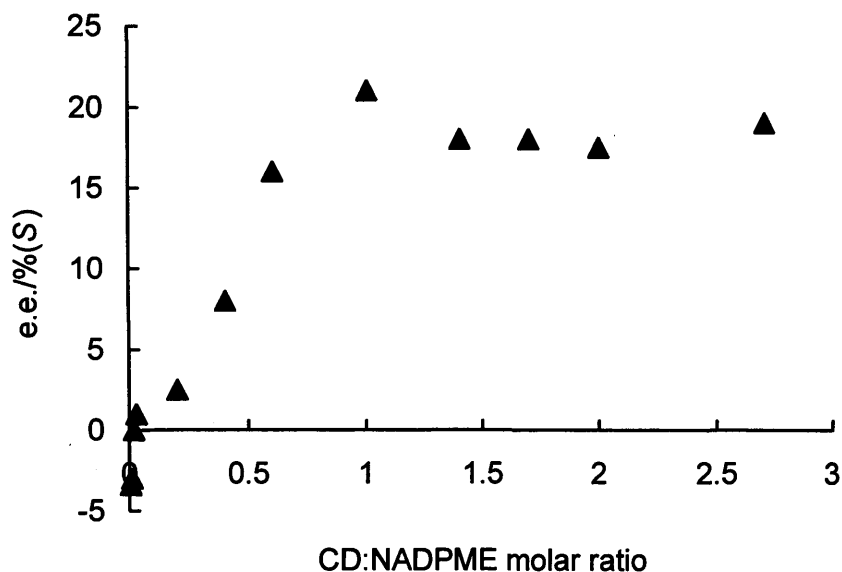


Figure 3.8.1 Variation of enantiomeric excess with CD:NADPME molar ratio. [NADPME = constant throughout, 100mg, 0.46 mmol]. A semi-logarithmic presentation of these results is contained in Figure 3.8.2.

In contrast to cinchonine, no saturation of the reaction solution occurred over the range of cinchonidine concentrations studied. This may be a contributory factor to the remarkable difference in chiral outcome between cinchonine- and cinchonidine-modified reactions for conditions involving the same modifier:NADPME molar ratios (Figure 3.8.2).

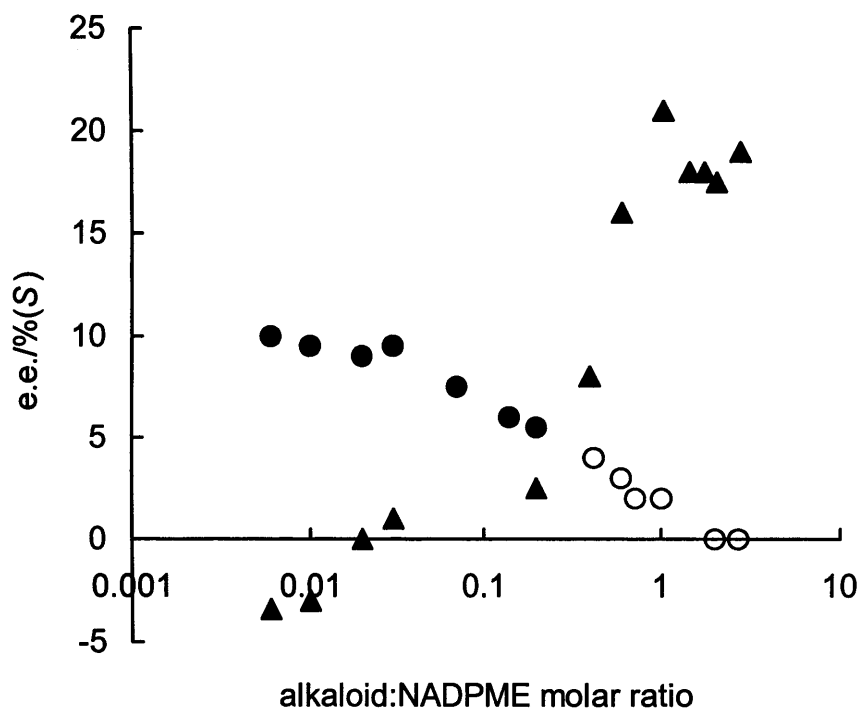


Figure 3.8.2 Semi-logarithmic presentation of the variation of enantiomeric excess with modifier:NADPME molar ratio. ●, cinchonine-modified reactions; ▲, cinchonidine-modified reactions.

### 3.8.2 Effect of Modifier on Rate

Uptake versus time curves for reactions involving various amounts of cinchonidine are shown in Figure 3.8.3. Reactions involved 2 g NADPME (to provide measurable hydrogen uptakes) and 1.0 g catalyst modified by 20 to 2100 mg cinchonidine. These conditions provided the same CD:NADPME molar ratios as those used under standard reaction conditions.

A fast consumption of hydrogen occurred in the initial few minutes of reaction. The amount consumed during these fast processes increased with the mass of cinchonidine present. Mass spectrometry (Figure 3.8.4) confirmed that reduction of the vinyl group in cinchonidine occurred during this period to form the 10,11-dihydroderivative; this occurred before any significant hydrogenation of NADPME. Thus, the effective modifier used in these reactions was 10,11-dihydrocinchonidine. NMR spectroscopy also indicated that partial hydrogenation of the quinoline ring in cinchonidine was occurring during the hydrogenation of NADPME.

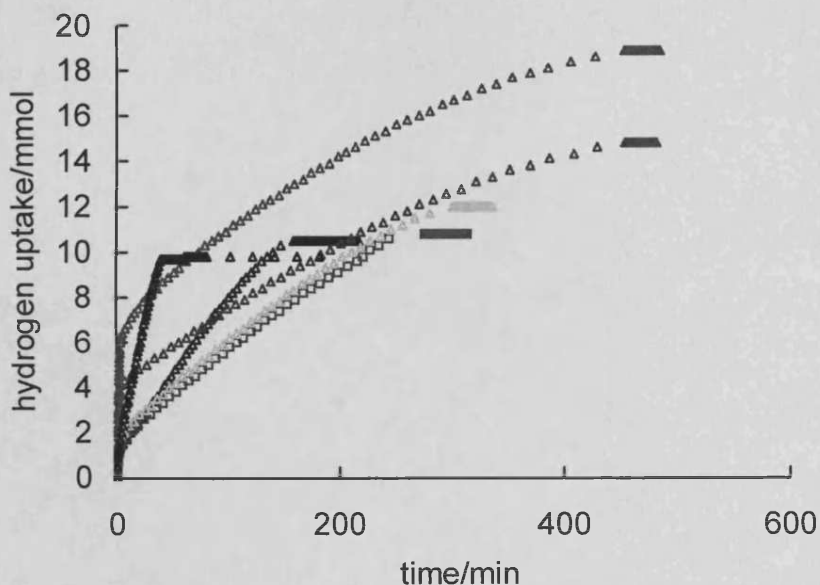


Figure 3.8.3 Hydrogen uptake curves observed in the hydrogenation of NADPME over cinchonidine modified palladium. Mass of cinchonidine:  $\Delta$ , 20 mg;  $\square$ , 60 mg;  $\circ$ , 200 mg;  $\diamond$ , 1.0 g;  $\nabla$ , 2.1 g; and in the absence of cinchonidine ( $\triangle$ ). For conditions see Table 3.8.2.

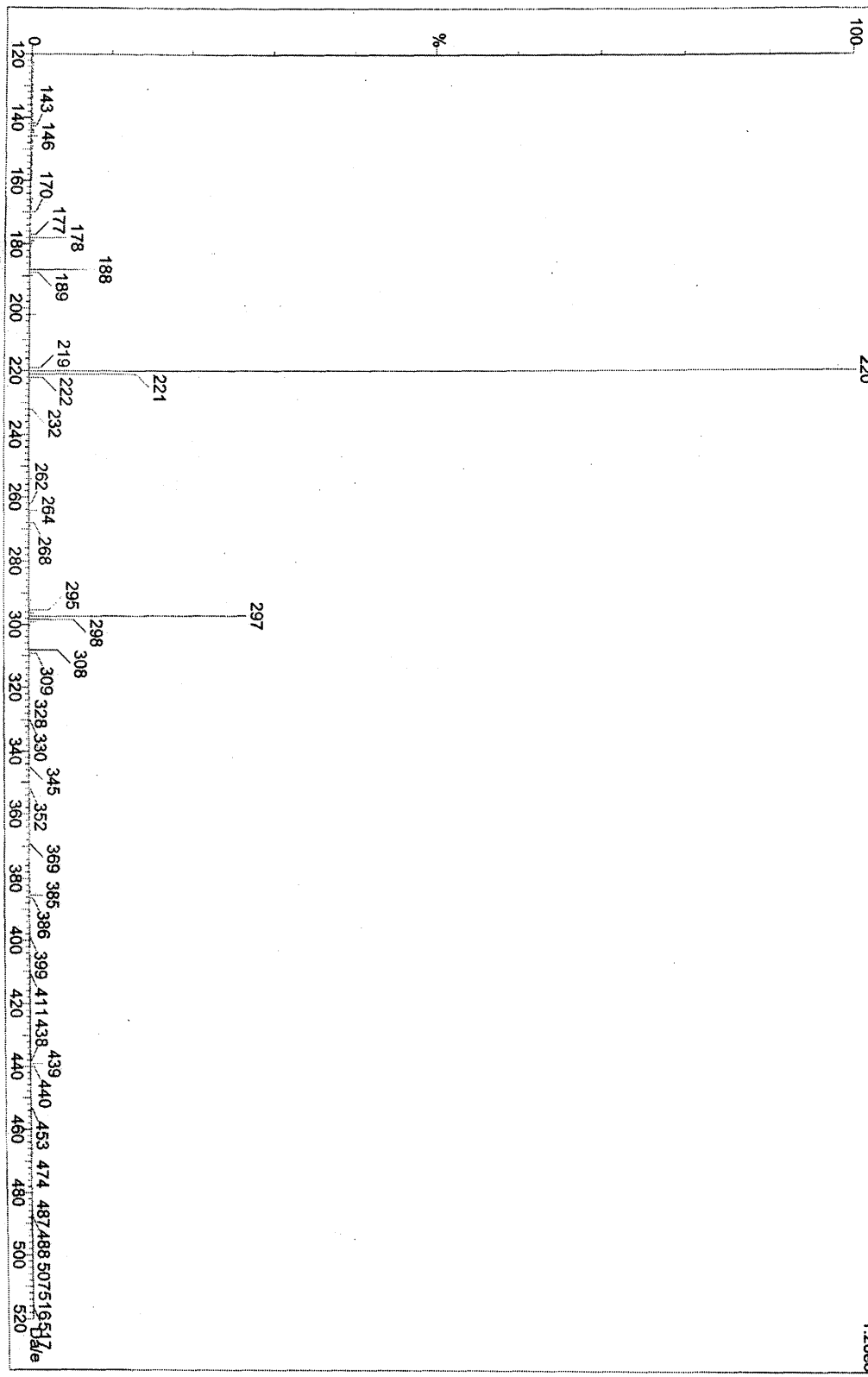


Figure 3.8.4 Mass spectrometry of hydrogenation product collected after 1 minute. [Conditions: 2.0 g NADPME, 1.0 g catalyst (2), 60 mg cinchonidine, 10 bar hydrogen pressure, T = 298 K, 1000 rpm].

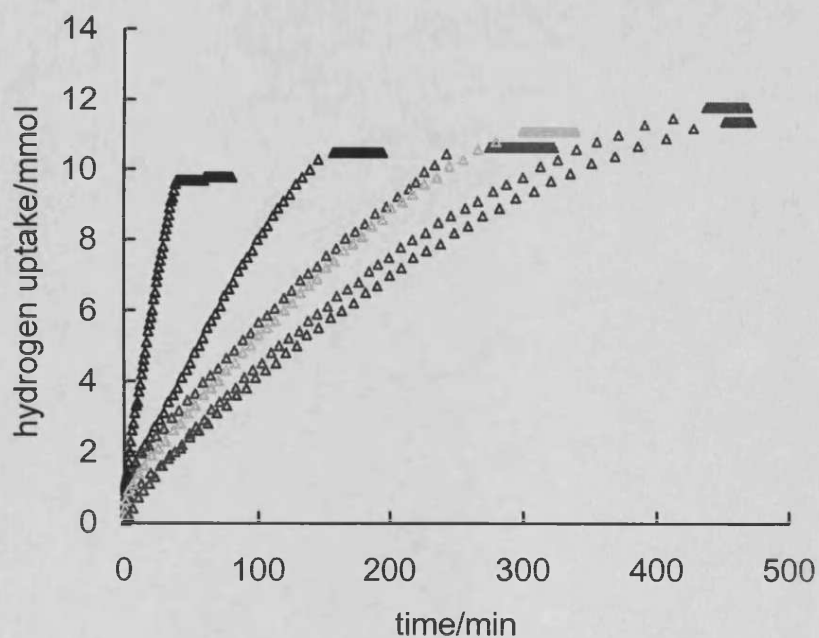


Figure 3.8.5 Hydrogen uptake curves obtained after the subtraction of the hydrogen uptake attributed to fast reduction of the vinyl group in cinchonidine. Mass of cinchonidine:  $\blacktriangle$ , 20 mg;  $\triangle$ , 60 mg;  $\blacksquare$ , 200 mg;  $\square$ , 1.0 g;  $\bullet$ , 2.1 g; and in the absence of cinchonidine ( $\Delta$ ).

Figure 3.8.5 shows uptake/time curves after subtraction of the uptake for the fast hydrogenation of the vinyl group in cinchonidine. Initial rates measured from these curves decreased with increasing mass of cinchonidine, with the fastest rate observed in the absence of modifier

Table 3.8.2 shows the initial rates determined from Figure 3.8.5 for hydrogenations of NADPME over catalyst modified by 20 to 2100 mg cinchonidine. The logarithmic plot (Figure 3.8.6) indicates that the rate varied with alkaloid concentration raised to the power  $-0.2$ .

Table 3.8.2 Initial rates measured for reactions over Pd/alumina modified by 20 to 2100 mg cinchonidine.

Mass of cinchonidine used /mg	Initial rate/mmol min <sup>-1</sup>
No cinchonidine	0.317
20	0.107
60	0.061
200	0.058
1000	0.042
2100	0.045

[Conditions: 20 ml methanol, 2.0 g NADPME, 1.0 g catalyst (2), 10 bar hydrogen pressure, T = 298 K, 1000 rpm, reaction time = 2 h].

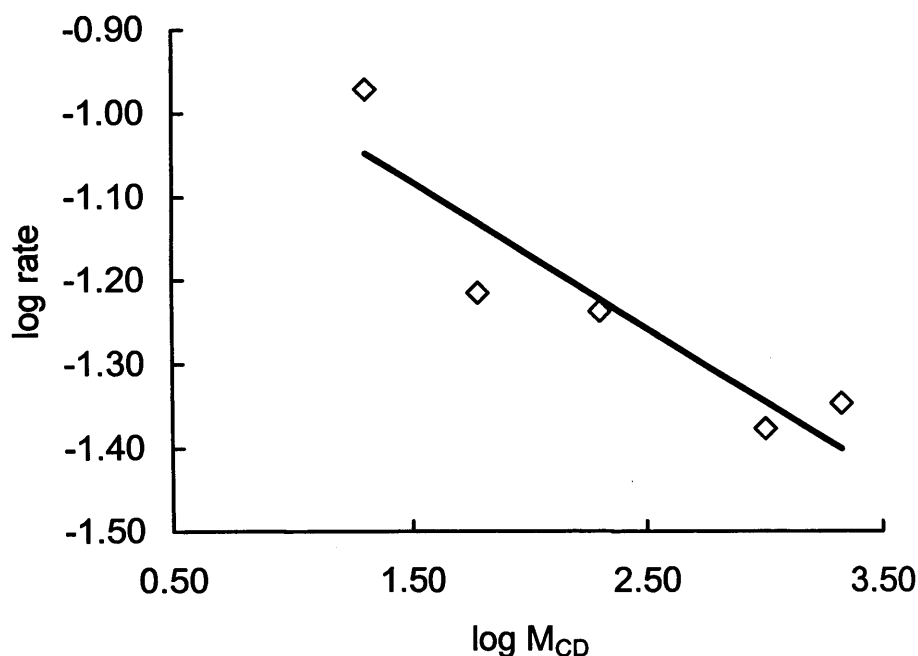


Figure 3.8.6 Logarithmic presentation of initial rate against mass of cinchonidine for NADPME hydrogenation over Pd/alumina. For rates and conditions see Table 3.8.2.

### 3.8.3 Reactions in Various Solvents

The variation of the sense and magnitude of the enantiomeric excess with CD:NADPME

molar ratio is shown in Table 3.8.3. The mass of NADPME (100 mg, 0.46 mmol) was constant throughout.

An inversion in enantioselectivity from R to S with increasing cinchonidine concentration was observed for hydrogenations in the primary alcohols methanol, ethanol and propan-1-ol. For these solvents a similar pattern of behaviour was observed, i.e. a low value of the enantiomeric excess in favour of the *R*-enantiomer with CD:NADPME molar ratios < 0.03, racemic product with CD:NADPME between 0.03 to 0.07, and an increasing enantioselectivity in favour of the *S*-enantiomer with CD:NADPME > 0.07.

Table 3.8.3 Variation of the sense and magnitude of the enantiomeric excess with cinchonidine concentration for reactions in various solvents

	e.e./%				
	CD:NADPME molar ratio				
	0.006	0.03	0.14	0.40	1.0
Methanol	3.4 ( <i>R</i> )	0	2.0 ( <i>S</i> )	8.0 ( <i>S</i> )	21.5 ( <i>S</i> )
Ethanol	2.0 ( <i>R</i> )	0	3.0 ( <i>S</i> )	7.0 ( <i>S</i> )	14.0 ( <i>S</i> )
Propan-1-ol	1.5 ( <i>R</i> )	0	2.5 ( <i>S</i> )	4.0 ( <i>S</i> )	9.5 ( <i>S</i> )
Propan-2-ol	5.0 ( <i>S</i> )	6.0 ( <i>S</i> )	7.0 ( <i>S</i> )	7.0 ( <i>S</i> )	10.0 ( <i>S</i> )
<sup>a</sup> DMF	0	7.0 ( <i>S</i> )	12.0 ( <i>S</i> )	17.0 ( <i>S</i> )	22.0 ( <i>S</i> )
<sup>b</sup> DCM	4.0 ( <i>S</i> )	5.0 ( <i>S</i> )	8.0 ( <i>S</i> )	8.0 ( <i>S</i> )	8.5 ( <i>S</i> )
<sup>c</sup> THF	2.5 ( <i>S</i> )	2.0 ( <i>S</i> )	2.5 ( <i>S</i> )	3.0 ( <i>S</i> )	3.0 ( <i>S</i> )

<sup>a</sup> *N,N*-dimethylformamide, <sup>b</sup> dichloromethane, <sup>c</sup> tetrahydrofuran

[Conditions: 10 ml solvent, 0.1 g NADPME, 0.05 g Pd/alumina (2), 10 bar hydrogen pressure, T = 298 K, 1000 rpm, reaction time = 3 h].

No inversion in the sense of the enantioselectivity was observed for propan-2-ol, dichloromethane, *N,N*-dimethylformamide or tetrahydrofuran. For these solvents enantioselectivity in favour of the *S*-enantiomer increased continuously with increasing mass of cinchonidine. For all solvents tested the highest enantioselectivities in favour of the *S*-enantiomer were observed at a CD:NADPME molar ratio of 1.0. The values were higher for solvents which have larger dielectric constants, in the order: DMF > methanol



> ethanol > propanol > DCM > THF (Table 3.8.4 and Figure 3.8.7). A similar correlation was observed for cinchonine modified hydrogenations. (Section 3.3).

Table 3.8.4 Correlation between the dielectric constant of the solvent and the value of enantiomeric excess

Solvent	Dielectric constant	e.e./%(S)
THF	7.6	3.0
DCM	8.9	8.5
Propanol	19.2	9.5
Ethanol	24.5	14.0
Methanol	32.7	21.5
DMF	36.7	22.0

[Conditions: 10 ml solvent, 100 mg NADPME, 50 mg catalyst (2), CD:NADPME molar ratio = 1.0, 10 bar hydrogen pressure, T = 298 K, 1000 rpm, reaction time = 3 h].

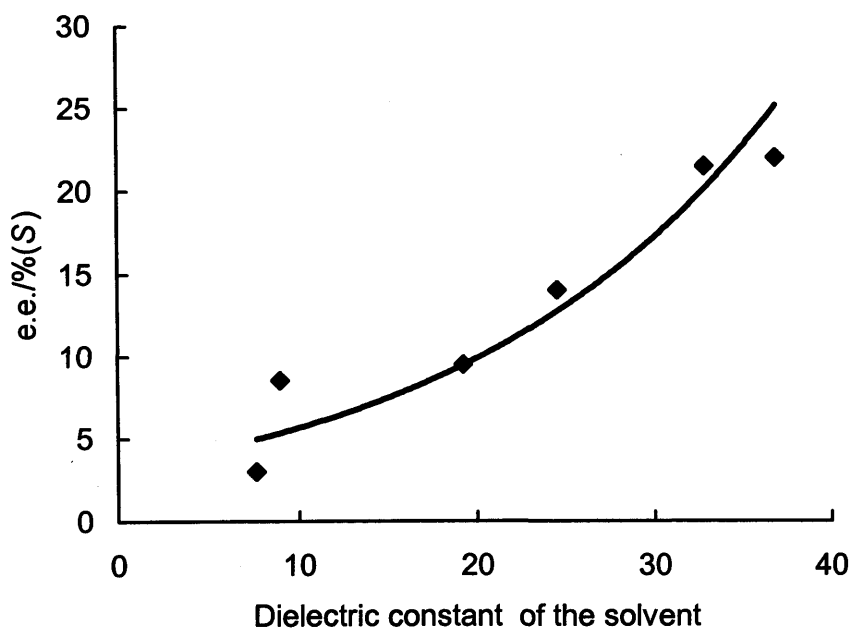


Figure 3.8.7 Variation of the value of the enantiomeric excess with the dielectric constant of the solvent. For conditions see Table 3.8.4.

### 3.8.4 Reactions in Mixed Solvents

The inversion in enantioselectivity observed for reactions carried out in methanol, ethanol and propanol was probed further by conducting hydrogenations in mixtures of these solvents with acetic acid. The variation of the sense and magnitude of the enantiomeric excess with CD:NADPME ratio for reactions in methanol/acetic acid, ethanol/acetic acid and dichloromethane/acetic acid is shown in Table 3.8.5.

The inversion in enantioselectivity observed for hydrogenations using methanol or ethanol as solvent was also observed for reactions carried out in mixtures of these solvents with acetic acid. However, the enantioselectivity in favour of the *R*-enantiomer observed in methanol and ethanol at low CD:NADPME ratios, was enhanced when acetic acid was present as a component of the solvent (Figure 3.8.8). Values of enantiomeric excess recorded in Table 3.8.5 for reactions carried out in DCM/acetic acid show no inversion in the sense of enantioselectivity with mass of cinchonidine.

Table 3.8.5 Variation of the sense and magnitude of the enantiomeric excess with CD:NADPME molar ratio for hydrogenations in three mixed solvents

	e.e./%				
	CD:NADPME molar ratio				
	0.006	0.02	0.40	0.60	1.0
Methanol/ Acetic acid	8.0 ( <i>R</i> )	5.5 ( <i>R</i> )	1.0 ( <i>R</i> )	3.0 ( <i>S</i> )	5.5 ( <i>S</i> )
Ethanol/ acetic acid	5.5 ( <i>R</i> )	3.0 ( <i>R</i> )	0	2.0 ( <i>S</i> )	4.0 ( <i>S</i> )
DCM/ acetic acid	7.0 ( <i>S</i> )	14.0 ( <i>S</i> )	14.0 ( <i>S</i> )	14.5 ( <i>S</i> )	14.0 ( <i>S</i> )

[Conditions: 9.95 ml methanol, ethanol or DCM, 0.05 ml acetic acid, 100 mg NADPME, 50 mg Pd/alumina (2), 10 bar hydrogen pressure, T = 298 K, 1000 rpm, reaction time = 3 h].

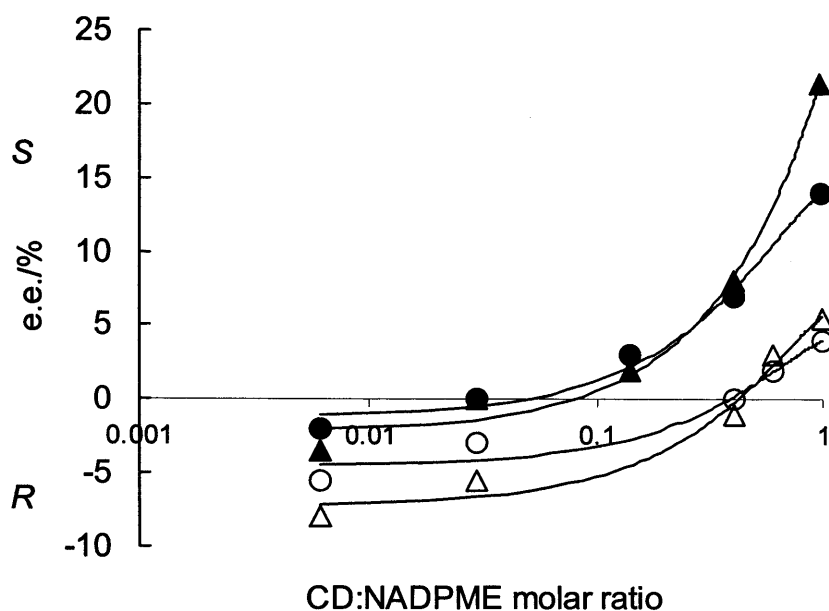


Figure 3.8.8 Semi-logarithmic presentation of the variation of the sense and the magnitude of enantiomeric excess with CD:NADPME molar ratio for reactions carried out in various solvents. Key: ▲, methanol; △, methanol/acetic acid; ● ethanol; ○, ethanol/acetic acid. For conditions see Table 3.8.3 and Table 3.8.5.

### 3.8.5 Variations on the Standard Reaction

Variations on the standard reaction were made to gather information regarding reactions occurring at high and low cinchonidine concentrations. The first was the variation of modifier structure and the second was the use of catalysts modified with cinchonidine prior to hydrogenation of NADPME.

#### 3.8.5.1 Quaternised cinchonidine

Reactions were carried out at two alkaloid:NADPME molar ratios, 0.006 and 1.0, using as modifier methyl cinchonidinium iodide (i.e. cinchonidine that had been quaternised with methyl iodide). The results are shown in Table 3.8.6.

Table 3.8.6 Conversions and values of enantiomeric excess for NADPME hydrogenation over catalyst modified by quaternised alkaloid

MeCD <sup>+</sup> I <sup>-</sup> :NADPME molar ratio	e.e. /%	Conversion /%
0.006	0	40
1.0	0	32

[Conditions: 10 ml methanol, 100 mg NADPME, 50 mg catalyst (2), 10 bar hydrogen pressure, T = 298 K, 1000 rpm, reaction time = 24 h].

Racemic product was observed for reactions conducted both at low and at high modifier concentrations. Incomplete conversion was observed over a 24 h period; this contrasts with 100% conversion in a 3 h period for reactions using cinchonidine as modifier.

### 3.8.5.2 Pre-modified catalyst

Initial rates and values of enantiomeric excess were recorded for reactions involving *in situ* modification (i.e. normal procedure) and for reactions carried out over catalyst that had been pre-modified with cinchonidine. Again two modifier concentrations were studied (Table 3.8.7).

For reactions involving a CD:NADPME = 0.006 similar values of enantiomeric excess were recorded for reactions over catalyst modified *in situ* and over catalyst that had been pre-modified. This is in contrast to the results observed at high cinchonidine concentrations, where the reactions carried out over the pre-modified catalyst showed a much reduced enantioselectivity.

The initial rates measured were lower for reactions over pre-modified catalyst than over *in situ* modified catalyst, at both high and low CD:NADPME molar ratios.

Table 3.8.7 Initial rates and values of enantiomeric excess for NADPME hydrogenation carried out over Pd/alumina modified *in situ* and over pre-modified Pd/alumina

CD:NADPME molar ratio	Reactions carried out <i>in situ</i>		Reactions carried out over pre-modified catalyst	
	<sup>a</sup> e.e. /%	<sup>b</sup> Initial rate /mmol min <sup>-1</sup>	<sup>a</sup> e.e. /%	<sup>b</sup> Initial rate /mmol min <sup>-1</sup>
no modifier	0	0.109	-	-
0.006	3.5 ( <i>R</i> )	0.072	3.0 ( <i>R</i> )	0.054
1.0	21.5 ( <i>S</i> )	0.044	3.5 ( <i>S</i> )	0.024

[<sup>a</sup> Conditions: 10 ml methanol, 100 mg NADPME, 50 mg catalyst (2), 10 bar hydrogen pressure, T=298 K, 1000 rpm, reaction time = 3 h. <sup>b</sup> Conditions: 20 ml methanol, 2.0 g NADPME, 1.0 g catalyst (2), 10 bar hydrogen pressure, T = 298 K, 1000 rpm, reaction time = 24 h]

### 3.8.6 Spectroscopic Investigations

<sup>1</sup>H NMR spectra of cinchonidine and cinchonidine with NADPME were recorded over the range of cinchonidine concentrations presented in Table 3.8.1. The primary aim of this investigation was to determine possible CD: NADPME interactions and to establish whether the conformation of cinchonidine was changing with concentration and /or with the presence of reactant. Unfortunately, the <sup>1</sup>H NMR spectra recorded for very low concentrations of CD with NADPME (molar ratios of 0.006 and 0.07) were inconclusive. This was a result of the far greater concentration of NADPME compared to cinchonidine present, which invariably led to an imbalance in the size of the peaks attributed to the protons of both compounds.

<sup>1</sup>H NMR spectra recorded for 7.5 mg CD in 0.5 ml deuterated methanol, and 7.5 mg CD with 5.0 mg NADPME in 0.5 ml deuterated methanol are shown in Figure 3.8.10 and 3.8.11 respectively. These molar ratios were comparable to that of 1:1 CD:NADPME molar ratio.

It is essential to assign the  $^1\text{H}$  NMR spectrum of cinchonidine in methanol before being able to study the effect of NADPME and /or acetic acid on the chemical shifts of protons associated with cinchonidine. Figure 3.8.9 illustrates the structure and proton numbering of cinchonidine and the assignment of these protons are presented in Table 3.8.8

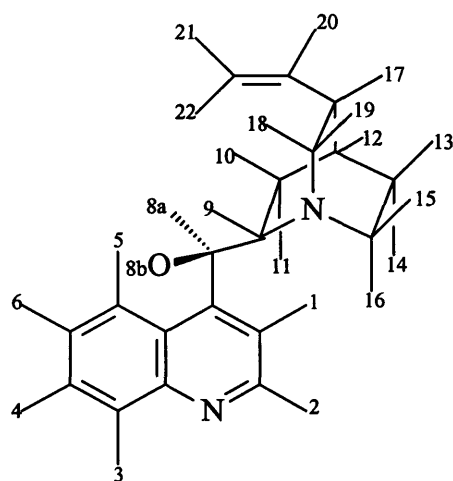


Figure 3.8.9 Structure and proton numbering of cinchonidine

Table 3.8.8  $^1\text{H}$  NMR chemical shifts (in ppm) for cinchonidine in  $\text{CD}_3\text{OD}$

Proton number	Chemical shift	Proton number	Chemical shift
1	7.74	12	1.79
2	8.84	13	1.55
3	8.24	14	1.84
4	7.79	15	2.66
5	8.08	16	3.62
6	7.67	17	2.33
8a	5.67	18	2.63
8b	6.04	19	3.09
9	3.12	20	5.76
10	1.50	21	4.89-4.99
11	1.86	22	4.89-4.99

All spectra were obtained at room temperature using a 400 MHz NMR spectrometer.

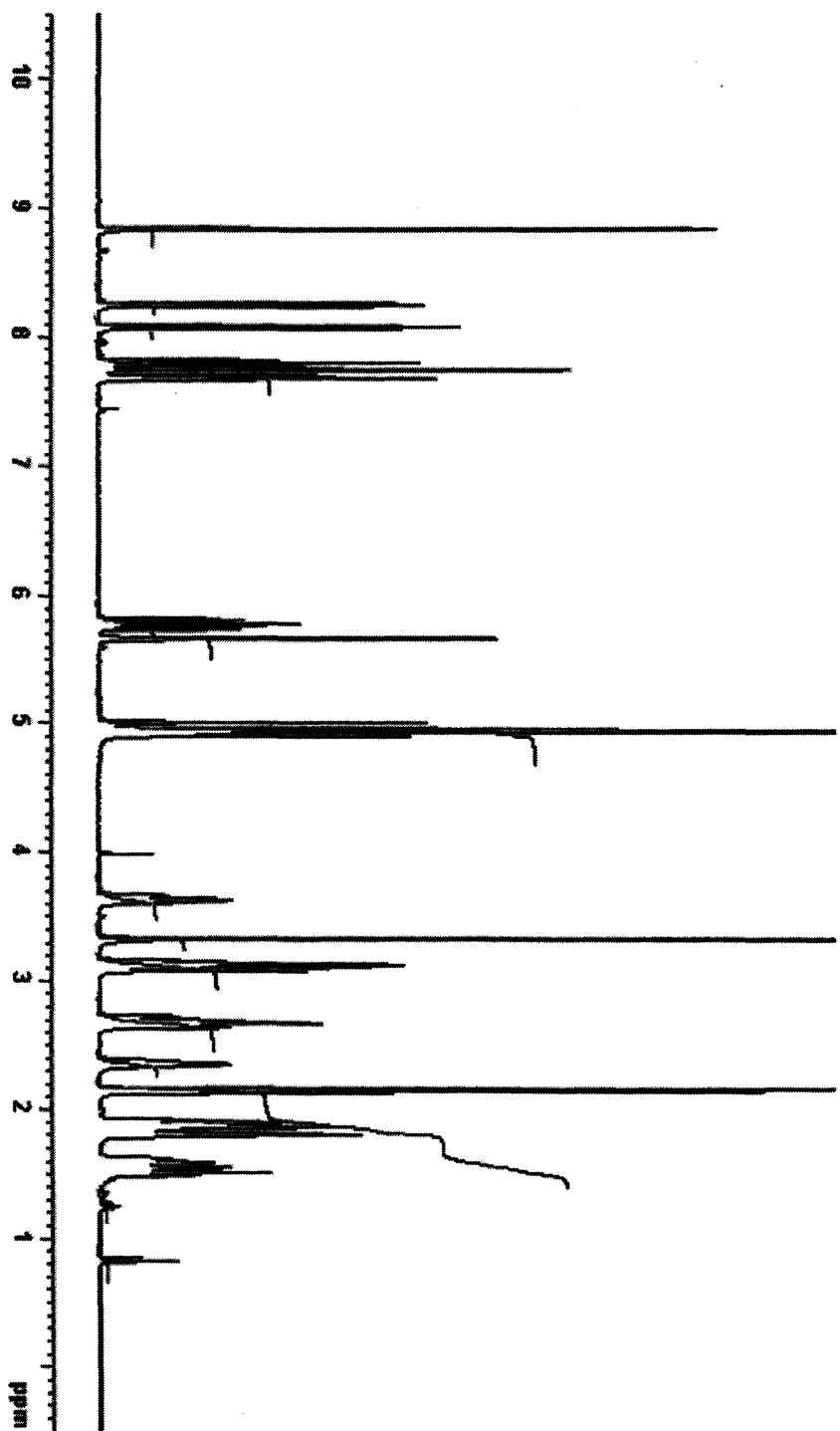


Figure 3.8.10  $^1\text{H}$  NMR spectra of cinchonidine (7.5 mg) in  $\text{CD}_3\text{OD}$  (0.5 ml).

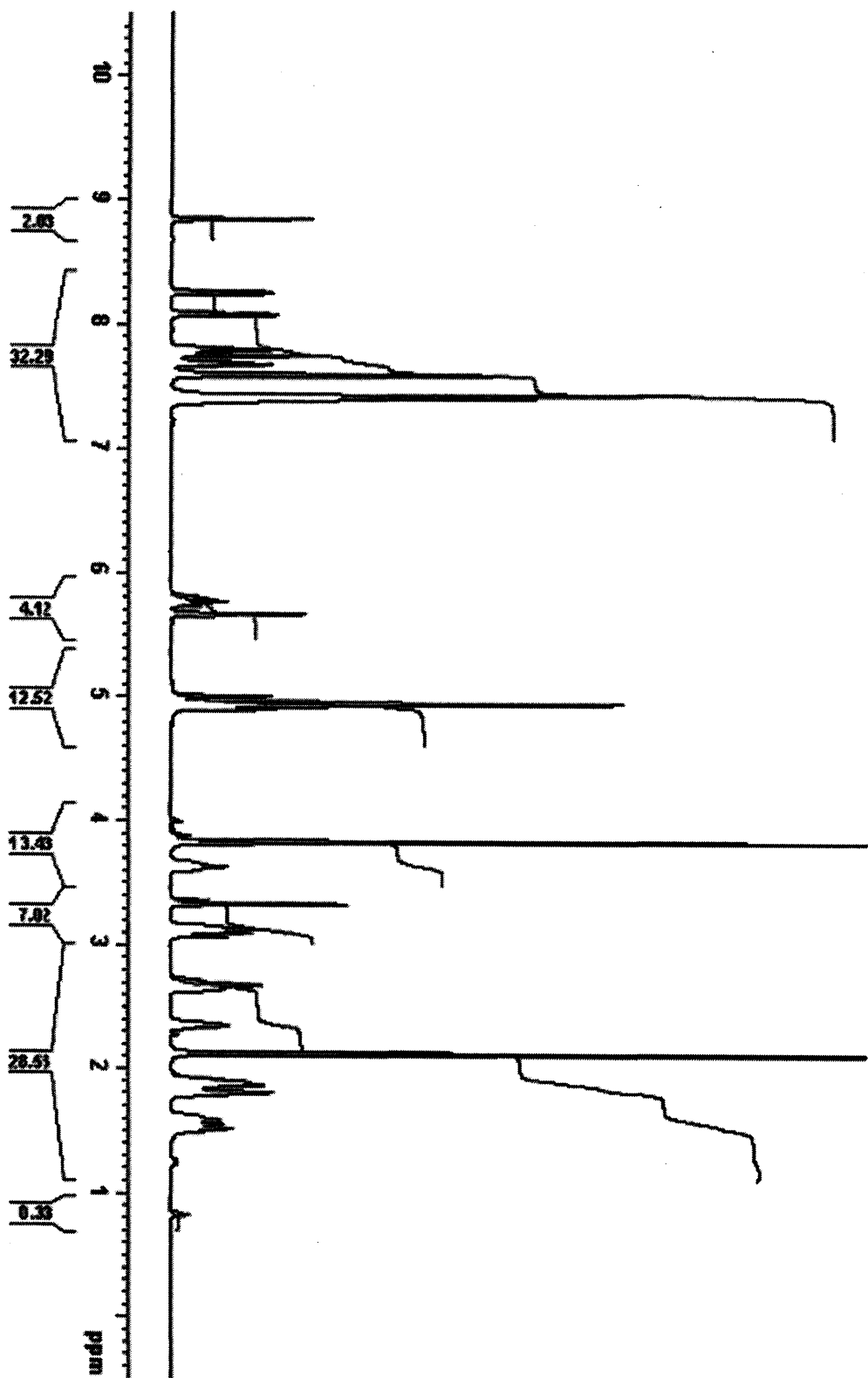


Figure 3.9.11  $^1\text{H}$ NMR spectra for cinchonidine (7.5 mg) and *N*-acetyl dehydrophenylalanine methyl ester, NADPME, (5.0 mg) in  $\text{CD}_3\text{OD}$  (0.5 ml).



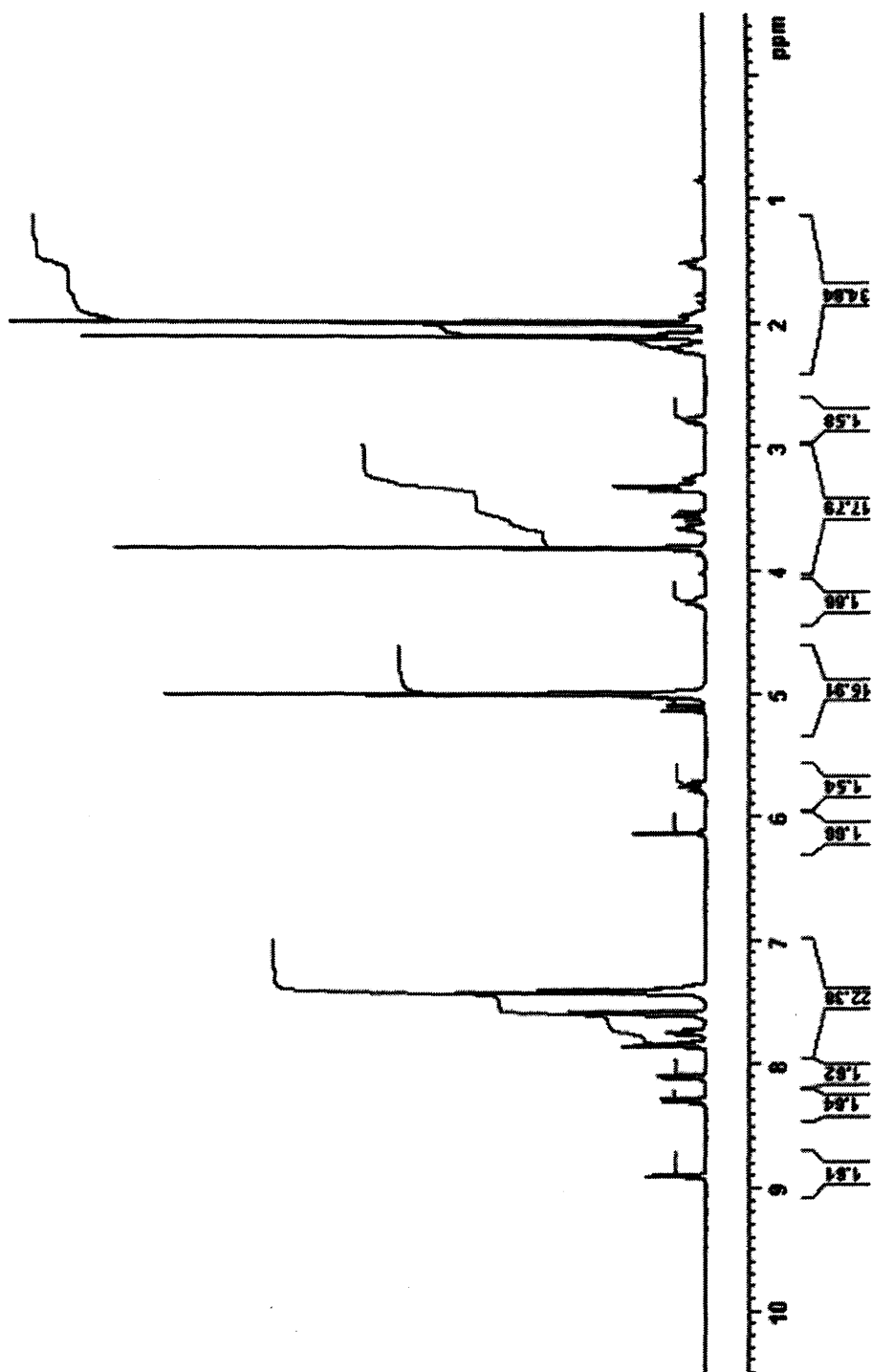


Figure 3.9.12 HNMR spectra for cinchonidine (7.5 mg), NADPME (5.0 mg) and acetic acid in  $CD_3OD$  (0.5 ml).

From the HNMR spectra obtained the signal attributed to the H<sub>8a</sub> proton was examined. For cinchonidine in CD<sub>3</sub>OD this signal was observed at 5.76 and was not altered by the addition of NADPME to the solution. However, the signal moved downfield to ~6.00 with the addition of acetic acid, indicating that conformational changes about the C<sub>8</sub> and C<sub>9</sub> bond in cinchonidine had occurred.

### 3.9 Reactions Involving Other Cinchona Alkaloids

Table 3.9.1 and Figure 3.9.1 shows the variation of enantiomeric excess with modifier:NADPME molar ratio for quinine-modified and quinidine-modified hydrogenations. Reactions were conducted over the same range of molar ratios as those of cinchonine and cinchonidine.

Table 3.9.1 Values of enantiomeric excess for NADPME hydrogenation conducted over quinine-modified Pd and quinidine-modified Pd.

Modifier:NADPME molar ratio	e.e./%	
	Quinine-modified reactions	Quinidine-modified reactions
0.007	2.0( <i>R</i> )	1.0 ( <i>S</i> )
0.01	0	1.0 ( <i>R</i> )
1	6.0( <i>S</i> )	7.5 ( <i>R</i> )
1.5	5.5 ( <i>S</i> )	7.5 ( <i>R</i> )
1.8	5.0 ( <i>S</i> )	8.0 ( <i>R</i> )

[Conditions: 10 ml methanol, 0.1 g NADPME, 0.05 g catalyst (2), 10 bar hydrogen pressure T =- 298 K, 1000 rpm, reaction time = 1 h].

The results show that both modifiers perform equally as well with the opposite sense in enantioselectivity being achieved; quinine giving an excess of the *S*-enantiomer and quinidine giving an excess of the *R*-enantiomer.

Inferior enantioselectivities are observed for both quinine and quinidine compared to those of cinchonine and cinchonidine. This may be attributed to the steric hindrance

associated with the former modifiers due to the O-methylated group present at position 4 on the quinoline moiety.

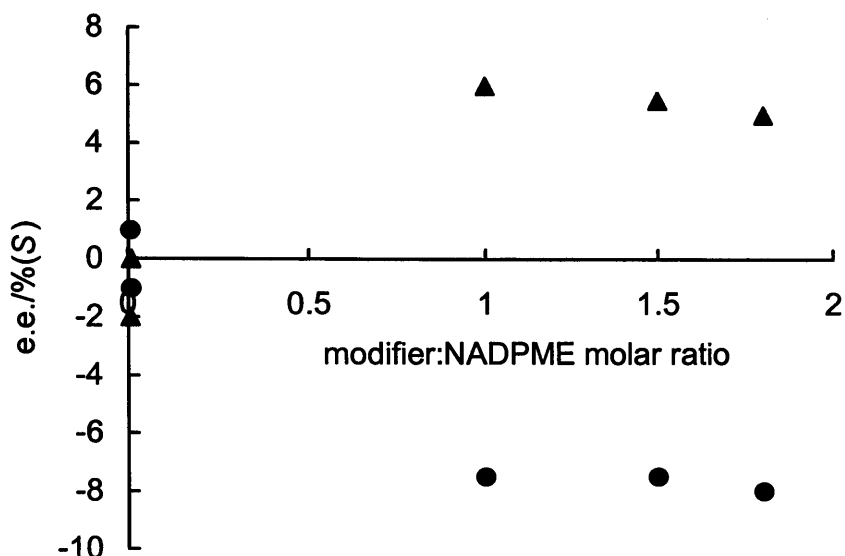


Figure 3.9.1 Variation of values of enantiomeric excess with modifier:NADPME molar ratio using, quinine (▲), and quinidine (●) as modifiers.

Interestingly the behaviour observed for cinchonine-modified reactions was not observed using the analogous modifier, quinidine. However, the same pattern in behaviour was observed for the analogous pair, quinine and cinchonidine.

The unusual pattern of behaviour observed for cinchonine-modified reactions may be attributed to the low solubility of cinchonine compared to that of the other cinchona alkaloids, which were soluble at all concentrations used.

However, in researching the solubility of all four modifiers it was found that the difference in solubility observed between cinchonine and cinchonidine was also repeated for quinidine and quinine but at much higher concentrations.

### 3.10 References

- 1 Y. Nitta, Y. Ueda, T. Imanaka, *Chem. Lett.*, (1994) 1095.

- 2 T. Mallat, A. Baiker, *App. Catal. A: Gen.*, **200** (2000) 3.
- 3 P.B. Wells, R.P.K. Wells, *Chiral Catalysts Immobilisation and Recycling*, ed. (DeVos et al.), Wiley-VCH, 2000, p123-154
- 4 P.B. Wells, K.E. Simons, J.A. Slipszenko, S.P. Griffiths, D.F. Ewing, *J. Mol. Catal. A: Chem.*, **146** (1999)159.
- 5 A. Tungler, T. Mathe, T. Tarnai, K. Fodor, G. Toth, J. Kajter, I. Kolossvary, B. Herenyi, R.A. Sheldon, *Tet. Asymm.*, **6** (1995) 2395.
- 6 W.R. Huck, T. Mallat, A. Baiker, *Catal. Lett.*, **80** (2002) 3.
- 7 T. Tarnai, A. Tungler, T. Mathe, J. Petro, R.A. Sheldon, G. Toth, *J. Mol. Catal. A: Gen.*, **102** (1995) 41.
- 8 K. Borszky, T. Mallat, R. Aeschman, W.B. Schweizer, A. Baiker, *J. Catal.*, **161** (1996) 451.
- 9 P. A. Meheux, A. Ibbotson, P. B. Wells, *J. Catal.*, **128** (1991) 387.
- 10 H. U. Blaser, H-P. Jalett, M. Garland, M. Studer, H. Thies, A. Wirth-Tijani, *J. Catal.*, **173** (1998) 282.
- 11 W.R. Huck, T. Mallat, A. Baiker, *New J. Chem.*, **26** (2002) 6.
- 12 T. Hall, PhD Thesis, University of Hull, 1997.
- 13 Y. Nitta, T. Kubota, Y. Okamoto, *Bull. Chem. Soc. Jap.*, **74** (2001) 2161.
- 14 J.A. Slipszenko, S.P. Griffiths, P. Johnston, K.E. Simons, W.A.H. Vermeer, P.B. Wells, *J. Catal.*, **179** (1998) 267.
- 15 I. Kun, B. Torok, K. Felfoldi, M. Bartok, *App. Catal. A: Gen.*, **203** (2000) 71.
- 16 K. Borszky, T. Burgi, Z. Zhaohui, T. Mallat, A. Baiker, *J. Catal.*, **187** (1999) 160.

# *Chapter 4*

## 4.1 Preliminary Considerations

### 4.1.1 A Comparison of Pd/alumina catalysts (1) and (2).

Most of the results presented in Chapter 3 were obtained using one of two 5% Pd/alumina catalysts. The catalysts were supplied by Johnson Matthey and were from different batches (99300 and 99306). The metal assay of catalyst (1) was 4.97% Pd with a palladium particle size distribution extending from 2 – 20 nm. The metal assay of catalyst (2) was 5.03% Pd with the same palladium particle size distribution. The water content of catalyst (1) was 1.70% and that of catalyst (2) was 0.30%.

This similarity in Pd loading and particle size was reflected in the similar performance of the catalysts towards NADPME hydrogenation. For reactions conducted under standard conditions catalyst (1) provided an enantiomeric excess of 10%(*S*), and catalyst (2) an excess of 8%(*S*). This small difference in performance may be attributed either to the difference in water content of the catalysts, since small additions of water have a favourable effect on enantiomeric excess (Section 3.3.2.1), or to experimental error as experimental error for duplicate experiments was estimated to be  $\pm 1.5\%$ .

Overall, the rates of reaction, enantioselectivities and the trends observed were similar for each of the two catalysts. For this reason comparisons of the results can be made without special reference to which catalyst was used.

### 4.1.2 Deuterium Tracer Work

The deuterium tracer study was undertaken to identify the bond undergoing saturation during NADPME hydrogenation. NADPME has the potential to exist in tautomeric forms (Figure 3.4.1) and it was important to determine whether the process under study was one of  $>C=C<$ , or  $>C=N-$  saturation. HNMR spectra obtained of the hydrogenation product (Table 3.4.1) showed that the integrals attributed to CH and CH<sub>2</sub> were each reduced in size when the reaction was carried out using deuterium instead of hydrogen, whereas the integrals associated with protons from other parts of the molecule, including

>NH, remained unaffected. The reduction in the size of these integrals was a result of deuterium addition having occurred at these locations in the molecule. Thus, NADPME hydrogenation was solely carbon-carbon double bond saturation; the tautomeric form made no measurable contribution to reaction.

The >CX- function in the reaction product showed the isotopic composition >C(H<sub>0.5</sub>D<sub>0.5</sub>)-, indicating that the isotopic composition of the adsorbed-X was 50%H, 50%D. This occurred despite D<sub>2</sub> being used as the deuterium source, and indicates that other processes contributed to adsorbed-H to the active palladium surface. These processes could have included (i) diffusion of adsorbed-H from the bulk of Pd particles to the surface and (ii) H-spillover from the OH-groups of the alumina support to the Pd particles. The latter is known to occur rapidly [1].

The >CX<sub>2</sub> function in the reaction product showed the composition >CH<sub>1.5</sub>D<sub>0.5</sub>. Since the added X-atom had the composition H<sub>0.5</sub>D<sub>0.5</sub>, this indicates that the H-atom bonded to this carbon atom in the reactant did not undergo exchange for deuterium. This is consistent with an absence of *E/Z* isomerisation in the reactant.

### 4.1.3 Comments on the Standard Reaction

Initial experimental work defined a set of standard conditions for the cinchonine-modified hydrogenation of NADPME (Section 3.1). It established that the only effective metal able to reduce the carbon-carbon double bond selectively, was palladium. This was not surprising and is consistent with other enantioselective hydrogenations involving reactants that have more than one reducible group present [2].

The use of various supported Pd catalysts highlighted the influence of the support on catalyst performance (Table 3.1.1). For reactions carried out in methanol under standard conditions Pd/alumina provided an enantiomeric excess of 10% (S) whereas under the same conditions, the value of the enantiomeric excess was nearly doubled using 5% Pd/titania. However, the advantage of titania as the support was not fully realised due to the effect of solvent and pH not being as influential for reactions over Pd/titania as they were for reactions over Pd/alumina. Thus, provided that each catalyst was used under the

most favourable conditions, Pd/alumina and Pd/titania performed equally well and provided similar values of the enantiomeric excess.

Generally, optima in enantioselectivity were achieved using CN:NADPME molar ratios of 0.01 - 0.07 over both 5% Pd/alumina and 5% Pd/titania (Table 3.7.1). The only exception was for reactions over 2% Pd/titania where a ratio of 0.16 was optimal. These molar ratios are comparable to those reported in the literature for enantioselective hydrogenations over cinchona-modified palladium. Reactants such as, tiglic acid, E-( $\alpha$ )-phenyl cinnamic acid and hydroxymethylpyrone all show optimum enantioselectivity at modifier:reactant molar ratios between 0.01-0.03 [2-4]. This contrasts with cinchona-modified platinum systems where much smaller amounts of modifier are required to induce high enantioselectivity, (e.g. in ethyl pyruvate and ketopantolactone hydrogenations, modifier:reactant ratios of 0.001 and 0.0005 respectively are sufficient [5-6]). The requirement for greater quantities of alkaloid to induce optima in enantioselectivity over palladium is not fully understood, but two possible explanations can be advanced. First, there is no rate enhancement associated with enantioselective hydrogenation over palladium. As a result significant racemic reaction occurs at unmodified sites thereby reducing enantioselectivity. Higher concentrations of alkaloid may increase alkaloid coverage, thereby reducing the number of unmodified sites available for racemic reaction. Second, the ability of Pd to hydrogenate the modifier as well as the reactant may reduce the concentration of the effective modifier present. Certainly, the modifier was reduced to the 10,11-dihydroderivative before any significant hydrogenation of the reactant occurred (Section 3.9). This reduction of the modifier is of no consequence, since cinchonine and 10,11-dihydrocinchonine are equally as effective modifiers (Table 3.1.3). However, as reaction proceeded partial hydrogenation of the quinoline ring of the modifier occurred. Baiker reported a similar finding in the cinchona-modified hydrogenation of 2-pyrones [7]. This is significant because it effects the strength of adsorption of the alkaloid and its effectiveness as a modifier. The consumption of the active form of the modifier during the enantioselective reaction would inevitably mean that higher concentrations of modifier are required in the reaction medium to produce the desired effect.

Values of enantiomeric excess varied only slightly with conversion and with temperature over the range of 268 K to 313 K (Table 3.1.5). However, there were significant decrease



s in enantioselectivity with hydrogen pressures below 7 and above 20 bar (Figure 3.1.4), and for this reason 10 bar was used as the standard pressure for reaction.

This variation of enantiomeric excess with hydrogen pressure contrasts with those of other cinchona-modified enantioselective reactions, where enantiomeric excess increases as a function of hydrogen pressure through to an optimum, with very little change thereafter [8].

## 4.2 Kinetics of Racemic and Enantioselective NADPME Hydrogenation

### 4.2.1 Competitive and Non-Competitive Adsorption under Reaction Conditions

The classical treatment of heterogeneous reaction kinetics, as exemplified in Laidler's textbook on chemical kinetics, provides equations which describe the surface coverages of reactants A, B, C...,  $\theta_A$ ,  $\theta_B$ ,  $\theta_C$ ... when these reactants adsorb competitively at an energetically uniform surface [9]. Thus, if A and B adsorb non-dissociatively in competition:

$$\theta_A = b_A[A]/(1 + b_A[A] + b_B[B]) \text{ and } \theta_B = b_B[B]/(1 + b_A[A] + b_B[B]) \quad (1)$$

where the symbols have their usual significance. These equations are valid when the site requirements for the adsorption of A and B are the same, and will be acceptable when the site requirements are similar. Molecular models show (i) that NADPME, if adsorbed in a mode with all  $\pi$ -systems parallel to an atomically flat surface, will obscure about 13 Pd atoms and (ii) that cinchonine, if adsorbed by the quinoline moiety, will obscure about 15 Pd atoms. In the treatment below, it will be assumed that these requirements are sufficiently similar to allow their competitive adsorption to be described by expressions of the type shown in equation (1) above. The situation for the dissociative adsorption of molecular hydrogen is quite different in that the site requirement is much reduced,

consisting of not more than two Pd atoms, and hence expressions analogous to those in equation (1) do not hold. The random adsorption of large molecules such as NADPME and cinchonine cannot provide a close-packed adlayer (unless lateral diffusion is very fast) and hence, at any instant during reaction, there will always be small areas of unoccupied palladium surface at which hydrogen can adsorb without competition. The surface coverage of hydrogen can, therefore, be expressed by the usual equation for non-competitive adsorption:

$$\theta_H = \frac{b_H^{0.5} P_H^{0.5}}{(1 + b_H^{0.5} P_H^{0.5})} \quad (2)$$

#### 4.2.2 Order in NADPME

The initial rate of reaction was independent of [NADPME] over the range 0.34 to 1.03 M for both racemic and alkaloid-modified reactions (Section 3.2), i.e. the order in NADPME was zero. Let us assume that the adsorption of NADPME occurs without dissociation and that it obeys the Langmuir equation. The rate of racemic (unmodified) reaction is then given by equation (1):

$$\text{reaction rate} = k \theta_{\text{NADPME}} f(\theta_H) = \frac{k b_R [\text{NADPME}] f(\theta_H)}{1 + b_R [\text{NADPME}]} \quad (3)$$

where  $k$  is the rate coefficient,  $b_R$  is the adsorption coefficient of the organic reactant, and  $f(\theta_H)$  describes the dependence of rate on hydrogen coverage achieved as a result of non-competitive adsorption. If NADPME is strongly adsorbed,  $b_R [\text{NADPME}] \gg 1$ , and equation (1) reduces to: reaction rate =  $k f(\theta_H)$ , i.e. rate is independent of [NADPME]. Thus, in the unmodified racemic reaction, the observed zero order implies that the majority of the active surface is occupied by adsorbed-NADPME.

When modifier is present it occupies a fraction of the surface, as indicated by the enantiomeric excess in the products. The situation is now one of competitive adsorption, and the appropriate equation for the surface coverage of NADPME, following equation (1), is:

$$\theta_{\text{NADPME}} = \frac{b_{\text{R}}[\text{NADPME}]}{1 + b_{\text{R}}[\text{NADPME}] + b_{\text{M}}[\text{CN}]} \quad (4)$$

and the equation for the reaction rate is:

$$\text{reaction rate} = k \theta_{\text{NADPME}} f(\theta_{\text{H}}) = \frac{k \cdot b_{\text{R}}[\text{NADPME}]}{1 + b_{\text{R}}[\text{NADPME}] + b_{\text{M}}[\text{CN}]} \cdot f(\theta_{\text{H}}) \quad (5)$$

In equations (4) and (5)  $b_{\text{M}}$  is the adsorption coefficient of the modifier.

Since both NADPME and CN are strongly adsorbed it can be assumed that  $b_{\text{R}}[\text{NADPME}] \gg 1$  and that  $b_{\text{M}}[\text{CN}] \gg 1$ . Furthermore, if reactant and modifier are approximately equally strongly adsorbed, so that  $b_{\text{R}} \sim b_{\text{M}}$ , then the high NADPME:CN ratio used under standard conditions means that  $b_{\text{R}}[\text{NADPME}] > b_{\text{M}}[\text{CN}]$  and that  $b_{\text{R}}[\text{NADPME}]$  is the dominant term in the denominator; equation (5) then reduces to equation (3). Thus, the zero order in NADPME observed for enantioselective reactions is consistent with simultaneous strong adsorption of both the reactant and the modifier.

### 4.2.3 Order in Hydrogen

The order in hydrogen pressure was 0.6 for both the unmodified and modified reactions. As indicated above, hydrogen is considered to adsorb non-competitively in this reaction so that its coverage is described by equation (2). If, in addition, its adsorption is weak so that  $b_{\text{H}}^{0.5} P_{\text{H}}^{0.5} \ll 1$  then the expression for the hydrogen coverage becomes:

$$\theta_{\text{H}} = b_{\text{H}}^{0.5} P_{\text{H}}^{0.5} \quad \text{or} \quad \theta_{\text{H}} \propto P_{\text{H}}^{0.5} \quad (6)$$

Thus, the simplest interpretation of an order of 0.6 in hydrogen is that the rate determining step involves the reaction of an adsorbed organic species with one hydrogen atom. It should be noted that this statement is true only when the adsorbed organic species concerned has *not* been formed by reaction with adsorbed hydrogen in some previous kinetically fast step (e.g. it would not be true for a reaction in which the rate-

determining step was the reaction of a half-hydrogenated state with adsorbed hydrogen (see Section 1.8).

Orders in hydrogen of one-half are not uncommon in enantioselective hydrogenation; the palladium-catalysed hydrogenations of tiglic acid and of methyl pyruvate (which proceeds via the enol and is therefore an alkenic hydrogenation) are examples [10,11].

#### 4.2.4 Activation Energy

The dependence of initial rate on temperature is shown on Figure 3.2.12. The plot of  $\ln(\text{initial rate})$  versus reciprocal temperature shows a shallow curve based on four points. The mean straight line provides a value for the activation energy of  $51 \text{ kJ mole}^{-1}$ . This value is sufficiently large to indicate that the reaction was not under diffusion control. This conclusion is supported by (i) the very slow rates observed (Table 3.2.5) and the independence of reaction rate on stirring speed (Figure 3.1.3). Thus the sense of the curvature in Figure 3.2.12, which might in other circumstances suggest a reduction in apparent activation energy with increasing temperature due to diffusion limitation, is attributed either to adventitious scatter of the points or to experimental uncertainty in the rate measurements.

#### 4.2.5 Dependence of Rate on Catalyst Mass

The results, both for the racemic and modified reactions, are remarkable in that the reaction rates increased more than in proportion to the amount of catalyst used (orders in catalyst mass: 1.5 for racemic reaction (Figure 3.2.3) and 1.2 for cinchonine modified reaction (Figure 3.2.8)). If diffusion of hydrogen through the solution to the catalyst surface had been determining reaction rate, then rates should have shown an order less than 1.0 in catalyst mass. If reaction was diffusion-free, then the rates should have been first order in catalyst mass. The orders greater than 1.0 may indicate that the reactant contained a small amount of impurity which acted as a poison and was progressively removed as larger amounts of catalyst were used. However, any such impurity, if it existed, was not detected analytically.

#### 4.2.6 Conclusions.

The orders of reaction are consistent with strong competitive adsorption of NADPME and cinchonine, and with non-competitive adsorption of hydrogen. The experimental conditions provided diffusion-free reaction.

#### 4.2.7 Variation of Enantiomeric Excess with Hydrogen Pressure and Catalyst Mass

The enantiomeric excess was recorded as a function of hydrogen pressure (Table 3.2.4) and of catalyst mass (Table 3.2.3). The variation with increasing hydrogen pressure was closely similar to that recorded under standard reaction conditions (Figure 3.1.4), indicating that the initial rise and subsequent fall in enantiomeric excess was independent of the scale on which the reactions were carried out (kinetic experiments: 3.0 g NADPME, 0.2 g catalyst; standard conditions: 0.5 g NADPME, 0.1 g catalyst). Enantiomeric excess was independent of catalyst mass, as expected for a diffusion-free reaction (Table 3.2.3) and was not influenced by the presence of any supposed impurity (see Section 4.3.5 above).

The dependence of enantiomeric excess on hydrogen pressure is a little odd. It appears that hydrogen pressures between 7 and 20 bar are effective in producing an enantioselective result whereas, both lower and higher hydrogen pressures are ineffective. The catalyst was used as received and as such would contain an O-adlayer on the Pd surface. This may be removed easily at high hydrogen pressure but at low hydrogen pressures (1 bar) the catalyst may be poorly reduced. This may result in the site ensembles being big enough to accommodate NADPME but not the NADPME:CN complex. Thus, more racemic hydrogenation of NADPME occurred resulting in the low value of enantiomeric excess observed.

For hydrogen pressures greater than 30 bar the low value of enantiomeric excess may be attributed to the detrimental effect of reducing the quinoline moiety of the modifier, a process which is known to occur slowly at 10 bar hydrogen pressure (Section 3.8). The reduction of this part of the modifier may cause the modifier to become tilted with respect to the surface and hence less effective (see Section 4.5.2) thus leading to lower values of the enantiomeric excess.

### 4.3 A Model for the Cinchonine-Modified Hydrogenation of NADPME

#### 4.3.1 Pathways to Products

When approaching a discussion of mechanism it is important to take into account at the start the range of types of processes that might contribute. The task then becomes one of judging the importance of each type of process so that the most important are identified. Figure 4.3.1 shows the possibilities. NADPME and cinchonine (or other cinchona alkaloid) are present in solution and there is the possibility that they will interact together in solution to form one or more adducts (step 1). All three species may adsorb on the

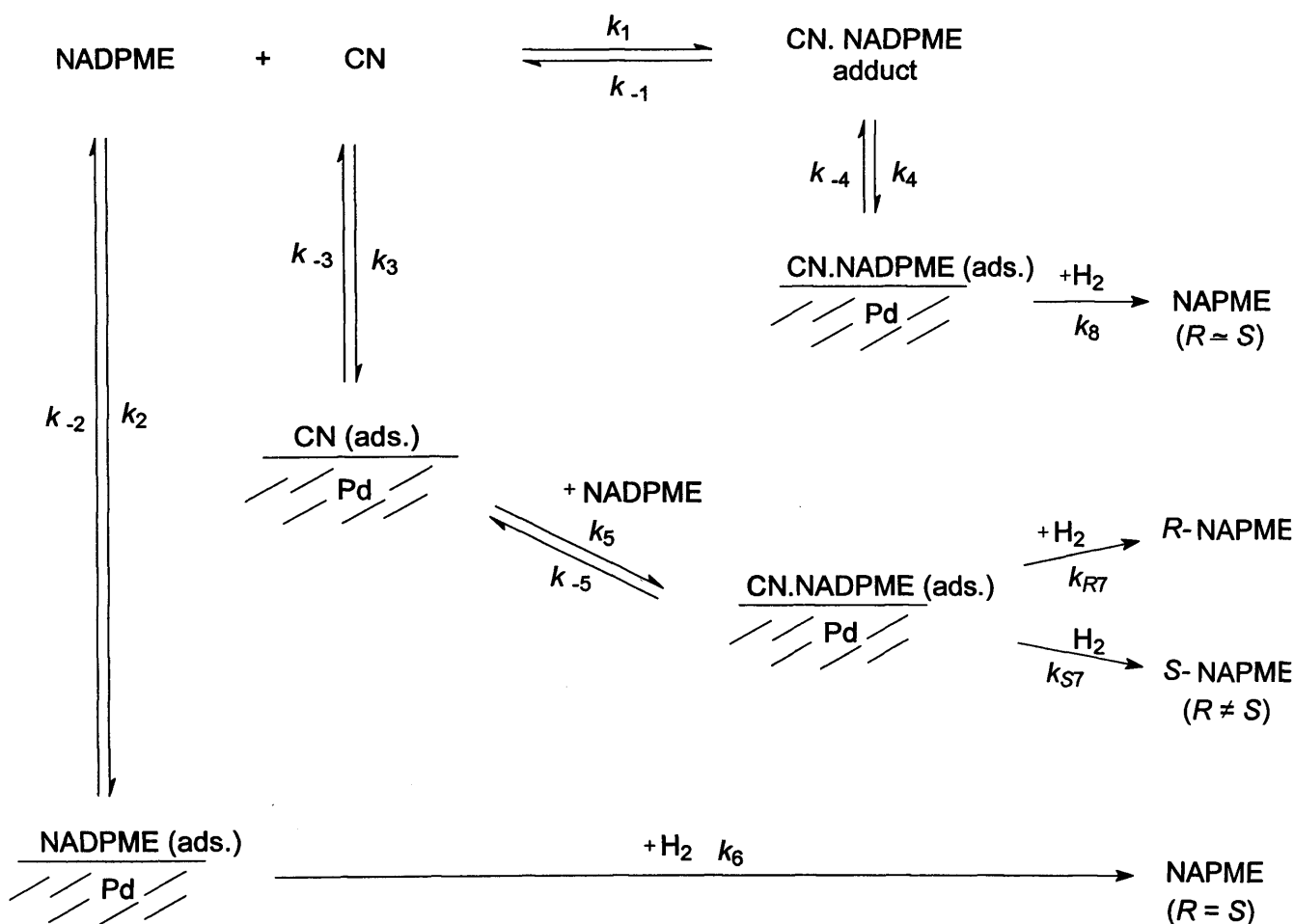


Figure 4.3.1 An illustration of the various pathways available for hydrogenation over cinchonine-modified palladium.

catalyst surface, giving NADPME(ads) by step 2, cinchonine(ads) by step 3, and adduct(ads) by step 4. It will be assumed that all three species are reversibly adsorbed. NADPME(ads) may then undergo hydrogenation to *N*-acetylphenylalanine methyl ester (NAPME) by step 6 and because this hydrogenation occurs without the participation of cinchonine the product will be a racemic mixture of *R*- and *S*-NAPME. The adsorbed adduct may be hydrogenated to NAPME by step 8; whether or not this step provides a racemic mixture will depend on the structure of the adduct, and this is discussed later. If, following cinchonine adsorption, NADPME is adsorbed in its vicinity (step 5) such that it can undergo selective enantioface adsorption, then adsorption by one enantioface will give *R*-NADPME on hydrogenation (step 7R), adsorption by the other enantioface will give *S*-NADPME (step 7S), and this fraction of the product will show an enantiomeric excess. The overall reaction will show a different enantiomeric excess which results from the sum of all three product pathways.

These three pathways to product will be considered in the order (i) adsorption and reaction of NADPME at alkaloid-modified Pd sites (steps 3,5,7), (ii) adsorption and reaction of NADPME at unmodified Pd sites (steps 2,6); and (iii) adsorption and reaction of adduct at Pd sites.

### 4.3.2 Adsorption and Reaction of NADPME at Alkaloid-Modified Sites

Because of the molecular complexity of the NADPME molecule, the discussion of its reaction at alkaloid-modified sites will be preceded by consideration of the adsorption and reaction of the free amine, dehydrophenylalanine methyl ester (DPME).

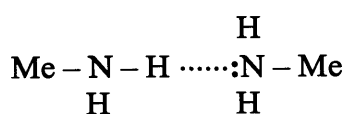
#### 4.3.2.1 Origin of the reactant-modifier interaction

Table 3.5.2 contains the information that the methyl ester of methylcinnamic acid was hydrogenated over cinchona-modified Pd/alumina and that it gave racemic product. This concurs with the literature in that Nitta and co-workers have shown that the methyl ester of phenylcinnamic acid is likewise reduced to racemic product [12], and Wells and co-workers have reported the same result for methyl tiglate [13]. In fact, there are no reports in the literature of the enantioselective hydrogenation of esters, so the enantioselective

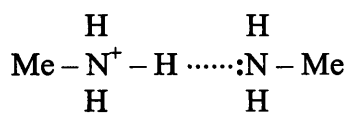
hydrogenation of DPME and NADPME observed in this investigation is exceptional. The chemical variation on passing from methylcinnamic acid methyl ester to DPME consists only in the replacement of a methyl group by an amine group, and hence there is an *a priori* case for supposing that it is the  $-\text{NH}_2$  group that interacts in some crucial way with cinchonine or cinchonidine. Likewise, in NADPME hydrogenation, the crucial interaction is supposed to be with the  $>\text{NH}$  portion of the  $-\text{NHAc}$  substituent.

In the hydrogenation of  $\alpha,\beta$ -unsaturated acids, such as phenylcinnamic acid and tiglic acid, it is the  $-\text{COOH}$  function of the reactant that undergoes H-bonding with the quinuclidine-N atom of the adsorbed modifier (Section 1.8.2) prior to selective enantioface adsorption. It is therefore likely that the interaction of DPME and of NADPME with adsorbed cinchona alkaloid is either by H-bonding between the  $>\text{NH}$  moiety of the reactant and the quinuclidine-N atom of the adsorbed modifier, or (if the quinuclidine-N is already protonated, see later) by H-bonding involving the lone pair on the  $\text{>N}$ -atom and quinuclidine- $\text{NH}^+$ .

Jeffery and Willock have calculated the relative strengths of these two types of H-bond for the cases of the interaction between two methylamine molecules (1) and the interaction of methylamine with protonated methylamine (2) [14].



(1)



(2)

The decreases in energy that occur on formation of these H-bonds from the constituent molecules at infinite separation are  $12 \text{ kJ mole}^{-1}$  and  $111 \text{ kJ mole}^{-1}$  respectively. Thus each type of interaction is favoured, the stronger interaction being of potential importance in media where protonation of the quinuclidine-N of the modifier is facile (see Section 4.5).



## 4.3.2.2 Reactant conformations

*DPME*

Modelling by Jeffery and Willock has identified two low energy conformations for free DPME (Figure 4.3.2). The lower energy conformation is shown as conformation-1 in Figure 4.3.2. The other conformation was higher in energy by  $46.4 \text{ kJ mole}^{-1}$  and was disregarded on energy grounds. Conformation-1 is not planar, the  $>\text{C}=\text{C}<$  to be hydrogenated being inclined at a dihedral angle of  $22.2$  degrees with respect to the phenyl ring. The mirror image of conformation-1, conformation-2, Figure 4.3.2, is (of course) of equal energy and conformational interconversion in the free state is assumed to be facile.

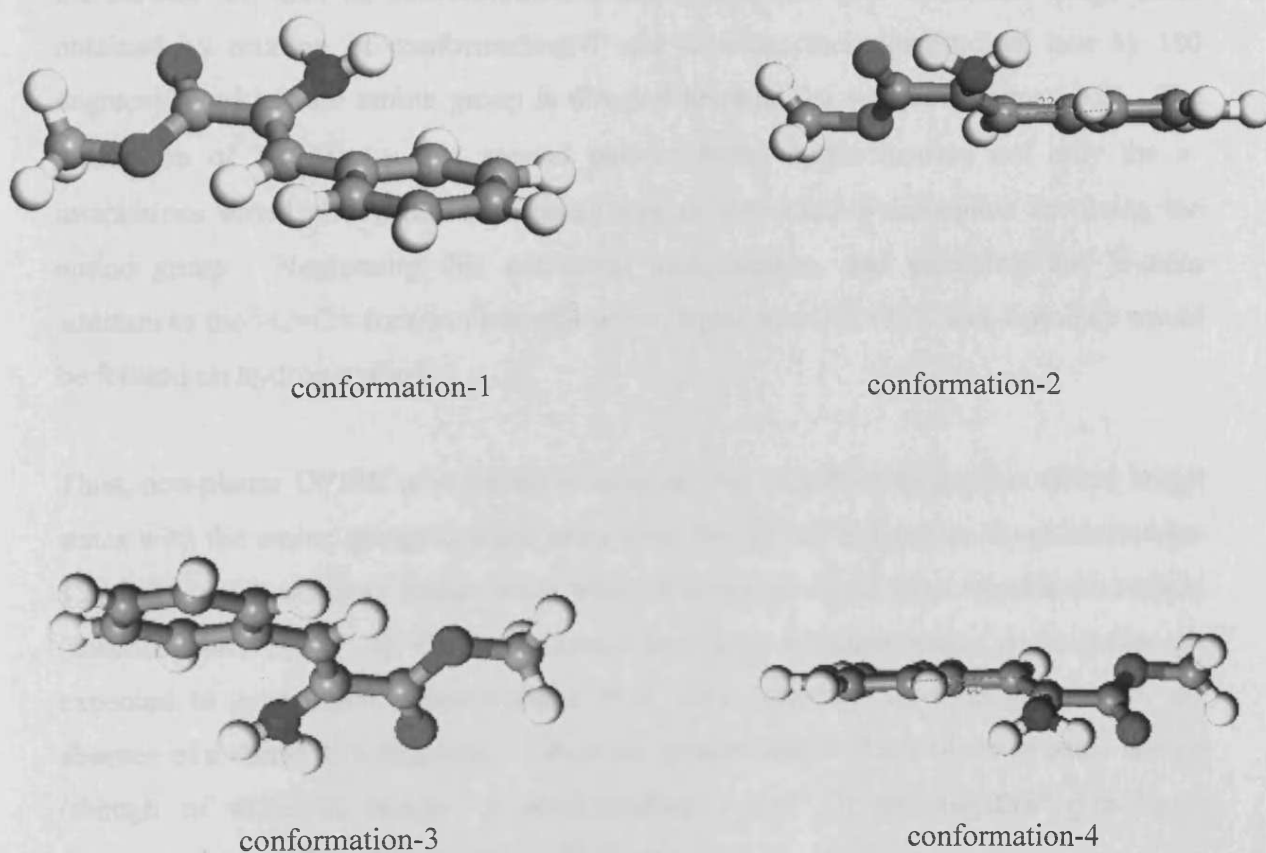


Figure 4.3.2 The four conformations for free DPME identified by molecular modelling  
●: carbon; ○: hydrogen; ●: nitrogen; ●: oxygen.

## 4.3.2.2 Reactant conformations

*DPME*

Modelling by Jeffery and Willock has identified two low energy conformations for free DPME (Figure 4.3.2). The lower energy conformation is shown as conformation-1 in Figure 4.3.2. The other conformation was higher in energy by  $46.4 \text{ kJ mole}^{-1}$  and was disregarded on energy grounds. Conformation-1 is not planar, the  $>\text{C}=\text{C}<$  to be hydrogenated being inclined at a dihedral angle of  $22.2$  degrees with respect to the phenyl ring. The mirror image of conformation-1, conformation-2, Figure 4.3.2, is (of course) of equal energy and conformational interconversion in the free state is assumed to be facile.

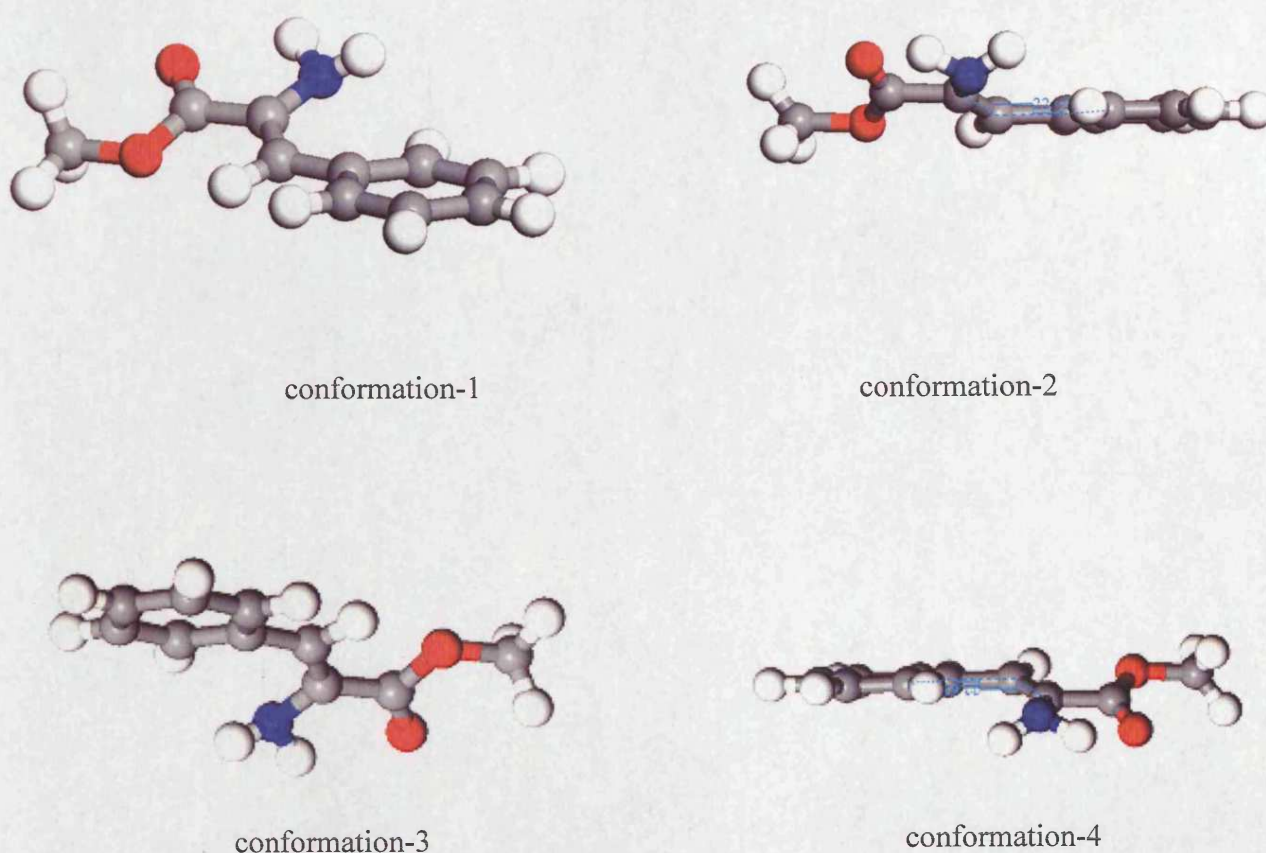


Figure 4.3.2 The four conformations for free DPME identified by molecular modelling  
●: carbon; ○: hydrogen; ●: nitrogen; ⊕: oxygen.

Consider conformation-1 adsorbed at a flat Pd surface. The molecule has three  $\pi$ -electron systems and it will be supposed that each interacts with the surface to some degree. However, phenylalanine methyl ester is the only reaction product, and hence the adsorbed state must be such as to permit the addition of two H-atoms to the  $>C=C<$  function. In common with other investigators, we assume that these H-atoms are transferred from the Pd surface and are added from below the plane of the adsorbed organic reactant. On this basis, adsorbed conformation-1 would give *S*-phenylalanine methyl ester on hydrogenation, whereas adsorbed conformation-2 would give *R*-product. Assuming these mirror image conformations to be of the same energy in their adsorbed states, equal amounts of *R*- and *S*-product would be formed on their hydrogenation.

For non-planar pro-chiral DPME, the molecule can be adsorbed not only as conformations-1 and -2 (mirror image states) with the amine group directed away from the surface but also as conformations-3 and -4 (another pair of mirror image states obtained by rotation of conformations-1 and -2 about their longitudinal axis by 180 degrees) in which the amine group is directed towards the surface (Figure 4.3.2). The adsorption of DPME by this second pair of states might involve not only the  $\pi$ -interactions noted above but also associative or dissociative adsorption involving the amine group. Neglecting this additional complication, and assuming that H-atom addition to the  $>C=C<$  function can still occur, equal amounts of *R*- and *S*-product would be formed on hydrogenation.

Thus, non-planar DPME is expected to exist as four adsorbed states, two mirror image states with the amine group directed away from the surface (adsorbate in conformations-1 and -2), and two mirror image states with the amine group directed towards the surface (conformations-3 and -4). Conformations-1 and -2 are of equal energy and together are expected to give equal concentrations of *R*- and *S*-product on hydrogenation in the absence of a chiral directing agent. Likewise, conformations-3 and -4 are of equal energy (though of different energy to conformations-1 and -2) and together give equal concentrations of *R*- and *S*-product on hydrogenation.

*NADPME*

The above considerations also apply in principle to NADPME. Jeffery and Willock have calculated some minimum energy states for NADPME and report that the lowest energy conformation is one which resembles conformation-1 of DPME with the acetyl group located over-and-above the phenyl group (Figure 4.3.3).

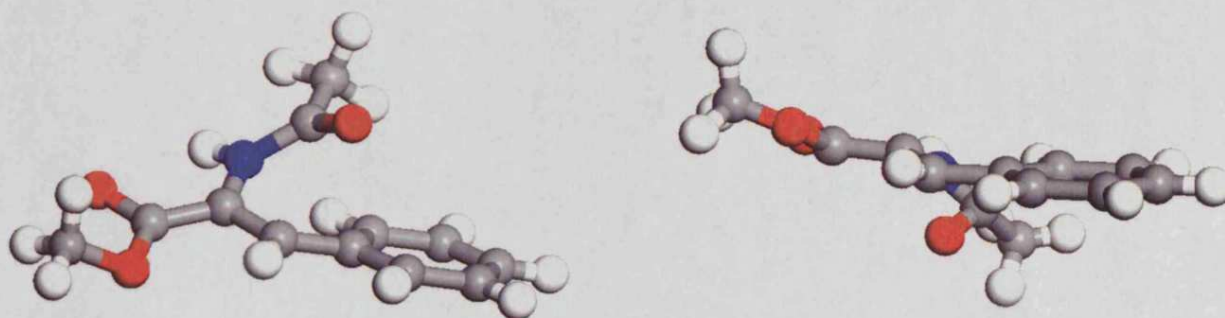


Figure 4.3.3 The two lowest energy conformations of NADPME obtained by molecular modelling.  $\ominus$  : carbon;  $\circ$  : hydrogen;  $\bullet$  : nitrogen;  $\bullet$  : oxygen.

The dihedral angle for this conformation is 13 to 18 degrees and hence there is a mirror image structure (conformation-2) of identical energy. Two other minimum energy conformations were identified in which rotation of the  $\text{-NHAc}$  group had occurred; these structures were of higher energy by 10.4 and 19.3  $\text{kJ mole}^{-1}$  and showed dihedral angles of 43 and 25 degrees respectively (structures not shown). In the lowest energy structure (Figure 4.3.3) the O-atom of the  $\text{-NHAc}$  group is directed away from the other two O-atoms in the structure whereas, in the other two structures the three O-atoms are in closer proximity and their mutual repulsions are accommodated to some degree by the enhanced dihedral angles.

Because of the increased three-dimensionality of NADPME in its lowest energy conformation, adsorption by modes equivalent to conformations-3 and -4 for DPME (i.e. with the amine group directed towards the surface) is not possible. Thus, in the developing mechanisms for NADPME hydrogenation it will be supposed that reactant molecules are adsorbed in their lowest energy configurations as conformations-1 and -2.



## 4.3.2.3 Reactant:modifier interaction at the enantioselective site

The adsorption of DPME and NADPME at the enantioselective site can now be considered. Figure 4.3.4 shows cinchonine in its open-3 configuration adsorbed at a Pd(111) surface. The adsorbed alkaloid molecule is arbitrarily located such that the two aromatic rings of the quinoline moiety are located directly above adjacent surface Pd atoms.

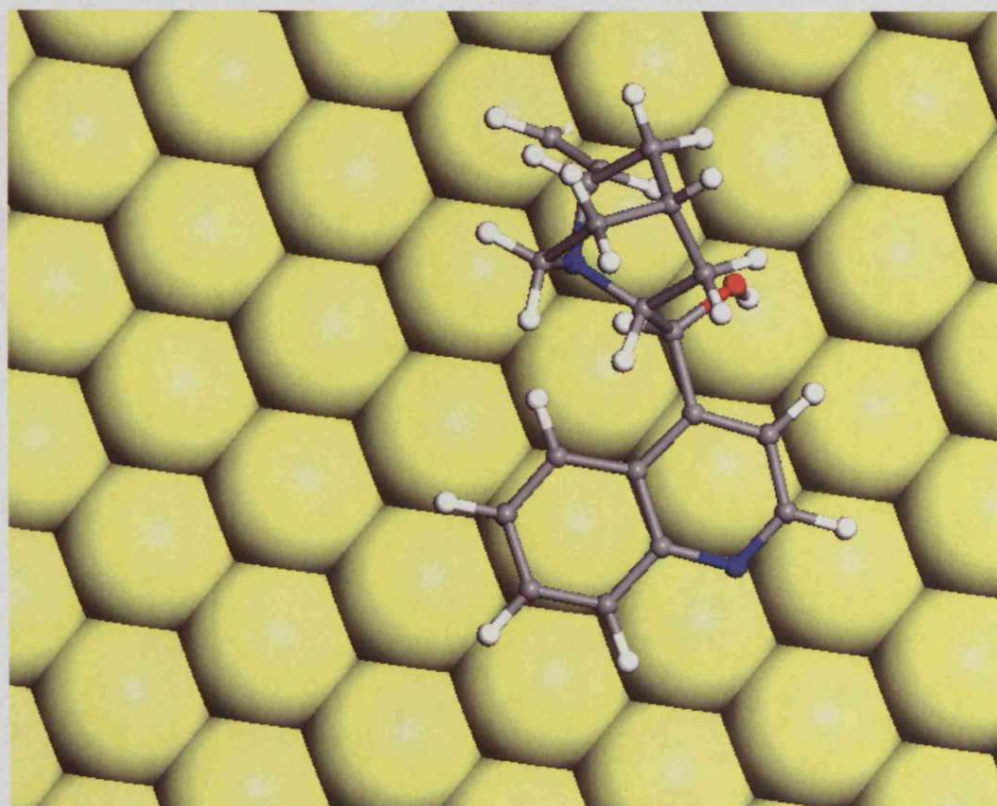
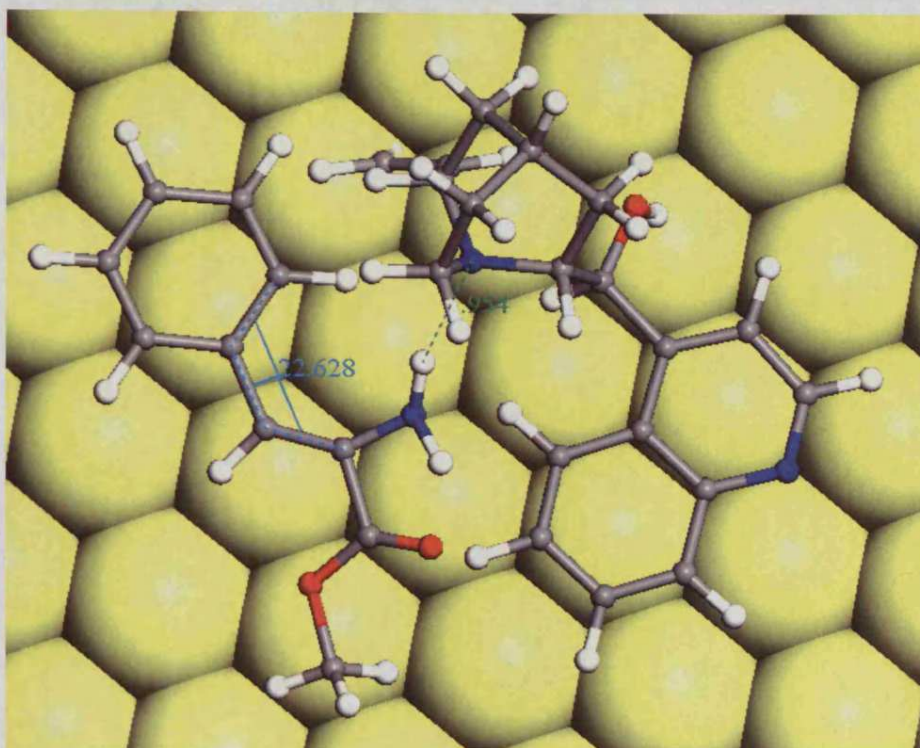
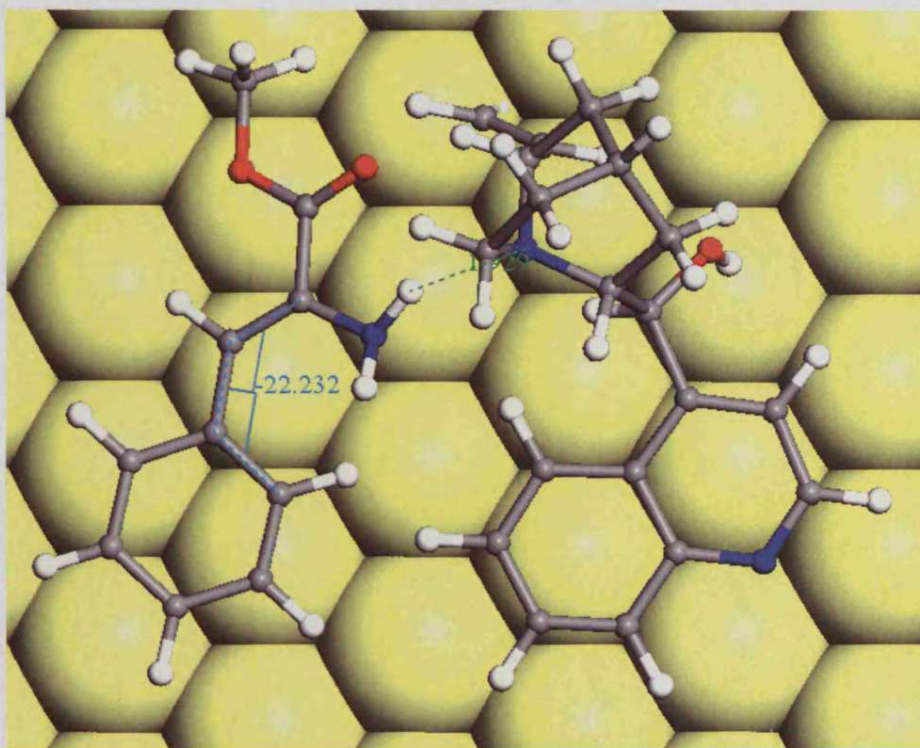


Figure 4.3.4 Cinchonine adsorbed on a Pd(111) surface. ● : carbon;  
○ : hydrogen; ● : nitrogen; ● : oxygen.

Step 5 of the Scheme in Figure 4.3.1 is envisaged to occur by DPME or NADPME approaching the surface through the fluid phase in such a way that a H-bond is formed between the >NH moiety of the reactant and the quinuclidine-N atom of the adsorbed modifier. This may occur before adsorption of the reactant, resulting in the formation of a *precursor state*. The precursor state may then dissociate, releasing the reactant molecule back to the fluid phase, or chemisorption of the reactant may occur at adjacent Pd atoms either by conformation-1 (a) or by conformation-2 (b) (Figure 4.3.5). These Figures show DPME adsorbed with the H-bond retained.



conformation-1 (a)



conformation-2 (b)

Figure 4.3.5 DPME adsorbed by each of its two conformations at the enantioselective site adjacent to cinchonine adsorbed in the open-3 conformation. Upon hydrogenation, (a) gives *S*-PME and (b) gives *R*-PME.



Such H-bond retention is not a necessary feature of the process. In principle, the precursor state fulfils two roles. It serves to bring the reactant into a closer spatial relationship with the modifier than would be achieved by simple van der Waals interaction, and it has a lifetime within which the reactant molecule can become aligned with the 'enantioselective site' more efficiently than would be the case during a simple molecular collision.

Figures 4.3.5 show the H-bond retained at a length of less than 0.2 nm and the  $C_{Ph}-C_{Ph}-C=C$  dihedral angle retained at 22 degrees, and there is no clear registration between the unsaturated functions of adsorbed DPME and the surface Pd atoms. It is likely, therefore, that the precursor state dissociates as DPME adsorbs, and that the  $>C=C<$  group adopts some optimum configuration with respect to the underlying Pd surface. If that optimum configuration involved  $\pi$ -adsorption to one Pd atom, then adsorbed-DPME in both conformations would move very slightly away from the adsorbed modifier.

Figures 4.3.5 (a) and (b) indicate the surface requirement for an enantioselective site. In each Figure, cinchonidine is adsorbed to two surface Pd atoms, but the alkaloid molecule as a whole obscures about 15 surface atoms, i.e. the van der Waals radii of the constituent atoms are such that 15 Pd atoms are no longer accessible to other adsorbing molecules (other than, possibly, hydrogen). Reactant DPME obscures 13 – 15 surface atoms in conformation-1 and 12 – 14 surface atoms in conformation-2. Four of these atoms are obscured jointly by reactant and modifier, so the total site requirement for the modifier-reactant complex is a minimum of 24 atoms for DPME in conformation-1 and 25 atoms for DPME in conformation-2.

#### 4.3.2.4 Enantioselective hydrogenation

##### *DPME*

Addition of two H-atoms to the  $>C=C<$  function of adsorbed-DPME in conformation-1 (a), (Figure 4.3.5) gives *S*-phenylalanine methyl ester whereas the corresponding addition to conformation-2 (b), (Figure 4.3.5) gives *R*-PME. The enantiomeric excess is therefore related to the populations of these conformations and their reactivities. Heterogeneous enantioselective hydrogenations over both Pd and Pt have been interpreted, without

exception, by supposing that different enantiofacial states have the same reactivities, and that the enantiomeric excess is determined by the relative surface coverages of the two enantiofacial forms. That assumption is made again here although, as noted in the Introduction (Section 1.9), it does not hold for the homogeneous enantioselective hydrogenation of NADPME. The relative surface coverages of conformations-1 and -2 ( $\theta_1/\theta_2$ ) are determined by the difference in their free energies of adsorption, thus:

$$\theta_1 / \theta_2 = \exp[\Delta G^\circ_1 - \Delta G^\circ_2] / RT$$

No values are available for the free energies of adsorption, and no calculations are available of the interaction in Figure 4.3.5. Consequently, no estimate can be made of the likely relative coverages of adsorbed conformations-1 and -2. However, the experimental result of DPME hydrogenation under standard conditions (Table 3.5.2) was that the enantiomeric excess was 11%(*S*), from which we conclude (given the assumptions made above) that conformation-1 was preferred to conformation-2 at the surface of the working catalyst.

In Figure 4.3.5 (a) the phenyl group of DPME is adjacent to the quinoline moiety of cinchonine, and the O-atom of the ester carbonyl is adjacent to the N-atom of the quinuclidine ring system. In Figure 4.3.5 (b) the phenyl group of DPME is adjacent to the quinuclidine ring system and the O-atom of the ester carbonyl is directed towards the quinoline ring system of the adsorbed modifier. These interactions would be strongly repulsive if experimental conditions were such as to cause compression of the surface adlayer; this will attract comment later.

#### *NADPME*

The situation on adsorption of NADPME as conformations-1 and -2 adjacent to adsorbed cinchonine in the open 3 conformation can be envisaged by consideration of Figure 4.3.5. For the adsorption of NADPME in conformation-1 the acetyl group substitutes the H-atom not involved in H-bonding to the alkaloid and is located above the phenyl and (to some extent) the quinolyl ring systems. For NADPME in conformation-2 formation of the precursor state requires a rotation of the -NHAc group so that the crucial H-bond can be formed to the quinuclidine-N atom of adsorbed cinchonine. Adsorption can then occur with the acetyl group directed above the ester function of the reactant and (to some



extent) the quinoline ring of the modifier. Although the presence of the acetyl group clearly congests the reactant-modifier complex, the congestion does not substantially modify the crucial interactions identified for DPME. Thus, typical values of the enantiomeric excess of 10%(*S*) recorded in the standard reactions indicate that adsorption as conformation-1 is slightly preferred over that of conformation-2.

#### 4.3.2.5 Modification by protonated cinchonine

It becomes evident in Section 4.5 below that, under certain conditions, the modifier is cinchonine protonated at the quinuclidine-N atom. In these circumstances, the H-bond in the precursor state is formed by interaction of the lone pair on the N-atom of NADPME with the protonic H-atom of the modifier. The DPME-modifier complexes are then as shown in Figures 4.3.6 and 4.3.7 (superseding Figure 4.3.5) and there is a slightly greater flexibility in accommodating the acetyl group when considering the NADPME-modifier complexes. Protonation of the quinuclidine-N did not of itself alter the chiral outcome of the reactant-modifier interaction.

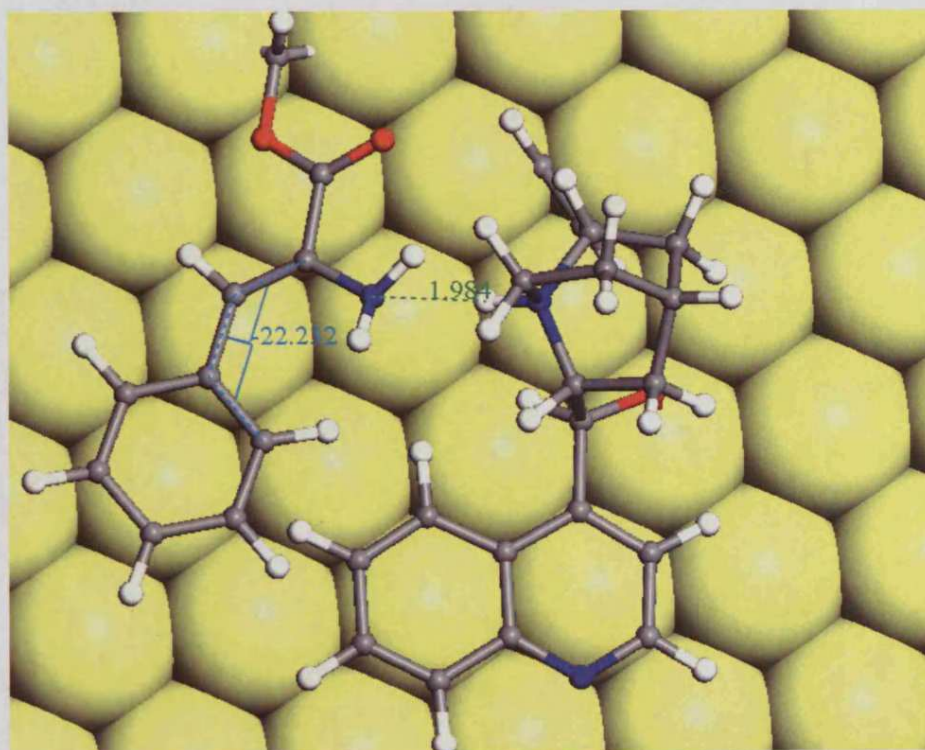


Figure 4.3.6 DPME adsorbed by conformation-1 at the enantioselective site adjacent to a protonated cinchonine molecule in the open-3 conformation. Upon hydrogenation gives *S*-PME. ● :carbon; ○ : hydrogen; ● : nitrogen; ● : oxygen.

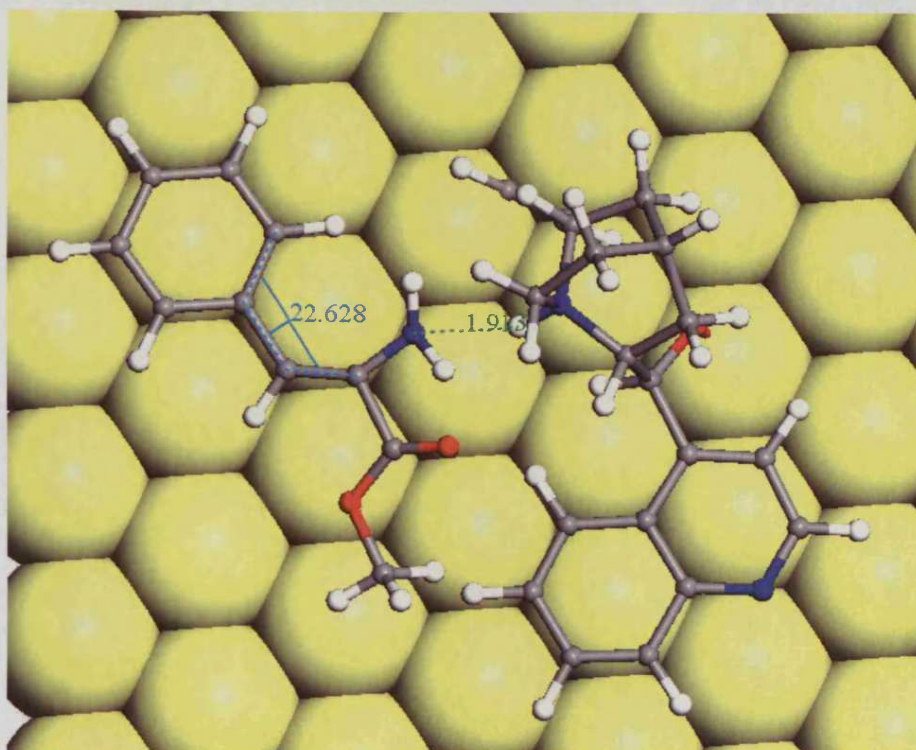


Figure 4.3.7 DPME adsorbed by conformation-2 at the enantioselective site adjacent to a protonated cinchonine molecule in the open-3 conformation. Upon hydrogenation gives *R*-PME. ● : carbon; ○ : hydrogen; ● : nitrogen; ● : oxygen.

The calculations for methylamine referred to above indicate that such a precursor state involving protonated cinchonine would be more stable than that involving the unprotonated form; the rate data available are insufficient to show whether this was kinetically significant.

### 4.3.3 Adsorption and Reaction of NADPME at Unmodified Sites

NADPME may adsorb at any element of vacant Pd surface provided a sufficient number of Pd atoms, probably about 12 in a 4 x 3 array (cf. Figure 4.3.5 for DPME), are exposed to the fluid phase. Only such ensembles adjacent to the chiral cleft of adsorbed cinchonine are locations at which the reactant can respond to the chiral environment created by the alkaloid. At all other locations adsorption will occur as either

conformation-1 or -2, the chances of each conformation being adsorbed being 50% over a very large number of such events. Consequently, the yields of *R*- and *S*-product will each be 50%, i.e. racemic reaction is obtained.

#### 4.3.4 Adducts in Solution and their Reaction at Surface Sites

Provided cinchonine is not protonated, its interaction with NADPME in solution is likely to be confined to a H-bonding interaction with the H-atom of the –NHAc group of the reactant, i.e. the precursor state interaction discussed above may also occur transiently in solution.

Figures 4.3.8 and 4.3.9 below indicates that cinchonine may be protonated under conditions where it functions effectively. Jeffery and Willock have carried out calculations which reveal that a variety of H-bonded adducts may have some stability, and that a H-bond can be formed to any of the three O-atoms of the NADPME structure. Two of the lowest energy adducts are shown in Figures 4.3.8 and 4.3.9; in one the H-bond is to the O-atom of the acetyl group and in the other it is to the carbonyl O-atom of the ester group. The  $C_{Ph}-C_{Ph}-C=C$  torsion angles in these species are 59 and 60 degrees respectively, indicating that resonance between the carbon-carbon double bond and the phenyl ring has been largely disrupted. If adduct (b) was to adsorb by the quinoline moiety of the alkaloid and the phenyl group of NADPME simultaneously it is not clear whether H-atom addition to the inclined carbon-carbon double bond could occur, and if it did, what would be the chiral outcome.

However, when similar calculations were carried out for methylcinnamic acid methyl ester, similar adducts were encountered, and one of these is also shown in Figure 4.3.9. Since methylcinnamic acid methyl ester is hydrogenated over cinchonine-modified Pd to give racemic product (Section 3.5.2) it would appear that any participation of such adducts in NADPME hydrogenation does not contribute to enantioselective hydrogenation, and that step 8 of the general mechanism (Figure 4.3.1), if it occurs at all, supplements the racemic product formed in step 6. In Figure 4.3.8 the colour of the atoms of both structures are the same as for those in Figure 4.3.9.



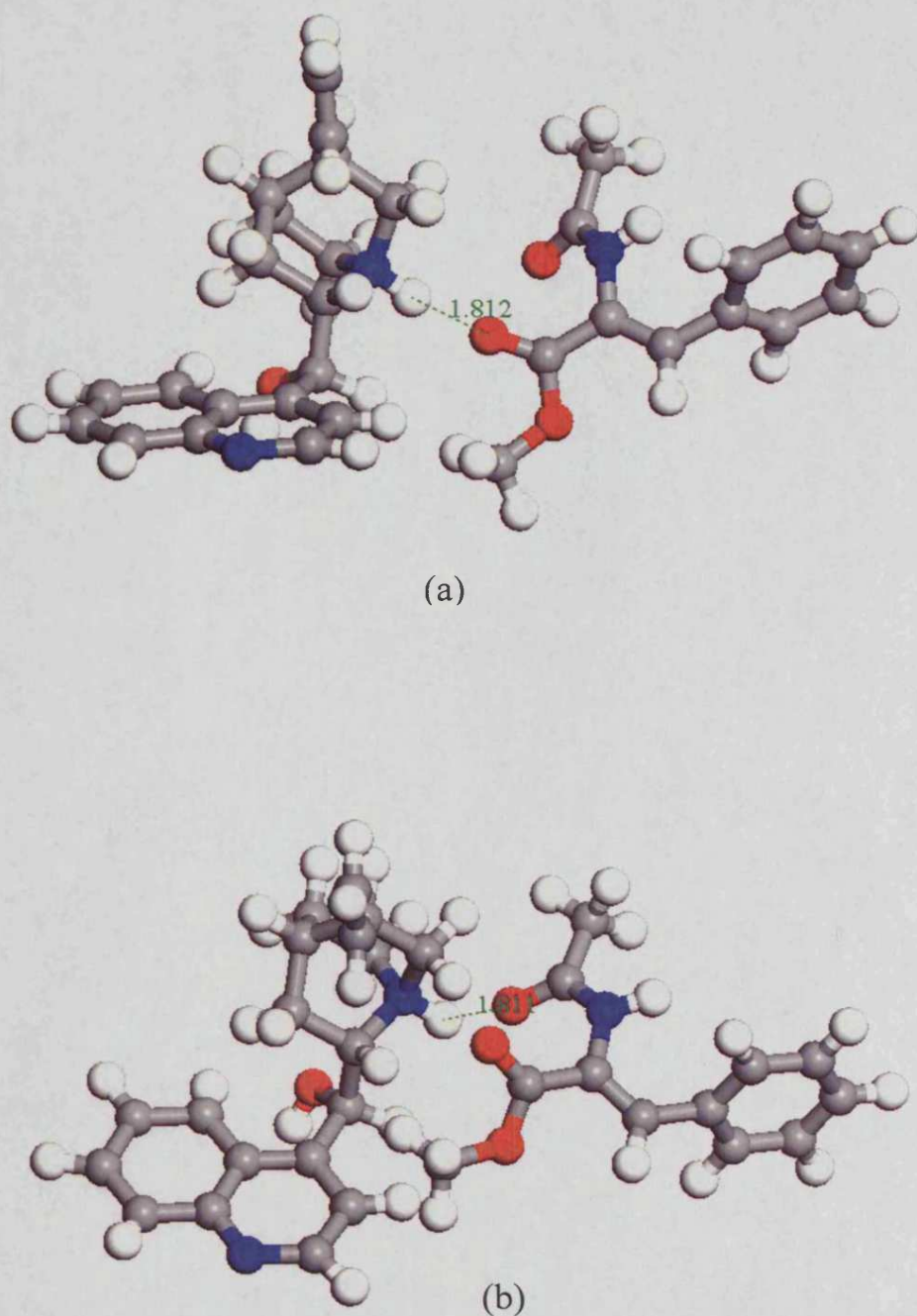


Figure 4.3.8 The low energy complexes formed between NADPME and cinchonine. In (a) there is H-bond between the carbonyl-O atom of the ester function of NAPME and the protonated quinuclidine-N atom of cinchonine (in the open-3 conformation); and in (b) there is a H-bond between the carbonyl-O atom of the acetyl group and the protonated quinuclidine-N of cinchonine.

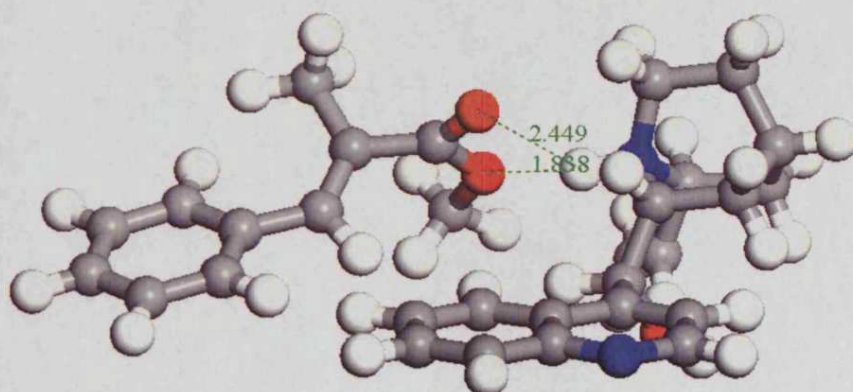


Figure 4.3.9 Adduct formation between the ester function in methyl cinnamate and the protonated quinuclidine-N of cinchonine. ● : carbon; ○ : hydrogen; ● : nitrogen; ● : oxygen.

One consequence of these calculations is that it has raised an awareness that a proportion of adsorbed protonated cinchonine molecules may, for a proportion of their lifetime in the adsorbed state, be involved in unproductive adduct formation, and thereby be prevented from functioning as effective modifiers creating enantioselective sites for NADPME hydrogenation.

#### 4.3.5 Conclusions

The above sections indicate that there is experimental evidence for the operation of each of the molecular processes indicated in steps 1 – 8 of Figure 4.3.1. Since the enantiomeric excess achieved in step 7 is not known, the relative importance of the various product-forming steps cannot be evaluated. However, given the very precise geometrical requirements to achieve enantioselection in steps 6 and 7, it is likely that the product yield by this pathway may be modest, in which case the inherent efficiency of the enantioselective process may have been high. For example, if steps 5 and 7 were the only product-forming steps and the former contributed two-thirds of the product with e.e. = zero then a measured enantiomeric excess of 14% would have corresponded to an enantiomeric excess provided by step 7 of 70%.

## 4.4 The Effect of Solvent

### 4.4.1 The Effect of Conformational Behaviour of Cinchona Alkaloids in NADPME Hydrogenation.

As indicated in the Introduction, cinchona alkaloids exhibit a rich conformational behaviour due to rotation about the single bonds in the molecule, i.e. C<sub>4</sub>' and C<sub>9</sub>, C<sub>8</sub> and C<sub>9</sub>, C<sub>3</sub> and C<sub>10</sub>, and C<sub>9</sub> and O. As a result, cinchonine and cinchonidine possess four states of minimum energy, identified as closed-1 and -2 and open-3 and -4 (Figure 1.8.5). Because each has a different dipole moment the relative abundance of these states as measured in solution by NMR depends on the polarity of the solvent. Thus, as the dielectric constant of the solvent increases, the energies of the closed-1 and -2 states approaches that of open-3. The closed-1 and -2 states having higher dipole moments are stabilised in the more polar solvents. The relative abundance of open-3 in various solvents is as follows: toluene ( $\epsilon = 2.34$ ) = 70%, diethylether ( $\epsilon = 4.3$ ) = 71%, THF ( $\epsilon = 7.6$ ) = 62%, DMF ( $\epsilon = 36.7$ ) = 33% and water ( $\epsilon = 78.5$ ) = 30% [15]. However, ethanol fails to conform to this correlation due to hydrogen bonding occurring between its OH group and the quinuclidine-N atom of the alkaloid, which stabilises the open-3 conformer: [Open-3] = 77% has been reported [15].

For many enantioselective hydrogenations there is a correlation between enantiomeric excess and the relative abundance of open-3 in solution, such that higher enantioselectivities are observed in apolar solvents [15]. Table 3.3.1 shows that for NADPME hydrogenation, this generalisation does not apply, since the enantioselectivity increases with the dielectric constant of the solvent. Thus, the population of the open-3 conformer in solution is not the prime determinant of enantioselectivity as solvent is varied. An alternative important influence on enantioselectivity is the configuration of the reactant in solution, as discussed in the next sub-section.

### 4.4.2 The Effect of Solvent on the Nature of the Modifier-Reactant Interaction

NADPME has the potential to exist as both a monomer and a dimer in solution, the two

forms being in dynamic equilibrium (Figure 4.4.5). The extent of dimerisation is expected to depend on the polarity of the solvent, such that more polar solvents will favour the monomer and the less polar (or the apolar) solvents the dimer.

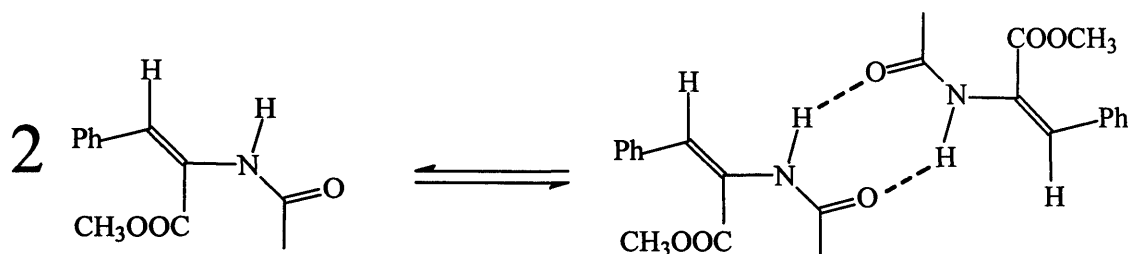


Figure 4.4.5 NADPME dimer formation.

Infra-red spectra obtained for NADPME in various solvents (not shown) did not provide conclusive evidence for dimer formation. However, the study of similar reactants has shown that dimerisation occurs in analogous systems [16].

Not only may NADPME form dimers in solution, it may also H-bond with cinchonine (a reactant-modifier interaction).

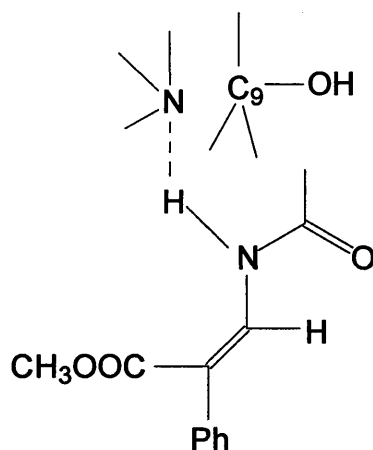


Figure 4.4.6 Representation of the NADPME monomer bonded to the quinuclidine-N atom of cinchonine

Figure 4.4.6 (above) shows a possible 1:1 H-bonding interaction between NADPME and cinchonine whereby the NH of the acetyl group of the reactant interacts with the quinuclidine-N of the modifier (assumed to be in the open-3 conformation). This system is analogous to that proposed by Nitta in the enantioselective hydrogenation of (E)-phenyl cinnamic acid over cinchona-modified Pd [3].

Another possibility is that an interaction may occur between the NADPME dimer and cinchonine. For this to occur both the quinuclidine-N and the OH at C<sub>9</sub> of the modifier are required for interaction with NADPME, as depicted in Figure 4.4.7. In this model three hydrogen bonds are formed:

- (i) one between the quinuclidine-N of the modifier and the NH group of the acetyl group of one NADPME molecule.
- (ii) one between the carbonyl group of the acetyl group of one molecule of NADPME and the NH-group of the acetyl group of the second molecule of NADPME; and
- (iii) one between the carbonyl group of the acetyl function of the second molecule of NADPME and the C<sub>9</sub>-OH of the modifier.

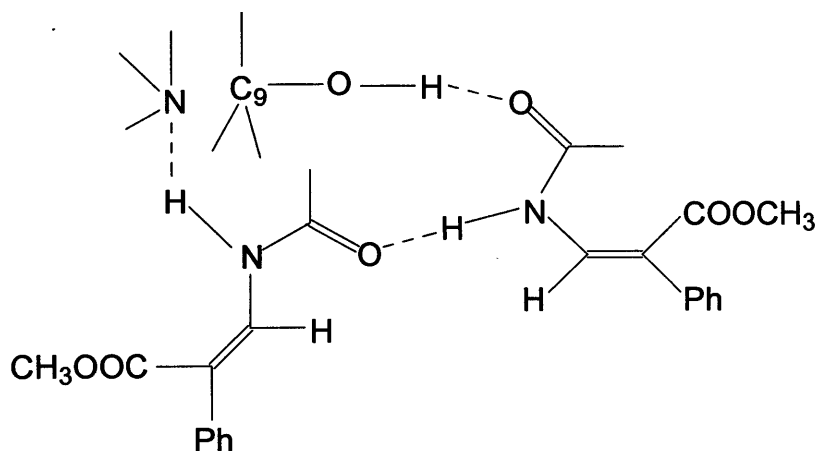


Figure 4.4.7 Representation of the NADPME dimer bonded to C<sub>9</sub>-OH and the quinuclidine-N atom of cinchonine

This model is analogous with that proposed by Baiker and co-workers in the hydrogenation of (Z)-2-methyl-2-butenoic acid. In that reaction enantioselectivity was lost when *either* the quinuclidine-N atom was quaternised *or* when the C<sub>9</sub>-OH was



replaced with O-Me, indicating the crucial reactant-modifier interaction required the participation of both functions of the modifier [17].

The effect of solvent on enantioselectivity will be different for each of these models. For example, if the important interaction is between the monomer and the modifier, then there will be a positive correlation between increasing dielectric constant of the solvent and enantioselectivity due to the stabilisation of the monomer in these solvents. However, if the important interaction is between dimer and modifier, then higher enantioselectivity will be favoured in apolar media.

Furthermore, structural changes made to the modifier at the quinuclidine-N and the C<sub>9</sub>-OH are diagnostic as to the reactant-modifier interaction involved. For the dimer-modifier interaction model, enantioselectivity will be lost when *either* quaternisation of the quinuclidine-N *and/or* the C<sub>9</sub>-OH is replaced by C<sub>9</sub>-OR whereas, for the monomer-modifier interaction model, enantioselectivity will only be lost on quaternisation of the quinuclidine-N (i.e it will be retained on replacing C<sub>9</sub>-OH by C<sub>9</sub>-OR).

Table 3.3.2 and Figure 3.3.2 shows that for NADPME hydrogenation enantioselectivity increases with increasing dielectric constant of the solvent. This implies that it is the monomer rather than the dimer of NADPME which interacts with the modifier. This is confirmed by the observation that quaternisation of the quinuclidine-N destroyed enantioselectivity and that replacement of the C<sub>9</sub>-OH with C<sub>9</sub>-OR resulted in no loss of enantioselectivity (Table 3.5.1).

#### 4.4.3 Conclusions

The results support a mechanism in which (i) NADPME monomer is in equilibrium with dimer in solution and (ii) the monomer-modifier interaction is crucial for the achievement of enantioselectivity. Variation of the extent of dimerisation in solvents of differing dielectric constant determines the solvent effect on enantiomeric excess. Thus, for a range of solvents of increasing dielectric constant, the proportion of cinchonine in the open-3 conformation is reduced (disfavouring high enantiomeric excess) but this is more than compensated by a reduced extent of dimer formation.

Using mixed solvents made further increases to dielectric constant of solvent and indeed had a positive effect on the value of enantiomeric excess. For water/methanol mixtures a 6% increase in enantiomeric excess was observed for mixtures containing between 2 and 3% by volume of water added (Table 3.3.3 and Figure 3.3.4) and similarly, for DMF/water mixtures a 15% increase in enantiomeric excess was observed for mixtures containing between 3 and 12% by volume of water added (Table 3.3.4 and Figure 3.3.5).

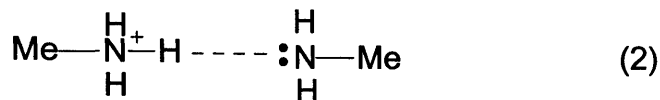
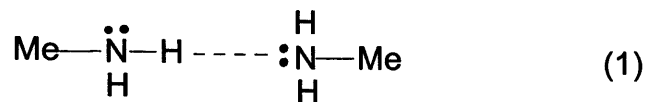
Interestingly, both water/solvent mixtures showed a similar pattern in behaviour in that, after the % by volume of water added exceeded that noted above, a decrease in enantioselectivity was observed. It is possible that under these conditions the dimerisation content of the equilibrium may be negligible. Hence, further increases made to the dielectric constant of the solvent only serves to reduce the proportion of the open-3 conformation in solution with the extent of monomer formation of NADPME remaining constant. Thus, a decrease in enantioselectivity occurs.

## 4.5 The Effect of pH on the Standard Reaction

### 4.5.1 The Reactant-Modifier Interaction

Section 4.3 argues that the reactant:modifier interaction required for this *enantioselective* reaction involves a N-H-N linkage and this can be established in two ways; either the NH group of NADPME can interact with the lone pair on the quinuclidine-N atom of the modifier, or the lone pair on the N-atom of NADPME can interact with the protonated-N of the modifier (both interactions requiring cinchonine to be in the open-3 conformation).

Calculations have been carried out [14] to assess the relative strengths of these interactions, using as a model the simplest amine, methylamine, (equations (1) and (2)). In each case the energy of the H-bonded state was compared with that of participating entities at infinite separation, and it was found that situation (2) was established to a considerably greater extent (for (1)  $\Delta E = 12 \text{ kJ mol}^{-1}$ ; for (2)  $\Delta E = 111 \text{ kJ mol}^{-1}$ ).



This suggests that the stronger interaction between NADPME and cinchonine would occur when one of the molecules is protonated. The pKa value for the quinuclidine-N of cinchonine is 10 and that for NADPME-N is 1.5. Thus, in a given solution protonation will occur more readily at the quinuclidine-N. Furthermore, experimental variables that influence this interaction will be expected to influence the value of the enantiomeric excess achieved.

#### 4.5.2 The Effect of Additives

The positive effect that acids have, either as solvent or as an additive, on the value of enantiomeric excess is a common feature of many enantioselective hydrogenations. For example, in the hydrogenation of ethyl pyruvate, much higher enantioselectivities are observed for reactions conducted in acetic acid (pKa = 4.7) than for those conducted in other solvents of comparable polarity [18]. The explanation offered is that in such media the modifier is completely protonated and exists almost entirely as the open-3 conformer [19, 20].

##### 4.5.2.1 Solutions containing acetic acid

For NADPME hydrogenation an optimum in enantiomeric excess was observed with the addition of acetic acid such that the pH of the solution was between 5.5 and 7.0 (Section 3.6, Table 3.6.1). Table 4.5.1 presents the ratios of protonated:unprotonated forms of the

modifier in solution at various pH values for protonation of both the quinuclidine-N and the quinoline-N functions.

At pH = 8.4 (standard reaction conditions) 97% of cinchonine molecules should be protonated at the quinuclidine-N and protonation of the quinoline-N should be negligible. For pH values between 5.5 and 7 the protonated forms increase to 99.99% and 33.33% for the quinuclidine-N and the quinoline-N atoms respectively. It is proposed that the increased concentrations of protonated modifier (which forms a stronger interaction with NADPME) and the open-3 conformer, are responsible for the observed increase in enantioselectivity.

Table 4.5.1 The ratios of protonated:unprotonated forms of modifier expected for various values of pH.

[QD-NH<sup>+</sup>] = protonated quinuclidine-N; [QD-N] = unprotonated quinuclidine-N; [Q-NH<sup>+</sup>] = protonated quinoline-N; [Q-N] = unprotonated quinoline-N.

pH of the reaction medium	[QD-NH <sup>+</sup> ]:[QD-N]	[Q-NH <sup>+</sup> ]:[Q-N]
2.0	$1.0 \times 10^8:1$	1600:1
4.0	$1.0 \times 10^6:1$	16:1
4.5	$3.2 \times 10^5:1$	5:1
5.5	$3.2 \times 10^4:1$	0.5:1
6.5	$3.2 \times 10^3:1$	0.05:1
7.0	1000:1	$1.6 \times 10^{-2}:1$
8.0	100:1	$1.6 \times 10^{-3}:1$
8.4	40:1	$6.3 \times 10^{-4}:1$
9.5	3:1	$5.0 \times 10^{-5}:1$
10.5	0.32:1	$5.0 \times 10^{-6}:1$
11.0	0.1:1	$1.6 \times 10^{-7}:1$

The ratios shown in this Table are calculated on assumption that the activity coefficients of the participating molecules and ions are unity in methanolic solution. These solutions were not ideal, but the trends in the ratios over many orders of magnitude are considered to be reliable.

For pH values lower than 5.5 a decrease in enantioselectivity was observed (Table 3.6.1). Table 4.5.1 clearly shows that significant protonation of the quinoline-N occurs in these solutions. This protonation interferes with the  $\pi$ -orbital system of the quinoline moiety increasing its susceptibility to hydrogenation at the Pd surface, an event which has been shown to occur slowly under standard reaction conditions (Section 3.8). Both protonation and reduction of the quinoline moiety (which is considered to be orientated parallel with the surface in the unperturbed state) may cause the modifier to become tilted with respect to the surface and hence less effective.

It should be noted that when the modifier used was cinchonine mono-hydrochloride (Section 3.5, Table 3.5.6) the pH of the reaction medium was 6.4. According to Table 4.5.1 the modifier remained almost entirely in the protonated form as it was dissolved, and the enantiomeric excess obtained (14.0%(S)) was almost the same as that observed for the cinchonine acidified to pH = 6.5 by use of acetic acid (16.0%(S)). This supports the proposal that cinchonine was extensively protonated under the conditions where it was most effective.

An interpretation of diminution in enantiomeric excess for high values of pH is given in Section 4.5.2.2 below.

#### 4.5.2.2 Solutions containing potassium hydroxide

The addition of potassium hydroxide to the reaction medium had a detrimental effect on enantioselectivity (Section 3.6, Table 3.6.2). This may be attributed to two factors. First, the proportion of modifier protonated at the quinuclidine-N decreases as the basicity increases, such that at a pH value of 11, only 1% of the modifier is expected to be protonated at this N-atom (Table 4.5.1). Thus, any H-bonding between reactant and alkaloid can only have been of the weaker type shown in equation (1), Section 4.5.1, resulting in fewer reactant molecules undergoing selective enantioface adsorption adjacent to adsorbed modifier, and hence in a lower enantioselectivity. Secondly, the addition of potassium hydroxide to the solution introduced potassium ions which may have adsorbed onto the palladium surface. This adsorption of potassium ions may have weakened the adsorption of the modifier, due to a lowering of electron density at the

palladium surface. This experimental result is comparable to that achieved in the Pd-catalysed hydrogenation of phenylcinnamic acid where the addition of small quantities of sodium hydroxide resulted in inferior values of enantioselectivity [21].

#### 4.5.2.3 Solutions containing trifluoroacetic acid

No significant effect on enantioselectivity was observed when pH was varied by addition of trifluoroacetic acid (Section 3.6, Figure 3.6.1) in marked contrast to the effect of addition of acetic acid.

A difference in the behaviour of these two acids in other enantioselective hydrogenations, such as 4-hydroxy-6-methyl-2-pyrone hydrogenation over cinchonidine-modified Pd has been reported [22]. The authors propose that trifluoroacetic acid can form ion-pairs in solution that interact with the quinuclidine-N of the modifier, as shown in Figure 4.5.1. This structure is thought to be the *actual chiral modifier* for the reaction.

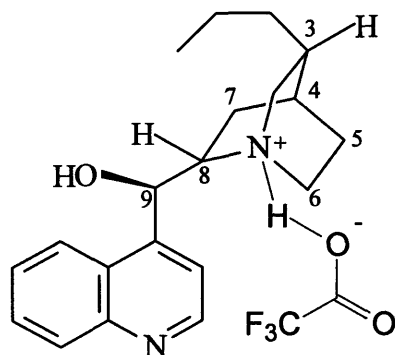


Figure 4.5.1 Cinchonidine- trifluoroacetic acid ion pair interaction

Thus, in the presence of trifluoroacetic acid the modifier is a cinchonine derivative, and enantioselective NADPME hydrogenation is not directly comparable with that catalysed by cinchonine in methanol/acetic acid solution.

### 4.5.3 The Effect of pH on the Optimum CN:NADPME Molar Ratio

The influence of pH on enantioselectivity had implications for the optimum mass of cinchonine used in 'standard reaction conditions'. Enantioselectivity increased through to an optimum as the quantity of cinchonine was increased from 0.5-10 mg (Section 3.1, Table 3.1.6). This is typical for cinchona-modified hydrogenations and is thought to be the result of the presence of a greater number of enantioselective sites at the catalyst surface as the modifier concentration is increased. However, further increase in the mass of cinchonine reduced the enantiomeric excess probably as a result of the formation of cinchonine saturated reaction media.

In the light of the effect of pH on enantioselectivity the optimum mass of cinchonine was re-assessed using reaction media buffered at pH = 6 (Section 3.6, Table 3.6.2 and Figure 3.6.3). By comparison with reactions conducted in unbuffered solutions, higher values of enantiomeric excess were recorded, although the relationship between enantioselectivity and modifier concentration remained the same. As discussed earlier this can be attributed to the higher concentration of the protonated open-3 conformer being present in buffered reaction media.

In contrast to reactions conducted in unbuffered reaction media, there was no substantial decrease in enantioselectivity for additions of cinchonine in the range 50 – 300 mg; and this was because cinchonine did not form saturated solutions in methanol/acetic acid solvent.

In conclusion the optimum mass of cinchonine was the same for buffered and unbuffered reaction media. However, the enantioselectivity was higher and was observed over a wider range of cinchonine concentrations for buffered solutions, a consequence of the greater presence of the protonated open-3 conformer of the modifier and no formation of saturated cinchonine solutions.

### 4.5.4 Conclusions

From the results presented in Section 3.6 it is evident that the pH of the reaction medium influences the value of enantiomeric excess achieved. In weakly acidic solutions the

effects are positive due to the higher concentrations of the protonated open-3 conformer. However, both lower and higher values of pH had a detrimental effect on enantioselectivity attributable either to significant protonation of the quinoline-N in strongly acidic media, or to deprotonation of the quinuclidine-N in basic media.

## 4.6 Effects of Other Experimental Variables

Alterations to reactant and modifier structure were undertaken in an attempt to throw more light on the interaction between NADPME and cinchonine which resulted in enantioselection (Section 3.5).

### 4.6.1 Variation in Reactant Structure

#### *Methylcinnamate (Table 3.5.2)*

It was important to verify accounts from the literature that  $\alpha$ ,  $\beta$ -unsaturated esters are not hydrogenated enantioselectively over cinchona-modified palladium [23]. Methyl cinnamate may be regarded as a variant of NADPME in which the *N*-acetyl group has been replaced by a methyl group. Methyl cinnamate produced racemic product on hydrogenation. This result is consistent with the literature and confirms that unsaturated esters are not enantioselectively hydrogenated.

#### *Dehydrophenylalanine methyl ester and its hydrochloride salt (Table 3.5.2)*

Replacement of the methyl group in methyl cinnamate by an amine generates in the molecule the functionality necessary to undergo enantioselective hydrogenation, as discussed earlier in Section 4.3. Both reactants provided slightly higher values of the enantiomeric excess than that achieved using NADPME. This may be attributed to favourable changes in the pH of the reaction medium as discussed in Section 4.5.



*N-acetyl dehydrophenylalanine (NADP, Table 3.5.1)*

It is well known that  $\alpha$ ,  $\beta$ -unsaturated acids can be enantioselectively hydrogenated to give values of enantiomeric excess in the range of 20 – 72% over cinchona-modified palladium [17, 23-25]. In these reactions the important interaction between modifier and reactant involves a H-bond between the OH of the carboxyl group and the quinuclidine-N of the modifier. Typically, for hydrogenations over cinchonine-modified palladium, an excess of the *R*-enantiomer is observed and for cinchonidine-modified palladium an excess of the *S*-enantiomer.

Hydrogenation of NADP resulted in an enantiomeric excess of only 5%(*S*). A possible explanation for this may be that two competing enantioselective interactions occurred between NADP and cinchonine, the first involving a H-bond between the NH group of NADP and the quinuclidine-N of the modifier giving an excess of the *S*-product, and the second involving a H-bond between the –OH of the carboxyl group and the quinuclidine-N of the modifier, giving an excess of the *R*-product. On this model, the two interactions would have exerted opposite enantiodirecting effects; the observed value of 5%(*S*) suggesting that the first-mentioned interaction was the more important.

*Various alkyl esters of NADP (Table 3.5.1).*

A decrease in enantioselectivity was observed with increasing size of the alkyl group in the ester function of NADPME. Although, molecular modelling shows the ester function to be directed away from the adsorbed modifier (Section 4.3) increasing its size may adversely influence this interaction in two ways. The first may involve intra molecular interactions between a given reactant molecule at one enantioselective site and an adjacent adsorbed modifier molecule on another and the second may involve unfavourable molecular interactions between reactant and the modifier molecule to which it was H-bonded. In either case, it appears clear that increases in the molecular volume of the (already large) reactant molecule makes adsorption at the enantioselective site adjacent to adsorbed cinchonine more difficult to achieve.

### *Various phenyl ring substituents of NADPME (Table 3.5.3)*

Alteration to the phenyl moiety of NADPME had very little effect on the value of enantiomeric excess. Two conclusions can be drawn. First, the electronic effects of the various substituents did not effect the enantioselective outcome of the reaction. Their effect on *rate* is unknown (except that complete reaction continued to be achieved in 3 h). However, since R- and S-product formation occurred by kinetically parallel paths, any small variations in gross rate are not expected to influence the enantiomeric excess. Second, the increased molecular volume of the MeO-substituted compound did not adversely influence the enantiomeric excess, which is surprising in view of the ester group effect noted on the preceding sub-section.

### 4.6.2 Variations in Modifier Structure

#### *10,11-Dihydrocinchonine (Table 3.5.6)*

It has been shown (Section 3.8) that the actual effective modifier for NADPME hydrogenation is dihydrocinchonine, as rapid reduction of the vinyl group in cinchonine occurs under the experimental conditions used. Hence, as expected, there was no difference in the value of enantiomeric excess achieved when the dihydro-compound was used to modify the catalyst surface.

#### *Cinchonine monohydrochloride (Table 3.5.6)*

Higher values of enantiomeric excess were achieved using cinchonine monohydrochloride as modifier. This is attributed to the higher concentration of the protonated form of the modifier present in acidic media and to the lower pH of the reaction medium. (This result is discussed with the effect of pH in Section 4.5).

*Alkyl-quaternised cinchonine (Table 3.5.6)*

A complete loss in enantioselectivity was observed for reactions carried out with quaternised alkaloid. This result confirmed the importance of the quinuclidine-N in providing an enantioselective interaction with the reactant, and is consistent with the literature which shows that many potentially enantioselective hydrogenations become racemic when the quinuclidine-N of a cinchona alkaloid is quaternised [26, 27].

*4-Chlorobenzoate quinidine (Table 3.5.6)*

This modifier was used as a test for the involvement of the C<sub>9</sub>-OH function in cinchonine in the enantioselective process, since 4-chlorobenzoate quinidine has no C<sub>9</sub>-OH function available for interaction with the reactant.

No change in the value of enantiomeric excess was observed, suggesting that the C<sub>9</sub>-OH function in cinchonine is not involved in the enantioselective interaction between reactant and modifier.

### 4.6.3 Conclusions

The most important inference from variation of reactant structure is that NADPME can be enantioselectively hydrogenated because of the presence of the N atom.

With regards to the modifier structure, the results have demonstrated the importance of the quinuclidine-N atom in achieving an enantioselective outcome and the positive influence on enantioselectivity of the protonated form of the modifier.

Overall, these results indicate that there is a monomer:modifier H-bonding interaction occurring between the N-atom of NADPME and the protonated quinuclidine-N of cinchonine. These conclusions are consistent with those drawn in Section 4.4 and 4.5 relating to solvent and pH effects respectively.

## 4.7 Hydrogenation of NADPME Catalysed by Pd/titania

There are various reports in the literature in which titania-supported catalysts outperform those of alumina, particularly for the hydrogenation of  $\alpha,\beta$ -unsaturated acids. In the Pd-catalysed hydrogenation of phenyl cinnamic acid, Nitta reports increases of 20 – 30% in the value of enantiomeric excess when the support was changed from alumina to titania under otherwise identical reaction conditions [28].

### 4.7.1 Method of Preparation of Pd/titania Catalysts

The method of preparation of Pd/titania catalysts made little difference to their performance in NADPME hydrogenation (Section 3.7, Table 3.7.1). However, the scale of the preparation did appear to influence performance, catalyst prepared on a 2 g scale showing better performance than those prepared on a 7 g scale. Although the reason for the failure to scale-up is unclear, it is known that the drying step involved in catalyst preparation can effect the distribution of the metal on the support [29]. For these samples, each was left to dry in the same size Buchner funnel, irrespective of the scale of the preparation. Thus, the two batches may have dried at different rates resulting in a different distribution of metal particles on the support.

### 4.7.2 Comparison of Pd/titania with Pd/alumina

A comparison of the performances of Pd/titania with that of Pd/alumina catalysts (1) and (2) (Section 3.7, Table 3.7.1) enabled the support effect to be quantified. Reactions over 5% Pd/titania prepared on the 7 g scale (Entry 6, Table 3.7.1) gave an enantiomeric excess of ~8%(*S*) which varied little with modifier:reactant ratio; this behaviour follows that shown by 5% Pd/alumina (1) and (2) (entries 3 and 4). However, 5% Pd/titania samples prepared on the 2 g scale (entries 1 and 2) gave values of enantiomeric excess which varied with reactant:modifier molar ratio, giving maxima of 16 – 17% (*S*). Under these conditions, there appears to be a beneficial effect of changing the support. However, the origin of this improvement may lie in the preparation techniques, because

5% Pd/alumina catalyst prepared in the laboratory also showed enantioselectivities that varied with modifier:reactant ratio, achieving 14.5%(*S*) under optimum conditions (entry 5). It may be significant that the best performing catalysts were those that had been freshly prepared. Certainly, titania-supported Pd did not show exceptional enantioselectivity.

Examination of the morphology of the catalysts revealed significant differences in their Pd particle size distributions (Figure 3.7.3 – 3.7.6). Pd/alumina contained Pd particles of ~ 7 nm in size, whereas Pd/titania contained Pd particles of ~ 4 nm in size. This difference may be responsible for a difference in performance as discussed in the next sub-section.

### 4.7.3 Effect of Palladium Loading

Table 3.7.2 shows the relationship between metal loading and performance in NADPME hydrogenation. The best performance was observed for 2% Pd/titania where values of enantiomeric excess reached 22%. This catalyst was unique in providing optimum performance at a higher CN:NADPME molar ratio than the other Pd/titania catalysts and unfortunately this was at the upper limit of the solubility of cinchonine. Thus, higher CN:NADPME molar ratios resulted in lower values of the enantiomeric excess which are attributed to the formation of saturated reaction media.

Figure 3.7.2 shows a smooth variation of enantiomeric excess with catalyst dispersion (as measured by the extent of CO adsorption in a pulsed flow system (Section 2.3.9) which suggests that there is an effect of particle size on enantioselectivity. The cubic particle model is adequate for the conversion of dispersion to mean particle size, and the values so obtained are shown in the third column of Table 4.7.1. As a check, 4.63% Pd/titania catalyst with a dispersion of 0.31 has a calculated Pd particle size of 4.1 nm which agrees with the value determined from electron microscopy of 4.2 nm (Figure 3.7.6). However, the metal particles in all supported metal catalysts exhibit a size distribution, and these values at best represent an estimate of the positions of the maxima in these distributions.

The morphology of the Pd particles is unknown. Of the platinum group metals (Ru, Rh, Pd, Os, Ir, Pt) palladium has the lowest melting point and is the most susceptible to sintering. It is probable therefore that the shape of the metal particles approximated to the cubo-octahedral symmetry expected for well annealed particles. Figure 4.7.1 shows

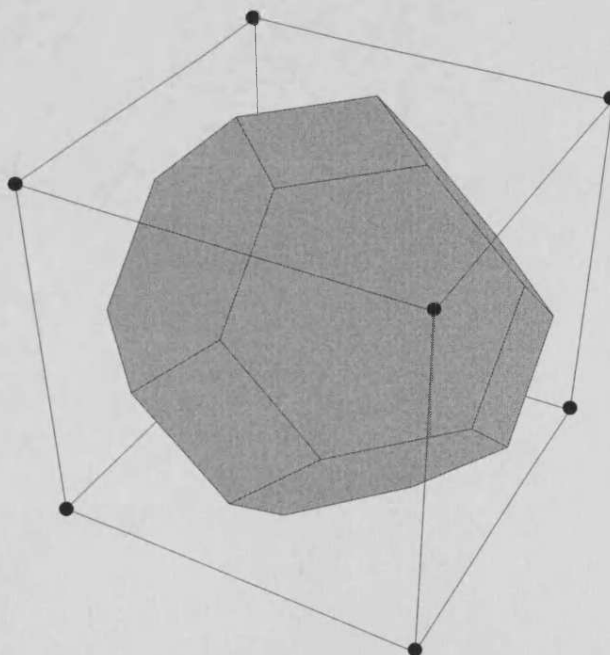
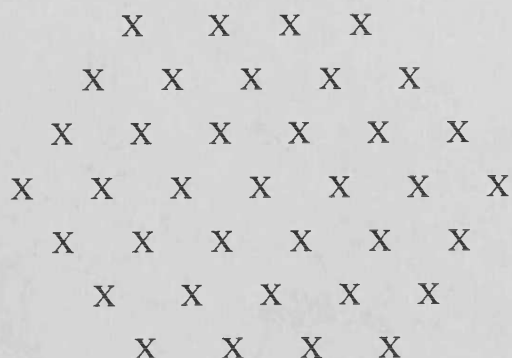


Figure 4.7.1 A faces exposed by a cubo-octahedral metal particle.

such a cubo-octahedral particle. As indicated in Table 4.7.1 2% Pd/titania, which showed the best performance, contained particles which, had they been cubes, would have contained about 10 atoms along each edge. The hexagonal faces of a cubo-octahedral particle contained within such a cube would have contained 4 atoms along the edge and successive rows of 4,5,6,7,6,5,4 atoms in the form of a  $\{111\}$  face, thus:-



and this face would therefore have contained 37 atoms. The atom populations of the corresponding hexagonal faces for the other Pd/titania catalysts are given in Table 4.7.1.

Table 4.7.1 Pd/titania catalysts. Observed loadings and derived dispersions, particle sizes and surface configurations based on the cubic and cubo-octahedral models of particle morphology.

Metal loading/%	Dispersion <sup>a</sup>	Pd particle size <sup>b</sup>		No. of Pd atoms constituting one hexagonal face <sup>d</sup>	Optimum e.e./%( <i>S</i> )
		/nm	No. of Pd atoms on a cube face <sup>c</sup>		
0.94	0.58	2.1	8 × 8	24	15
1.8	0.46	2.7	10 × 10	37	22
4.63	0.31	4.1	15 × 15	75	16
9.71	0.20	6.3	24 × 24	217	14
19.89	0.13	10.4	38 × 38	547	12

<sup>a</sup> by CO adsorption;

<sup>b</sup> calculated on the cubic particle model; <sup>c</sup> in a (100) configuration; <sup>d</sup> in a (111) configuration

It may be argued that a 'perfect' catalyst particle would be one that contained facets which exposed exactly the number and arrangement of surface atoms required to form one enantioselective site (i.e. exactly the number and arrangement required for the adsorption of one molecule of cinchonine, one molecule of NADPME, and hydrogen). From the Figures contained in Section 4.3, it appears that an array of 25 or so atoms would be sufficient. Smaller arrays that would not accommodate cinchonine would provide sites for racemic hydrogenation, and larger sites would provide sites for both enantioselective and racemic hydrogenation. On this basis it would appear that the Pd particles present in 2% Pd/titania might well have been the most suitable for enantioselective NADPME hydrogenation, and indeed the highest enantiomeric excess was indeed observed with this catalyst.

In methyl pyruvate hydrogenation over cinchonidine-modified Pt it has been reported that EUROPT-1, (6.3 % Pt/silica) which contains Pt particles in a distribution that peaks at 1.8 nm, gave high values of the enantiomeric excess (typically 70%), whereas a 0.1%

Pt/silica containing 0.7 nm Pt particles gave low values [11,30]. It was proposed that the 0.7 nm particles were ineffective because they did not provide for simultaneous adsorption of modifier and reactant. In retrospect, it would have been interesting if the present study had included a 0.5% Pt/titania catalyst; the model predicts it would have provided an enantiomeric excess significantly below 15%(*S*).

No information was available concerning Pd particle size in Pd/alumina (1) and (2). Values of the enantiomeric excess given by samples of catalyst (1) reduced at various temperatures between 423 and 673 K showed no meaningful variation (Table 3.1.2). It would be expected that an unsintered catalyst would have undergone a degree of sintering over this temperature range, giving rise to a variation in enantiomeric excess. The absence of such a variation suggests that the catalysts were reduced during manufacture at such a temperature that no further change occurred during the experiments described in Table 3.1.2.

## 4.8 Reactions Involving Other Cinchona Alkaloids

Cinchonine was the alkaloid modifier used most extensively in this investigation. However, to understand its behaviour, it is necessary to view it in a wider context; to do this, the behaviours of three other naturally occurring cinchona alkaloids, cinchonidine, quinidine, and quinine were investigated.

Cinchonine and cinchonidine have the same molecular mass and contain the same structural elements, differing only in their configurations at the chiral carbons C<sub>8</sub> and C<sub>9</sub> (Section 2.1.3, Figure 2.1.8). They have been described as 'near enantiomers' and in many enantioselective hydrogenations they behave equivalently except that one provides an excess of *R*-product and the other an excess of *S*-product [17]. However, the situation is more complex in the case of NADPME hydrogenation, where inversions in the sense of the enantioselectivity sometimes occurred as modifier concentration was varied.



Quinidine is 6'-methoxy cinchonine and quinine is 6'-methoxy cinchonidine. In the Pt-catalysed hydrogenation of methyl pyruvate these alkaloids behaved like cinchonine and cinchonidine except that they provided lower values of the enantiomeric excess [11]. The lower performance was attributed to steric hindrance at the enantioselective site caused by the methoxy substituent.

One property which distinguishes these alkaloids is their solubility in common solvents, cinchonine being less soluble than cinchonidine and quinidine than quinine. Of these four alkaloids, cinchonine showed the lowest solubility and it was only in cinchonine-modified reactions that saturation limits were reached and the ability to explore the system was thereby limited.

#### 4.8.1 Variation of Enantiomeric Excess with Modifier:Reactant Ratio

For cinchona-modified hydrogenations the value of the enantiomeric excess varied with the mass of modifier added to the reactor. Since the volume of the reaction mixture and the quantity of NADPME were retained constant, the results in Chapter 3 have been expressed in terms of the variation of enantiomeric excess with modifier:reactant molar ratio.

The chiral outcomes of NADPME hydrogenations using all four modifiers with modifier:reactant ratios in the range 0.006:1 to 2.7:1 are reported in Chapter 3. Here, reactions involving low modifier:reactant ratios (defined as <0.03:1) are discussed first, followed by reactions involving high modifier:reactant (defined as >0.03:1 and <2.7:1). Except where otherwise stated, all reactions were carried out in methanol over Pd/alumina (2).

##### 4.8.1.1 Reactions involving low modifier:reactant ratios

*Cinchonine and cinchonidine (Section 3.1, Tables 3.1.6 and 3.8.1).*

Cinchonine (and its 10,11-dihydroderivative) afforded values of the enantiomeric excess in favour of the *S*-enantiomer (~10%(*S*)) which changed little with cinchonine:NADPME molar ratio over the range 0.006 to 0.03. Cinchonidine with the opposite stereochemistry

at C<sub>8</sub> afforded an excess of the opposite enantiomer (3.5%(R)). These results are shown in Figure 4.8.1 (open diamond and square points).

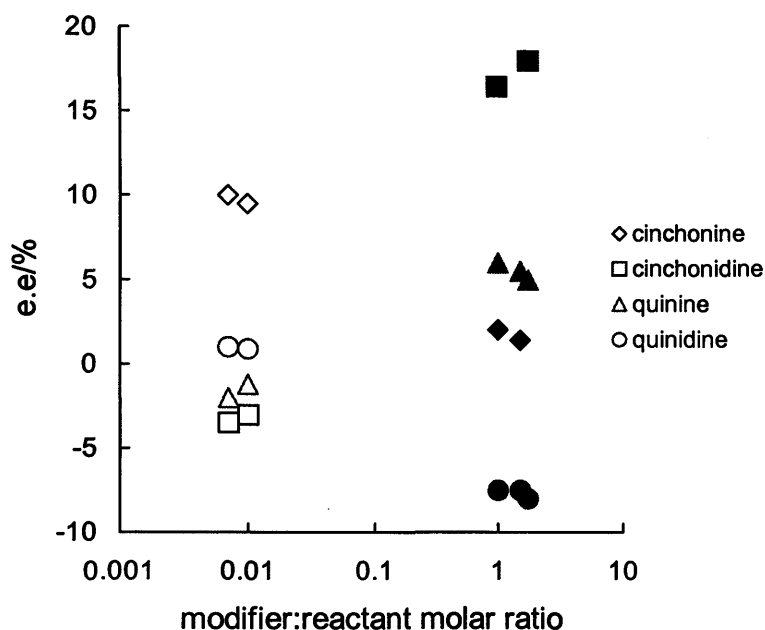


Figure 4.8.1 Semi-logarithmic presentation of the variation of enantiomeric excess with modifier:NADPME molar ratio.

At first sight these results were surprising because, as stated above, cinchonine normally favours *R*-enantiomer formation and cinchonidine *S*-enantiomer formation in the Pd-catalysed hydrogenation of  $\alpha,\beta$ -unsaturated acids. However, the results are consistent with the general experience that these modifiers favour the formation of opposite enantiomers.

#### *Quinine and quinidine (Section 3.9, Table 3.9.1).*

At a modifier:NADPME ratio of 0.007 quinine provided e.e. = 2.0%(*R*) and quinidine 1.0%(*S*) and these values changed slightly to zero and 1.0%(*R*) at a ratio of 0.01. These results are shown in Figure 4.8.1 as the open triangles and circles. The reason for this poor performance is unclear. However, recent reports in which the adsorption strengths of the cinchona alkaloids were examined, revealed that quinine and quinidine adsorb much more weakly on the catalyst surface than cinchonine and cinchonidine [31]. It is therefore possible that these modifiers are required in greater concentrations in solution

to provide the same surface coverage as those of cinchonine and cinchonidine and thus to provide a significant enantioselective outcome. Indeed, these two modifiers do provide values of enantiomeric excess at much high modifier concentrations and this result will be discussed below.

#### 4.8.1.2 Reactions at high modifier:reactant molar ratio

High ratios were defined above as  $>0.03:1$  and  $<2.7:1$ .

##### *Quinine and quinidine (Section 3.9, Table 3.9.1).*

At modifier:reactant ratios of 1:1 to 1.8:1) quinine and quinidine performed equally well and showed a reversal in the sense in enantioselectivity, quinidine giving e.e. =  $\sim 8\%(R)$  and quinine  $\sim 6\%(S)$ . This behaviour is represented on Figure 4.8.1 as the filled triangles and circles.

Thus, the effect of increasing the amount of modifier in the reactor was to move the enantioselectivity of quinidine from a slight *S*-excess to a more substantial *R*-excess, and that of quinine from a slight *R*-excess to a more substantial *S*-excess. Furthermore, the values of enantiomeric excess achieved are inferior to those of cinchonine and cinchonidine and may be a result of the additional steric hindrance associated with the methoxy group of quinine and quinidine.

##### *Cinchonine (Section 3.1, Table 3.1.6) and cinchonidine (Section 3.8, Table 3.8.1).*

Consider the behaviour of cinchonidine before that of cinchonine. Figure 4.8.1 shows how enantioselectivity varied from a weak *R*-preference to a strong *S*-preference ( $\sim 20\%(S)$ , filled square points) on passing from low to high cinchonidine:reactant ratio conditions. This trend in behaviour follows that of quinine but is more marked. For cinchonine, the Figure shows that enantioselectivity varied from a strong *S*-preference to a weak *S*-preference ( $\sim 2\%(S)$ , filled diamond points) over the same range of conditions. In this, the behaviour of cinchonine followed that of quinidine in an almost parallel fashion although there was no reversal in the optical preference. For cinchonine, reaction

solutions under the high ratio conditions shown in Figure 4.8.1 are saturated with cinchonine, and it may be speculated that a reversal in the sense of the enantioselectivity might have occurred had its solubility been as high as that of the other three alkaloids.

Thus, Figure 4.8.1 shows that there is a consistency of behaviour as between cinchonine and cinchonidine on the one hand, and between quinidine and quinine of the other. The situation is a demanding one in terms of interpretation because at many modifier:reactant ratios both cinchonine and cinchonidine give an enantioselectivity in favour of *S*-product. However, the starting point from which an interpretation is developed must be the recognition that all four modifiers are showing consistent family behaviour.

Examination of the molecular modelling presented in Section 4.3 for the interaction between DPME and cinchonine revealed two important considerations when interpreting the effect of alkaloid concentration on the observed sense of the enantioselectivity. First, the interaction leading to the formation of the *S*-product requires slightly more room on the catalyst surface compared to that of *R*-product formation. Secondly, and perhaps more importantly, the interaction leading to *S*-product formation (Figure 4.3.5) clearly shows that the phenyl ring of DPME is adjacent to the quinoline moiety of cinchonine and the O-atom of the ester carbonyl is adjacent to the quinuclidine-N atom. Although the quinuclidine ring is not adsorbed on the catalyst surface and as such will have Pd atoms which are 'unoccupied' underneath the ring, there would be insufficient space to accommodate the ester group of DPME if experimental conditions were such to cause compression of the surface ad layer. This interaction would then encounter strong repulsive forces resulting in this interaction no longer being as favourable. Additionally, the O-atom of the carbonyl ester group of DPME would be in close proximity to the quinuclidine-N atom with which it may interact. This type of interaction is similar to that shown for adduct formation in Figure 4.3.8 and is not thought to have an enantioselective outcome. As a result more of the modifier may be 'locked-up' in interactions leading to racemic products.

In contrast, the interaction leading to *R*-product formation (Figure 4.3.6) shows that the phenyl ring is adjacent to the quinuclidine moiety and the ester carbonyl adjacent to the quinoline moiety. For experimental conditions where compression of the surface ad layer are in effect, it may be possible for the phenyl ring of DPME (adsorbed flat and parallel)

to move closer to cinchonine by occupying some of the 'free' Pd atoms underneath the quinuclidine moiety. Furthermore, no adverse interactions between the O-atom of the carbonyl ester group of DPME and the quinuclidine-N atom would occur. Thus, this interaction would require less space on the catalyst surface compared to that leading to the formation of the *S*-enantiomer and would not encounter the undesirable interactions between the carbonyl-O atom of DPME and the quinuclidine-N atom. Hence under conditions where there is high surface coverage of the modifier (this is, compression of the surface ad layer) the interaction leading to *R*-product formation would be more favourable.

This proposal supports the results obtained for the decline in the value of enantiomeric excess with cinchonine;NADPME molar ratios between 0.03 – 0.2:1, this is at cinchonine concentrations prior to the formation of saturated reaction media (Table 3.1.6). Over this range the value of enantiomeric excess decreased in favour of the *S*-enantiomer from 10% to 5.5%. This may be attributed to the interaction leading to *S*-product formation encountering strong repulsive forces as high surface coverage of the modifier was achieved and thus, becoming more unfavourable leading to the observed decrease in enantioselectivity.

The model predicts that if cinchonine concentration was further increased, further decreases in the value of enantiomeric excess in favour of the *S*-enantiomer would be observed, with a possibility of an inversion in enantioselectivity as the interaction leading to *R*-product formation became more favourable. Unfortunately, this prediction could not be investigated due to the formation of saturated reaction media above CN:NADPME molar ratios of 0.2:1.

The low solubility of cinchonine was not observed for the other three cinchona alkaloids and as a result, reactions involving these modifiers could be conducted over a much higher concentration range enabling the model outlined above to be tested.

The results obtained from molecular modelling of DPME with cinchonine can be used to incorporate cinchonidine with DPME, since they contain the same structural elements, differing only in their configurations at C<sub>8</sub> and C<sub>9</sub>. Thus, similar interactions as those shown in Figures 4.3.5 and 4.3.6 exist when cinchonidine is the adsorbed modifier. In summary, the interaction shown for cinchonine with DPME leading to *S*-product formation will give *R*-product formation for cinchonidine and DPME. Likewise, the

interaction shown for cinchonine with DPME leading to *R*-product formation will give *S*-product formation for cinchonidine and DPME.

For cinchonidine and DPME the interaction leading to *R*-product formation requires the more space on the catalyst surface and additionally involves the phenyl ring of DPME being adjacent to the quinoline moiety. Thus, when there is a high surface coverage of the modifier such that compression of the surface ad layer occurs, *R*-product formation will be less favoured resulting from the strong repulsive forces occurring between the ester group of DPME and the quinuclidine ring of cinchonidine. Under these experimental conditions the preferred interaction is then that leading to *S*-product formation. Thus, for reactions with cinchonidine as modifier, as the concentration of cinchonidine is increased so the value of enantiomeric excess will vary as well as the stereochemical outcome. This thereby lends an interpretation to the inversion in enantioselectivity observed with increasing modifier concentration from a weak *R*-preference at low modifier concentration to a strong *S*-preference at high modifier concentrations.

In conclusion, the sense of enantioselectivity achieved for cinchona-modified reactions may be dependent on the solution concentration and ultimately the surface coverage of the modifier. Experimental conditions that effect this equilibrium may not only effect the value of enantiomeric excess but also the stereochemical outcome of the reaction. Variation of experimental conditions with cinchonidine as modifier has been studied and the results will be discussed below.

## 4.8.2 Variation of Experimental Conditions for Cinchonidine-Modified Reactions

### 4.8.2.1 Effect of modifier on rate

Rate of reaction decreased with increasing modifier concentration with the fastest rate observed in the absence of modifier, i.e. for racemic hydrogenation. However, the value

of enantiomeric excess increased with increasing modifier concentration (Section 3.8.1). This is typical for cinchona-modified Pd reactions and is consistent with the literature [32-34]. The lack of rate enhancement such as is observed in pyruvate ester enantioselective hydrogenation, results in significant racemic reaction occurring at unmodified sites, thereby reducing enantioselectivity (see Section 4.4.5). Higher concentrations of modifier may increase modifier surface coverage and thus reduce the number of unmodified sites for racemic reaction leading to higher enantioselectivity. The observed decrease in rate is a result of the modifier occupying a larger fraction of the catalyst surface and thereby reducing the total number of available active sites at which hydrogenation can take place.

#### 4.8.2.2 Solvent effects

Results discussed thus far involved reactions conducted in methanol. For cinchonidine-modified hydrogenations the effect of solvent was investigated further (Section 3.8, Table 3.8.3). There are two important conclusions to be drawn from these results. First, an excess of the *S*-enantiomer was achieved in the majority of reactions and that optima occurred at CD:NADPME molar ratios of 1:1. Furthermore, the value achieved at this optimum increased with increasing dielectric constant of the solvent (Table 3.8.4). A similar correlation was observed for cinchonine-modified hydrogenations and an explanation for this behaviour has been offered in Section 4.4. To summarise, the more polar the solvent the greater the stabilisation of the monomeric form of NADPME and as the NADPME monomer is required for interaction with the modifier there is an increase in enantioselectivity with increasing polarity of the solvent.

Second, the only inversion in enantioselectivity to form an excess of *R*-products occurred at low modifier concentrations and only in the primary alcohol solvents, methanol, ethanol and propanol. These results are difficult to interpret. However, solvents should not be considered simply as indifferent media in which the dissolved material diffuses in order to distribute itself evenly; it is not just an host environment in which a reaction can take place. Use of physical constants such as the dielectric constant of the solvent does not adequately represent solute/solvent interactions and in this case catalyst/solvent interactions. It is well known that liquids that possess hydroxyl groups have the potential to hydrogen bond with each other (leading to their higher boiling points) and with other

molecules. The crucial interaction between cinchonidine and NADPME involves H-bonding and it is quite possible that when these interactions are taking place in alcoholic solvents they may be influenced by the H-bonding capability of the solvent itself.

Furthermore, the solvation energy of a solvent, which estimates the ability of the solvent to solvate a solute molecule, is different for different solvents [35]. This ability may effect the surface coverage of the modifier on the surface, such that the greater the solvation ability of the solvent, the fewer solute molecules (modifier) will be adsorbed at the catalyst surface. Thus, the use of the same concentration of modifier in different solvents will not necessarily provide the same surface coverage of modifier on the surface. This may contribute to the various rates observed for reactions conducted in different solvents (Section 3.3, Table 3.3.2).

Additionally, evidence in the literature has shown that methanol can adsorb on the catalyst surface and dissociate to form adsorbed carbon monoxide and hydrogen [36]. If these reactions take place, a fraction of the catalyst surface will be occupied and this again may affect the surface coverage of modifier. If this were correct and inversion in enantioselectivity only takes place under low surface coverage of the modifier, then no inversion in enantioselectivity in THF is observed as a result of the higher surface coverage of the modifier in this solvent compared to that of methanol.

Although, inversions in the sense of the enantioselectivity are not commonplace there are several reports of this phenomenon in the literature. In the catalytic hydrogenation of the C=N double bond in pyruvic acid oxime,  $\text{MeC(=NOH)COOH}$  over ephedrine-modified Pd/C the enantiomeric excess was 10%(*S*) in 2-propanol as solvent, but 3%(*R*) in dioxane [37]. The workers report a complex H-bonding compound between oxime and cinchonidine, both in solution and on the catalyst surface. Small changes in the balance of these intermediates in different solvents have been proposed to account for these inversions in enantioselectivity. HNMR spectroscopy for NADPME and cinchonidine did not reveal any immediate changes attributable to hydrogen bonding or complex formation as the concentration of cinchonidine was increased (Section 3.8 Figures 3.9.10 – 3.9.12). However, there is now spectroscopic evidence in the literature [38] of slow processes occurring, and additional information might have been obtained had the spectra been collected over a time period equivalent to that of a reaction (i.e. 3 h).



#### 4.8.2.3 Reactions in acetic acid mixtures

##### *Reactions in methanol/acetic acid and in ethanol/acetic acid (Section 3.9, Table 3.8.5)*

For reactions conducted in alcoholic/acetic acid mixtures there was an increase in enantioselectivity in favour of the *R*-enantiomer at low modifier concentrations. This may be attributed to the protonation of the modifier and the greater abundance of the open-3 conformer in these solutions, as discussed in Section 4.5. However, at high modifier concentrations (1:1 molar ratio) the value of enantiomeric excess dropped significantly from 21%(*S*) to ~5%(*S*). Acetic acid is sometimes used industrially to clean catalyst surfaces and it may be that under these conditions the high surface coverage of the modifier is being lowered by the acetic acid. Hence, as surface coverage decreases so there is a decrease in enantioselectivity in favour of the *S*-enantiomer (which is proposed as the preferred interaction at high surface coverage).

##### *Reactions in DCM/acetic acid*

For DCM no inversion in enantioselectivity was observed at low or high modifier concentrations and a possible explanation for this has been considered in sub-section 4.8.2.2. When acetic acid was present as a component of the solvent the value of enantiomeric excess was enhanced in favour of the *S*-enantiomer. This may be attributed to the positive effects associated with the prevailing pH (Section 4.5).

#### 4.8.2.4 Effect of varying standard conditions

##### *Quaternised Cinchonidine*

Reactions were carried out using methyl cinchonidium iodide at low and high concentrations (Section 3.8, Table 3.8.6). Racemic products were observed for both concentrations and this supports the widely held view that the quinuclidine-N atom of the modifier plays a crucial role in the enantioselective reaction.

### 4.8.1 Conclusion

For cinchonidine-modified hydrogenations enantioselectivity is lost when the alkaloid is quaternised. This is consistent with the analogous experiment using quaternised cinchonine. It is therefore proposed that a similar interaction as between cinchonine and NADPME involving a N-H-N linkage, also applies for cinchonidine and NADPME.

The value of enantiomeric excess increased with increasing dielectric constant of the solvent and further supports the model of a 1:1 interaction between a monomer of NADPME and the modifier.

The behaviour of the cinchona alkaloids in terms of the value of enantiomeric excess and the stereochemical outcome achieved appears to be dependent on the solution concentration and ultimately the surface coverage of the modifier. Experimental conditions that effect this equilibrium will undoubtedly effect the value of enantiomeric excess and the sense of enantioselectivity observed.

## 4.9 References

1. Strong Metal-Support Interactions, R. T. K. Baker, S. J. Tauster, J. A. Dumesic, Oxford University Press, (1986).
2. W.R. Huck, T. Burgi, T. Mallat, A. Baiker, *J Catal.*, **193** (2000) 1.
3. Y. Nitta, K. Kobiro, *Chem. Lett.* **165** (1995).
4. T. J. Hall, P. Johnston, W. A. H. Vermeer, S. R. Watson, P. B. Wells, *Stud. Surf. Sci. Catal.*, **101** (1996) 221.
5. H.-U. Blaser, H. P. Jalett, D. M. Monti, A. Baiker, J. T. Wehrli, *Stud. Surf. Sci. Catal.*, **67** (1991) 147.

6. M. Schurch, O. Schwalm, T. Mallat, J. Weber, A. Baiker, *J. Catal.*, **169** (1997) 275.
7. W.R. Huck, T. Burgi, T. Mallat, A. Baiker, *J. Catal.*, **200** (2001) 171.
8. J. Wang, Y. Sun, C. LeBlond, R. N. Landau, D. G. Blackmond, *J. Catal.*, **161** (1996) 759.
9. K. J. Laidler, 'Chemical Kinetics', McGraw Hill, New York, (1950), pp256-320.
10. T. J. Hall, PhD Thesis, University of Hull, 1997.
11. I. M. Sutherland, A. Ibbotson, R. B. Moyes, P. B. Wells, *J. Catal.*, **125** (1990) 77.
12. Y. Nitta, K. Kobiro, Y. Okamoto, *Chem. Lett.*, (1996) 897.
13. T.J. Hall, P. Johnston, W.A.H. Vermeer, S. R. Watson, P. B. Wells, *Stud. Surf. Sci. Catal.*, **101** (1996) 221.
14. Ed Jefferey, personal communication.
15. T. Burgi, A. Baiker, *J. Am. Chem. Soc.*, **120** (1998) 12920
16. H-bonding for analogous systems
17. K. Borszky, T. Burgi, Z. Zhaohui, T. Mallat, A. Baiker, *J. Catal.*, **187** (1999) 160.
18. A. Baiker, *J. Mol. Catal. A*, **115** (1997) 473.
19. G. D. H. Dijkstra, R. M. Kellogg, H.J. Wynberg, *J. Org. Chem.*, **55** (1990) 6121.
20. G. D. H. Dijkstra, R. M. Kellogg, H.J. Wynberg, *Recl. Trav. Chim. Pays-Bas*, **108** (1989) 195.

21. Y. Nitta, *Chem. Lett.*, **635** (1999).
22. W.-R. Huck, T. Burgi, T. Mallat, A. Baiker, *J. Catal.*, **205** (2002) 213.
23. P.B. Wells, R.P.K. Wells, *Chiral Catalysts Immobilisation and Recycling*, ed. (DeVos et al.), Wiley-VCH, 2000, p123-154.
24. A. Tugler, G. Fogassy, *J. Mol. Catal. A: Chem.*, **173** (2001) 231.
25. I. Kun, B. Torok, K. Felfoldi, M. Bartok, *App. Catal. A: Gen.*, **203** (2000) 71.
26. G. Webb, P.B. Wells, *Catal. Today*, **12** (1992) 319
27. T. Mallat, A. Baiker, *App. Catal. A: Gen.*, **200** (2000) 3.
28. Y. Nitta, Y. Ueda, T. Imanaka, *Chem. Lett.*, (1994) 1095.
29. G. C. Bond, *Heterogeneous Catalysis Principles and Applications*, Oxford Science Publications (second edition, 1987), Chapter 7, p79.
30. Preparation and properties of a Pt/silica and its comparison with EUROPT-1. S.D. Jackson, M.B.T. Keegan, G.D. McLellan, P.A. Meheux, R.B. Moyes, G. Webb, P.B. Wells, R. Whyman, and J. Willis, in 'Preparation of Catalysts V' (Eds G. Poncelet, P.A. Jacobs, G. Grange and B. Delmon, Elsevier, Amsterdam, 1991) 135-144.
31. W-R. Huck, T. Mallat, A. Baiker, *Catal. Lett.*, Vol. 87, **3-4** (2003) 241.
32. T. Tarnai, A. Tugler, T. Mathe, J. Petro, R.A. Sheldon, G. Toth, *J. Mol. Catal. A: Gen.*, **102** (1995) 41.
33. K. Borszky, T. Mallat, R. Aeischman, W.B. Schweizer, A. Baiker, *J. Catal.*, **161** (1996) 451.

- 34 P. A. Meheux, A. Ibbotson, P. B. Wells, *J. Catal.*, **128** (1991) 387.
- 35 C. Reichardt in 'Solvents and Solvent Effects in Organic Chemistry', (2<sup>nd</sup> Edition), VCH-Weinheim, 1988, pp27-35.
- 36 Adsorption of methanol on a catalyst surface
- 37 K. Borszky, T. Mallat, R. Aeschiman, W.B. Schweizer, A. Baiker, *J.Catal.*, **161** (1996) 451.
- 38 X. Li, PhD Thesis, Cardiff University, 2001.

